Monitoring enzyme activity by using mass-encoded peptides and multiplexed detection

Dissertation zur Erlangung des naturwissenschaftlichen Doktorgrades der

Julius-Maximilians-Universität Würzburg

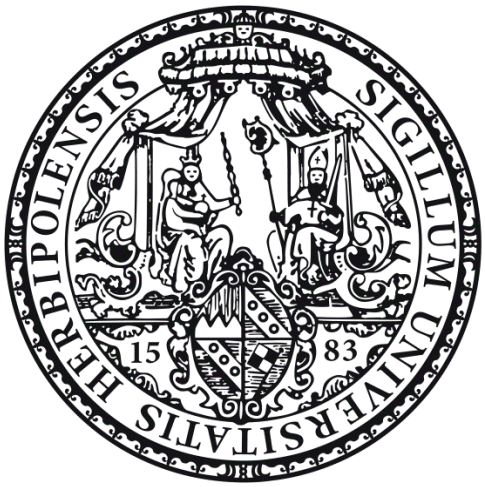

vorgelegt von

Katharina Anna Dodt

aus Darmstadt

Würzburg 2020

Eingereicht bei der Fakultät für Chemie und Pharmazie am

_____

Gutachter der schriftlichen Arbeit

1. Gutachter: _____

2. Gutachter: _____

Prüfer des öffentlichen Promotionskolloquiums

1. Prüfer: _____

2. Prüfer: _____

3. Prüfer: _____

Datum des öffentlichen Promotionskolloquiums

_____

Doktorurkunde ausgehändigt am

_____

Die vorliegende Arbeit wurde in der Zeit von Oktober 2015 bis Oktober 2019 am Institut für Pharmazie und Lebensmittelchemie der Bayerischen Julius-Maximilians-Universität Würzburg unter der Anleitung von Herrn Prof. Dr. Dr. Lorenz Meinel und Frau PD Dr. Tessa Lühmann angefertigt.

To my parents

TABLE OF CONTENTS

Summary **1**

Zusammenfassung **5**

Chapter 1: A complete and versatile Protocol: Decoration of cell-derived matrices with mass-encoded peptides for multiplexed enzyme activity detection **9**

Chapter 2: Mass-encoded reporters reporting proteolytic activity from within the extracellular matrix **63**

Chapter 3: Soluble mass reporters for detection of enzyme activity and multiplexed analysis **109**

Conclusion and outlook **154**

Abbreviations **168**

Acknowledgments **170**

Documentation of authorship **172**

SUMMARY

Cell culture models are helpful tools to study inflammatory diseases, like rheumatoid arthritis (RA), osteoarthritis (OA), arteriosclerosis or asthma, which are linked to increased matrix metalloproteinase (MMP) activity. Such cell culture models often focus on the secretion of cytokines and growth factors or the direct effects of disease on tissue destruction. Even though the crucial role of MMPs in inflammatory diseases is known, the results of MMP studies are contradictious and the use of MMPs as biomarkers is inconsistent. MMPs play an important role in disease pathology, as they are involved in elastin degradation in the walls of alveoli in chronic obstructive pulmonary disease (COPD), tumor angiogenesis and metastasis and in cartilage and bone degradation in arthropathies. In RA and OA MMPs are secreted by osteocytes, synoviocytes, and by infiltrating immune cells in response to the increased concentration of inflammatory mediators, like growth factors and cytokines. MMPs are zinc and calcium-dependent proteinases and play an important role in physiological and pathological extracellular matrix (ECM) turn over. Their substrate specificity gives them the ability to degrade all major ECM components, like aggrecan, elastin, gelatin, fibronectin and all types of collagen even the triple helix of collagen monomers. The ECM consists of two large three-dimensional cross-linked macromolecule classes: one are fibrous proteins, like collagen and elastin fibers that are responsible for ECM's structure, tensile strength, resiliency, reversible extensibility, and deformability and the second class is comprised of proteoglycans composed of glycosaminoglycan (GAG) chains covalently attached to protein cores that are multifunctionally involved in signaling pathways and cell interactions. ECM is present within all tissues and organs and changes in ECM structure contribute to pathogenesis, e.g. wounded and fibrotic tissue, COPD or tumours.

This thesis primarily focuses on the development of a diagnostic peptide system, that enables to gain information on MMP activity from ECM by deploying the isobaric mass encoding strategy. The core element of the developed system is an isotopically labelled peptide sequence (mass tag), that is released in response to elevated levels of MMPs and allows multiplexed detection in tandem mass spectrometry (LC-MS/MS). The mass reporters possess a modular structure with different functionalities. C-terminal either a transglutaminase (TG) recognition sequence or a high molecular weight polyethylene glycol (PEG) moiety was attached to immobilize the mass reporters covalently or

physically at the injection site. The following matrix metalloproteinase substrate sequence (MSS) is incorporated in two different versions with different sensitivity to MMPs. The MSS were applied in pairs for relative quantification consisting of the cleavable version synthesized with natural L-amino acids and the noncleavable D-amino acid variant. The mass tag was synthesized with isotopically labelled amino acids and is separated from the MSS by a UV light-sensitive molecule. N-terminal the mass tag is followed by a tobacco etch virus protease (TEV) sensitive sequence, that is responsible to separate the mass tag from the affinity tag, which was either the Strep-tag II sequence or biotin and were added for purification purposes.

Chapter 1 presents a step-by-step protocol on how to design a mass tag family allowing for multiplexed analysis by LC-MS/MS. The multiplexing is achieved by developing an isobar mass tag family with four family members, which are chromatographically indistinguishable, but due to the mass encoding principles they fragment in distinct y-type ions with a mass difference of 1 or 2 Da each in MS^2. Furthermore, it is explained how to covalently attach the mass reporter peptides onto ECM by the activated calcium-catalyzed blood coagulation transglutaminase factor XIII (FXIIIa). The lysine of mass reporter's TG sequence (D-domain of insulin-like growth factor-I (IGF-I)) and a glutamine in fibronectin are covalently crosslinked by FXIIIa and build an isopeptide bond. Elevated levels of MMP release the mass reporters from ECM by recognizing the inter-positioned MSS.

The designed mass reporters were able to monitor enzyme activity in an *in vitro* setting with cell-derived ECM, which was shown in **Chapter 2.** The modular structured mass reporters were investigated in a proof of concept study. First, the different modules were characterized in terms of their MMP responsiveness and their sensitivity to TEV protease and UV light. Then the FXIIIa-mediated coupling reaction was detailed and the successful coupling on ECM was visualized by an immunosorbent assay or confocal laser scanning microscopy. Finally, the immobilized mass reporters on ECM were incubated with MMP-9 to investigate their multiplexing ability of MMP activity. The cleaved mass reporter fragments were purified in three steps and mass tags were analyzed as mix of all four in LC-MS/MS.

Chapter 3 describes the change from an immobilizing system as seen in chapter 1 and 2 to a soluble enzyme activity monitoring system that was applied in an osteoarthritic mouse model. Instead of the immobilizing TG sequence the C-terminal MMS was extended with

two amino acids where one holds an azide moiety to perform a strain-promoted azide-alkyne cycloaddition to a high molecular weight dibenzocyclooctyne-polyethylene glycol (DBCO-PEG), which was chosen to retain the mass reporters at the injection site. Furthermore, the N-terminal affinity tag was extended with a 2.5 kDa PEG chain to increase the half-life of the mass reporter peptides after MMP release. The systems biocompatibility was proved but its enzyme monitoring ability in an *in vivo* setting could not be analyzed as samples degraded during shipping resulting from the Chinese customs blocking transport to Germany.

In summary the diagnostic peptide system was developed in two variants. The immobilized version one from chapter 1 and 2 was designed to be covalently attached to ECM by the transglutaminase-mediated cross-linking reaction. In an *in vitro* setting the functionality of the mass reporter system for the detection of MMP activity was successfully verified. The second variant comprises of a soluble mass reporter system that was tested in an OA mouse model and showed biocompatibility. With these two designed systems this thesis provides a flexible platform based on multiplexed analysis with mass-encoded peptides to characterize cell culture models regarding their MMP activity, to deploy cell-derived ECM as endogenous depot scaffold and to develop a mass tag family that enables simultaneous detection of at least four mass tags.

ZUSAMMENFASSUNG

Zellkulturmodelle sind hilfreiche Werkzeuge, um entzündliche Krankheiten, wie rheumatoide Arthritis (RA), Osteoarthritis (OA), Arteriosklerose und Asthma, die mit einer erhöhten Aktivität von Matrixmetalloproteinasen (MMPs) verbunden sind, zu untersuchen. Viele Zellkulturmodelle fokussieren sich hauptsächlich auf die Sekretion von Zytokinen und Wachstumsfaktoren oder die direkten Effekte der Entzündung auf die Gewebezerstörung. Obwohl die zentrale Rolle der MMPs in entzündlichen Erkrankungen bekannt ist, wird die Untersuchung von MMPs in diesen Zellkulturmodellen vernachlässigt. MMPs spielen eine wichtige Rolle in der Krankheitsentstehung, da sie am Abbau von Elastin in den Wänden der Alveolen bei chronisch obstruktiver Lungenerkrankung (COPD), an der Gefäßneubildung und Metastasenbildung von Tumoren und an Knorpelabbau und Knochenzerstörung in Gelenkerkrankungen beteiligt sind. In RA und OA werden MMPs von Osteozyten, Synoviozyten und infiltrierenden Immunzellen als Antwort auf erhöhte Konzentrationen an entzündlichen Mediatoren, wie Wachstumsfaktoren und Zytokinen, sekretiert. MMPs sind Zink- und Calcium-abhängige Proteinasen, die eine wichtige Rolle beim physiologischen und pathologischen Turnover der extrazellulären Matrix (EZM) spielen. Ihre Substratspezifität verleiht ihnen die Fähigkeit alle Hauptkomponenten der EZM, wie Aggrecan, Elastin, Gelatin, Fibronectin und alle Typen des Kollagens, sogar die dreifach-Helix der Kollagenmonomere, abzubauen. Die EZM besteht aus zwei großen, drei-dimensional vernetzten Makromolekülklassen: zu der ersten Klasse zählen die faserigen Proteine, wie Kollagen- und Elastinfasern, die für die Struktur der EZM, ihre Zugfestigkeit, Elastizität, reversible Dehnbar- und Verformbarkeit verantwortlich sind und zur zweiten Klasse gehören die Proteoglykane, die aus Glykosaminoglykanketten (GAG), die kovalent an Kernproteine gebunden sind, bestehen und zusammen multifunktional in Signalwege und Zellinteraktionen involviert sind. Jedes Gewebe und Organ ist mit EZM ausgekleidet und Änderungen in der EZM Struktur können zur Krankheitsentstehung beitragen, z.B. bei verletztem und fibrotischem Gewebe, COPD oder Tumoren.

Diese Promotion fokussiert sich primär auf die Entwicklung eines diagnostischen Peptidsystem, das es ermöglicht durch die Anwendung der isobaren massencodierten Strategie Informationen über MMP Aktivität der EZM zu gewinnen. Eine isotopenmarkierte Peptidsequenz stellt dabei das Kernelement des entwickelten Systems dar, welche als Antwort auf erhöhte MMP Level von der EZM freigegeben wird und eine

gebündelte Detektion per Tandem-Massenspektrometrie (LC-MS/MS) erlaubt. Die Massenreporter besitzen einen modularen Aufbau mit unterschiedlichen Funktionalitäten. Am C-terminalen Ende wurde entweder eine Transglutaminase (TG) Erkennungssequenz oder eine hochmolekulare Polyethylenglykol (PEG) Einheit angehängt, um die Massenreporter kovalent oder physikalische am Applikationsort zu immobilisieren. Die darauffolgende eingeschobene Matrixmetalloproteinase Substratsequenz (MSS) wurde in zwei verschiedenen Versionen mit unterschiedlicher MMP Sensitivität angewendet. Die MSSs werden für die relative Quantifizierung jeweils in Paaren verwendet, wobei die spaltbare Variante mit natürlichen L-Aminosäuren synthetisiert wird und die nicht-spaltbare Sequenz mit D-Aminosäuren. Der Mass tag wird mit isotopenmarkierten Aminosäuren versehen und ist von dem MSS durch ein lichtsensitives Molekül getrennt. N-terminal des Mass tags folgt die TEV Protease-sensitive Peptidsequenz, die zur Abspaltung des Affinitäts-tags vom Mass tag eingebaut wurde. Zur Aufreinigung dient ein Affinitätstag, der entweder aus der Strep-tag II Sequenz oder Biotin besteht.

In **Kapitel 1** werden Schritt-für-Schritt Protokolle präsentiert, für die Gestaltung und Entwicklung einer Gruppe von isotopenmarkierten Peptiden, die eine simultane Analyse per LC-MS/MS zulassen. Die gleichzeitige Detektion wird dadurch erreicht, dass jedes Gruppenmitglied in der Summe die gleiche Molekülmasse besitzt, aber aufgrund der angewandten isobaren Isotopenmarkierungen fragmentieren diese in MS^2 in spezifische y-Typ Ionen, die einen Massenunterschied von 1 oder 2 Da besitzen. Zudem wurde erklärt, wie die Massenreporter Peptide durch den aktivierten, Calcium-abhängigen Blutkoagulationsfaktor XIII (FXIIIa) kovalent an die EZM gebunden werden. Bei der enzymatischen Reaktion wird durch das Quervernetzen des Lysins der TG Aminosäuresequenz (der D-Domäne von IGF-I) der Massenreporter mit dem Glutamin der Aminosäureerkennungssequenz in Fibronectin eine Isopeptidbindung gebildet. Die Freisetzung der Massenreporter von der EZM erfolgt aufgrund des erhöhten MMP Level und geschieht durch die Spaltung der dazwischenliegenden MSS.

Die entwickelten Massenreporter waren in der Lage die Enzymaktivität in einer aus Fibroblasten stammenden *in vitro* Umgebung aus EZM zu beobachten, was in **Kapitel 2** dargestellt wird. Die modulare Struktur der Massenreporter wurde in einer Machbarkeitsstudie untersucht. Zuerst wurden die verschiedenen Module bezüglich ihrer Ansprechempfindlichkeit auf MMP und ihrer Sensitivität gegenüber der TEV Protease und UV-Licht charakterisiert. Dann wurden die vier Peptide FXIIIa-vermittelt an die EZM

gekoppelt und die erfolgreiche Kopplung an EZM wurde mit Hilfe eines immunologischen Verfahrens oder konfokaler Laser-Scanning-Mikroskopie visualisiert. Abschließend wurden die auf der EZM immobilisierten Massenreporter mit MMP-9 inkubiert, um deren Fähigkeit der gleichzeitigen Detektion von MMP Aktivität zu untersuchen. Die abgespalteten Massenreporterfragmente wurden in drei Schritten aufgereinigt und die vier isotopenmarkierten Tags wurden als Mix mittels LC-MS/MS analysiert.

Kapitel 3 beschreibt die Änderung der aus Kapitel 1 und 2 bekannten immobilisierten System zu einem löslichen System, das die Enzymaktivität in Körperflüssigkeiten bestimmen soll und in einem Mausmodell für Osteoarthritis getestet wurde. Anstelle der immobilisierenden TG Sequenz wurde der C-Terminus der MSS um zwei Aminosäuren erweitert. Eine Aminosäure trägt eine Azidgruppe um eine Azid-Alkin Cycloaddition mit einem hochmolekularen PEG durchzuführen, die ausgewählt wurde, um die Massenreporter an der Injektionsstelle zurückzuhalten. Des Weiteren wurde der Affinitäts-tag mit einer 2.5 kDa PEG-Kette erweitert, um die Halbwertszeit des von MMPs freigesetzten Massenreporterpeptides zu erhöhen. Die Biokompatibilität des Systems wurde erwiesen, allerdings war es nicht möglich die MMP Aktivität in einem *in vivo* Model zu zeigen, da eine Analyse der Proben aufgrund von Versand- und Zollproblemen und damit verbundenen Instabilitäten nicht möglich war.

Zusammenfassend wurde ein diagnostische Peptidsystem bestehend aus zwei Varianten entwickelt. Die zu immobilisierende Version aus Kapitel 1 und 2 wurde so konzipiert, dass die Peptide durch die Transglutaminase vermittelte Quervernetzungsreaktion kovalent an EZM gebunden werden. In einem *in vitro* Model wurde die Funktionalität des Massenreporter Systems hinsichtlich der Detektion von MMP Aktivität erfolgreich bestätigt. Die zweite Variante, bestehend aus einem löslichen Massenreporter System, wurde in einem Osteoarthritis Mausmodel getestet und zeigte Biokompatibilität. Mit diesen zwei entworfenen Systemen stellt diese Dissertation eine flexible Plattform zur Verfügung, die basierend auf der multiplexen Detektion von isotopenmarkierten Peptiden, für die Charakterisierung von Zellkulturmodellen bezüglich deren MMP Aktivität genutzt wird, die zelluläre EZM als endogenes Depot anwendet und die durch die Entwicklung einer Familie aus isotopenmarkierten Tags eine simultane Detektion von mindestens vier Tags erlaubt.

CHAPTER 1: A COMPLETE AND VERSATILE PROTOCOL: DECORATION OF CELL-DERIVED MATRICES WITH MASS-ENCODED PEPTIDES FOR MULTIPLEXED ENZYME ACTIVITY DETECTION

*Katharina Dodt[1], Stephanie Lamer[2], Andreas Schlosser [2], Tessa Lühmann[1], Lorenz Meinel[1]**

[1] Institute of Pharmacy and Food Chemistry, University of Wuerzburg, Am Hubland, 97074, Wuerzburg, Germany

[2] Rudolf-Virchow-Center for Experimental Biomedicine, University of Wuerzburg, 97080 Wuerzburg, Germany

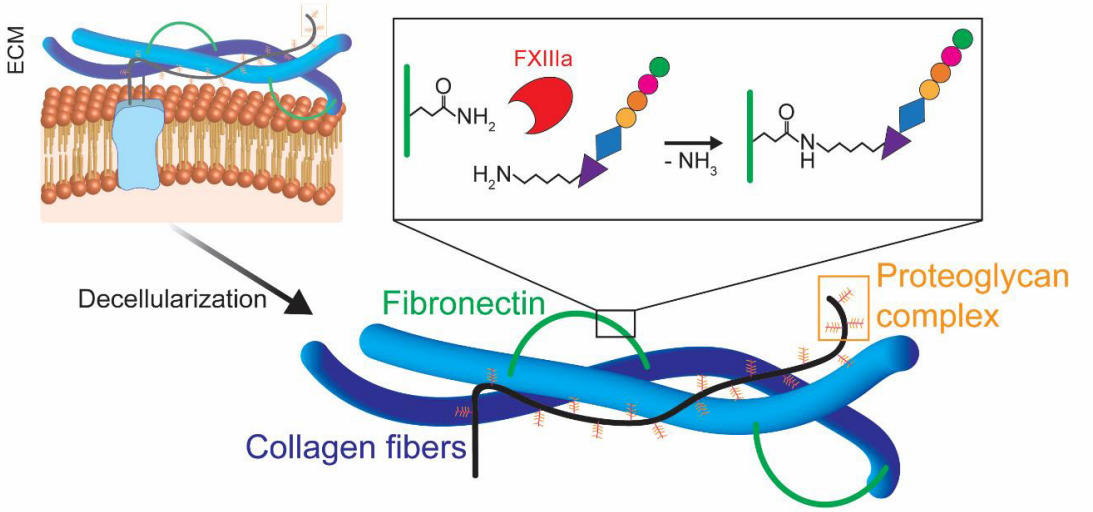

Chapter 1: A complete and versatile Protocol: Decoration of cell-derived matrices with mass-encoded peptides for multiplexed enzyme activity detection

Abstract

This article provides guidance toward a platform technology for monitoring enzyme activity within the extracellular matrix (ECM) assessed by quantifying reporters secreted into the cell culture supernatant and analyzed by tandem mass spectrometry. The reporters are enzymatically and covalently bound to the ECM by transglutaminases (TG) using the peptide sequence of human insulin-like growth factor I's (IGF-I) D-domain which is known to be bound to the ECM by transglutaminase. The IGF-I D-domain sequence is followed by a peptide sequence cleaved by the intended target protease. This protease-sensitive peptide sequence (PSS) is cleaved off the ECM and can be used to monitor target-enzyme activity by employing a down-stream mass tag designed according to isobaric mass encoding strategies, i.e. the combination isotopically labeled, heavy amino acids. Thereby, cleavage events are linked to the appearance of encoded mass tags, readily allowing multiplexing. This article presents the design and synthesis of these mass reporters. It further aims at detailing the search for peptide sequences responding to target proteases to facilitate future work on enzyme activity measurement for enzymatic activities of hitherto unknown enzymes. In conclusion, the goal of this article is to arm scientists interested in measurements of local enzymatic activities within the ECM with robust protocols and background knowledge.

Keywords: diagnostics; isotopically labelled peptide; tandem mass spectrometry; proteinase; extracellular matrix; transglutaminase

1. Introduction

Detailed insight into inflammatory processes is key for understanding many (patho-) physiological processes including response to infection/immunity or regeneration. For example, persisting inflammation may turn into a chronic inflammation with tissue damage such as in asthma,[1] arthritis,[2, 3] inflammatory bowel disease,[4] or arteriosclerosis.[5] Osteoarthritis (OA) and rheumatoid arthritis (RA) are inflammatory conditions affecting joints, with matrix metalloproteinase (MMP) expression being upregulated in chondrocytes[6, 7] and disease-elevated MMP levels in cartilage[8] and synovial fluid.[9] However, healthy states also have balanced proteolytic activity, e.g. the interplay of extracellular active enzymes such as MMPs and tissue inhibitors of metalloproteinases (TIMPs) as part of the physiological remodeling process of the ECM.[10, 11] MMP activity is critically regulated on the transcriptome level and post-translationally including activation of pro-enzymes (pro-MMPs) or by other biological means including control of MMP secretion rates, inhibition of enzyme activation, and inhibition of activated enzymes.[12] These events are intrinsically related to the ECM, as it is this extracellular, three-dimensional, and highly organized network being enzymatically remodeled. Thereby, the maintenance, growth and differentiation of cells growing on ECM may change in response to protease-mediated ECM remodeling. The ECM has been traditionally seen as providing structural support to cells by means of a mixture of macromolecules, including collagens, elastins, and proteoglycans such as laminin, or fibronectin, decorin, or thrombospondin.[13] However, ECM function goes beyond structural support e.g. by virtue of ECM-receptors, moieties controlling the binding, stability, and activity of cytokines and growth factors and by the presentation of catalytic enzymes. All of these are potentially being modulated by proteolytic ECM remodeling in health and disease.[14-16] According to MMP's substrate specificity, they have the ability to degrade all major ECM components,[11] with collagen being a main degradation substrate.[17]

As mentioned, aberrant enzyme activity is often found in disease states including cancer,[18] muscular injury,[19] arthritis, asthma,[20] or arteriosclerosis.[21] It is for the insights into these and other inflammatory conditions that diagnostic peptide systems have been previously suggested for profiling disease progression.[22] For example, enzyme activity was previously determined by an intravenously injected fluorescently labeled peptide conjugate - the peptide being sensitive for a disease-associated protease - coupled to nanoparticles or gold-nanoparticles. The fluorescent label was released at the site of disease following proteolysis

and *in vivo* imaging and urine analysis.[23-25] Another system was developed consisting of a near-infrared fluorescence probe (NIRF) with a cathepsin B-sensitive probe comprised of a copolymer of poly-L-lysine sterically protected by methoxypolyethylene glycols and modified with the fluorochrome Cy5.5 for early detection of OA.[26, 27] These diagnostic systems are encouraging but arguably share one aspect in that they only report one time point, for example the moment in which the sensor reaches the joint. The challenges resulting from multiplexing with photoactive moieties such as absorption overlap, substrate cross-reactivity or loss of sensitivity[28] are overcome by replacing these with quantum dots[28] or mass-encoded peptides.[22] These systems typically require a targeting strategy if administered intravenously and a need for sufficient accumulation in target tissues. Thus, their effectiveness is critically determined by their targeting ability. When targeting is not accurate, it is not limited to one site, but various, maybe unintended sites are reached at the same time. This leads to the risk of obtaining biased information as signals reflect events from multiple sites at the same time. Finally, these systems only report in active disease, if the respective target proteases are already upregulated, as is observed in liver fibrosis or cancer.[18] They propably also have limited ability of reporting for example a beginning flare – as typically one would not use these in asymptomatic windows. These considerations prompted us to provide protocols leading to alternative reporters of inflammation. The reporters are localized within the ECM by means of their transglutaminase peptide sequence enabling local sensor-immobilization at the ECM - more specifically including localization at fibronectin - by means of co-administered transglutaminase. Transglutaminase activity is Ca^{2+} dependent and catalyzes an acyl-transfer from γ-carboxamide of glutamine donors on the ECM to ε-amines acceptors, like the lysine within the IGF-I D-chain of the mass reporters forming an iso-peptide bond.[29] Similar reactions have previously been used to enzymatically (hence site-specifically) modify peptides and proteins with PEG [30-37], to incorporate peptides in fibrin gels,[38-41] or for surface decoration.[42] This manuscript details the use of two transglutaminases for covalently immobilizing the sensors at the site of intended diagnosis:

a) human tissue transglutaminase (TG2) is responsible for ECM macromolecule crosslinking, transmembrane signaling, and mediating cell surface adhesion,[43, 44]
b) and activated A-subunits of plasma coagulation factor XIII (FXIIIa)), which play an important role in the cross-linking of fibrin clots in blood coagulation and in wound healing, were used.

One application is covalently depositing the sensors on ECM (either cell culture ECM, tissue engineered ECM, or (remaining to be shown) future use *in vivo*. Because of the covalent bond at the site of application, reporting occurs from these local sensor-depots, avoiding off-site information. As mentioned before, the systems outlined here indirectly report cleavage of the proteolytic activity through isobaric mass encoding strategies. This strategy was selected to maximize both sensitivity (through liquid chromatography – tandem mass spectrometry (LC-MS/MS)) and to allow virtually unlimited multiplexing ability (through the large flexibility of isobaric coding strategies). However, the cleaved reporters need to be primed for tandem mass spectrometric quantification by a series of purification and specific cleavage steps, following previously presented strategies. In one study they developed ironoxide nanoworms modified with disease-associated protease sensitive linkers and a mass-encoded peptide. These were shown to accumulate in fibrotic liver or tumor tissue following passive targeting. The protease-sensitive peptide sequence is cleaved and the mass-encoded peptide was released and secreted with urine. From there, it is processed and analyzed by LC-MS/MS.[22] By using the reporters in pairs (one protease sensitive sequence being synthesized with L-amino acid (AA) and the internal control being synthesized with D-amino acid (aa), resulting in an identical molecular weight), relative quantification by LC-MS/MS became possible for the following reason: Once the balanced mass tags (having been recorded in MS^1 with one identical mass) are fragmented for MS^2 by collision with a collision gas, each disintegrates into distinct and encoded fragments. Next, the relative comparison of these fragment signals, resulting from the L- and D-reporters, is used for the readout of proteolytic activity. As mentioned, the purification of the balanced mass tags involves multiple steps. Upon harvest of the matrix surrounding medium (cell culture supernatant, biological fluids), the remaining AA from the PSS of the diagnosed cleavage event were separated from the rest of the reporter fragment (including the balanced mass tag) by UV light. For that, a photo-cleavable molecule (3-amino-3-(2-nitrophenyl)propionic acid) is inter-positioned between the mass tag and the PSS. To isolate the reporter fragments from the matrix the reporters N-terminally carry biotin-aminohexanoic acid, which was used for affinity purification. Lastly, a tobacco etch virus (TEV) protease sequence allows the separation of the balanced mass tag and the biotin label and leaves the mass tag sequence ready for liquid chromatography tandem mass spectrometry (**Figure 1**).

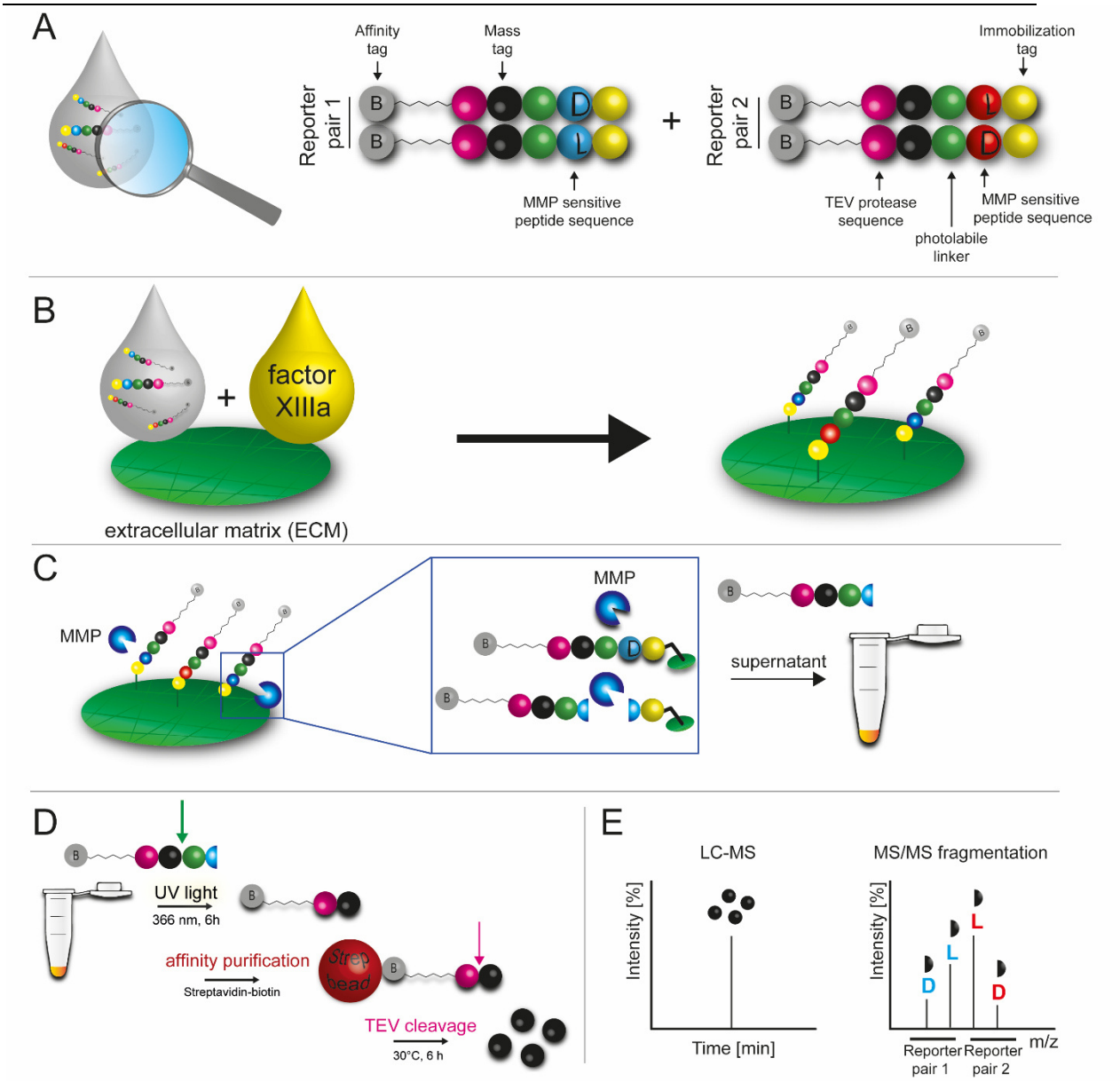

Figure 1 (A) The reporter peptides consist of six modules: an affinity tag (grey), TEV protease sequence (pink), the mass-encoded peptide (black), a photolabile linker (green), a MMP sensitive peptide sequence (blue or red) and an immobilization tag (yellow). The four reporter peptides were used in a mix of all four. (B) The two reporter pairs were bound to the extracellular matrix by FXIIIa. Each reporter pair is identical, with the exception of the MMP substrate sequence which is synthesized either with D- or L- amino acids, respectively. (C) Inflammatory MMPs cleave the MMP sensitive peptide sequence synthesized of L-amino acid but not the D-amino acid version of each reporter pair. Thereby the D-amino acid variant reports on background events such as nonspecific ECM adsorption or nonspecific turnover of the ECM (internal control), whereas the L-amino acid variants report on background events and specific MMP activity. (D) The supernatant containing the cleaved reporter fragments were purified in three consecutive steps. First by UV irradiation, second by streptavidin-biotin affinity purification and third by cleavage with TEV protease to release the mass tags. (E) All mass tags have the same parent mass (LC-MS) and fragment into specific ions, which were detected by the second quadrupole (MS^2). This figure was adapted from "Mass-encoded reporters reporting inflammation from within the extracellular matrix" and reproduced with permission from [45]Copyright ACS Publications.

2. Materials

2.1. Reagents and Supplies

- (+)-Sodium L-ascorbate (Sigma Aldrich A4034)
- (3-Aminopropyl)triethoxysilane 99 % (APTES) (Sigma Aldrich 440140)
- One-Step™ Turbo TMB-ELISA Substrate Solution (34022, Thermo Fisher)
- 6-Biotinylamino-hexanoic acid (Bio-Ahx-OH) (Iris Biotech RL-2025)
- Eight-well NuncTM Lab-TekTm II Chamber SlideTM System (VWR 734-2061)
- Acetic anhydride (Sigma Aldrich 33214)
- Acetonitrile (VWR 83639.320)
- AcTEV Protease (Invitrogen 12575-015)
- Amino acids (natural, non-natural and isotopically labelled):
    - Fmoc-L-Ala-OH A Sigma Aldrich
    - Fmoc-L-Ala (^{13}C)-OH ^{+1}A Cambridge Isotope Laboratories
    - Fmoc-L-Ala ($^{13}C_3$)-OH ^{+3}A Cambridge Isotope Laboratories
    - Fmoc-L-Ala ($^{13}C_3$, ^{15}N)-OH ^{+4}A Cambridge Isotope Laboratories
    - Fmoc-D-Ala-OH a Iris Biotech
    - Fmoc-D-Arg(Pbf)-OH r Iris Biotech
    - Fmoc-L-Asn(Trt)-OH N Iris Biotech
    - Fmoc-L-Gln(Trt)-OH Q Sigma Aldrich
    - Fmoc-D-Gln(Trt)-OH q Iris Biotech
    - Fmoc-L-Glu(otBu)-OH E Sigma Aldrich
    - Fmoc-Gly-OH G Sigma Aldrich
    - Fmoc-Gly (^{15}N)-OH ^{+1}G Cambridge Isotope Laboratories
    - Fmoc-Gly ($^{13}C_2$)-OH ^{+2}G Cambridge Isotope Laboratories
    - Fmoc-Gly ($^{13}C_2$, 15N)-OH ^{+3}G Cambridge Isotope Laboratories
    - Fmoc-L-His(Trt)-OH H Sigma Aldrich
    - Fmoc-D-His(Trt)-OH h Iris Biotech

o Fmoc-L-Ile-OH	I	Sigma Aldrich
o Fmoc-D-Ile-OH	I	Iris Biotech
o Fmoc-L-Leu-OH	L	Sigma Aldrich
o Fmoc-D-Leu-OH	l	Iris Biotech
o Fmoc-L-Lys(Trt)-OH	K	Sigma Aldrich
o Fmoc-L-Phe-OH	F	Sigma Aldrich
o Fmoc-L-Phe (^{15}N)-OH	$^{+1}$F	Cambridge Isotope Laboratories
o Fmoc-L-Phe (Ring$^{13}C_6$)-OH	$^{+6}$F	AnaSpec
o Fmoc-L-Pro-OH	P	Sigma Aldrich
o Fmoc-D-Pro-OH	p	Iris Biotech
o Fmoc-L-Ser(tBu)-OH	S	Sigma Aldrich
o Fmoc-L-Ser(tBu) (^{15}N)-OH	$^{+1}$S	Cambridge Isotope Laboratories
o Fmoc-D-Ser(tBu)-OH	s	Iris Biotech
o Fmoc-L-Tyr(tBu)-OH	Y	Sigma Aldrich

- Anti-fibronectin (rabbit) (Sigma Aldrich F3648)
- Bovine calf serum (Sigma Aldrich 12133C)
- Dichloromethane (Fisher Chemical D/1852/17)
- Diethyl ether (Jäklechemie 451675)
- Dulbecco's Modified Eagle's Medium - high glucose (Sigma Aldrich D5796)
- Ethylenediaminetetraacetic acid (Sigma Aldrich E9884)
- Fibrogammin (kindly provided by CSL Behring)
- Filtropur S 0.2 (Sarstedt 83.1826.001)
- Fmoc-(S)-3-amino-3-(2-nitrophenyl)propionic acid (ChemImpex 15606)
- Fmoc-Rink amide AM resin (Iris Biotech BR-1340)
- Gelatin from bovine skin (Sigma Aldrich G9391)
- Glutaraldehyde solution 50 wt. % in H_2O (Sigma Aldrich 340855)
- Goat anti-Rabbit IgG (H+L), Alexa Fluor 488 conjugate (Merck Millipore AP132JA4)
- Greiner CELLSTAR® 96 well plates with 0.34 cm^2 growth surface per well (Sigma Aldrich M3687)

- Greiner culture flasks, tissue culture treated surface area 75 cm^2 (Sigma Aldrich C7231)
- H_2SO_4 (95-97 % V/V) (Sigma Aldrich 30743-M)
- Human MMP-1 ELISA (Thermo Fisher Scientific EHMMP1)
- Human MMP-8 ELISA (Thermo Fisher Scientific EHMMP8)
- Human MMP-9 Quantikine ELISA (R&D Systems DMP900)
- Hydrochloric acid 37 % (Bernd Kraft 05430.4200)
- Isopropyl alcohol (Sigma Aldrich I9516)
- KH_2PO4 (Grüssing GmbH 12018)
- Luer Stopper (MultiSynTech V000LS100)
- MMP-9, Monomer, Human Neutrophil (Sigma Aldrich 444231-5µg)
- *N,N′*-Diisopropylcarbodiimide (DIC) (Sigma Aldrich 38370-100mL)
- *N,N*-Diisopropylethylamin (DIPEA) (Carl Roth 2474.1)
- *N,N*-Dimethylformamide (Fisher Chemical D/3841/17)
- Na_2HPO4 (Grüssing GmbH 12147)
- NORM-JECT 10 mL syringe (B. Braun Melsungen AG NJ-4606108)
- NORM-JECT 20 mL syringe (B. Braun Melsungen AG NJ-4606205)
- Oxyma (Novabiochem 8.51086.0100)
- Penicillin-streptomycin (Sigma Aldrich P4333)
- Pierce™ BCA protein assay kit (Thermo Fisher Scientific 23225)
- Piperidine, 99 % (Alfa Aesar A12442)
- PP-Reactor 10 mL with PE frit (MultiSynTech V100PE086)
- Sera-Mag-streptavidin-coated beads, medium (GE Healthcare 30152103010150)
- Sodium L-ascorbate (Sigma Aldrich A7631)
- Streptavidin-Cy5 (Sigma Aldrich, GEPA45001)
- Streptavidin-HRP conjugate (Sigma Aldrich RPN1231)
- Trifluoroacetic acid (TFA) (Sigma Aldrich 302031)
- Triisopropylsilane (TIS) (Sigma Aldrich **233781)**
- Triton X-100 (Sigma Aldrich T9284)
- Trizma base (TRIS base) (Sigma Aldrich T6066)
- Trypsin-EDTA solution (Sigma Aldrich T3924)
- TWEEN 20 (Sigma Aldrich P2287)

- Ultrapure water (prepared by MilliQ Reference A+ water purification system equipped with Q-pod remote dispenser, Merck Millipore)

The provided supplier serves as orientation and may be replaced by another source.

2.1.1. Buffers and Solutions

- Fibrogammin was activated by addition of 20 U/mL thrombin in TBS with 2.5 mM $CaCl_2$ to activated FXIIIa, which was aliquoted (182 U/mL)
- Phosphate buffered saline (PBS) (137 mM NaCl, 2.68 mM KCl, 4.29 mM Na_2HPO_4, 1.47 mM KH_2PO4 in ddH_2O, pH 7.4)
- Triton-X-ammonia buffer (0.5 % Triton™ X-100, 20 mM NH_4OH in PBS pH 7.4)
- Tris buffered saline + TWEEN 20 (TBST) (100 mM Tris, 150 mM NaCl in ddH_2O, 0.1 % TWEEN 20, pH 7.4)
- Tris buffered saline (TBS) (100 mM Tris, 150 mM NaCl in ddH_2O, pH 7.4)
- TG buffer (50mM Tris-HCl, 150 mM NaCl, 2,5 mM $CaCl_2$)
- MMP buffer (50 mM Tris, 150 mM NaCl, 1 µM $ZnCl_2$, 10 mM $CaCl_2$, pH 7.4)
- TEV buffer (50mM Tris-HCl, 1 mM DTT; 0.5 mM EDTA, pH 8.0)
- Acetate buffer (50 mM sodium acetate, 1 M NaCl, pH 5.3)
- DMEM containing heat-inactivated BCS (10 %), penicillin G (100 U/mL) and streptomycin (100 µg/µL)
- DMEM containing heat-inactivated BCS (10 %), penicillin G (100 U/mL) and streptomycin (100 µg/µL) + 56.24 µg/mL sodium L-ascorbate

2.1.2. Equipment

- Agilent Infinity II 1260 HPLC system equipped with a flexible pump (G7104C) vial sampler (G7129C), MCT (G7116A) and VWD (G7114A)
- Fast protein liquid chromatography (FPLC) (Äkta Pure, Äkta Explorer, GE Healthcare, Pittsburgh, USA)
- Freeze dryer Alpha 1-4 (Martin Christ Gefriertrocknungsanlagen GmbH, Osterode, Germany)

- High-resolution AOBS SP2 confocal laser scanning microscope (Leica microsystem, Wetzlar, Germany) with a 63x N.A. 1.4-0.60 Oil I BL HCX PL APO I objective
- LaChromUltra UPLC system equipped with a L-2160U Pump, L-2200U autosampler, L- 2300 column oven, L-2400U UV detector (Hitachi, VWR)
- Shimadzu LC-MS 2020 equipped with a DGU-20A3R degassing unit, a LC20AB liquid chromatograph, and a SPD-20A UV/Vis detector (Shimadzu Scientific Instruments, Columbia, MD, USA)
- Liberty Blue peptide synthesizer (CEM, Matthews, USA)
- Luminescence spectrometer LS50B (Perkin Elmer, Waltham, USA)
- Orbitrap Fusion Tribrid mass spectrometer (Thermo Fisher) equipped with a PicoView Ion Source (New Objective) and coupled to an EASY-nLC 1000 (Thermo Scientific)
- Orital Shaker KS 130 basic (IKA, Staufen, Germany)
- SpectraMax 250 absorbance microplate reader, spectrophotometer (Molecular Devices, San Jose, USA)
- TurboVap LV evaporator (formerly Zymark now Biotage, Uppsala, Sweden)
- Universal UV Lamp (CAMAG, Berlin, Germany)
- Vacuum concentrator plus (Eppendorf, Wesseling-Berzdorf, Germany)
- VirTis AdVantage Plus freeze-dryer (SP Scientific, Warminster, USA)
- General: magnetic stir plate, hemocytometer, chromatography columns (Agilent, Phenomenex), research pipettes (Eppendorf Research plus pipette 0.1-2.5 µL, 1-10 µL, 10-100µL, 100-1000µL), centrifuge (Eppendorf centrifuge 5840 R, Eppendorf Minispin), freezer (−20 °C and −80 °C), thermoblock (Eppendorf thermomixer comfort, AccuBlock Mini Labnet), shaker (VWR Minishaker), roller mixer (Stuart roller mixer SRT1), Vortex Genie 2 (Bender&Hobein AG), incubator (Thermo Fisher Scientific HeraCell 150i), Class II biological safety cabinet (Thermo Fisher Scientific Safe 2020)

3. Procedures

These protocols provide an overview of how to synthesize mass reporters with a mass-encoded peptide as core module to perform multiplexed detection by tandem mass spectrometry. After synthesis of isotopically labelled peptides, prestudies were performed to characterize the peptides regarding their sensitivity to proteases (here MMPs and TEV protease) and UV light. Furthermore, the multiplexing ability of mass tags was demonstrated. These fully characterized mass reporters can then be used to decorate cell-derived ECM, which is prepared by NIH 3T3 fibroblasts, and protocols for this purpose are provided as well. The release of mass reporters from ECM by MMPs is explained, and mass tag analysis by tandem mass spectrometry demonstrated. The quantitative and qualitative detection of mass reporters on ECM and their cleavage by proteases (here MMP) can optionally be visualized by an immune assay or confocal laser scanning microscopy (CLSM) (**Figure 2**).

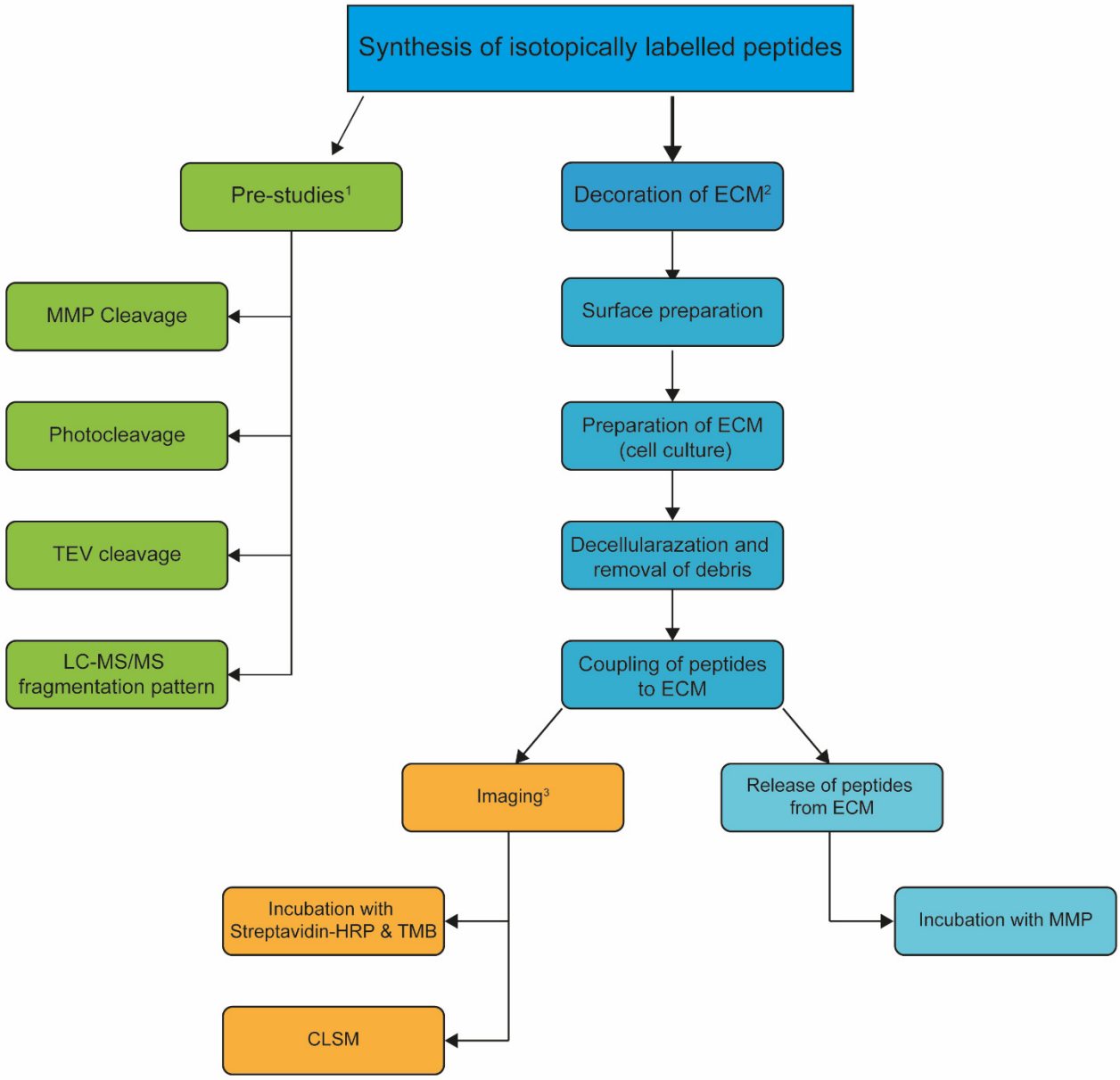

Figure 2 Left arm of the flowchart shows the prestudies that were performed to characterize the individual modules of the mass-encoded peptides. After characterization the isotopically labelled mass reporters were used for decoration of ECM. This workflow starts with preparing surfaces for cell seeding and ECM production. After cells were lysed and washed out, the mass reporters were coupled to ECM by coadministration of FXIIIa. The release of mass reporters in response to an inflammatory stimulus (MMP-9) was performed and analyzed by LC-MS/MS. Optionally, the detection of mass reporters on ECM and their cleavage by MMPs can be visualized by an ELISA or CLSM.

3.1. Development of diagnostic peptides

In this section, the design, synthesis and characterization of isotopically labelled peptide constructs, especially the isotopically enriched mass tag sequence, are described. The mass reporters consist of six functional modules. Module #1 at the N-terminus is biotin-aminohexanoic acid that is used for affinity purification and peptide detection and relative quantification on ECM. The TEV protease substrate sequence, module #2, is incorporated to separate the balanced mass tag from the affinity tag in the course of purification by TEV protease. Module #3 is the isotopically labelled mass tag, which is comprised of the same amino acid sequence in all four mass reporters but with different isotopic labels to create distinct fragment ions in liquid chromatography - tandem mass spectrometry. The photosensitive molecule #4, ((S)-3-amino-3-(2-nitrophenyl)propionic acid, ANP), presents a second cleavage site C-terminal to the balanced mass tag to cleave off the remaining amino acid residues from the adjacent PSS in the purification process. The PSS module #5 consists of two different PSS, both respond to matrix metalloproteinases, but with different kinetics, and they serve to release the balanced mass tag from the ECM in response to elevated MMP levels. The C-terminal module #6 is the TG sequence that was used to immobilize the peptide on ECM by Ca^{2+}-catalyzed transglutaminase reaction (**Figure 3**).

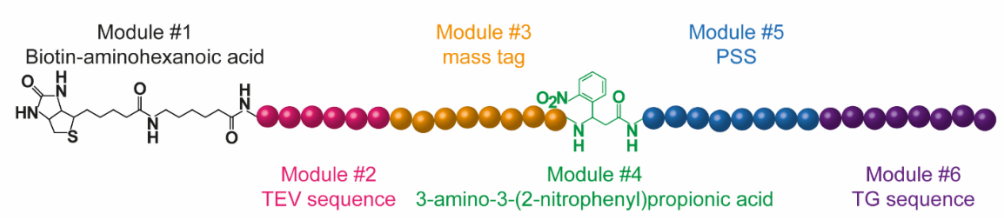

Module	Name	Sequence
Module #2	TEV	ENLYFQ
Module #3	Mass tag	SAEGPGFr
Module #5	L-PSS1	GPQGIAGQ
	D-PSS1	GpqGiaGq
	L-PSS2	GPSGLLAH
	D-PSS2	GpsGllah
Module #6	TG	PLKPAKSA

Figure 3 Overview of six modules of mass reporters and amino acid sequences of modules in one-letter code. Amino acids written in capital letter depict L-amino acids, and small letters depict D-amino acids.

The mass reporter family with four members varies in two modules- number 5 and 3. For module #5 two different PSSs were chosen and used in the MMP-sensitive L-amino acid version and in the noncleavable D-amino acid version serving as negative, internal control and resulting in two PSS pairs. The mass tag module #3 consists of the same amino acid sequence for each mass reporter but with different isotopic labels within the mass tag. Detecting the balanced mass tags simultaneously in LC-MS/MS allowed backtracking to the assigned PSS. The strategy was to apply all four mass reporters in a mixture at the same time as all four reporters bind equally well to ECM in the presence of FXIIIa as previous studies showed.[45]

3.1.1. Design of mass tags

The balanced mass tag functions as diagnostic tool to monitor the activity of specific proteases. The aim is to synthesize a library of isotopically labelled peptide sequences (balanced mass tags), sharing a common parent mass, which can fragment mainly in y_4- or y_5-ions in tandem mass spectrometry, to receive one or two major peptide fragments that can be enriched with heavy amino acids. Y-type fragment ions occur after breakage of the peptide bond between two amino acids. The peptide fragment containing the N-terminus is calleda b-type fragment ion, whereas fragments containing the C-terminus are called y-ions. The numbers indicate the number of amino acid residues in the fragment ion, e.g. y_4-fragment ions contain 4 AA counting from the C-terminus (here PGFr), y_5-fragment ions contain 5 AA (here GPGFr), and so on. Amino acids, which are known to enhance selective cleavages for a specific type of fragment ion, were selected. In previous studies, it was found that proline-containing peptides show a very distinct fragmentation pattern. Mainly y-type fragment ions are produced in collision induced dissociation (CID) by cleavage of the amide bond N-terminal to the proline residue.[46] Moreover, it was reported that the cleavage C-terminal to the acidic residues dominate the fragmentation pattern when an N-terminal arginine is present, and aspartic acid is at least in a distance of one amino acid, or glutamic acid has at least a distance of three amino acids to arginine.[47] In accordance with these findings, three mass tag sequences were designed, and their fragmentation pattern predicted (**Figure 4A**). The mass tag sequences were shown in single-letter code, and the colored amino acids displayed those AA that are mainly responsible for bond breakage in MS^2 and building fragment ions. Regarding the retention time and the fragmentation pattern

mass tag sequence number 1 (S1) was chosen for further experiments. Since the S1 sequence faced some problems due to aspartimide-formation during peptide synthesis, it was decided to exchange aspartic acid for glutamic acid, which is not prone to the occurring problem and possess the same fragmentation characteristics as aspartic acid but with decreased prevalence.[48] Furthermore, the C-terminal arginine (R) was used in its D-version, which is why it is displayed with a small character (r), because the L-amino acid caused coupling problems with the neighboring ANP molecule due to sterically hindrance. In previous studies, the mass-encoded peptide sequence contained primarily D-amino acids to prevent proteolysis by endogenous human enzymes.[22] So far, this isotopically labelled peptide library is intended to be used in *in vitro* settings, and thus proteolytic degradation can be neglected. In case of an *in vivo* application or the use of body fluids, proteolytic degradation by C- and N-terminal exopeptidase activity should be less critical as both ends are protected, N-terminally by biotinaminohexanoic acid, which is not a substrate of exopeptidases. C-terminally the four remaining amino acids from the cleaved PSS may be cleaved off but exoproteases will stop at the photolabile (S)- 3-amino-3-(2-nitrophenyl)propionic acid) linker, and hence the intermediate mass tag remains protected from these activities. Furthermore, evaluation of target protease activity is performed by using the mass reporters in pairs (with the cleavable L-PSS and the noncleavable D-PSS) and building the ratio of L and D mass tags, arguing that as long as these are used in pairs the reporter and its internal control (= D-variant) undergo comparable degradation: hence, the relative ratios supposedly remain constant after ECM release. According to MS^2 spectra, it was shown that y_4-, y_5- and y_6- fragment ions dominate the cleavage pattern (**Table 1**). The principles of isobaric mass encoding[49, 50] were applied to create a family of mass reporters.[22] Here, four mass tags centered on the y_4-, y_5- and y_6-ions by enriching the trimer of Pro-Gly-Phe (PGF) with heavy amino acids to produce variants of approximately 1 or 2 Da each were constructed (**Figure 4B**). The differences between the reporters are not exactly 1 or 2 Da, because the isotopically labelled amino acids contain ^{13}C and ^{15}N isotopes, which have a mass difference to their lighter version of 1.00335 Da and 0.997035 Da for carbon and nitrogen, respectively. The use of amino acids with mixed isotope labels was chosen to gain a higher number of possible variations. The introduced mass shift was balanced by isotope enrichment within the remaining residues (SAEG, SAE) to produce peptides with an identical parent mass but distinct y_4-, y_5-, or y_6- fragment ions. The mass tag octamers were analyzed as a mix of all four mass tags and are

indistinguishable in LC-MS but show distinct fragment ions in tandem mass spectrometry (MS^2) (**Figure 4B**).

Table 1 Mass tag sequence SAEGPGFr with its parent mass of 825.42 Da fragments in MS^2 in y_4-, y_5-, and y_6-reporter ions with their distinct ion mass[a].

A

Balance		Reporter	Balance	y4-Reporter	$[M+H]^+$	$[M+2H]^{2+}$
S $^{+4}$A E G	–	P $^{+2}$G F r	366.32	477.55	825.42	413.21
S $^{+3}$A E G	–	P $^{+3}$G F r	365.32	478.55	825.42	413.21
$^{+1}$S $^{+1}$A E G	–	P $^{+3}$G $^{+1}$F r	364.32	479.55	825.42	413.21
S A E G	–	P G $^{+6}$F r	362.32	481.55	825.42	413.21

B

Balance		Reporter	Balance	y5-Reporter	$[M+H]^+$	$[M+2H]^{2+}$
S $^{+4}$A E	–	G P $^{+2}$G F r	308.27	534.6	825.42	413.21
S $^{+3}$A E	–	G P $^{+3}$G F r	307.27	535.6	825.42	413.21
$^{+1}$S $^{+1}$A E	–	G P $^{+3}$G $^{+1}$F r	306.27	536.6	825.42	413.21
S A E	–	G P G $^{+6}$F r	304.27	538.6	825.42	413.21

C

Balance		Reporter	Balance	y6-Reporter	$[M+H]^+$	$[M+2H]^{2+}$
S $^{+4}$A	–	E G P $^{+2}$G F r	162.12	663.3	825.42	413.21
S $^{+3}$A	–	E G P $^{+3}$G F r	161.12	664.3	825.42	413.21
$^{+1}$S $^{+1}$A	–	E G P $^{+3}$G $^{+1}$F r	160.12	665.3	825.42	413.21
S A	–	E G P G $^{+6}$F r	158.12	667.3	825.42	413.21

[a]The balancing ion was isotopically labelled to balance the mass shift introduced by labelling the reporter ions to maintain an identical parent mass for all four mass reporters.

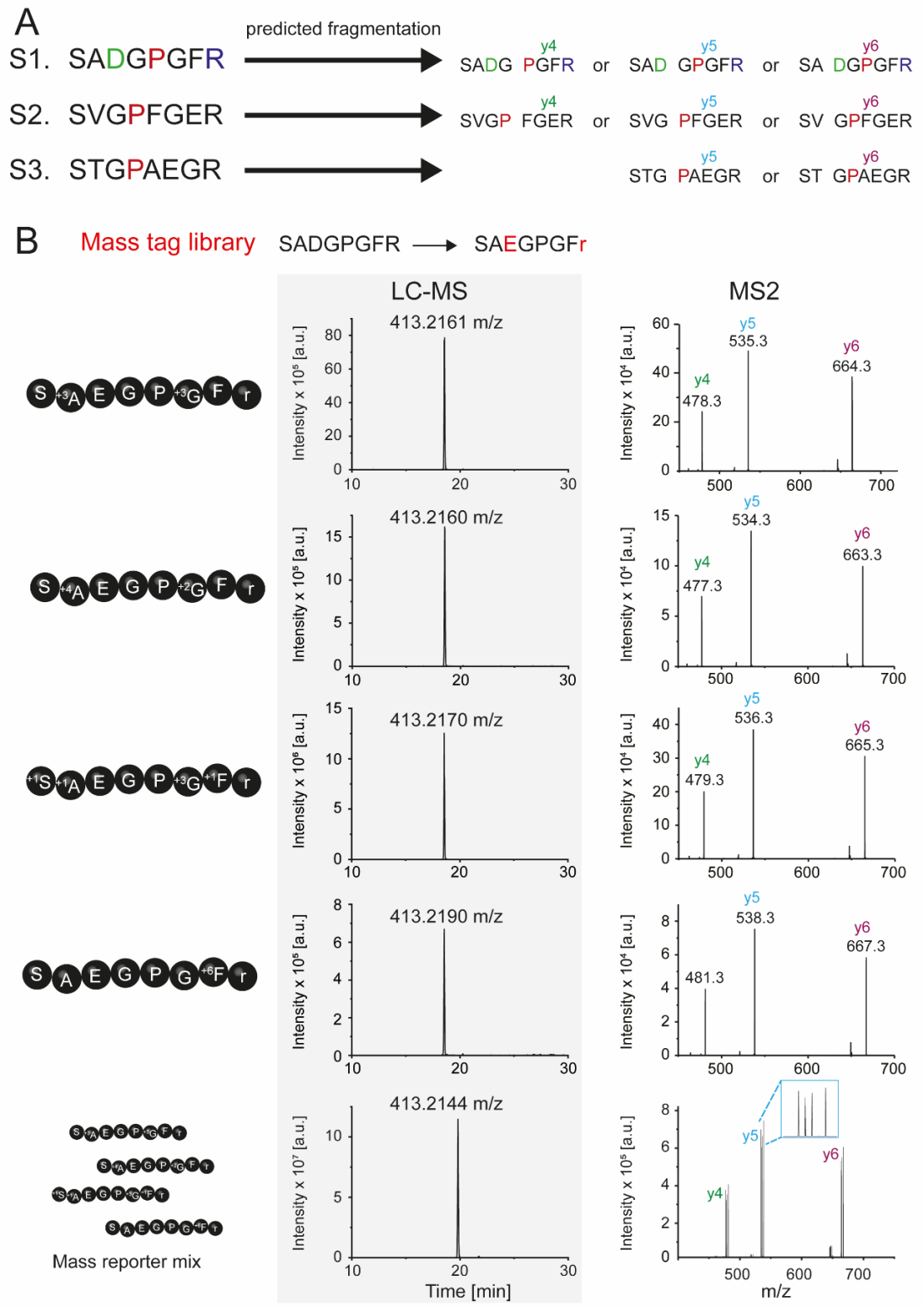

Figure 4 (A) Three initial mass tag sequences (S1-3) were designed, and their fragmentation was predicted. The mass tag sequences are shown in single-letter code, and the colored amino acids displayed those AA that are mainly responsible for bond breakage in MS² and building fragment ions. (B)The mass tag library is depicted with its four family members that all possess a mass shift of + 6 Da but with distinct isotopic labelling. Extracted ion chromatogram and MS² spectra are shown for the four mass tag family members separately and when they were analyzed simultaneously as a mass reporter mix.

3.1.2. Protease-sensitive sequences (PSS)

The diagnostic peptide was designed for detection of elevated enzyme activity. As model system, protease-sensitive sequences for matrix metalloproteinases were chosen, which are known to show elevated levels in inflammatory disease, e.g. rheumatoid arthritis or osteoarthritis.[9, 21, 51] The MMP-substrate sequence 1 (PSS-1) is originated from collagen, which is one main substrate of MMPs.[11] The sequence was already successfully used to detect peri-implant disease by being cleaved by upregulated MMPs in salvia and releasing a bitter substance that display the patient oral inflammation.[34] According to previous findings, the relative cleavage rate was improved by the exchange of amino acids in position P'1-4 to Leu, Ala or His for MMP-1, -8 and -9 as compared to the hydrolysis of the peptide sequence GPQG~IAGQ.[52] Therefore, the already known sequence GPQGIAGQ was altered, and a second PSS with an amino acid sequence of GPSGLLAH that has a better cleavage rate, hence is cleaved faster, was chosen. This effect was confirmed by MMP cleavage experiments (as described below: *4.2.1 Cleavage by matrix metalloproteinases*) as well as by MEROPS – the Peptidase database that predict that a peptide sequence is cleaved better by MMP-9, if position 1' is a leucine instead of an isoleucine as it applies in PSS-2 (https://www.ebi.ac.uk/merops/cgi-bin/pepsum?id=M10.004;type=P).

The PSSs were synthesized either with naturally occurring L-amino acids, which present a sequence that is sensitive to MMPs (L-PSS-1 and -2), or non-natural D-amino acids were used for synthesis and result in a sequence that is not sensitive to MMPs and therefore not cleaved (D-PSS-1 and -2). The specific D-linkers, D-PSS-1 or -2, served as internal negative control. It was used for analysis to build a ratio between the signal intensity of the L- and D-reporter, respectively. With this negative control, the extent of cleavage events of the cleavable L-linker by MMPs can directly be determined in relation to the noncleavable D-linker in the same sample (**Figure 1E**).

3.1.3. Peptide Synthesis

Instead of synthesizing peptide constructs and performing the following purification steps, peptides can be purchased. Here, synthesis was performed by the fully automated peptide synthesizer "Liberty Blue" equipped with built-in software.

Warning: This step utilizes several substances that, if not properly handled, can pose a danger. Please refer to the respective guidelines regarding proper handling and disposal of

the chemicals used. While these guidelines might vary, please refer to the respective safety datasheets for basic information. We have highlighted some of these chemicals in bold script when they are used first.

We recommend performing all steps under a fume hood and utilizing full SPE equipment.

Timing of peptide synthesis:

- Peptide synthesis (per peptide) = 6-8 h
- Peptide purification (per peptide) = 4 h
- Lyophilization for 2 mL = overnight (12-24 h)

3.1.3.1 Fully automated peptide synthesis

Note: We utilized a fully automated microwave peptide synthesizer (Liberty Blue, CEM GmbH, Kamp-Lintfort). The protocol contains remarks specific for this device, but can be adapted to any available peptide synthesizer.

1. The following settings were chosen: scale (0.1), C-terminus (amide), resin type (not preloaded), resin swelling (high swelling), resin cycle (0.1 resin swelling HS) and final deprotection cycle (0.1 no final deprotection HS). Note: Since non-natural amino acids were used the bottle setup has to be adjusted on some systems.

2. If not stated otherwise 0.1 – single coupling (HS) cycle was used. Modified cycles were used for the following amino acids:
    a. His — 0.1 – single 50 °C 10 min coupling (HS)
    b. ANP — 0.1 – double 50 °C 10 min coupling
    c. Arg — 0.1 – double Arg 75 °C coupling (HS)
    d. all amino aicds from TEV sequence — 0.1 – double coupling (HS)
    e. isotopically labelled AS — standard coupling 90 °C
3. Note: usually 5 equiv of amino acids are added. For non-natural amino acids or isotopically labelled amino acids, only 2 or 2.5 equivalents are added.
4. Weigh all amino acids in 50 mL tubes (or appropriate container) and weigh resin in reactor.
5. Mix or dissolve activator and deprotector with appropriate amount of **DMF** and connect to the synthesizer.

6. Dissolve amino acids in DMF and make sure the ANP is protected from light (e.g.by aluminum foil).
7. Fmoc-deprotection was performed with 20 % **piperidine** in DMF at 90 °C for 1 min, and amino acid coupling was performed with the activators **DIC/Oxyma** at 90 °C for 2 min followed by three washing cycles with DMF.
8. Do not remove the Fmoc-group of the last amino acid!
9. After synthesis transfer the resin to a 20 mL polypropylene reactor with a polyethylene frit, which is fitted with a Luer stopper and wash the resin with 3 mL of DMF five times.
10. To block potentially free N-terminal amino groups, manually perform an N-acetylation step with 75 µL acetic anhydride and 135 µL **DIPEA** in 3 mL of DMF for 25 min at room temperature on an orbital shaker.
11. Perform Fmoc-deprotection manually by using 40 % (V/V) **piperidine in DMF** for 3 min and 20 % (V/V) piperidine in DMF for 12 min at room temperature and then wash resin 5 times with DMF.
12. Weigh 1.5 equiv of N-(+)-Biotinyl-6-aminohexanoic acid in a 15 mL falcon tube and dissolve it in 2.5 mL **DMSO**. Before adding 2.5 mL of 0.5 M **HOBt** in DMF make sure that all powder is dissolved. Then add 200 µL of DIC and 150 µL of DIPEA for carboxylic activation and add mixture to resin.
13. Incubate overnight at room temperature on an orbital shaker.
14. Wash peptide three times with DMF and repeat step 15 but incubate this time only for at least 2 h.
15. After five washing steps with DMF, dry peptide by washing three times with **DMC** and three times with **diethyl ether** and then store dried peptide on an orbital shaker for at least 1 h.

3.1.3.2 Peptide cleavage from solid support

Cleavage was performed to cleave peptide from resin and to remove all side protecting groups of amino acids to be available for further reactions.

Warning: This step utilizes several substances that, if not properly handled, can pose a danger. Please refer to the respective guidelines regarding proper handling and disposal of the chemicals used. While these guidelines might vary, please refer to the respective safety datasheets for basic information. We have highlighted some of these chemicals in bold script when they are used first.

1. Prepare 5 mL of cleavage solution containing **TFA:TIS:**H_2O (95:2.5:2.5, V/V/V), add to dried peptide and incubate for 3 h at room temperature on an orbital shaker.
2. Prepare approximately 20 mL of ice-cold diethyl ether in a 50 mL falcon tube and collect the cleavage solution in ether. Note: A white, cloudy turbidity appears due to the precipitating peptide.
3. Store precipitating peptide on ice for at least 15 min or at -20 °C overnight.
4. Centrifuge at 4 °C with 3000 rpm for 5 min and discard supernatant.
5. Add approximately 20 mL ice cold **diethyl ether** and vortex and then repeat step 4 and 5 until a total of three washed was performed.
6. Dry the pellet under the fume hood for at least 2 h.

Note: protect peptide from light.

3.1.3.3 Peptide purification

Warning: This step utilizes several substances that, if not properly handled, can pose a danger. Please refer to the respective guidelines regarding proper handling and disposal of the chemicals used. While these guidelines might vary, please refer to the respective safety datasheets for basic information. We have highlighted some of these chemicals in bold script when they are used first.

The peptide was purified from side products by reversed phase chromatography using an FPLC system (GE Healthcare Äkta Pure, Life sciences, Freiburg, Germany) with a Luna 15u C18(2) 100Å column (21.2 mm × 250 mm, Phenomenex Inc., Torrance, CA). Please note: FPLC purification is well established in our lab. We have optimized workflows and workup strategies to make use of the generally less harsh conditions during FPLC purification opposed to HPLC purification. Part of the workflow is to determine purity either by analytical HPLC or HPLC-MS. However, for samples containing impurities, coeluting with peptides, and depending on available instrumentation, HPLC methods might have to be developed.

1. Prepare your sample by dissolving the peptide pellet in 25 % acetonitrile in water with **0.1 % TFA**.
2. Equilibrate column with 25 % **acetonitrile + 0.1 % TFA** in water + 0.1 % TFA with at least 1 column volume (CV).

3. Prepare 10 mL superloop for sample application on column and load sample on the column with a maximum flow rate of 2 mL/min. Note: check tube connections for any leakage during method set up.
4. Wash column with two CV to elute nonbinding impurities.
5. Elute peptide with a linear gradient from 25 – 100 % acetonitrile + 0.1 % TFA in water + 0.1 % TFA over 8 CV at a flow rate of 4 mL/min.

Note: repeat purifications might be necessary. We repeated FPLC purification twice to receive a peptide purity of over 90 %; this will be dependent on the specific system in use.

6. Collect the eluent in 2 mL fractions in 15 mL falcon tubes protected from light.
7. Perform LC-MS measurements with samples from peak fractions to determine the molecular weight and purity (see example in [45]).
8. Evaporate acetonitrile from fractions with the correct peptide mass by treating the samples with nitrogen in TurboVap LV Evaporator for at least 1.5 h.
9. Prepare samples for freeze-drying: close falcon tubes with appropriate lids and punch three holes in the lid. Before the lyophilisation process, freeze samples at –80 °C for at least 30 minutes. Freeze-drying was performed with Freeze Dryer Alpha 1-4 with -53 °C for the primary drying process and 3,010 mbar.
10. Dissolve the lyophilized peptides in ultrapure water and lyophilize them again with VirTis Benchtop Freeze dryer with a condenser temperature of -79.0 °C and 14 µbar.
11. Store lyophilized peptides at –80 °C until use.

3.2. Characterization

Timing of characterization of isotopically labelled peptides:

- MMP cleavage = 48 h
- Photocleavage = 6 h
- TEV cleavage = 6 h

3.2.1. Cleavage by Matrix Metalloproteinases

The matrix-metalloproteinase substrate sequences L-and D-PSS-1 and L-and D-PSS-2 were incubated with MMP in a time- and concentration-dependent manner. To ensure the

stability against MMP of the modules #1, 2 and 3 they were individually incubated with MMP and showed no cleavage after 15 h (data not shown).

1. Dissolve lyophilized matrix metalloproteinase substrate sequences, PSS-1 (GPQGIAGQK$_{(N3)}$Q) and PSS-2 (=GPSGLLAHK$_{(N3)}$Q) in MMP buffer to a final concentration of 1 mM. Note: K$_{(N3)}$ is used as abbreviation for L-azidolysine. Here, the ε-amino group of lysine's side chain is exchanged by an azide functional group.
2. For the concentration-dependent experiment, prepare a 10-fold MMP-Mix, consisting of MMP-1, -8, -9 with the concentration range from 0.16 nM to 16 nM.
3. Use 40 µL peptide solution and add 4µL of 10x MMP-Mix amount of MMP-Mix and incubate reaction mixtures at 37 °C for 24 h.
4. Peptide solution incubated only in MMP buffer served as negative control.
5. Stop the protease activity by adding 50 mM EDTA to a final concentration of 1 mM and heat the mixture up to 95 °C for 15 min.
6. Analyze cleavage efficiency by RP-HPLC (Zorbax Eclipse XDB-C18 column, elution with a linear acetonitrile gradient from 5 % up to 65 % in 16 min), determine main peak area and calculate relative ratio of cleaved to uncleaved peak (see example Supporting Information in [45]).
7. For the time-dependent release experiment use 30 µL of each peptide and mix it with MMP-1, MMP-8 or MMP-9 with a final enzyme concentration of 35.1 nM, 13.2 nM or 10.6 nM, respectively (according to the MMP concentrations in synovial fluid from patients with RA[12]). Prepare three samples for each time point.
8. Incubate peptides with MMP buffer as negative control.
9. Incubate samples at 37 °C with gentle agitation for 30 min, 2, 4, 6, 24 and 48 h.
10. At the specific time point stop reaction by adding 1.66 µL of 50 mM EDTA solution to a final concentration of 1 mM and heat the reaction mixture to 95 °C for 15 min (see example in Figure 2 of [45]).
11. Analyze samples by RP-HPLC as described under *4.3.2*, step 11.

3.2.2. Photo-cleavage and affinity purification

To confirm photosensitivity of incorporated ANP, the L-amino acid reporter 2 (not isotopically labelled, Biotin-Ahx-ENLYFQSAEGPGFR-(ANP)-GPSGLLAHPLKPAKSA) was irradiated with UV light at 366 nm for 6 . Afterwards,

cleaved products were separated by affinity purification with streptavidin-coated magnetic beads and analyzed by MALDI.

1. Prepare 100 µL of (0.5 mg/mL) L-amino acid reporter 2 in MQW and fill it in a 1.5 mL Eppendorf tube and place it 10 cm under an UV lamp (8 W).
2. Cover UV lamp and sample with a cardboard box and irradiate sample for 6 h. Note: use specific UV safety eyewear with colored glasses and UV skin protection lotion to protect your eyes and hands from UV light.
3. Prepare streptavidin-coated magnetic beads by using 37.5 µL beads and wash them with PBS twice to remove preservatives.
4. Equilibrate beads by washing them three times with binding buffer (e.g. TBS)
5. Dilute samples to 300 µL with TBS and add it to beads.
6. Resuspend the slurry and incubate for 30 min on a benchtop shaker.
7. Transfer supernatant to new Eppendorf tube.
8. Wash beads three times with washing buffer (TBS + 2 M urea, pH 7.5)
9. Elute biotinylated peptide fragment by adding 100 µL elution buffer (2 % SDS)
10. Resuspend the slurry and incubate at 95 °C for 5 min.
11. Shortly centrifuge the sample and collect supernatant containing the fragment biotin-Ahx- ENLYFQSAEGPGFr.
12. Use Ziptip columns to desalt and purify the sample for MALDI measurements.

3.2.3. Cleavage of TEV site by TEV protease

Warning: This step utilizes several substances that, if not properly handled, can pose a danger. Please refer to the respective guidelines regarding proper handling and disposal of the chemicals used. While these guidelines might vary, please refer to the respective safety datasheets for basic information. We have highlighted some of these chemicals in bold script when they are used first.

We recommend performing all steps under a fume hood and utilizing full SPE equipment.

To confirm cleavage between TEV sequence and the balanced mass tag, the peptide constructs were incubated with TEV protease (10 U/µL) for 6 h and then analyzed by HPLC and ESI-MS. Note: store TEV protease on ice until usage.

1. Prepare 200 µL of 0.5 mM peptide solution in TEV protease buffer (50 mM TRIS-HCl, 0.5 mM EDTA, 1 mM **DTT**, pH 8.0)
2. Prepare 30 µL peptide solution per Eppendorf tube.
3. Add 2.74 µL or 2.76 µL of TEV protease for reporter pair 1 (L- and D-version) or reporter pair 2 (L- and D-version), respectively.
4. Prepare negative control by pipetting 2.74 µL or 2.76 µL TEV buffer to reporter pair 1 (L- and D-version) or reporter pair 2 (L- and D-version), respectively.
5. Preheat Thermomixer to 30 °C.
6. Incubate samples in Thermomixer at 30 °C for 6 h with 300 rpm. Note: protect samples from light by using brown Eppendorf tubes and cover Thermomixer with aluminum foil.
7. Preheat a second Thermomixer to 95 °C.
8. Incubate samples at 95 °C for 10 min to inactivate TEV protease.
9. Centrifuge samples at 13.4 x 1000 rpm for 2 min.
10. Transfer 25 µL to HPLC vials with 100 µL glass inserts.
11. Prepare HPLC.
    a. Connect Zorbax-Eclipse XDB-RPC18 column to HPLC.
    b. Wash column with 100 % CAN + 0.1 % TFA for at least 5 CV.
    c. Equilibrate column with 5 % ACN/H_2O + 0.1 % TFA for at least 5 CV.
    d. Perform two blank runs before starting to measure your samples.
    e. Injection volume of samples = 20 µL.
    f. column oven was set to ambient temperature (22 °C).
    g. a stepwise acetonitrile gradient was run from 5 – 60 % in 16 min and from 65 – 95 % in 2 min; detector was set at 214 nm wavelength.
12. HPLC Analysis was performed with ChemStation OpenLab software. Integrate peaks from uncleaved peptide construct to determine main peak area before and after incubation with TEV protease. Calculate cleavage efficiency by comparing cleaved to uncleaved peak areas.
13. Use the remaining 5 µL in HPLC vial to confirm cleavage at the right target site by ESI-MS.
14. Desalt and purify samples from TEV protease for MS by using Ziptips and proceed according to the instructor's manual.

3.3. Decoration of ECM with isotopically labelled peptides

NIH 3T3 fibroblasts secrete extracellular matrix as structural component for adhesion, migration and tissue organization.[29] The cells were cultured and maintained in DMEM containing heat inactivated BCS (10 %), penicillin G (100 U/mL) and streptomycin (100 µg/µL). After cell seeding on glass or plastic surfaces, sodium L-ascorbate was added to the medium. The antioxidant was added as it is an essential cofactor for collagen biosynthesis.[53] After 7 days, cells were removed to obtain the cell-free three-dimensional cell-derived matrix that served as depot scaffold for isotopically labelled mass reporters. Steps 1 - 3 were performed according to Gutmann *et al.*[47]

Overview of steps and timing:

Step 1: Surface preparation

- Surface preparation = 2 h
- Gelatin coating = 2 h

Step 2: Cell culture and ECM preparation

- Cell seeding = 1 h
- ECM production by NIH3T3 cells = 7 d
- Maintenance = 1 - 2 h/daily

Step 3: De-cellularization and removal of cells and cellular debris

- Decellularization = 4 h

Step 4: Decoration of ECM with mass reporters

- transglutaminase reaction of D-chain peptide sequence of mass reporter constructs with fibronectin

Step 5: Detection of mass reporter constructs on ECM

- immunoassay with Streptavidin-HRP and TMB substrate to quantify peptide amount on ECM

Step 6: Release of mass reporters from ECM

- incubation with MMP-9

3.3.1. Preparation of ECM in 96-well plates and 8-well LabTek Chambers

ECM was prepared in 8-well Nunc™ Lab-Tek™ II Chamber Slide™ Systems for microscopy or in Greiner CELLSTAR® 96-well plates. In brief:

3.3.1.1 Surface preparation

Note: Steps 1 - 4 of surface preparation do not have to be performed under laminar air flow (LAF).

1. Precoat 8-well LabTek chambers with 2 % APTES solution. Add 300 µL of 2 % APTES solution per well and incubate for 15 min at room temperature. Note: Prepare solution immediately before use, as APTES solution is only stable for 20 min.
2. Discard solution and wash wells four times with 300 µL of ultrapure water for 5 min. Note: Make sure to follow proper precautions and protocols when discarding toxic substances.
3. Freshly prepare 0.125 % glutaraldehyde solution, add 300 µL/well and incubate for 30 min at room temperature.
4. Discard solution and wash wells four times with 300 µL of ultrapure water for 5 min.
5. Place empty LabTek Chambers without lid in LAF box and irradiate with UV light for 1 h.

Note: Perform gelatin coating immediately before cell seeding.

Note: Eight-well LabTek® chambers as well as CELLSTAR® 96-well plates have to be treated with gelatin for a better adherence of NIH3T3 cells to the surface.

6. Prepare 2 % gelatin in PBS for gelatin coating.
7. Perform filtration through a sterile 0.22 µm PES filter (Filtropur S 0.2) and add 300 µL per well and incubate for 1 h under LAF.
8. Wash wells three times with sterilized PBS and leave wells filled with PBS until cells are added.

3.3.1.2 Cell culture and ECM preparation

NIH 3T3 fibroblasts (CRL-1658; ATCC, Manassas, VA) were maintained in 75 cm^2 culture flasks in growth medium (DMEM high glucose, containing heat-inactivated BCS (10 %), penicillin G (100 U/mL) and streptomycin (100 µg/µL)) at 37 °C under CO_2 (5 %). For

ECM production, NIH3T3 cells should at least be in passage 20. Do not allow cells to reach 100 % confluency to retain correct phenotype.[48]

Note: cells should always be handled under LAF box and treated with sterilized or sterile filtered solutions.

Note: handle and prepare cells according to Gutmann *et al*. for cell seeding.

1. Count cells under light microscope with a hemocytometer according to the manufacturer's instructions.
2. Dilute cells with fresh medium to $2x10^5$ cells/mL for 96-wells plates and to $1.7x10^5$ cells/mL for Lab Tek chambers.
3. Aspirate PBS from wells of 96-well plate and LabTek chambers.
4. Seed cells:
    a. 8-well LabTek Chambers 300 µL/well = $5x10^4$ cells/well
    b. 96-well plate 150 µL/well = $3x10^4$ cells/well
5. Incubate cells at 37 °C, 5 % CO_2 for 24 h.

Note: Perform medium exchange according to Gutmann *et al*.

Note: Gently aspirate the growth medium without touching the ground and replace the medium by gently pipetting on the wall to avoid disruption and detachment of the matrix.

3.3.1.3 De-cellularization and removal of cellular debris

Decellularization can take place at day 7 after cell seeding, when cells were kept in growth medium with 10 % BCS. Matrices should be handled with care during decellularization process and further treatment due to strong destabilization of generated matrices after cell extraction. For detailed explanation see Gutmann et al.'s publication,[47] here in short.

1. Rinse matrix two times with PBS and then incubate with double distilled water for 15 min and again for 30 min at room temperature. Note: cells should be detaching during incubation.
2. Rinse matrix three times with PBS and incubate matrix with triton-X-ammonium buffer for 10 min at 37 °C, 5 % CO_2.
3. Rinse matrix five times with PBS.

4. Store matrix in PBS with penicillin G (100 U/mL) and streptomycin (100 µg/mL) for storage at 4 °C. Note: storage place should be without severe vibration because matrix can detach from surface.

3.3.2. Coupling of peptides to fibronectin of ECM

For the transglutaminase-mediated immobilization reaction FXIII (Fibrogammin) was activated by incubation with 20 U/mL thrombin in TBS and 2.5 mM $CaCl_2$ for 30 min at 37 °C. Tissue culture treated 96-well plates were used for binding efficiency studies. The mass reporters' working concentration was determined to 7.5 nmol/mL, as the incubation of higher peptide amounts on ECM did not increase the amount of covalently attached peptides, but nonspecific adsorption increased in a concentration dependent manner. Furthermore, the use of 20 U/mL activated FXIII compared to the use of 20 U/mL recombinant human tissue transglutaminase (rhTG2) was able to immobilize a higher amount of peptide under the same conditions. As a result, FXIIIa was used for further immobilization experiments (e.g. Figure 4 in [45]). Moreover, the mass reporters were applied in a mixture because all four peptides bind equally well to ECM at the working concentration. The N-terminal immobilization tag consisting of the amino acid sequence of IGF-I D-domain served for covalent attachment. The D-domain's lysine was used as acetyl group acceptor, whereas the glutamines of fibronectin in cell-derived ECM functioned as acyl group donors.

Note: According to the supplier (Zedira) for rhTG2 1 unit is defined as the formation of 1 µmol of hydroxamate per min from Z-Gln-Gly-OH and hydroxylamine at pH 6.0 at 37 °C. For FXIII the supplier (CSL Behring) stated, one unit is defined as the clotting ability of 1 mL normal pooled plasma. Thrombin units are defined as cleaving more than 90 % of a test protein in PBS at 16 °C in 22 h.

Timing for decoration of ECM with isotopically labelled peptides:

- Sample preparation = 30 min
- Transglutaminase reaction = 30 min
- washing steps = 30 min

1. Rinse matrix three times with 150 µL PBS to wash out PBS + penicillin + streptomycin in which it was stored.

2. Perform bicinchonic acid (BCA) assay with a peptide standard according to the manufacturer's manual for concentration determination of four isotopically labelled peptide constructs.
3. Mix isotopically labelled peptides in equal molar ratios and dilute mix with TG buffer to a total final concentration of 7.5 nmol/mL.
4. Prepare mixture of mass reporters and mix with 20 U/mL activated FXIII. Note: Perform mixing by carefully pipetting up and down because FXIIIa is very sensitive to shear stress! Do not vortex!
5. Add 100 µL/well of mass reporter mix + FXIIIa and incubate matrix at 37 °C, 5 % CO_2 for 30 min.
6. After incubation discard supernatant and rinse matrix three times with 150 µL TBST and three times with 150 µL PBS.

3.4. Imaging

3.4.1. Detection of immobilized peptide on ECM with Streptavidin-HRP and TMB substrate

Use ECM in 96-well plates with immobilized mass reporters. The N-terminal biotin tag was used to detect peptides on ECM with streptavidin-HRP conjugate and TMB substrate. The biotin-streptavidin complex is the strongest noncovalent biological interaction known, with a dissociation constant of $K_d = 10^{-15}$ M. The conjugated horseradish-peroxidase oxidizes the TMB substrate and induce a color shift from colorless to blue and allow UV/VIS spectrometric detection. After addition of acid, the color shifts to yellow. The biotinylation ratio of peptide to biotin is 1:1.

Timing of imaging procedures:

- peptide quantification via HRP-TMB = 2 h
- CLSM:
    - sample preparation = 2 d
    - use of microscope = 4 h

1. Prepare appropriate volume of streptavidin-HRP (1:5000) in PBS (100 µL/well).
2. Add 100 µL diluted Streptavidin-HRP to each well and incubate matrix for 1 h at room temperature with slightly agitation. Note: use multichannel pipette to make sure that incubation time is the same for each well.

3. Discard supernatant and rinse wells three times with 150 µL of TBST and three times with 150 µL of PBS.
4. Prepare appropriate volume of 1-Step Turbo TMB-ELISA substrate solution immediately before use Note: the TMB solution should be clear. If it already appears blue or green TMB solution is contaminated and need to be purchased again.
5. Add 100 µL of TMB solution to each well with a multichannel pipette and incubate for 15 min at room temperature in the dark. Note: Alternatively, the development of blue color can be followed by kinetic measurements at 605 nm wavelength with the plate reader.
6. After 15 min, stop reaction by adding 50 µL 2 M sulfuric acid. A color shift from blue to yellow can be observed.
7. Measure absorbance at 450 nm wavelength.

3.4.2. CLSM: Visualization of peptide immobilization to ECM

ECM in Eight-well LabTek chambers is used for microscopic imaging.

1. Wash ECM three times with 300 µL PBS to remove P/S.
2. Couple isotopically labelled peptide to ECM according to previous mentioned protocol in chapter 5.3.2. *Coupling of peptides to fibronectin of ECM*. Note: This time no peptide mix is prepared. Each peptide construct is coupled in a separate well.
3. Wash ECM three times with 300 µL of TBST, once with 300 µL of acetate buffer and three times with 300 µL of PBS.
4. Prepare anti-fibronectin rabbit antibody (primary antibody) and dilute 1:400 in PBS.
5. Add 300 µL/well primary antibody and incubate at 2 - 8 °C overnight.
6. Wash three times with 300 µL of TBST and three times with 300 µL of PBS.
7. Prepare secondary antibody goat anti-rabbit IgG AF488 by diluting it 1:500 in PBS and add 300 µL/well.
8. Add 0.3 µL/well streptavidin-Cy5 and incubate both antibody and streptavidin-Cy5 simultaneously for at least 1 h at room temperature with slightly agitation and in the dark. Note: cover LabTek chambers with aluminum foil to protect dyes from light.

9. Thoroughly wash each well five times with 300 µL of TBST and three times with 300 µL of PBS.
10. For analysis, use a confocal microscope. Here, an AOBS SP2 confocal laser scanning microscope (Leica microsystem, Wetzlar, Germany) with a 63x N.A. 1.4-0.60 Oil I BL HCX PL APO I objective was used.
11. After microscoping, prepare an 8 nM MMP-9 solution by dilution of enzyme in MMP buffer.
12. Add 300 µL/well MMP-9 solution or MMP buffer as negative control and place LabTek chambers into a petri dish. Seal petri dish with parafilm and cover it from light with aluminum foil.
13. Incubate at 37 °C, 5 % CO_2 for 48 h.
14. After incubation, wash each well five times with 300 µL of TBST and three times with 300 µL of PBS.
15. For analysis, use a confocal microscope. Here, an AOBS SP2 confocal laser scanning microscope (Leica microsystem, Wetzlar, Germany) with a 63x N.A. 1.4-0.60 Oil I BL HCX PL APO I objective was used (**S6**).

3.5. Bioresponsive release of mass reporters from ECM and read-out

The bioresponsive release of mass reporters from ECM by recombinant MMP-9 was performed as a proof of concept. The incubation process and the following purification steps were (**Figure 1C, D**):

Steps and timing:

Step 1: Incubation of mass reporter decorated ECM with MMP-9 for 48 h.

Step 2: Collection of supernatant and irradiation at 366 nm for 6 h.

Step3: Affinity purification with Streptavidin-beads (~ 3 h).

Step4: Cleavage of balanced mass reporters from beads by TEV protease, TEV protease incubation: ~ 6 h.

Step5: Collection of supernatant and analysis by LC-MS/MS.

3.5.1. Incubation with MMP-9

1. Use ECM decorated with isotopically labelled peptides (refer to "5.3.2 C*oupling of peptide to fibronectin of ECM*").
2. Determine appropriate volume of MMP solution, 100 µL per well is needed.
3. Dilute MMP-9 (100 µg/mL = 1.08 µM) with MMP buffer to a final concentration of 8 nM. Note: store MMP-9 on ice until use. Avoid freeze-thaw cycles as the enzyme's activity decrease.
4. Add 100 µL/well MMP-9 solution and seal 96-well plate with parafilm.
5. Incubate 96-well plate in cell culture incubator at 37 °C, 5 % CO_2 for 48 h for optimum performance of MMP.
6. Collect supernatant and transfer it to new Eppendorf tubes. Note: if samples are not further treated right away store them in the fridge (2-8 °C) for storage of less than 24 h or store them in the freezer (-20 °C or -80 °C) for long time storage (> 24 h).

3.5.2. Purification of released mass tags

Mass reporters have to be purified from supernatant (MMP buffer). It is important to isolate the balanced mass tag sequence since this sequence shows the specific fragmentation pattern in LC-MS/MS.

3.5.2.1. Photo-cleavage

Photo cleavage was performed to separate the balanced mass tag from four remaining amino acid residues of PSS. The photosensitive molecule is placed between the balanced mass tag and PSS and is cleaved by irradiation with UV light at 366 nm. Note: take care to not expose skin to UV light for prolonged times and wear safety goggles with tinted glasses.

1. Place open Eppendorf tubes containing the supernatant from previous step in a rack and place it under UV lamp with a distance of 10 cm to the light source.
2. Turn on the UV lamp with a wavelength of 366 nm.
3. Cover the experiment setup with a cardboard box to make sure that only light of a specific wavelength reaches the samples.
4. Irradiate samples for 6 h. Note: if samples are not further treated right away store them in the fridge (2-8 °C) for storage of less than 24 h or store them in the freezer (-20 °C or -80 °C) for long time storage (> 24 h).

3.5.2.2. Affinity purification with Streptavidin-coated magnetic beads

Affinity purification with beads was performed to remove cleaved PSS residue from mass reporter solution and to bind mass reporters to a solid support, which subsequently helps to separate balanced mass tag from remaining N-terminal TEV sequence and affinity tag (Biotin-Ahx).

1. Resuspend beads in the original vial by vortexing.
2. Calculate the amount of beads required based on their binding capacity (on average 4000 pmol nominal biotin binding capacity per mg wet beads, 10 mg/mL) and transfer the beads to a new Eppendorf tube.
3. Wash beads with 500 µL PBS to remove preservatives.
4. Place the tube containing the beads on a magnet for ~ 1 min and remove supernatant by aspiration with a pipette while the tube is on the magnet.
5. Repeat washing steps for a total of three washes.
6. After the last washing step and removal of supernatant add same volume of washing buffer as the initial volume to the beads.
7. Prepare samples by diluting them with PBS to a final volume of 300 µL.
8. Add appropriate volume of beads to each Eppendorf tube with biotinylated samples.
9. Incubate for 30 min at room temperature with gentle rotation of the tube on the roller mixer in the dark.
10. Wash the coated beads five times with 300 µL of PBS.

3.5.2.3. TEV cleavage

Biotinylated mass reporters which are now immobilized on streptavidin beads via their biotin moiety are incubated with TEV protease to release and separate balanced mass tags. The cleavage takes place between Gln (Q) and Ser (S) of the TEV sequence and results in pure balanced mass tag.

1. Prepare 100 µL /per sample of TEV buffer and add 0.5 U/µg peptide TEV protease
2. Resuspend beads in 100 µL TEV buffer + TEV protease.
3. Incubate samples for 6 h at 30 °C with gentle agitation.
4. Collect supernatant, transfer it to new Eppendorf tubes, and store at -80 °C or -20 °C until LC-MS/MS measurements.

Note: TEV protease units are defined as follows: 1 U cleaves 85 % of 3 µg of a control substrate according to the supplier (ThemoFisher).

3.5.3. LC-MS/MS measurements and analysis

Timing of LC-MS/MS measurements:

- Preparation of samples = 1 h
- Measurements = 4 h/sample
- data analysis = 6 h

3.5.3.1. C18 clean up with StageTips

Warning: This step utilizes several substances that, if not properly handled, can pose a danger. Please refer to the respective guidelines regarding proper handling and disposal of the chemicals used. While these guidelines might vary, please refer to the respective safety datasheets for basic information. We have highlighted some of these chemicals in **bold** script when they are used first.

Use C-18 StageTips for purification, desalting and concentration slightly modified according to Rappsilber *et al*[49].

Buffer A and B are needed for sample preparation.

- Buffer A: **0.3 % TFA in 2 % acetonitrile**
- Buffer B: **0.3 % FA in 60 % acetonitrile**

1. Prepare each Stage Tip with three discs of C-18 Empore SPE Discs (3 M) in a 200 µL pipet tip.
2. Wet and equilibrate the tips with 1 x 50 µL methanol, 1 x 50 µL buffer B and 2 x 50 µL buffer A using stage tipping centrifuge (Sanation lab solutions).
3. Use 100 µL of sample volume and acidify samples with formic acid to a final concentration of 0.5 % formic acid.
4. Load acidified samples onto the StageTips using Eppendorf centrifuge 5424 with 1500 x g.
5. Wash with 3 x 50 µL buffer A using stage tipping centrifuge.
6. Elute peptides with 2 x 20 µL buffer B using Eppendorf centrifuge with 1500 x g.
7. Dry eluents in vacuum concentrator (Eppendorf) and store them at -20 °C.
8. Prior to NanoLC-MS/MS analysis dissolve peptides in 2 % acetonitrile + 0.1 % formic acid.

3.5.3.2 NanoLC-MS/MS Analysis Fusion

NanoLC-MS/MS analysis of purified balanced mass tags, which were released from ECM by recombinant MMP-9, was performed on an Orbitrap Fusion™ Tribrid™ Mass Spectrometer (Thermo Fisher) equipped with a PicoView Ion Source (New Objective) and coupled to an EASY-nLC 1000 (Thermo Scientific). Use 0.1 % (v/v) formic acid in water as eluent A and 0.1 % (v/v) formic acid in 80 % acetonitrile as eluent B.

1. Pack capillary columns (PicoFrit, 30 cm x 150 µm ID, New Objective) with ReproSil-Pur 120 C18-AQ, 1.9 µm (ReproSil was purchased from Dr. Maisch, GmbH, Ammerbuch-Entringen, Germany).
2. Load purified and desalted peptide samples on capillary column
3. Separate sample with a 30 min linear gradient from 3 % to 40 % eluent B and a flow rate of 500 nL/min.
4. Acquire MS and MS/MS scans in the Orbitrap analyzer with a resolution of 60,000 for MS scans and 15,000 for MS/MS scans.
5. Use a data-dependent targeted MS/MS method with a fixed cycle time of 3 s with a target mass of m/z 413.2144 (corresponding to the doubly charged mass tag) and set the target mass HCD collision energy to 20 % normalized collision energy and the isolation window to 0.5 m/z to minimize peak overlapping from isotopic peaks.
6. Exclude singly charged precursors from selection and set mass tolerance to 22 ppm. Note: Mass tolerance has to be adjusted if a mass reporter set with more than the described four mass reporters is used.
7. Measure nontarget masses by using standard parameters (35 % normalized collision energy, isolation window 2.5 m/z, dynamic exclusion with repeat count of 1 and an exclusion duration of 30 s).
8. Increase the injection time from 50 ms for nontarget masses to 500 ms for target mass.
9. Set minimum signal threshold for precursor selection for nontarget masses to 50,000 and for target mass no threshold.
10. Use predictive AGC with an AGC target value of 2e5 for MS scans and 5e4 for MS/MS scans.
11. Use EASY-IC for internal calibration.

3.5.3.3. Data analysis

For data analysis Thermo Xcalibur™ 3.0 software (Thermo Fisher) was used.

1. Set mass tolerance in global mass options to 22.0 ppm and set mass precision to four decimals.
2. Choose in chromatogram ranges two traces and depict plot type total ion current (TIC) and base peak, respectively. Define the range for the base peak as 413.2144, which is the doubly charged mass tag ion.
3. To display the MS2 spectrum, select in chromatogram ranges a third trace and set plot type to base peak, set no ranges and select the scan filter with only hcd20.
4. Display the mass peaks in the MS2 spectra as spectrum list to show the signals intensities.
5. Calculate the intensity ratio of L-amino acid reporter to D-amino acid reporter after incubation with MMP-9 and the ratio of L/D after incubation in buffer.
6. To obtain overall mass tag release or PSS cleavage subtract the averaged L/D ratio after incubation in buffer from the averaged L/D ratio after MMP-9 incubation.
7. The following formula was used: $\left[\frac{L_{MMP}}{D_{MMP}} - \frac{L_{buffer}}{D_{buffer}}\right]$ = relative protease activity

3.5. Timing

The total experimental timeline is on the scale of roughly 2.5 - 3 weeks. However, this takes into account incubation times, cell growth, etc. This means the time can be considerably shorter, depending on which matrix is used and which optional experiments are performed.

Peptide synthesis (per peptide) **Total time: 22-36 h**

- Peptide synthesis = 6-8 h
- Peptide purification = 4 h
- Lyophilization for 2 mL = overnight (12-24 h)

Characterization of isotopically labelled peptides **Total time: ca. 60 h**

- MMP cleavage = 48 h
- Photo-cleavage = 6 h
- TEV cleavage = 6 h

ECM production **Total time: ca. 9 h (+ cell growth)**

- Surface preparation = 2 h
- Gelatin coating = 2 h
- Cell seeding = 1 h
- ECM production by NIH3T3 cells = 7 d
- Maintenance = 1-2 h/daily
- Decellularization = 4 h

Decoration of ECM **Total time: ca. 1.5 h**

- Peptide coupling to ECM
    - Sample preparation = 30 min
    - Transglutaminase reaction = 30 min
    - washing steps = 30 min

Imaging **Total time: ca. 48-54 h**

- peptide quantification via HRP-TMB = 2 h
- CLSM:
    - sample preparation = 48 h
    - use of microscope = 4 h

Bioresponsive release of mass reporters **Total time: ca.111 h**

- MMP incubation = 48 h
- SF incubation = 48 h
- Purification of balanced mass tags from supernatant
    - Irradiation with UV light = 6 h
    - Affinity purification = 3 h
    - TEV cleavage = 6 h

LC-MS/MS measurements **Total time: ca. 11 h (+ 4 h/sample)**

- Samples preparation = 1 h
- Measurements = 4 h/sample
- data analysis = 6 h

3.6. Troubleshooting

Table 2 Troubleshooting for different critical steps.

Problem	Cause	Solution
Missing amino acid in peptide	a. Fmoc-group was not properly removed b. carboxylic acid was not activated	a. check temperature, deprotecting and coupling reagents b. perform double coupling c. increase coupling time d. use another activation reagent
No MMP cleavage	a. insufficient MMP activation b. thiol residues in peptide or buffer	a. activate MMP again with 50 mM APMA solution, 6h, 37 °C b. alkylation of thiols with e.g. iodoacetamide
Transglutaminase reaction not working	a. FXIIIa is very sensitive to shear stress b. no calcium for enzyme available. c. FXIIIa not active	a. handle enzyme with care. Mix only by pipetting up and down b. check if calcium is in reaction buffer c. the reaction interferes with calcium-chelators like EDTA d. check FXIIIa activity in an activity assay
ECM detaching after decellularization		a. use heat inactivated BCS b. after incubation with triton-X buffer only use pipette for supernatant removal c. Check if sodium L-ascorbate is not oxidized yet
TMB solution turns green during incubation	a. Too much peptide was immobilized on ECM b. Streptavidin-HRP was not washed away properly	a. check peptide concentration b. next time intensify washing steps with TBST and PBS, or try 1 wash step with sodium acetate buffer, pH 5.3
Stage Tips clog during sample preparation for LC-MS/MS	a. remaining proteins in sample after three purification steps	a. intensify washing steps with TBST or PBS
No mass tag signal in LC-MS/MS measurements	a. mass tag concentration in supernatant of 96-well plate too low b. loss of mass tag during purification steps	a. start experiment with a higher concentration of mass tags. b. make sure that PSL is cleaved by MMP and mass tag is released.

4. Anticipated Results

The resulting isotopically encoded reporters simultaneously report cleavage events in an exemplary inflamed *in vitro* condition. The reporter pairs were immobilized within 3D engineered ECM and released by a specific cleavage event, here by MMP-9. After a three-step purification process the simultaneous detection of the two reporter pairs in LC-MS/MS was demonstrated resulting in the determination of relative proteolytic activity at the cleavage site.

Note: We have recently published a first study based on this system.[45] We refer to results published there as a very good example of how well these protocols work and of typical experimental data. Especially Supplementary figures S6 and S7 (for CLSM results) and S12 (LC-MS/MS) therein are examples of how we would expect the protocols to perform.

The ECM is a network-like structure mainly composed of fibrillar proteins and polysaccharides, function as structural support and provide instructional signals to its environment.[54, 55] In previous studies, the composition of the ECM was studied by mass spectrometry-based proteomics and it was shown that it is highly tissue-specific.[56] Engineered ECM from NIH 3T3 fibroblast in cell cultures were described as a fibrillar mesh of fibronectin, collagen I and III but not IV and minor traces of unorganized laminin and perlecan.[57] Furthermore, the ECM is a highly dynamic meshwork that is constantly remodelled either enzymatically or nonenzymatically.[54, 58] MMPs play a major role in ECM degradation as their main substrate is a collage-like recognition sequence.[12, 17, 59] In this study, the mass reporters were covalently immobilized on 3D engineered ECM in the presence of FXIIIa and released by cleavage of the PSS-1 or -2. To ensure that MMPs are responsible for the proteolytic release of reporters and not ECM degradation, a synthetic, nondegradable matrix with a transglutaminase peptide sequence or solid surfaces might present an alternative, e.g. PEG hydrogels with lysine or glutamine available for transglutaminase reactions[60] or gold nanoparticles containing glutamine residues.[61]

To overcome this problem and to differentiate nonspecific release due to ECM degradation or unknown events from specific proteolysis of PSSs the mass reporters were applied in pairs (**Figure 1A**). The reporter incorporating the cleavable L-amino acid variant of the PSS report both nonspecific, undetermined background release and specific proteolysis, while the corresponding D-amino acid variant reports background only. The signal intensity of L-reporter normalized to its D-reporter gives a good estimation of the

proteolytic versus the background events. The details of this calculation were stated in a previous manuscript [45]. To determine the proteolytic activity within the ECM the ratio of the reporter pairs from the incubation with buffer only were subtracted from the ratio of the reporter pair after incubation in presence of MMP.

A possibility to expand the capacity of mass reporters is the use of another standard. Here, the use of reporters in pairs using the D-variant for normalization is presented. Instead of creating a corresponding noncleavable variant of the incorporated linker, a general noncleavable linker might be used as negative control. Here, this would have led to the screening of three different MMP sensitive peptide sequences using only one mass tag as control reporter.

The mass reporter library might be expanded by increasing the incorporation of isotopically labelled amino acids into the mass tag peptide sequence. While maintaining the amino acid sequence of SAEGPGFr of the mass tag, in theory the maximal number of mass reporters is 18if the centred y-fragment ion is y_4. For mass reporters centered on another y-ion (e.g. y_5 or y_6), this number differs, due to the number of amino acids determining the labelling possibilities. The total isotopic labelling of the final reporters must be handled cautiously, since the mass-encoded amino acids were labelled with a mix of ^{15}N- and ^{13}C-atoms, or with ^{15}N- or ^{13}C-atoms only. Hence, a difference in the monoisotopic molecular mass occurs. To ensure the detection of all mass tags in LC-MS^1, the mass tolerance must be adapted. In this study, amino acids with different isotopic labels were used, and thus the window for mass tolerance had to be expanded to 22 ppm; otherwise the doubly charged mass tag (413.2144 m/z) in LC-MS^1 was not targeted and fragmented in MS^2 (**Figure 5**).

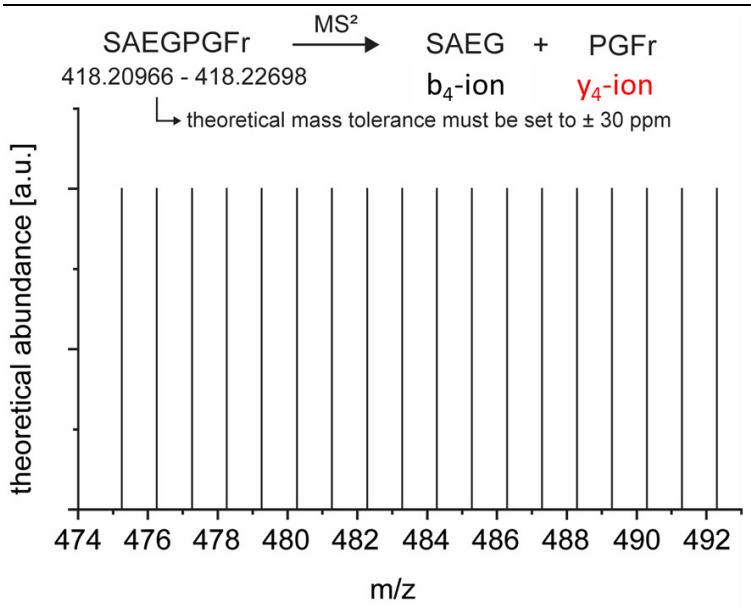

b_4-ion	y_4-ion	m/z (y_4 only)
$^{+4}S^{+4}A^{+6}E^{+3}G$	PGFr	475,25436
$^{+4}S^{+3}A^{+6}E^{+3}G$	$^{+1}$PGFr	476,25139
$^{+4}S^{+3}A^{+6}E^{+2}G$	P^{+2}GFr	477,26107
$^{+4}S^{+3}A^{+6}E^{+1}G$	P^{+3}GFr	478,2581
$^{+4}S^{+3}A^{+6}EG$	$^{+1}P^{+3}$GFr	479,26146
$^{+4}S^{+1}A^{+6}E^{+1}G$	$^{+1}P^{+3}G^{+1}$Fr	480,26481
$^{+4}SA^{+6}E^{+1}G$	PG^{+6}Fr	481,27449
$^{+4}SA^{+6}EG$	$P^{+1}G^{+6}$Fr	482,27784
$S^{+3}A^{+6}EG$	$P^{+2}G^{+6}$Fr	483,2812
$SA^{+6}E^{+2}G$	$P^{+3}G^{+6}$Fr	484,27823
$SA^{+6}E^{+1}G$	$^{+1}P^{+3}G^{+6}$Fr	485,28159
$SA^{+6}EG$	$P^{+1}G^{+10}$Fr	486,28494
$S^{+4}AE^{+1}G$	$^{+6}PG^{+6}$Fr	487,2883
$S^{+3}AE^{+1}G$	$^{+6}P^{+1}G^{+6}$Fr	488,29165
$SAE^{+3}G$	$^{+6}P\ ^{+2}G^{+6}$Fr	489,29501
$SAE^{+2}G$	$^{+6}P^{+3}G^{+6}$Fr	490,29204
$SAE^{+1}G$	$^{+6}PG^{+10}$Fr	491,2954
SAEG	$^{+6}P^{+1}G^{+10}$Fr	492,29875

Figure 5 Theoretical MS² spectra of an expanded mass tag library centered on the y4-reporter ion. The mass difference between the mass tags is approximately 1 Da, depending on the used labelled amino acids with either ^{13}C or ^{15}N isotopes or both. As mentioned, the mass tolerance must be adjusted when using more than four mass reporters; here for example the mass tolerance has to be set to ± 30 ppm.

The selection of the module #5 (PSS) aims at minimizing off-target effects and at only reporting the occurrence of one specific cleavage event. By choosing the matrix metalloproteinase substrate sequences, it was possible to detect MMP activity. The incorporated MMP sensitive linkers vary in their cleavage kinetics/profile to extend the observation period (e.g. Figure 2 in [45]) or may be substrate to different enzyme isoforms (e.g. MMP-1 or MMP-8 or MMP-9) reflecting the occurrence and participation of the different members of the MMP family in inflammation.[62-65] The mass reporter system is highly flexible and can be adapted to future needs and may easily be expanded to other proteases,[66, 67] pH-,[68] temperature-,[69] or reactive oxygen species (ROS)[70] – sensitive systems.[32] For example, the pH significantly decreases in inflamed tissue[71] or in cancer micro-environment.[72, 73] A proton-sensitive system was deployed for targeted drug delivery in previous studies using polymer-drug conjugates, which disintegrate in response to increased acidity.[74, 75] The enzymatic activity of cathepsin B, a cancer associated protease,[76] was also used to release cytotoxic drugs at the target site by cleaving the peptide bond between a dipeptide and a p-aminobenzylcarbonyl ether spacer. The dipeptide consisted of a basic amino acid (Cit, Arg, Lys) and a hydrophobic amino acid (Phe, Val).[77-79]

These presented protocols for purification of cleaved mass reporters before LC-MS/MS may also be employed for screening the initial concentration of mass reporter mixes or the

binding efficacy for each reporter to ECM. For example, new reporters were designed by exchanging the module #5, the protease-sensitive sequence, and a mix of all reporters were prepared. Before applying the mix to ECM, the following procedure helps to check if the reporters were mixed equimolar: expose the mixture to UV light of 366 nm and enrich it by adding streptavidin-coated beads. The reporters are now coupled to the beads, and in the presence of TEV protease the mass tag is cleaved. The supernatant containing the mass tags is analyzed by LC-MS/MS, and by comparing the signal intensity of each reporter the relative concentration of each reporter in the mix is determined. The same signal intensities reflect an equal concentration. Furthermore, a similar procedure helps to determine the binding efficacy of each reporter to ECM. After simultaneous incubation of the reporter mix and FXIIIa and thorough washing, the detection of immobilized reporters succeeds after release from ECM by UV irradiation and cleavage of the photolabile linker, following the aforementioned purification steps with streptavidin-coated beads and TEV protease. The measurements of isolated mass tags and their relative signal intensities in LC-MS/MS mirror the proportion of immobilization on ECM.

Possible *in vitro* applications for the mass reporter system is to screen proteolytic activity of enzymes in different buffers or microenvironments. The mass reporters are immobilized within the ECM, and the target protease is added in different buffers, whether it be with surfactants, especially high concentration of salts or antioxidants. The detection of signals in LC-MS/MS and their relative intensities represent the outcome of screening with the highest signal intensities reflecting the best cleavage conditions. The characterization of cell cultures or organoids display another possible application area. If the target protease's cleavage sequence is well-known, it is incorporated in the mass reporter and the presence of the target protease is monitored by cleavage of a corresponding sensitive peptide sequence and the coupled mass tag, and analyzed by LC-MS/MS. In case the enzyme's specificity is unknown, the extended mass reporter library in combination with many potential cleavable peptide sequences is used and the detection of a signal in LC-MS/MS reflect whether a cleavage event occurred or not. This procedure constitutes one way to determine the recognition peptide sequence of unknown proteases (e.g. of bacteria or viruses) for possible future diagnostic applications, like the detection of an infection by incorporating the peptide sequence into a chewing gum.[34]

Since the PSS-1 and -2 respond to a specific MMP threshold, the characterization of cell cultures regarding MMP activity might be pursued. The PSSs-1 and -2 were designed with different amino acid sequences and show distinct MMP sensitivity. The concentration threshold of L-PSS-1 was 8 nM in a Mix of MMP-1, -8 and -9, whereas L-PSS-2 was already cleaved at concentrations higher than 3.2 nM (Figure 2 in [45]).

These protocols provide the knowledge for using the mass reporters in an *in vitro* setting, while also *in vivo* applications might be possible in the future. One viable idea is to inject different reporter pairs into one area with each of the pairs reporting for one distinct proteolytic turnover event or to inject various pairs at multiple sites with each pair encoding for a preset proteolytic event at the site at which it got injected. These possibilities are featured through the covalent and rapid coupling onto ECM and the leverage of multiplexing.[22, 80] Furthermore, the mass reporters may be used to detect early disease-associated elevated levels of a target protease as they respond to a distinct protease threshold. They were immobilized on ECM by FXIIIa and were released as soon as the target protease exceed a specific concentration. The future application of the mass reporters is advisable in tissues with upregulated enzymes, e.g. in inflammatory disease like RA in the synovial gap. Elevated levels of matrix metalloproteinases indicate the presence or onset of an inflammatory disease, e.g. rheumatoid arthritis (RA),[81, 82] asthma,[83, 84] chronic obstructive pulmonary disease (COPD),[85, 86] chronic wounds,[65, 87] and myopathies.[19, 62] The mass reporters can be applied even before disease-associated changes occur. As soon as the target enzyme activity exceed a threshold the enzyme's presence can be monitored by measuring the cleaved mass reporter peptides in supernatant of ECM by LC-MS/MS. The elevated enzyme concentrations may occur earlier than clinical symptoms like pain, swelling and impaired function, thus providing an early detection system for the onset of an inflammation.

Another possible future *in vivo* application field of the mass reporter system is to monitor postsurgical infections. For example, for RA patients after knee replacement surgery is it important to early detect an acute postsurgical prosthetic bacterial infection typically occurring up to three months after surgery that can lead to implant replacement.[88] Often infections are triggered by *Staphylococcuc aureus,*[89] secreting virulence factors such as the metalloprotease aureolysin and serine-protease V8.[90, 91] Aureolysin possesses a specific N-terminal peptide cleavage site after a large hydrophobic residue.[90] It was reported that

several peptide sequences were identified which are specifically cleaved by aureolysin and might be used to detect the onset of a bacterial infection.[92] The beauty of this reporter family is that different protease-sensitive linkers can be chosen and applied simultaneously. It allows to monitor infection by *S. aureus* not only by linking the PSL for aureolysin to a mass tag but also by coupling a second linker sensitive to serine-protease V8 to a second mass tag with the same amino acid sequence as the first but different isotopic labels. Multiplexed detection would allow simultaneous analysis of both mass tags from only one sample.

Furthermore, enzyme activity is changing in the progression of an inflammation, so that the severity of an inflammation can be monitored. For example, the concentration of MMP-8 and MMP-9 was measured in synovial fluid from rheumatoid arthritis patients, and an increase in enzyme concentrations in advanced stage compared to early stage RA was observed.[9] With the optimized mass tag reporter family, the enzyme activity not only at a certain time point is measurable (like with enzyme-linked immunosorbent assay (ELISA)) but also the development of enzyme activity over a specific period of time. This is achieved by comparing the signal intensity peaks from the L-reporter to its D-equivalent. The changes in L/D ratio depict the extent of increased enzyme activity.

5. Summary

The mass reporters consisting of an affinity tag, followed by TEV peptide sequence, the mass tag sequence, and 3-amino-3-(2-nitrophenyl)propionic acid, a photosensitive molecule that is positioned next to a protease-sensitive sequence and the TG-sequence (D-chain of IGF-I) provide a detection system for *in vitro* enzyme activity. The elevated levels of proteases cleaved the incorporated PSS with L-amino acids but not the D-amino acid version and released the mass tag containing reporter fragment. After a three-step purification the mass tags were analyzed by tandem mass spectrometry. Their signal intensity ratio of L-amino acid reporter to D-amino acid reporter after incubation in buffer (control) was subtracted from the intensity ratio after incubation with MMP-9 and referred to a specific cleavage event of the applied PSS. Since the mass reporters were locally immobilized, the protease activity in different tissues (e.g. diseased and healthy) can be observed and measured simultaneously by drawing only one sample.

The outlined protocols offer a step-by-step instruction on how to (i) design the mass encoded peptide sequences that can be analyzed by tandem mass spectrometry and provide multiplexed measurements, (ii) incorporate a protease-sensitive linker into the sequence that is cleaved by specific disease-associated proteases, and (iii) use the IGF-I D-domain to covalently couple the mass reporters to ECM by transglutaminase catalyzed reaction.

Abbreviations

AA	Amino acid
AF488	Alexa fluor 488
AGC	Automated gain control
ANP	Fmoc-(*S*)-3-amino-3-(2-nitrophenyl)propionic acid
BCA	Bicinchoninic acid
BCS	Bovine calf serum
Biotin-Ahx	Biotin-aminohexanoic acid
BSA	Bovine serum albumin
CID or HCD	collision induced dissociation or high-energy collision dissociation
CLSM	Confocal laser scanning microscopy
DCM	Dichlormethane
DIC	N,N′-Diisopropylcarbodiimide
DIPEA	Diisopropylethylamin
DMEM	Dulbecco's Modified Eagle Medium
DMF	Dimethylformamid
DMSO	Dimethyl sulfoxide
ECM	Extracellular matrix
EDTA	Ethylenediaminetetraacetate
ELISA	Enzyme linked immunosorbent assay
FXIIIa	activated factor XIII
HRP	Horseradish peroxidase
IGF-I	Insulin-like growth factor I
LAF	Laminar air flowLC-MS/MS Tandem mass spectrometry
Mt	Mass tag
MMP	Matrix metalloproteinase
PBS	Phosphate buffered saline
Pen/Strep or P/S	Penicillin and Streptomycin
PSS	Protease-sensitive sequence
PTFE	Polytetrafluoroethylene
TEV	Tobacco Etch Virus
TFA	Trifluoracetic acid
TIS	Triisopropylsilane
TMB	3,3′,5,5′-Tetramethylbenzidine

Acknowledgments

Technical support is kindly acknowledged for Dr. Büchner and his team from the Organic Chemistry Department of the University of Wuerzburg regarding MALDI and ESI-MS measurements and for Matthias Beudert and Niklas Hautpstein who supported the confocal laser scanning microscopy images. Financial support is kindly acknowledged by the German Research Foundation (DFG) through the Sino-German Center (Grant # ME3820/3-1).

References

1. Kay, A. B., Asthma and inflammation. *Journal of Allergy and Clinical Immunology* **1991,** *87* (5), 893-910.
2. Goldring, M. B.; Otero, M., Inflammation in osteoarthritis. *Curr Opin Rheumatol* **2011,** *23* (5), 471-8.
3. Berenbaum, F., Osteoarthritis as an inflammatory disease (osteoarthritis is not osteoarthrosis!). *Osteoarthritis Cartilage* **2013,** *21* (1), 16-21.
4. Rubin, D. C.; Shaker, A.; Levin, M. S., Chronic intestinal inflammation: inflammatory bowel disease and colitis-associated colon cancer. *Front Immunol* **2012,** *3*, 107.
5. Hansson, G. K., Inflammation, atherosclerosis, and coronary artery disease. *N Engl J Med* **2005,** *352* (16), 1685-95.
6. Freemont, A. J.; Hampson, V.; Tilman, R.; Goupille, P.; Taiwo, Y.; Hoyland, J. A., Gene expression of matrix metalloproteinases 1, 3, and 9 by chondrocytes in osteoarthritic human knee articular cartilage is zone and grade specific. *Ann Rheum Dis* **1997,** *56* (9), 542-9.
7. Shlopov, B. V.; Lie, W. R.; Mainardi, C. L.; Cole, A. A.; Chubinskaya, S.; Hasty, K. A., Osteoarthritic lesions: involvement of three different collagenases. *Arthritis Rheum* **1997,** *40* (11), 2065-74.
8. Woessner, J. F., Jr.; Gunja-Smith, Z., Role of metalloproteinases in human osteoarthritis. *The Journal of rheumatology. Supplement* **1991,** *27*, 99-101.
9. Yoshihara, Y.; Nakamura, H.; Obata, K.; Yamada, H.; Hayakawa, T.; Fujikawa, K.; Okada, Y., Matrix metalloproteinases and tissue inhibitors of metalloproteinases in synovial fluids from patients with rheumatoid arthritis or osteoarthritis. *Ann Rheum Dis* **2000,** *59* (6), 455-461.
10. Nagase, H.; Visse, R.; Murphy, G., Structure and function of matrix metalloproteinases and TIMPs. *Cardiovasc Res* **2006,** *69* (3), 562-73.
11. Murphy, G.; Knauper, V.; Atkinson, S.; Butler, G.; English, W.; Hutton, M.; Stracke, J.; Clark, I., Matrix metalloproteinases in arthritic disease. *Arthritis research* **2002,** *4 Suppl 3*, S39-49.
12. Jablonska-Trypuc, A.; Matejczyk, M.; Rosochacki, S., Matrix metalloproteinases (MMPs), the main extracellular matrix (ECM) enzymes in collagen degradation, as a target for anticancer drugs. *J Enzyme Inhib Med Chem* **2016,** *31* (sup1), 177-183.
13. Hay, Cell Biology of Extracellular Matrix. **1991**.
14. Bateman, J. F.; Boot-Handford, R. P.; Lamande, S. R., Genetic diseases of connective tissues: cellular and extracellular effects of ECM mutations. *Nat Rev Genet* **2009,** *10* (3), 173-83.
15. Humphrey, J. D.; Dufresne, E. R.; Schwartz, M. A., Mechanotransduction and extracellular matrix homeostasis. *Nat Rev Mol Cell Biol* **2014,** *15* (12), 802-12.
16. Hynes, R. O., The extracellular matrix: not just pretty fibrils. *Science* **2009,** *326* (5957), 1216-9.
17. Van Doren, S. R., Matrix metalloproteinase interactions with collagen and elastin. *Matrix Biol* **2015,** *44-46*, 224-31.
18. Klein, G.; Vellenga, E.; Fraaije, M. W.; Kamps, W. A.; de Bont, E. S., The possible role of matrix metalloproteinase (MMP)-2 and MMP-9 in cancer, e.g. acute leukemia. *Crit Rev Oncol Hematol* **2004,** *50* (2), 87-100.
19. Schoser, B. G.; Blottner, D.; Stuerenburg, H. J., Matrix metalloproteinases in inflammatory myopathies: enhanced immunoreactivity near atrophic myofibers. *Acta Neurol Scand* **2002,** *105* (4), 309-13.
20. Hoshino, M.; Nakamura, Y.; Sim, J.; Shimojo, J.; Isogai, S., Bronchial subepithelial fibrosis and expression of matrix metalloproteinase-9 in asthmatic airway inflammation☆☆☆★★★. *Journal of Allergy and Clinical Immunology* **1998,** *102* (5), 783-788.
21. Hu, J.; Van den Steen, P. E.; Sang, Q. X.; Opdenakker, G., Matrix metalloproteinase inhibitors as therapy for inflammatory and vascular diseases. *Nat Rev Drug Discov* **2007,** *6* (6), 480-98.

22. Kwong, G. A.; von Maltzahn, G.; Murugappan, G.; Abudayyeh, O.; Mo, S.; Papayannopoulos, I. A.; Sverdlov, D. Y.; Liu, S. B.; Warren, A. D.; Popov, Y.; Schuppan, D.; Bhatia, S. N., Mass-encoded synthetic biomarkers for multiplexed urinary monitoring of disease. *Nature biotechnology* **2013,** *31* (1), 63-70.
23. Warren, A. D.; Gaylord, S. T.; Ngan, K. C.; Dumont Milutinovic, M.; Kwong, G. A.; Bhatia, S. N.; Walt, D. R., Disease detection by ultrasensitive quantification of microdosed synthetic urinary biomarkers. *J Am Chem Soc* **2014,** *136* (39), 13709-14.
24. Lin, K. Y.; Kwong, G. A.; Warren, A. D.; Wood, D. K.; Bhatia, S. N., Nanoparticles that sense thrombin activity as synthetic urinary biomarkers of thrombosis. *ACS Nano* **2013,** *7* (10), 9001-9.
25. Lee, S.; Cha, E. J.; Park, K.; Lee, S. Y.; Hong, J. K.; Sun, I. C.; Kim, S. Y.; Choi, K.; Kwon, I. C.; Kim, K.; Ahn, C. H., A near-infrared-fluorescence-quenched gold-nanoparticle imaging probe for in vivo drug screening and protease activity determination. *Angew Chem Int Ed Engl* **2008,** *47* (15), 2804-7.
26. Lai, W. F.; Chang, C. H.; Tang, Y.; Bronson, R.; Tung, C. H., Early diagnosis of osteoarthritis using cathepsin B sensitive near-infrared fluorescent probes. *Osteoarthritis Cartilage* **2004,** *12* (3), 239-44.
27. Weissleder, R.; Tung, C. H.; Mahmood, U.; Bogdanov, A., Jr., In vivo imaging of tumors with protease-activated near-infrared fluorescent probes. *Nature biotechnology* **1999,** *17* (4), 375-8.
28. Lowe, S. B.; Dick, J. A.; Cohen, B. E.; Stevens, M. M., Multiplex sensing of protease and kinase enzyme activity via orthogonal coupling of quantum dot-peptide conjugates. *ACS Nano* **2012,** *6* (1), 851-7.
29. Franco-Barraza, J.; Beacham, D. A.; Amatangelo, M. D.; Cukierman, E., Preparation of Extracellular Matrices Produced by Cultured and Primary Fibroblasts. *Curr Protoc Cell Biol* **2016,** *71*, 10 9 1-10 9 34.
30. Braun, A. C.; Gutmann, M.; Mueller, T. D.; Luhmann, T.; Meinel, L., Bioresponsive release of insulin-like growth factor-I from its PEGylated conjugate. *J Control Release* **2018,** *279*, 17-28.
31. Fontana, A.; Spolaore, B.; Mero, A.; Veronese, F. M., Site-specific modification and PEGylation of pharmaceutical proteins mediated by transglutaminase. *Advanced drug delivery reviews* **2008,** *60* (1), 13-28.
32. Luhmann, T.; Meinel, L., Nanotransporters for drug delivery. *Curr Opin Biotechnol* **2016,** *39*, 35-40.
33. Lühmann, T.; Spieler, V.; Werner, V.; Ludwig, M. G.; Fiebig, J.; Mueller, T. D.; Meinel, L., Interleukin-4-Clicked Surfaces Drive M2 Macrophage Polarization. *Chembiochem* **2016,** *17* (22), 2123-2128.
34. Ritzer, J.; Luhmann, T.; Rode, C.; Pein-Hackelbusch, M.; Immohr, I.; Schedler, U.; Thiele, T.; Stubinger, S.; Rechenberg, B. V.; Waser-Althaus, J.; Schlottig, F.; Merli, M.; Dawe, H.; Karpisek, M.; Wyrwa, R.; Schnabelrauch, M.; Meinel, L., Diagnosing peri-implant disease using the tongue as a 24/7 detector. *Nat Commun* **2017,** *8*.
35. Sato, H., Enzymatic procedure for site-specific pegylation of proteins. *Advanced drug delivery reviews* **2002,** *54* (4), 487-504.
36. Spieler, V.; Ludwig, M. G.; Dawson, J.; Tigani, B.; Littlewood-Evans, A.; Safina, C.; Ebersbach, H.; Seuwen, K.; Raschig, M.; Ter Mors, B.; Muller, T. D.; Meinel, L.; Luhmann, T., Targeting interleukin-4 to the arthritic joint. *J Control Release* **2020,** *326*, 172-180.
37. Wu, F.; Braun, A.; Lühmann, T.; Meinel, L., Site-Specific Conjugated Insulin-like Growth Factor-I for Anabolic Therapy. *ACS BIOMATER-SCI ENG* **2018,** *4* (3), 819-825.
38. Sakiyama-Elbert, S. E.; Hubbell, J. A., Development of fibrin derivatives for controlled release of heparin-binding growth factors. *Journal of Controlled Release* **2000,** *65* (3), 389-402.
39. Sanborn, T. J.; Messersmith, P. B.; Barron, A. E., In situ crosslinking of a biomimetic peptide-PEG hydrogel via thermally triggered activation of factor XIII. *Biomaterials* **2002,** *23* (13), 2703-2710.

40. Schense, J. C.; Hubbell, J. A., Cross-linking exogenous bifunctional peptides into fibrin gels with factor XIIIa. *Bioconjug Chem* **1999,** *10* (1), 75-81.
41. Ehrbar, M.; Rizzi, S. C.; Schoenmakers, R. G.; Miguel, B. S.; Hubbell, J. A.; Weber, F. E.; Lutolf, M. P., Biomolecular hydrogels formed and degraded via site-specific enzymatic reactions. *Biomacromolecules* **2007,** *8* (10), 3000-7.
42. Song, W.; Tang, Z.; Zhang, D.; Li, M.; Gu, J.; Chen, X., A cooperative polymeric platform for tumor-targeted drug delivery. *Chem Sci* **2016,** *7* (1), 728-736.
43. Fesus, L.; Piacentini, M., Transglutaminase 2: an enigmatic enzyme with diverse functions. *Trends in Biochemical Sciences* **2002,** *27* (10), 534-539.
44. Akimov, S. S.; Krylov, D.; Fleischman, L. F.; Belkin, A. M., Tissue transglutaminase is an integrin-binding adhesion coreceptor for fibronectin. *J Cell Biol* **2000,** *148* (4), 825-38.
45. Dodt, K.; Lamer, S.; Driessen, M.; Bölch, S.; Schlosser, A.; Lühmann, T.; Meinel, L., Mass-encoded reporters reporting proteolytic activity from within the extracellular matrix. *ACS Biomaterials Science & Engineering* **2020**.
46. Vaisar, T.; Urban, J., Probing the proline effect in CID of protonated peptides. *J Mass Spectrom* **1996,** *31* (10), 1185-7.
47. Huang, Y.; Tseng, G. C.; Yuan, S.; Pasa-Tolic, L.; Lipton, M. S.; Smith, R. D.; Wysocki, V. H., A data-mining scheme for identifying peptide structural motifs responsible for different MS/MS fragmentation intensity patterns. *J Proteome Res* **2008,** *7* (1), 70-9.
48. Sullivan, A. G.; Brancia, F. L.; Tyldesley, R.; Bateman, R.; Sidhu, K.; Hubbard, S. J.; Oliver, S. G.; Gaskell, S. J., The exploitation of selective cleavage of singly protonated peptide ions adjacent to aspartic acid residues using a quadrupole orthogonal time-of-flight mass spectrometer equipped with a matrix-assisted laser desorption/ionization source. *International Journal of Mass Spectrometry* **2001,** *210* (1-3), 665-676.
49. Ross, P. L.; Huang, Y. L. N.; Marchese, J. N.; Williamson, B.; Parker, K.; Hattan, S.; Khainovski, N.; Pillai, S.; Dey, S.; Daniels, S.; Purkayastha, S.; Juhasz, P.; Martin, S.; Bartlet-Jones, M.; He, F.; Jacobson, A.; Pappin, D. J., Multiplexed protein quantitation in Saccharomyces cerevisiae using amine-reactive isobaric tagging reagents. *Mol Cell Proteomics* **2004,** *3* (12), 1154-1169.
50. Thompson, A.; Schafer, J.; Kuhn, K.; Kienle, S.; Schwarz, J.; Schmidt, G.; Neumann, T.; Johnstone, R.; Mohammed, A. K.; Hamon, C., Tandem mass tags: a novel quantification strategy for comparative analysis of complex protein mixtures by MS/MS. *Anal Chem* **2003,** *75* (8), 1895-904.
51. Parks, W. C.; Wilson, C. L.; Lopez-Boado, Y. S., Matrix metalloproteinases as modulators of inflammation and innate immunity. *Nat Rev Immunol* **2004,** *4* (8), 617-29.
52. Nagase, H. F., G., Human matrix metalloproteinase specificity studies using collagen sequence-based synthetic peptides. *Biopolymers* **1996,** *40*.
53. Pinnell, S. R., Regulation of collagen biosynthesis by ascorbic acid: a review. *Yale J Biol Med* **1985,** *58* (6), 553-9.
54. Frantz, C.; Stewart, K. M.; Weaver, V. M., The extracellular matrix at a glance. *J Cell Sci* **2010,** *123* (Pt 24), 4195-200.
55. Naba, A.; Pearce, O. M. T.; Del Rosario, A.; Ma, D.; Ding, H.; Rajeeve, V.; Cutillas, P. R.; Balkwill, F. R.; Hynes, R. O., Characterization of the Extracellular Matrix of Normal and Diseased Tissues Using Proteomics. *J Proteome Res* **2017,** *16* (8), 3083-3091.
56. Shao, X.; Taha, I. N.; Clauser, K. R.; Gao, Y. T.; Naba, A., MatrisomeDB: the ECM-protein knowledge database. *Nucleic Acids Res* **2020,** *48* (D1), D1136-D1144.
57. Yamada, K. M., Extracellular Matrix. *Current Protocols in Cell Biology* **2009,** *45* (1), 10.0.1-10.0.3.
58. Walma, D. A. C.; Yamada, K. M., The extracellular matrix in development. *Development* **2020,** *147* (10).

59. Murphy, G.; Nagase, H., Progress in matrix metalloproteinase research. *Mol Aspects Med* **2008,** *29* (5), 290-308.
60. Ranga, A.; Lutolf, M. P.; Hilborn, J.; Ossipov, D. A., Hyaluronic Acid Hydrogels Formed in Situ by Transglutaminase-Catalyzed Reaction. *Biomacromolecules* **2016,** *17* (5), 1553-60.
61. Chandrawati, R.; Stevens, M. M., Controlled assembly of peptide-functionalized gold nanoparticles for label-free detection of blood coagulation Factor XIII activity. *Chemical Communications* **2014,** *50* (41).
62. Choi, Y. C.; Dalakas, M. C., Expression of matrix metalloproteinases in the muscle of patients with inflammatory myopathies. *Neurology* **2000,** *54* (1), 65-71.
63. Galis, Z. S.; Sukhova, G. K.; Lark, M. W.; Libby, P., Increased expression of matrix metalloproteinases and matrix degrading activity in vulnerable regions of human atherosclerotic plaques. *The Journal of clinical investigation* **1994,** *94* (6), 2493-503.
64. Goldring, M. B.; Otero, M.; Plumb, D. A.; Dragomir, C.; Favero, M.; El Hachem, K.; Hashimoto, K.; Roach, H. I.; Olivotto, E.; Borzi, R. M.; Marcu, K. B., Roles of inflammatory and anabolic cytokines in cartilage metabolism: signals and multiple effectors converge upon MMP-13 regulation in osteoarthritis. *European cells & materials* **2011,** *21*, 202-20.
65. Nwomeh, B. C.; Liang, H. X.; Cohen, I. K.; Yager, D. R., MMP-8 is the predominant collagenase in healing wounds and nonhealing ulcers. *J Surg Res* **1999,** *81* (2), 189-95.
66. Elsadek, B.; Graeser, R.; Warnecke, A.; Unger, C.; Saleem, T.; El-Melegy, N.; Madkor, H.; Kratz, F., Optimization of an albumin-binding prodrug of Doxorubicin that is cleaved by prostate-specific antigen. *ACS Med Chem Lett* **2010,** *1* (5), 234-8.
67. Tanihara, M.; Suzuki, Y.; Nishimura, Y.; Suzuki, K.; Kakimaru, Y.; Fukunishi, Y., A novel microbial infection-responsive drug release system. *J Pharm Sci* **1999,** *88* (5), 510-4.
68. Lee, E. S.; Na, K.; Bae, Y. H., Super pH-sensitive multifunctional polymeric micelle. *Nano Lett* **2005,** *5* (2), 325-9.
69. Choi, S. W.; Zhang, Y.; Xia, Y., A temperature-sensitive drug release system based on phase-change materials. *Angew Chem Int Ed Engl* **2010,** *49* (43), 7904-8.
70. de Gracia Lux, C.; Joshi-Barr, S.; Nguyen, T.; Mahmoud, E.; Schopf, E.; Fomina, N.; Almutairi, A., Biocompatible polymeric nanoparticles degrade and release cargo in response to biologically relevant levels of hydrogen peroxide. *J Am Chem Soc* **2012,** *134* (38), 15758-64.
71. Geborek, P.; Saxne, T.; Pettersson, H.; Wollheim, F. A., Synovial fluid acidosis correlates with radiological joint destruction in rheumatoid arthritis knee joints. *J Rheumatol* **1989,** *16* (4), 468-72.
72. Barar, J.; Omidi, Y., Dysregulated pH in Tumor Microenvironment Checkmates Cancer Therapy. *Bioimpacts* **2013,** *3* (4), 149-62.
73. Kato, Y.; Ozawa, S.; Miyamoto, C.; Maehata, Y.; Suzuki, A.; Maeda, T.; Baba, Y., Acidic extracellular microenvironment and cancer. *Cancer Cell Int* **2013,** *13* (1), 89.
74. Ye, W. L.; Zhao, Y. P.; Na, R.; Li, F.; Mei, Q. B.; Zhao, M. G.; Zhou, S. Y., Actively targeted delivery of doxorubicin to bone metastases by a pH-sensitive conjugation. *J Pharm Sci* **2015,** *104* (7), 2293-303.
75. Lv, S.; Tang, Z.; Zhang, D.; Song, W.; Li, M.; Lin, J.; Liu, H.; Chen, X., Well-defined polymer-drug conjugate engineered with redox and pH-sensitive release mechanism for efficient delivery of paclitaxel. *J Control Release* **2014,** *194*, 220-7.
76. Mort, J. S.; Buttle, D. J., Cathepsin B. *The International Journal of Biochemistry & Cell Biology* **1997,** *29* (5), 715-720.
77. Toki, B. E.; Cerveny, C. G.; Wahl, A. F.; Senter, P. D., Protease-mediated fragmentation of p-amidobenzyl ethers: a new strategy for the activation of anticancer prodrugs. *J Org Chem* **2002,** *67* (6), 1866-72.
78. Dubowchik, G. M.; Firestone, R. A., Cathepsin B-sensitive dipeptide prodrugs. 1. A model study of structural requirements for efficient release of doxorubicin. *Bioorganic & Medicinal Chemistry Letters* **1998,** *8* (23), 3341-3346.

79. Dubowchik, G. M.; Mosure, K.; Knipe, J. O.; Firestone, R. A., Cathepsin B-sensitive dipeptide prodrugs. 2. Models of anticancer drugs paclitaxel (Taxol®), mitomycin C and doxorubicin. *Bioorganic & Medicinal Chemistry Letters* **1998,** *8* (23), 3347-3352.
80. Ross, P. L.; Huang, Y. N.; Marchese, J. N.; Williamson, B.; Parker, K.; Hattan, S.; Khainovski, N.; Pillai, S.; Dey, S.; Daniels, S.; Purkayastha, S.; Juhasz, P.; Martin, S.; Bartlet-Jones, M.; He, F.; Jacobson, A.; Pappin, D. J., Multiplexed protein quantitation in Saccharomyces cerevisiae using amine-reactive isobaric tagging reagents. *Mol Cell Proteomics* **2004,** *3* (12), 1154-69.
81. Ishiguro, N.; Ito, T.; Oguchi, T.; Kojima, T.; Iwata, H.; Ionescu, M.; Poole, A. R., Relationships of matrix metalloproteinases and their inhibitors to cartilage proteoglycan and collagen turnover and inflammation as revealed by analyses of synovial fluids from patients with rheumatoid arthritis. *Arthritis & Rheumatism* **2001,** *44* (11), 2503-2511.
82. Tchetverikov, I.; Ronday, H. K.; Van El, B.; Kiers, G. H.; Verzijl, N.; TeKoppele, J. M.; Huizinga, T. W.; DeGroot, J.; Hanemaaijer, R., MMP profile in paired serum and synovial fluid samples of patients with rheumatoid arthritis. *Ann Rheum Dis* **2004,** *63* (7), 881-3.
83. Vignola, A. M.; Riccobono, L.; Mirabella, A.; Profita, M.; Chanez, P.; Bellia, V.; Mautino, G.; D'Accardi, P.; Bousquet, J.; Bonsignore, G., Sputum metalloproteinase-9/tissue inhibitor of metalloproteinase-1 ratio correlates with airflow obstruction in asthma and chronic bronchitis. *Am J Respir Crit Care Med* **1998,** *158* (6), 1945-50.
84. Simpson, J. L.; Scott, R. J.; Boyle, M. J.; Gibson, P. G., Differential proteolytic enzyme activity in eosinophilic and neutrophilic asthma. *Am J Respir Crit Care Med* **2005,** *172* (5), 559-65.
85. Mercer, P. F.; Shute, J. K.; Bhowmik, A.; Donaldson, G. C.; Wedzicha, J. A.; Warner, J. A., MMP-9, TIMP-1 and inflammatory cells in sputum from COPD patients during exacerbation. *Respir Res* **2005,** *6*, 151.
86. Vernooy, J. H.; Lindeman, J. H.; Jacobs, J. A.; Hanemaaijer, R.; Wouters, E. F., Increased activity of matrix metalloproteinase-8 and matrix metalloproteinase-9 in induced sputum from patients with COPD. *Chest* **2004,** *126* (6), 1802-10.
87. Wysocki, A. B.; Staiano-Coico, L.; Grinnell, F., Wound fluid from chronic leg ulcers contains elevated levels of metalloproteinases MMP-2 and MMP-9. *J Invest Dermatol* **1993,** *101* (1), 64-8.
88. Soriano, A.; Garcia, S.; Bori, G.; Almela, M.; Gallart, X.; Macule, F.; Sierra, J.; Martinez, J. A.; Suso, S.; Mensa, J., Treatment of acute post-surgical infection of joint arthroplasty. *Clin Microbiol Infect* **2006,** *12* (9), 930-3.
89. Martinez-Pastor, J. C.; Macule-Beneyto, F.; Suso-Vergara, S., Acute infection in total knee arthroplasty: diagnosis and treatment. *Open Orthop J* **2013,** *7*, 197-204.
90. Drapeau, G. R., Role of metalloprotease in activation of the precursor of staphylococcal protease. *J Bacteriol* **1978,** *136* (2), 607-13.
91. Karlsson, A.; Saravia-Otten, P.; Tegmark, K.; Morfeldt, E.; Arvidson, S., Decreased amounts of cell wall-associated protein A and fibronectin-binding proteins in Staphylococcus aureus sarA mutants due to up-regulation of extracellular proteases. *Infect Immun* **2001,** *69* (8), 4742-8.
92. Gonzalez, D. J.; Okumura, C. Y.; Hollands, A.; Kersten, R.; Akong-Moore, K.; Pence, M. A.; Malone, C. L.; Derieux, J.; Moore, B. S.; Horswill, A. R.; Dixon, J. E.; Dorrestein, P. C.; Nizet, V., Novel phenol-soluble modulin derivatives in community-associated methicillin-resistant Staphylococcus aureus identified through imaging mass spectrometry. *J Biol Chem* **2012,** *287* (17), 13889-98.

1 Chapter 1: A complete and versatile Protocol: Decoration of cell-derived matrices with mass-encoded peptides for multiplexed enzyme activity detection

CHAPTER 2: MASS-ENCODED REPORTERS REPORTING PROTEOLYTIC ACTIVITY FROM WITHIN THE EXTRACELLULAR MATRIX

*Katharina Dodt[1], Stephanie Lamer[2], Marc Drießen[1], Sebastian Bölch[3], Andreas Schlosser[2], Tessa Lühmann[1], Lorenz Meinel[1,]**

[1] Institute of Pharmacy and Food Chemistry, University of Wuerzburg, Am Hubland, 97074 Wuerzburg, Germany

[2] Rudolf-Virchow-Center for Experimental Biomedicine, University of Wuerzburg, Josef-Schneider-Str. 2, 97080 Wuerzburg, Germany

[3] Department for Orthopedic Surgery, Koenig-Ludwig-Haus, University of Wuerzburg, Brettreichstrasse 11, 97074, Wuerzburg, Germany

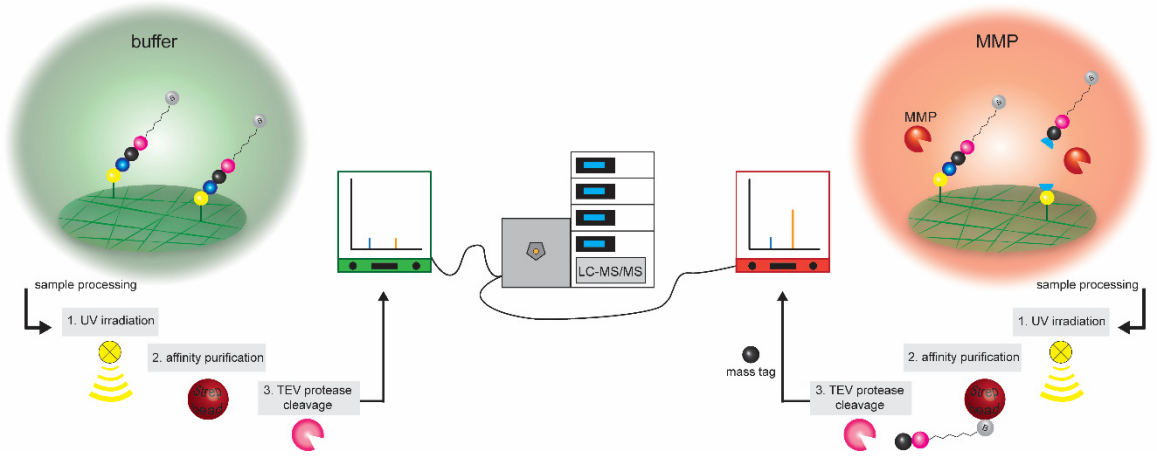

Abstract

Reporting matrix metalloproteinase (MMP) activity directly from the extracellular matrix (ECM) may provide critical insights to better characterize 2D and 3D cell culture model systems of inflammatory diseases and potentially leverage *in vivo* diagnosis. In this proof of concept study, we designed MMP-sensors, which were covalently linked onto the ECM by co-administration of the activated transglutaminase factor XIIIa (FXIIIa). Elements of the featured MMP-sensors are the D-domain of Insulin-like growth factor I (IGF-I) through which co-administered FXIIIa covalently links the sensor to the ECM followed by an MMP sensitive peptide sequence and locally reporting on MMP activity, an isotopically labeled mass tag encoding for protease activity, and an affinity tag facilitating purification from fluids. All sensors come in identical pairs, other than the MMP sensitive peptide sequence, which is synthesized with L-amino acids or D-amino acids, the latter serving as internal standard. As proof of concept for multiplexing, we successfully profiled two MMP-sensors with different MMP sensitive peptide sequences reporting MMP activity directly from engineered 3D ECM. Future use may include covalently ECM bound diagnostic depots reporting MMP activity from inflamed tissues.

Keywords: diagnostic; isotopically labelled peptide; matrix metalloproteinases; extracellular matrix; transglutaminase; tandem mass spectrometry

Introduction

MMPs drive ECM turnover and structural tissue destruction in inflammatory and degenerative arthropathies.[1-3] The proteinases are secreted by both the resident cells of joint tissue and invading cells[4] in response to proinflammatory cytokines, including TNF-α and IL-1β.[5-7] They are present in all disease stages but with different temporal patterns. For example, MMP-1 and -3 are upregulated in early stages of rheumatoid arthritis (RA) and decrease in later stages. In contrast, MMP-8 and -9 start with low levels in early-stage RA and increase with disease progression.[8] Several 3D cell culture models describing aspects of these diseases were developed including systems secreting MMPs.[9] In another study, *in vitro* canine arthritis model chondrocytes secreted proinflammatory cytokines, enzyme mediators (MMP-3, MMP-13) and their catabolites in presence of IL-1β and TNF-α[10] as was observed in co-culture systems of activated macrophages and chondrocytes.[11]

Previously, MMP activity was deployed for bioresponsive diagnostic use and MMP-driven drug delivery applications. For example, an MMP-sensitive peptide linker was formulated into a chewing gum and responded to upregulated salivary and inflammatory proteases of peri-implant disease in the oral cavity by releasing a bitter-tasting molecule, thereby alarming a patient of possible inflammatory complication.[12] Similar systems were used for the release of biopharmaceuticals, including a MMP sensitive peptide for releasing myostatin-inhibitors in response to myositis[13] or to cleave off a half-life prolonging 30kDa polyethylene glycol (PEG)-chain from IGF-I to recover wildtype protein features at the site of disease.[14] In addition, MMPsensitive peptide sequences were used for drug delivery[15-17], or prodrug activation.[18, 19] Protease-sensitive linkers for diagnostic reasons have been the subject to previous studies, including uses like *in vivo* imaging.[20-22] Other studies used tandem mass spectrometry or a paper lateral flow assay. For example, mass-encoded peptides were coupled to a MMP-9 sensitive amino acid sequence, which then was conjugated to iron oxide nanoworms for the diagnosis of liver fibrosis.[23] Another study employed reporters conjugated to nanoparticles via protease-sensitive substrates to diagnose thrombosis and colorectal cancer from urine.[24] The transglutaminase FXIII calcium-dependently catalyzes the covalent formation N-ε-(γ-glutamyl)lysine protein-to-protein or peptide-to-peptide iso-peptide bonds. FXIII is part of the coagulation cascade and is activated by thrombin in presence of Ca^{2+}-ions. FXIIIa stabilizes the fibrin clot by its cross-linking ability. This transglutaminase activity was successfully applied to

covalently load cytokines and growth factors onto hydrogels,[25, 26] tethering biological active peptides to surfaces,[27] or to incorporate peptides into fibrin gels.[28-30]

The major component of the ECM is a three-dimensional and highly organized network composed of fibrous proteins (like collagens of various types), glycoproteins such as fibronectin and laminin and proteoglycans (heparan sulfate, chondroitin sulfate). The components provide tensile strength, elasticity and reversible extensibility or deformation.[31] Each tissue exhibits a unique ECM composition in order to perform cell signaling or, cell-tissue interactions.[32] In this study, we used ECM obtained from NIH 3T3 fibroblasts tissue cultures, a murine cell line. This protocol leads to an artificial ECM characterized by mesh-like fibronectin, collagen type I and III, but not IV and small amounts of laminin and perlecan.[31] 3D ECM generated with these NIH 3T3 fibroblasts has previously been compared to naturally produced ECM. It was shown that the artificial ECM exhibited similarities in terms of matrix composition and geometry compared to natural ECM templates.[33]

Here, we present a proof of concept study for a multiplexed diagnostic peptide depot holding a transglutaminase (TG) sequence for covalently anchoring the mass reporter system (=sensor) to ECM through FXIIIa. The mass tag design followed isobaric mass encoding strategies,[34] allowing the measurement of proteolytic activity in inflamed environment by tandem mass spectrometry. The peptide system consists of two reporter pairs, each pair having the identical MMP sensitive sequence, where one is synthesized with L-amino acids and the other one with noncleavable D-amino acids (internal control). Both pairs have a different sensitivity to MMPs to provide a first proof of concept for (simultaneous) multiplexing of proteolytic activities. The mass reporter pairs were applied in a mix of all four individual reporters (**Figure 1A**). Co-administration of mass reporter mix with FXIIIa immobilized the sensors onto ECM, forming a depot of inflammation-reporting diagnostics (**Figure 1B**). Upon proteolysis, the cleavage of the MMP sensitive peptide sequence occurred and fragments containing the mass tags were released into the incubation medium (**Figure 1C**). To isolate the mass tag peptide sequence from incubation medium and to free it from the adjacent affinity tag and the four remaining amino acid residues remaining from MMP sensitive peptide sequence cleavage, three purification steps were performed: (1) irradiation with UV light, (2) affinity purification with streptavidin-coated beads, (3) incubation with TEV protease (**Figure 1D**). Lastly, the mass tags were analyzed by tandem mass spectrometry, within which the four mass tags eluted at the same

retention time in LC-MS[1] due to their identical parent mass. These fragmented into individual reporter ions in MS[2] with each mass tag having a distinct fragmentation encoding for the respective reporter (**Figure 1E**).

Results

Design of the mass reporter system

We developed protease activity reporter depots for locally monitoring protease activity. The sensors (mass reporters) emulate various functionalities by integration of six functional modules. The mass reporters were designed in pairs and applied as a mix of all four (**Figure 1A**). The C-terminal module #1 consists of the IGF-I D-domain (binding site Lys 68) by which the mass reporters get covalently coupled to the ECM in presence of FXIIIa, which is applied simultaneously with the mass reporter mix (**Figure 1B, S1**).[13, 14, 35-37] This immobilization tag is followed by module #2, the MMP sensitive peptide sequence designed for cleavage in tissue inflammation by various MMPs (**Figure 1C**). The 'MMP sensitive peptide sequence 1' was selected from a previous study on MMP-reporting chewing gums monitoring the oral cavity for protease activity.[12] The amino acid sequence of 'MMP sensitive peptide sequence2' was designed for faster cleavage.[38] Each of the two MMP sensitive peptide sequences have a mirrored version of D-amino acids serving as negative MMP control and resulting in four mass reporters forming two reporter pairs with each pair having one sensor of L- and D-amino acids. Once the mass reporters are released from ECM by proteolysis of the MMP sensitive peptide sequence, the supernatant containing the mass reporters is processed further. Module #3 is a photolabile linker. This enables photoseparation of the MMP sensitive peptide sequence or remaining amino acids from a cleaved MMP sensitive peptide sequence from the subsequent elements of the cleaved mass reporters, one step of the purification process for LC-MS/MS[39, 40] (**Figure 1D**). Module #4 introduces a balanced mass tag for the isobaric mass encoding strategy.[41] The mass reporter further holds module #5, a tobacco etch virus (TEV) protease sequence, to separate module #6 from the mass tags after the cleaved reporter fragments were bound to streptavidin-coated beads by their biotin-label, module #6, in the purification step 2 before LC-MS/MS analysis (**Figure 1D**). Module #6, the biotin label with a hexyl spacer group, is further used for quantification on ECM with streptavidin-horseradish peroxidase (HRP) and 3,3′,5,5′-tetramethylbenzidin (TMB) substrate. The mass tags were designed

having an identical amino acid sequence and an overall introduced mass shift of 6 Da. As the mass tags all share the same parent mass, they were efficiently collected by LC-MS and then fragmented into distinct fragment ions in the second quadrupole (MS/MS or MS^2) allowing the use of identical reporters while differentiation through this isobaric design is possible (**Figure 1E**).[23]

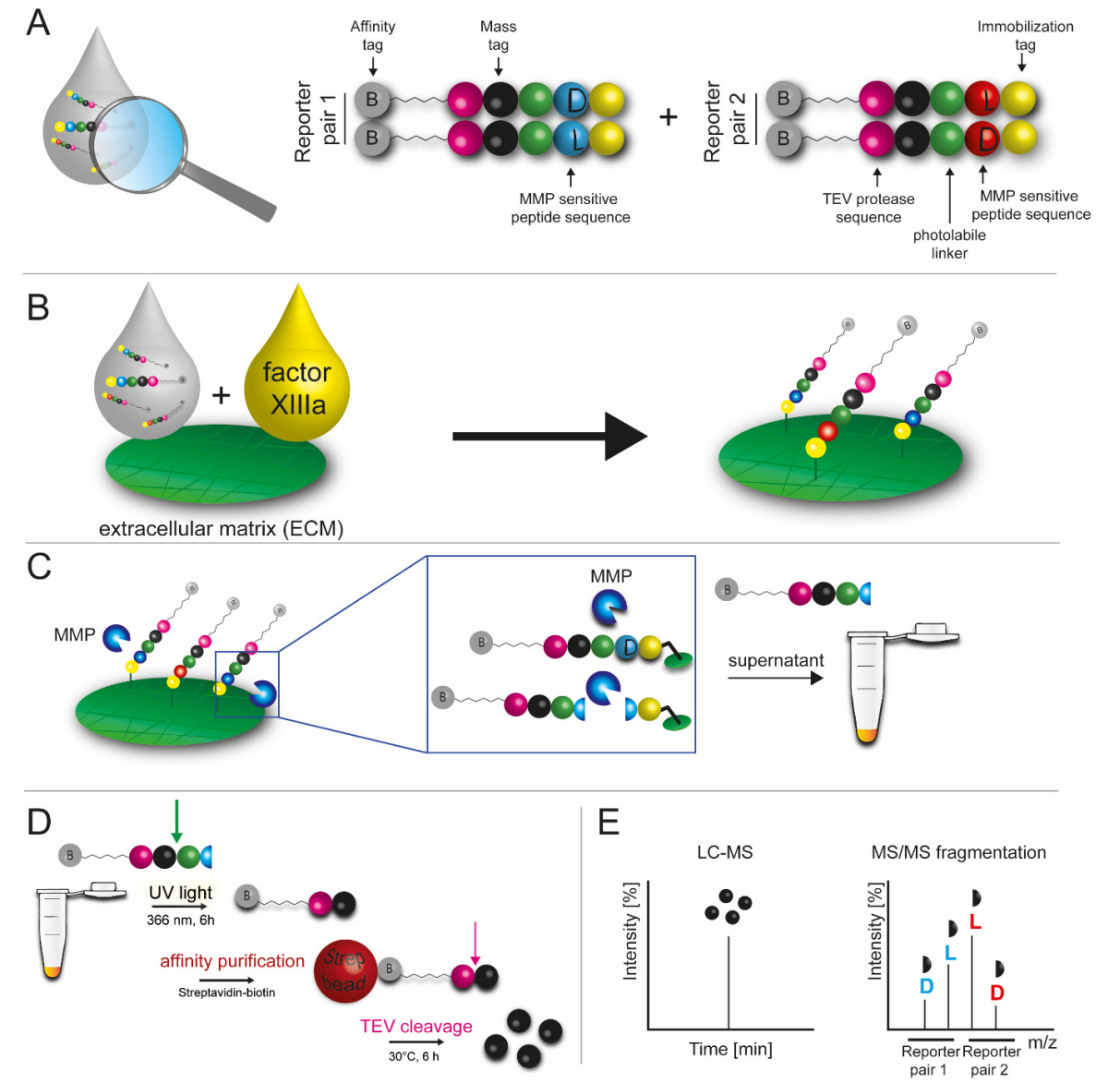

Figure 3 (A) The reporter peptides consist of six modules: an affinity tag (grey), TEV protease sequence (pink), the mass-encoded peptide (black), a photolabile linker (green), a MMP sensitive peptide sequence (blue or red), and an immobilization tag (yellow). The four reporter peptides were used in a mix of all four. (B) The two reporter pairs were bound to the extracellular matrix by FXIIIa. Each reporter pair is identical, with the exception of the MMP substrate sequence, which is either synthesized with D- or L- amino acids. (C) Inflammatory MMPs cleave the MMP sensitive peptide sequence synthesized of L-amino acid but not the D-amino acid version of each reporter pair. Thereby the D-amino acid variant reports on background events such as unspecific ECM adsorption or unspecific turnover of the ECM (internal control), whereas the L-amino acid variants report on background events and specific MMP activity. (D) The supernatant containing the cleaved reporter fragments was purified in three consecutive steps. first by UV irradiation, second by streptavidin-biotin affinity purification, and third by cleavage with TEV protease to release the mass tags. (E) All mass tags have the same parent mass (LC-MS) and fragment into specific ions, which were detected by the second quadrupole (MS^2).

System responsiveness to MMPs

The MMP responsiveness of MMP sensitive peptide sequences 1 and 2 was analyzed by HPLC by comparing the area under the curve of the peptide sequence in absence and presence of MMPs. In our experiments, time-dependent cleavage of MMP sensitive peptide sequences was performed with MMP concentrations of 35.1 nM, 13.2 nM and 10.6 nM for MMP-1, MMP-8 and MMP-9, respectively, approximating previously reported MMP concentrations found in synovial fluid of rheumatoid arthritis patients.[8] MMP-9 cleaved half of the L-amino acid 'MMP sensitive peptide sequences 1' - consisting of GPQGIAGQK$_{N3}$Q –within 5.6 h and plateaued after 20 h with an overall cleavage of 79. ± 11.1 %. 'MMP sensitive peptide sequences 1' responded slower to MMP-1 or MMP-8, with final cleavage efficiencies of 14.2 ± 3.3 % and 11.2 ± 1.1 %, respectively. (**Figure 2A, S2**). The concentration-dependent experiments were performed using an equimolar mix of MMP -1, -8, and -9, with the abscissa depicting the total MMP concentration, e.g., 16 nM = 5.33 nM MMP-1 + 5.33 nM MMP-8 + 5.33 nM MMP-9 (**Figure 2B, D**). Exposure of reporter pair 1 to MMP-1, -8 and -9 for 24 h cleaved the L-amino acid but not the MMP sensitive peptide sequences containing D-amino acids [GpqGiaGqK$_{N3}$Q]. It also demonstrated that the MMP sensitive peptide sequence does to respond to a sharp threshold of MMP concentration, hence being nonresponsive at below 2.5 nM and fully responsive at 8 nM (**Figure 2B, S3**). 'MMP sensitive peptide sequences 2' rapidly responded to MMP-9, resulting in 50 % cleavage within 2.5 h and full cleavage within less than 10 h. This MMP sensitive peptide sequences also responded to MMP-1 – and to a much lower extent to MMP-8 (11.3 ± 1.1 % after 48 h) - resulting in 50 % cleavage within about 20 h and reaching plateau in about 45 h (**Figure 2C, S4**). The 'MMP sensitive peptide sequences 2' did not respond at MMP levels below 0.5 nM but was already fully cleaved at concentrations of 3.2 nM within 24 h. The D-amino acid reporter was not cleaved (**Figure 2D, S5**). 'MMP sensitive peptide sequences 1' has been described before as inter-positioned linker to detect peri-implant disease in response to elevated levels of MMPs or to bioresponsively release myostatin inhibitor in myositis.[12, 13] Furthermore, previous studies on MMP substrate sequences showed that the exchange of amino acids in position P'1-4 to leucine, alanine or histidine improved relative cleavage rate for MMP-1, MMP-8 and MMP-9 as compared to the hydrolysis of sequence Gly-Pro-Gln-Gly~Ile-Ala-Gly-Gln.[38] Following these findings, we exchanged the amino acids in position P´1 + 2 to leucine, P´3 to alanine and P´4 to histidine for 'MMP sensitive peptide sequences 2' to

increase the enzyme cleavage rate compared to 'MMP sensitive peptide sequences 1'. Indeed, cleavage experiments (**Figure 2A, C**) showed the expected outcome in line with afore mentioned studies and MEROPS entries – a peptidase database helping the selection of cleavable peptide sequences - which had leucine instead of isoleucine in position P1' to increase MMP-9 activity (https://www.ebi.ac.uk/merops/cgi-bin/pepsum?id=M10.004;type=P). Immobilizing these two different MMP sensitive peptide sequences with distinct cleavage kinetics allowed us to extend the observation period of protease activity and having a noticeable mass reporter release over 48 h in our *in vitro* setting. Moreover, the noncleavable MMP sensitive peptide sequences synthesized with D-amino acids served as negative controls and their cleavage resistance to MMP-1, -8 and -9 has been demonstrated (**Figure 2B, D**).

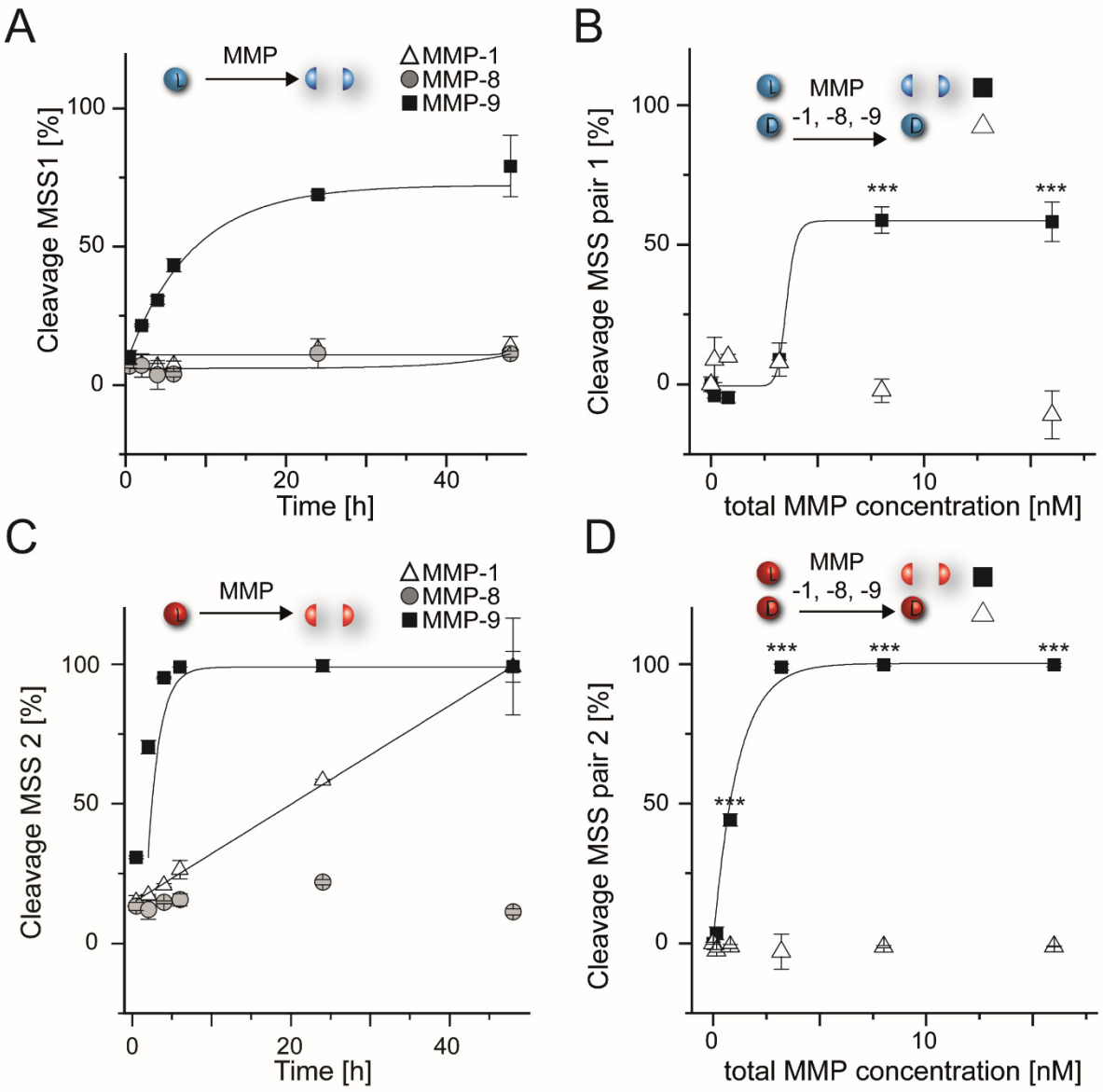

*Figure 2: MMP cleavage of the (A) 'MMP sensitive peptide sequences 1' (GPQGIAGQK$_{N3}$Q) in response to MMP-1, MMP-8, or MMP-9 over 48 h and (B) in response to an equimolar combination of these three MMPs as a function of overall MMP concentration when incubated for 24 h. The corresponding 'MMP sensitive peptide sequences 1' with D-amino acids (negative control) was not cleaved (GpqGiaGqK$_{N3}$Q). MMP cleavage of the (C) 'MMP sensitive peptide sequences 2' (GPSGLLAHK$_{N3}$Q) in response to MMP-1, MMP-8, or MMP-9 and (D) in response to the combination of these three MMPs as a function of overall MMP concentration when incubated for 48 hs. The corresponding 'MMP sensitive peptide sequences 2' with D-amino acids (negative control) was not cleaved (GpsGllahK$_{N3}$Q). Mean ± standard deviation (n = 3; two-sided Student's t-Test * = p < 0.05, ** = p < 0.01, *** = p < 0.001). The curve fit was applied as guide for the eye.*

Immobilization of mass reporters on ECM

The covalent binding of the reporter pairs by FXIIIa to an engineered ECM was analyzed by measuring stability of the mass reporter-decorated ECM after 48 h both in presence and

absence of MMP-9 (**Figure 1B, C or 3A and 3D**). A concentration series (0.75, 7.5, 15 and 30 nmol/mL) of the L-reporter 2 (without isobaric coding) was incubated with 20 U/mL FXIIIa or 20 U/mL recombinant human transglutaminase 2 (rhTG2) or in absence of transglutaminase. Quantification was performed by the reporters' N-terminal biotin label on the ECM by ELISA. ECM's binding capacity was limited at a peptide concentration of 7.5 nmol/mL as seen by the reached plateau. When ECM was incubated with peptides but without transglutaminase, the unspecific binding was concentration-dependent and increased with higher peptide concentrations. Peptide depot formation was performed with 7.5 nmol/mL mass reporters in further experiments to achieve maximum amount of ECM bound peptide and minimize unspecific adsorption (**Figure 3B**). To demonstrate that all four mass reporters possess equal binding capabilities to ECM, they were incubated in presence and absence of FXIIIa and quantified by ELISA. The incubation with FXIIIa showed that the two reporter pairs bind equally well to ECM, while all mass reporters also experienced similar unspecific adsorption to the ECM in the absence of FXIIIa (**Figure 3C**). The incubation with MMP-9 or buffer for 48 h of immobilized mass reporters did not affect the amount of D-amino acid reporter of reporter pair 2 and slightly but significantly of reporter pair 1. Exposure to MMP resulted in statistically reduced amounts of both L-amino acid reporters on the ECM (**Figure 3E**). The binding to and the proteolytic cleavage off the ECM were further detailed by confocal laser scanning microscopy (CLSM) (**Figure 3F, S6, S7**). The mass reporters bound to fibronectin in the presence of FXIIIa and remained bound for 48 h in buffer. Exposure to MMP-9 reduced the amount of mass reporters on the ECM as assessed qualitatively (**Figure 3F**).

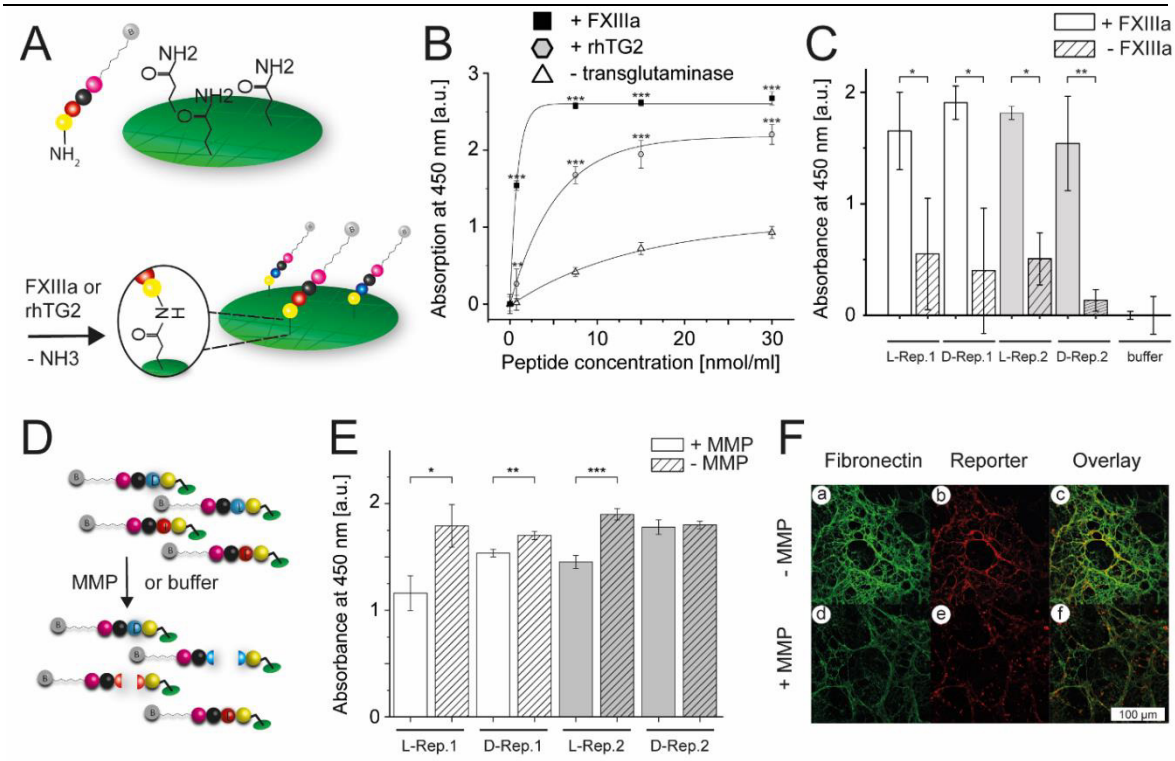

*Figure 3 (A) Transglutaminase catalyzed crosslinking reaction of the peptide's immobilization tag and ECM. (B) Concentration-dependent immobilization of peptide to ECM with either activated human FXIIIa or recombinant human tissue transglutaminase 2 (rhTG2). (C) The amount of reporter decorated onto ECM by FXIIIa was comparable for both reporter pairs and is significantly higher for reporters incubated in presence of FXIIIa than in absence of FXIIIa. All mass reporters showed unspecific adsorption to the ECM in the absence of FXIIIa (mean ± standard deviation (n = 3); no differences according to ANOVA. (D) Immobilized mass reporters were incubated with MMP-9 to release the mass tag containing mass reporter fragment. (E) Cleavage of L-amino acid reporter 1 and 2 was significantly different after 48 h incubation with MMP-9 compared to incubation in buffer. The peptide amount of D-amino acid reporter 1 on ECM was slightly but significantly reduced and of D-amino acid reporter 2 not. (F) CLSM images of ECM bound L-amino acid reporter 2 incubated in buffer (a)-(c) or with MMP-1, -8 and -9 (d)-(f) for 48 h. Mean ± standard deviation; two-sided Student's t-Test * = $p < 0.05$, ** = $p < 0.01$, *** = $p < 0.001$. The curve fit was applied as guide for the eye.*

Purification of mass tags

We now tested the separation, purification, and mass tag release (**Figure 1D, E**). For this purpose, first reporter pair 1 and 2 with L- and D-amino acids were characterized by RP-HPLC and ESI-MS (**Figure 4A**). These analyses showed high peptide purity in HPLC and identified the correct mass of $[M+H]^+$ = 3653.1 g/mol and $[M+H]^+$ = 3677.2 g/mol for reporter pair 1 and 2, respectively.

Irradiation with UV light (λ = 366 nm) cleaved (*S*)-3-amino-3-(2-nitrophenyl)propionic acid by a radical reaction mechanism,[42, 43] separating the amide bond between the photo-sensitive molecule and the mass tag peptide sequence and leaving the mass tag comprising the reporter fragment with a C-terminal amide. Hence, UV-photolysis separated the immobilization tag/ MMP sensitive peptide sequence of the reporter from its mass tag/TEV protease sequence/affinity tag part (**Figure 4B, S8**). The L-amino acid version of reporter

pair 2 (not isotopically labelled) was exemplarily used to demonstrate the photolysis step. For the purpose of isolating the cleaved N-terminal biotinylated peptide fragment from incubation medium, it was purified by affinity purification with streptavidin beads and eluted with 2 % SDS in tris-buffered saline. The reaction was measured by MALDI-TOF, showing the mass of the L-reporter pair 2 before photolysis (singly charged, 3671.9 m/z; **Figure 4C**) and after affinity purification with streptavidin-beads indicating that only the mass tag/TEV protease sequence/affinity tag part remained (singly charged, 1953.9 m/z; expected mass = 1952.2 m/z; **Figure 4D, S9**).

In the standard purification process, the next step after photolysis was the addition of magnetic beads coated with streptavidin to the remaining mass tag/TEV protease sequence/affinity tag part to separate it from the photocleaved peptide fragments by binding the peptide comprising the mass tag to beads via their biotin label. The release of mass tags from the streptavidin beads was performed by incubation with TEV protease, by cleaving the peptide bond between the glutamine of the TEV sequence and the serine of the mass tag sequence. TEV cleavage completed after incubating for 6 h (**Figure 4E, S10**).

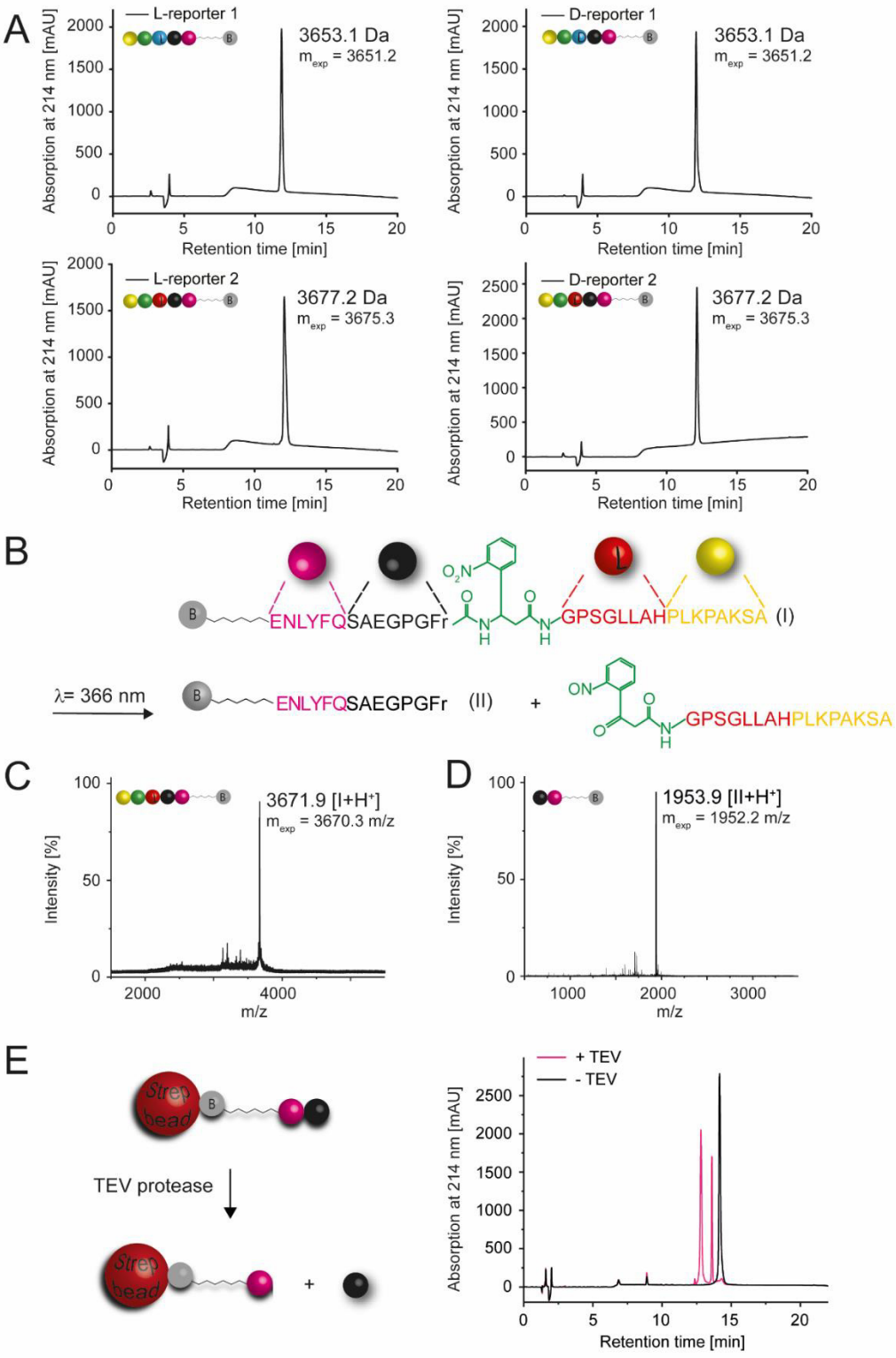

*Figure 4 (A) RP-HPLC chromatograms of reporter pair 1 and 2 and the corresponding masses measured by ESI-MS. (B) Structures of L-amino acids reporter 2 (compound I) containing the affinity tag (gray), the TEV protease sequence (pink), the mass tag (black), an internal UV-sensitive linker (green), followed by the MMP sensitive peptide sequences (here in red), and the immobilization tag (yellow). The free biotinylated mass tag (compound II) was generated after photolysis (~366 nm). LC-MS spectra of compound I (**C**) before (singly charged, 3671.9458 m/z; expected mass = 3670.3 m/z) and (**D**) after (singly charged, 1953,9275 m/z; expected mass = 1952.2 m/z) exposure to UV light. (**E**) Biotinylated mass reporter is bound to magnetic streptavidin beads during purification. To obtain mass tag, the beads were incubated with*

TEV protease. RP-HPLC chromatogram of L-amino acid reporter 2 in presence (pink) and absence (black) of TEV protease.

Mass tag design

The mass tag peptide sequence was designed to form y-type fragment ions in MS^2 following cleavage of the peptide bond between two specific amino acids.[23] To enhance specific amide bond cleavage, proline was inserted in the centre of the sequence - deploying previously reported insights on optimizing y-type ions on amide bond cleavage – N-terminal to the proline residue in collision induced dissociation (CID).[44] Furthermore, it was reported that the cleavage C-terminal to the acidic residues dominated the fragmentation pattern when a N-terminal arginine is present and aspartic acid is at least in a distance of one amino acid or glutamic acid has at least a distance of three amino acids to arginine.[45] According to these findings, our initial mass tags (**Figure S11**) were successfully designed resulting in three major y-ion fragments following CID (**Figure 5A**). As our mass tag library was designed by isobaric mass encoding,[23] the individual members of our mass tag family shared the same parent mass but show unique and distinguishable ions after fragmentation by tandem mass spectrometry. We produced four mass tags centred not only on one fragment ion but on three, namely y_4-, y_5- and y_6-fragment ions. These three reporter ions contained the peptide sequence Pro-Gly-Phe (PGF, highlighted in grey). The reporter ions were produced by enriching the trimer with heavy amino acids during peptide synthesis producing variants differentiated by 1 Da for the reporter pair 1 and by 2 Da for the reporter pair 2. The introduced mass shift was balanced by enriching the balancing ion (SAE or SAEG or SAEGP) with isotopically labelled amino acids. In conclusion a peptide library was developed with four mass tag sequences having identical parent mass but fragment into distinct y-type ions in tandem mass spectrometry. Each mass tag sequence was assigned to a specific MMP sensitive peptide sequence (**Figure 5B**). The mixture of the four mass tags was chromatographically indistinguishable, with each peptide having the same retention time and mass (**Figure 5C**). The mass-to-charge ratio of 413.2 (*m/z*) further fragmented in MS^2 and yielded four separable y-type fragment ions. The four reporter ions corresponding to each MMP sensitive peptide sequence were found with slightly different intensities (**Figure 5D**).

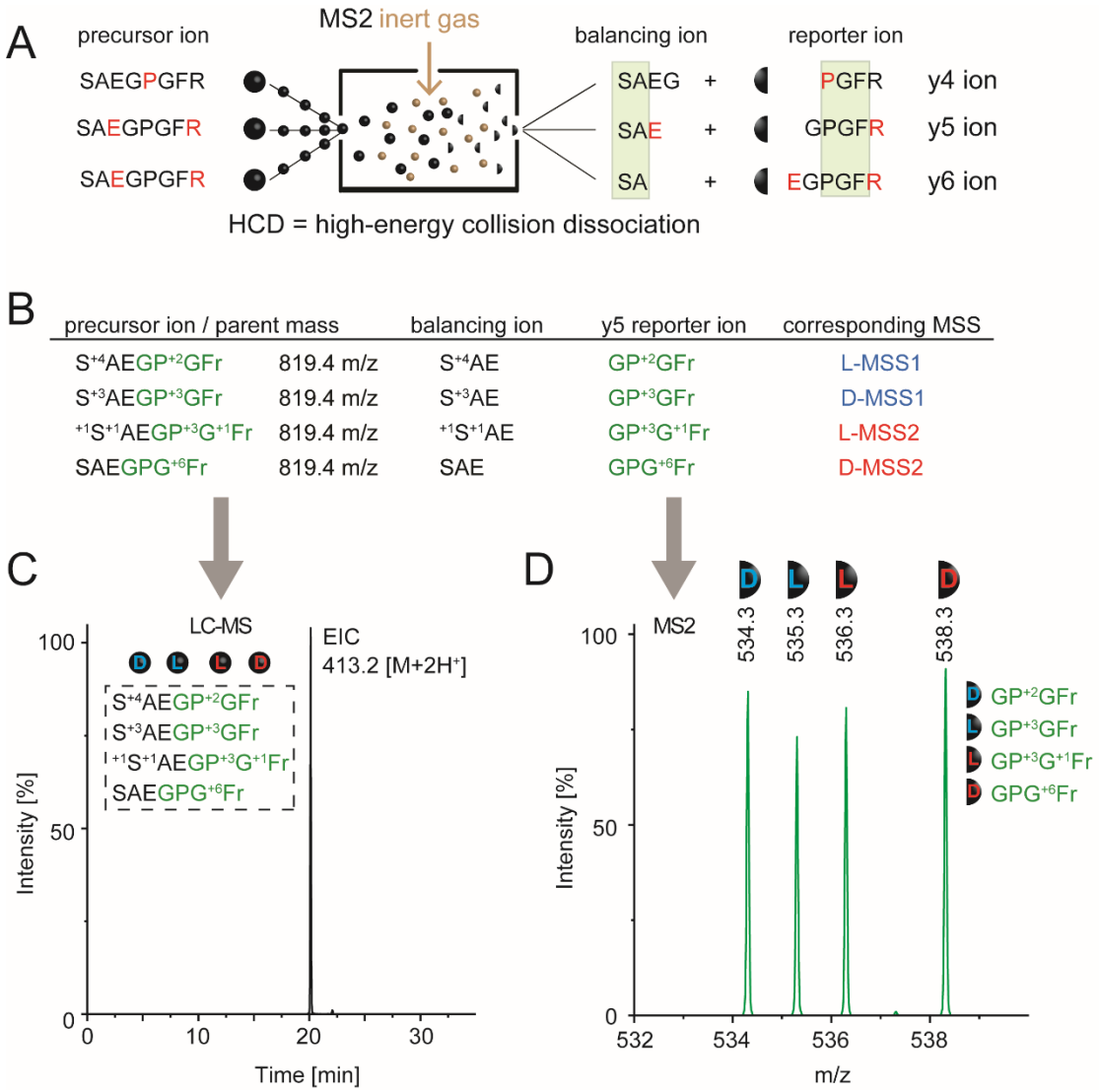

*Figure 5 (A) Overview of fragmentation pattern of mass tags. Insertion of proline, arginine, and glutamic acid influences fragmentation to y-type reporter ions (these amino acids are depicted in red). The precursor ion is selected in MS and subsequently mixed with inert gas for high-energy collision dissociation where reporter ions are created. (B) Precursor ions of reporter pairs 1 and 2 possess same parent masses but distinct reporter ions. These correlate directly with the specific MMP sensitive peptide sequences of the respective reporter pairs. (C) Extracted ion chromatogram (EIC) of a 4-plex peptide mixture (413.2144 ± 22ppm m/z). The entire multiplexed mix was chromatographically indistinguishable. (**D**) MS^2 spectrum of peptide mixture after high energy collision-induced dissociation. Individual mass tags were identified using unique y_5 reporter ions (534.3 – 538.3 m/z).*

Proof of concept

Lastly, the overall functionality including multiplexing was tested as a proof of concept. The two reporter pairs were covalently immobilized onto the ECM by FXIIIa followed by MMP incubation, photolysis, streptavidin-bead purification, release of the mass tags by TEV protease cleavage, and finally mas tag collection by LC-MS[1] and fragmentation and

analysis by MS^2 (**Figure 1D, E**). Before immobilization to ECM, the reporter pairs were purified and analyzed by LC-MS/MS (**Figure S12A**). The reporter pairs were incubated in buffer (**Figure 6A**) or with MMP-9 (**Figure 6B**) for 48 h, and the supernatant was processed as outlined above and analyzed. Due to the experimental setup, variations in absolute intensities between replicates are expected. However, structurally identically reporter pairs are expected to behave identical in this experimental setup. Hence, we choose to normalize to the noncleavable D-linker (i.e., all values are L/D ratios for each condition and reporter pair, each averaged over n=5 experiments) (**Figure 6C**). Overall cleavage was 0.29 ± 0.06 and 0.39 ± 0.22, for reporter pairs 1 and 2, respectively, calculated by subtracting the relative values (ratio of L- and D-reporter intensity after incubation in buffer) from the corresponding ratio after MMP incubation (ratio of L-and D-reporter intensity after MMP incubation) (**Figure 6D**). Is the outcome of subtraction zero, it presents that no cleavage event took place, while the result of 1 means the protease activity increased twice as much as compared to the negative control (incubation in buffer).

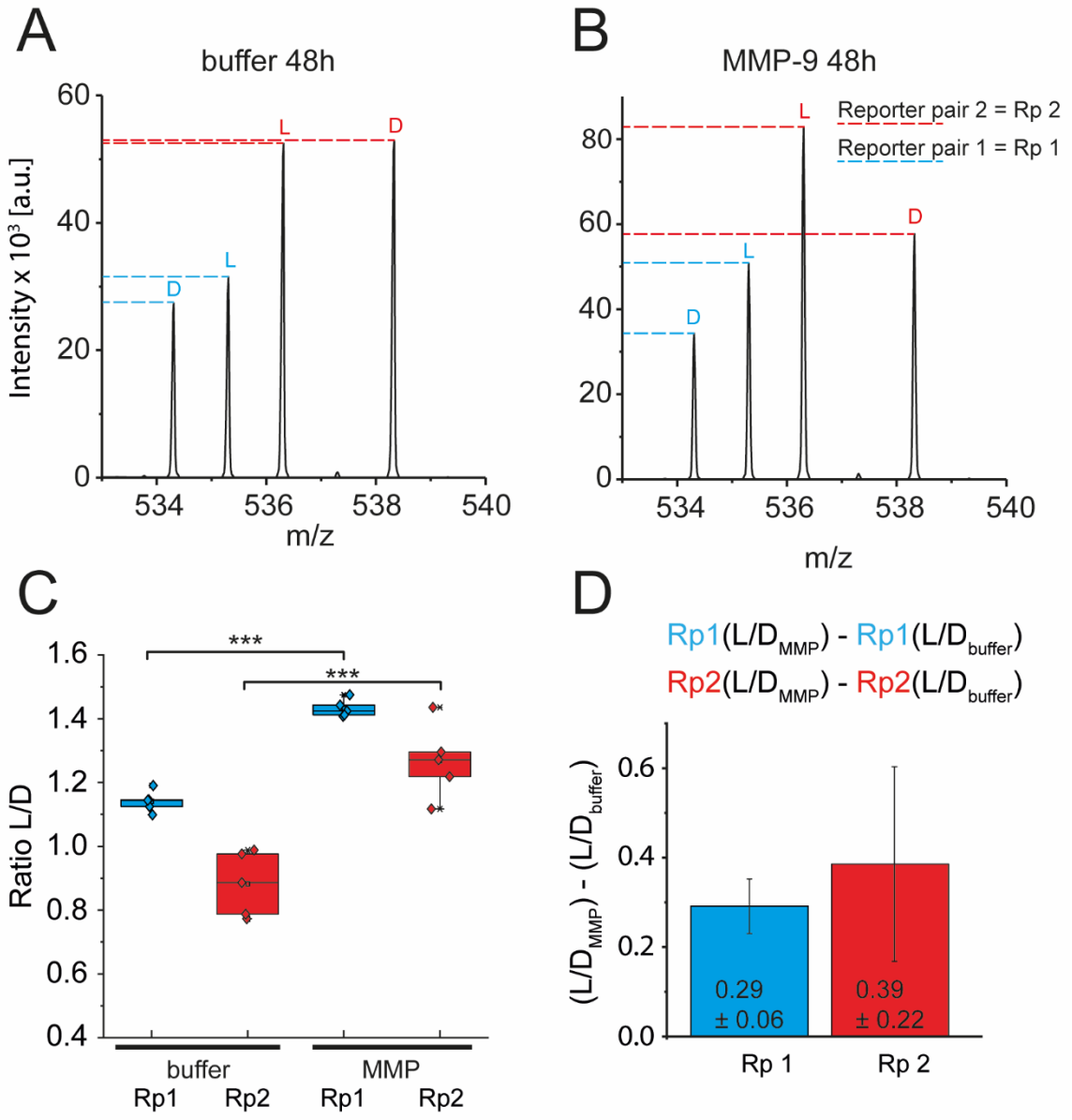

*Figure 6 The mass reporters were immobilized on ECM and incubated with either buffer or MMP-9. (A) MS^2 spectra after incubation in buffer for 48 h. (B) After incubation with MMP-9, the L- to D-reporter ratio of the signal intensities increased as seen by MS^2. (C) For each experiment setup, the L-reporter is normalized to its corresponding D-reporter (n=5). (D) Normalized cleavage rates obtained by subtracting the mean L/D ratio after incubation in buffer from the mean L/D-ratio after MMP-9 incubation (n=5, standard deviation was obtained by propagation of error). The subtraction resulted in values of 0. 29 ± 0.06 and 0.39 ± 0.22 for reporter pair 1 and 2, respectively. Values are depicted as mean ± standard deviation, two-sided Student's t-test with ***p < 0.001.*

Discussion

An MMP-sensor system with six different functional modules was developed, characterized, and a proof of concept study was performed. These sensors are based on two distinctive MMP sensitive peptide sequences designed for proteolytic cleavage. Both MMP sensitive peptide sequences were incubated in a time and concentration-dependent manner

with MMP-1, -8, -9 each or with a mix of MMP-1, -8 and -9. This revealed a higher cleavage efficiency for 'MMP sensitive peptide sequence 2' compared to 'MMP sensitive peptide sequence 1' for MMP-9 and MMP-1. The N-terminal TG immobilization sequence effectively formed a depot on ECM when incubated with FXIIIa, as detected by an immunosorbent assay with streptavidin-HRP and TMB substrate and as confirmed by CLSM. Photolysis and affinity purification followed by TEV incubation isolated the mass tags from neighboring functional modules as a prerequisite for LC-MS/MS quantification. The system's multiplexing ability refers to the detection of multiple proteases from one sample and was approached here by quantifying four mass reporters after buffer or MMP-9 incubation. These elute as one peak in LC-MS^1 and fragment into distinct patterns in MS^2. Our *in vitro* proof-of-concept experiment demonstrated the systems responsiveness to MMPs and its ability of mass tag detection after purification.

Previous studies with 'MMP sensitive peptide sequence 1' demonstrated an impact of the surface to which it was bound on cleavage efficacy.[12, 13] Qualitatively similar results were found here, with cleavage efficiency being slower from ECM bound MMP sensitive peptide sequences than from MMP sensitive peptide sequences in solution. To put these differences into perspective, the relative cleavage (defined as the ratio of cleavage seen for the L-amino acid sequences over its D-amino acid internal standard) of the first and second reporter pairs was 1.43- and 1.27-fold within 48 h from ECM and were approximately 80- to 100-fold higher in solution. We can only speculate on the cause of these observations, being it limited access of the proteases to ECM bound MMP sensitive peptide sequences due to steric hindrance or competition with cleavage of ECM molecules or both – however, the data confirms the limited information obtained from protease experiments with reporters in solution for reporters ultimately intended to report from surfaces. Hence, future studies building off this proof-of-concept study might evaluate the performances on living ECM or living tissues, which may differ from the outcome reported here on nonliving, decellularized ECM - which was treated with alkaline ammonium hydroxide and Triton X-100 to lyse and wash off cells, a process potentially altering the content of glycosaminoglycans and ECM structure.[31, 46, 47] Furthermore, the approach might be used for the profiling of biological fluids (e.g., synovial fluid from knee joint) or potentially for *in vivo* use (e.g., following intra-articular depot formation in inflamed or re-flaring joints with analysis of the cleaved mass reporters from urine, plasma, or perhaps even saliva samples).[48, 49] Other applications may detail proteolytic profiles in tissue remodelling

processes,[50, 51] wound healing,[52] chronic nonhealing wounds,[53] or delayed wound closure.[54] However, several validation steps should precede such *in vivo* applications, one consideration being plasma stability of the ECM-released cleaved mass reporters (biotin-affinity tag/TEV sequence/mass tag/light-sensitive molecule and the four amino acids remaining from MMP cleavage).

Differentiating general cleavage within the ECM from specific cleavage at the MMP sensitive peptide sequence was perhaps the major challenge for our intention. For example, the "background proteolysis" of the ECM in presence of MMP will lead to unspecific release of ECM reporters. In addition, there are known and unknown "background" effects related to manufacturing and handling, including the input ratio of D- and L- reporters for enzymatic binding or efficacy of washing of the decorated ECM, possibly leaving behind physically adsorbed reporters without covalent linkage to the ECM. Consequently, our system needed a design differentiating "background" effects from specific effects at the MMP sensitive peptide sequence of the reporters. To meet these challenges, we decided to use reporters in pairs (**Figure 1A**). One reporter pair is used within the experimental condition, which is to be measured. The outcome from this experiment reported by the 'MMP sensitive peptide sequence' made of D-amino acids measures all background. The outcome of the reporter composed of a 'MMP sensitive peptide sequence' made of L-amino acids measures all background and, additionally, measures specific cleavage at the 'MMP sensitive peptide sequence'. The normalization of signal intensities for each 'MMP sensitive peptide sequence' pair to the value of its D-variant (i.e., background signal) provides a good estimation of the specific proteolysis events vs background, as discussed before (**Figure 6C**), especially since we observed that in our hand, amounts of reporter pairs incorporated into the ECM were not identical *ab initio* (as demonstrated by differences in signal intensity despite identical handling and chemical structure) (**Figure 6A**). We largely attribute this to handling difficulties during manufacturing (e.g., weighing accuracy) but it might also reflect other undetermined sources (e.g., chemical cleavage, background UV radiation, etc.) contributing to variation. This leads to an average starting or 'background' ratios (in buffer) of 0.88 ± 0.10 for reporter pair 2 and, 1.14 ± 0.03 for reporter pair 1 over all 5 experiments. To determine protease efficacy, we then subtracted the respective mean ratios of each reporter pair in buffer from their counterpart after MMP incubation (**Figure 6D**). These numbers give a good estimation of 'L-MMP sensitive peptide sequence' cleavage over the general background and confounding factors

throughout the whole experiment, as the 'D-MMP sensitive peptide sequence' served as an efficient internal standard. Future improvement of the manufacturing of this system and proper validation might render this normalization step unnecessary in the future.

One aspect as of the current design's feasibility for *in vivo* application is the use of the sensors in pairs, i.e., including an internal control or 'standard'. This means as long as these pairs are used, all events (biological as well as technical) such as challenges in plasma, enrichment, LC-MS analysis can be controlled and would not impact the sensor/control ratio (here L/D of 'MMP sensitive peptide sequence) after ECM release. N- and C-terminal exopeptidase activity in plasma must be confirmed but should be less critical as both ends are protected N-terminally by biotinaminohexanoic acid and C-terminally; even if the four remaining L-amino acids of the MMP sensitive peptide sequence should be cleaved off, the exonucleases will stop at the photo-labile ((S)-3-amino-3-(2-nitrophenyl)propionic acid) linker at the latest, and hence the intermediate mass tag remains protected from exopeptidase cleavage during plasma transport. Another focus will be on half-life increase of the sensors for read-out from plasma or perhaps saliva (not necessarily required for sampling from urine). For this, common platforms may be deployed, more prominently PEGylation,[55, 56] but perhaps also oligomerization e.g., with sialic acid[57] or palmitic acid.[58] Following such or similar adaptation, the system would complement concentration-based immunochemical assessments by activity read-outs, hence reporting efficacy of the enzyme rather than its presence. One convenience of this system is the modular design and the broad applicability. The MMP sensitive peptide sequence gets readily adapted to report a novel suite of MMP activity in another indication, while immobilization by co-administration with FXIIIa should have potential at any site at which sufficient ECM matrix is available. The system may be further developed in the future replacing the MMP sensitive peptide sequences by sensors responding to other stimuli such as other proteases,[59, 60] pH-,[61] temperature-,[62] or reactive oxygen species (ROS).[63] Lastly, multiplexing has been restricted to two reporter pairs in this proof-of-principle study but may be vastly extended when needed reporting an enormous amount of information directly from within the ECM.

Conclusion

We demonstrated proof of concept for a MMP-responsive diagnostic system responding from enzymatically built depots reporting on MMP levels from within cell-derived matrices. The use of mass reporters in pairs – with one MMP sensitive peptide sequence built with L-amino acids, the internal control with D-amino acids – allows purification through multiple steps without loss of relative quantitative information for the pair. Therefore, the sensor pairs translate local MMP cleavage events into relative information cues as a prerequisite for reliable quantitative read-out by tandem mass spectrometry (LC-MS/MS). This is featured by means of an identical parent mass of all mass tags in the MS^1 detector subsequently being fragmented into a set of encoded y-type ions, allowing precise allocation of mass tag to the originally cleaved sensor molecule in MS^2. We restricted this evaluation to two reporter pairs – the platform, however, has substantial leverage for multiplexing and reporting various events from within the ECM. Future studies aim at adapting and profiling this diagnostic for the realization of minimally invasive enzymatic depots *in vivo* with read-out from urine, plasma, and perhaps saliva, reporting inflammation from within the inflamed ECM.

Experimental section

Materials

The following chemicals were purchased from Sigma Aldrich (Taufkirchen, Germany): N, N-diisopropylcarbodiimide (DIC), ethyl cyanohydroxyiminoacetate (Oxyma), hydroxybenzotriazole (HOBt), trifluoroacetic acid (TFA), triisopropylsilane (TIS), acetic anhydride, ethylenediaminetetraacetic acid, Dulbecco's Modified Eagle's Medium - high glucose, bovine calf serum, penicillin-streptomycin, gelatin from bovine skin, glutaraldehyde solution 50 wt. % in H_2O, anti-fibronectin (rabbit), streptavidin-Cy5, streptavidin-HRP conjugate, Triton™ X-100. Piperidine was purchased from Alfa Aesar (Haverhill, USA), and AcTEV Protease from Invitrogen (Carlsbad, USA). N, N-diisopropylethylamine and Roti®Block was purchased from Carl Roth GmbH + Co. KG (Karlsruhe, Germany). All amino acids, rink-amide resin, and 6-biotinylamino-hexanoic acid were purchased from Iris Biotech (Marktredwitz, Germany) and isotopically labelled amino acids were purchased from Cambridge Isotope Laboratories Inc (Tewksbury, USA), except for Fmoc-Phenylalanine (Ring$^{13}C_6$) which was purchased from Anaspec (Seraing,

Belgium). Matrix metalloproteinases (MMP-1, MMP-8, MMP-9), acetonitrile (ACN), and methanol were purchased from VWR (Darmstadt, Germany). Fmoc-(S)-3-amino-3-(2-nitrophenyl)propionic acid was purchased from ChemImpex (Wood Dale, USA), recombinant human tissue transglutaminase (rhTG2) from Zedira (Darmstadt, Germany) and goat anti-rabbit IgG (H+L), Alexa Fluor 488 conjugate from Merck Millipore (Burlington, USA). The following kits or chemicals were purchased from Thermo Fisher Scientific (Waltham, USA): Pierce™ BCA Protein Assay Kit, 1 -Step™ Turbo TMB-ELISA Substrate Solution, N, N-dimethylformamide and dichloromethane. Fibrogammin (FXIII) was kindly provided by CSL Behring (Marburg, Germany).

Peptide synthesis

Isotopically labelled peptides were synthesized using the fully automated Liberty blue peptide synthesizer (CEM). The peptide synthesis is based on solid phase Fluorenylmethoxycarbonyl (Fmoc)-strategy and coupling reagents were DIC/Oxyma in DMF. Fmoc-deprotection is performed with 20 % piperidine in DMF at 75 °C for 3 minutes followed by five washing steps with 2.5 mL DMF each. The coupling settings for all amino acids were 90 °C for 2 minutes, except for histidine, which was coupled with 50 °C for 10 minutes. Amino acid number 18 and the following were double coupled with the appropriate method. There was no final Fmoc-deprotection performed. The resin was transferred from the synthesizer's reactor to a 20 mL syringe with polyethylene frit and plastic fit (MultiSynTech GmbH, Witten, Germany) to manually perform N-acetylation with 75 µl acetanhydride and 135 µL DIPEA in 2 mL DMF for 25 minutes at room temperature. Manual Fmoc-deprotection was conducted with 40 % (V/V) piperidine in DMF for 3 minutes and 20 % (V/V) piperidine in DMF for 12 minutes at room temperature and 5 washing steps using DMF. The last amino acid like compound, 6-Biotinylamino-hexanoic acid, was coupled to the free N-terminal amino group in 0.5 M HOBt in DMF solution with 10 eq. DIC (1mmol) and 5 eq. DIPEA (0.5mmol) for eight hours at room temperature and a second coupling was carried out overnight. The resin was washed five times with 3 mL DMF and dried with dichloromethane (DCM) and diethyl ether. Peptide cleavage from resin was performed with TFA:TIS:H_2O (95:2.5:2.5) for 3 hours at room temperature. The peptides were precipitated from the cleavage solution with diethyl ether,

centrifuged, the supernatant was discarded, and the pellet was dried under very mild airflow. The four synthesized sequences were as follows:

a. BioAhx-ENLYFQ-S^{+3}AEGP^{+3}GFr-X-GPQGIAGQ-PLKPAKSA
b. BioAhx-ENLYFQ-S^{+4}AEGP^{+2}GFr-X-GpqGiaGq-PLKPAKSA
c. BioAhx-ENLYFQ-$^{+1}$S^{+1}AEGP^{+3}G^{+1}Fr-X-GPSGLLAH-PLKPAKSA
d. BioAhx-ENLYFQ-SAEGPG^{+6}Fr-X-GpsGllah-PLKPAKSA

BioAhx = N-(+)-Biotinyl-6-aminohexanoic acid
X = Fmoc-(*S*)-3-amino-3-(2-nitrophenyl)propionic acid
Small letters depict D-amino acids

Peptide purification

The peptide pellets were dissolved in acetonitrile/water + 0.1 % TFA and purified by reversed phase chromatography using a FPLC system (GE Healthcare Äkta Pure, Life sciences, Freiburg, Germany) with Luna 10u C8 100A column (250 mm × 21.2 mm, Phenomenex Inc., Torrance, CA) equilibrated by water containing 0.1 % TFA and acetonitrile (ACN) containing 0.1 % TFA (95:5 v/v). A stepwise acetonitrile gradient from 25 % to 80 % in 12 column volumes and from 80 % to 100 % in two column volumes with 1mL/min flow rate was used for elution and UV-absorbance was monitored at λ = 214 nm. The collected fractions were analysed by LC-MS, acetonitril was evaporated and samples were freeze dried in Freeze Dryer Alpha 1-4 (Martin Christ Gefriertrocknungsanlagen GmbH, Osterode, Germany). The lyophilized peptides were stored at – 80 °C until use.

MALDI-MS, ESI-MS

Matrix-assisted laser desorption ionization (MALDI)-MS spectra were acquired in the linear positive mode by using an ultrafleXtreme mass spectrometer (Bruker Daltonics, Bremen), equipped with a 355 nm smartbeam-II™ laser. For the external calibration 1 µL of a CsI_3 solution (40 mg/mL in acetonitrile) was mixed with 1µL of a DCTB (*trans*-2-[3-(4-tert-Butylphenyl)-2-methyl-2-propenylidene]malononitrile) solution (20 mg/mL in acetonitrile) and 0.5 µL of the mixture were spotted onto the stainless steel target. Samples were desalted using ZipTipC18 pipette tips (C18 resin, Millipore) following the manufacturer's instructions. One µL of the eluate was embedded in a matrix, consisting of equal parts of α-cyano-4-hydroxycinammic acid solution (saturated in 40% ACN/ 60% H_2O/ 0.1% TFA)) and TA-solvent. 0.5 µl of the mixture were dropped onto the stainless

steel target (MTP 384 target plate ground steel, Bruker Daltonics #8280784) and 2000 shots were accumulated for each measurement.

The samples were analyzed by LC-MS on a microTOF-Q III (Bruker Daltonics) equipped with an ESI Ion Source (Apollo II) and coupled to a Thermo Ultimate 3000 HPLC System. The samples were either loaded on a reversed phase C18 column (Synergi, 4 µm, Fusion-RP 80 Å, 250 x 2 mm) or directly injected. The separation on the C18 column was performed with a flow of 0.5 mL/min over 35 minutes using a step gradient of 5 % acetonitrile in Millipore water and 0.1 % TFA to 65 % in 16 minutes and 95 % in 2 minutes. The MS spectra were recorded continuously in the range m/z 250 – 3000 with the following settings: capillary voltage -4.5 kV, end plate voltage – 4 kV, nitrogen nebulizer pressure 1.0 bar, dry gas flow 6 L/min, dry temperature 180 °C; Funnel 1 was 300 Vpp and Funnel 2 RF 400 Vpp, Hexapole RF 400 Vpp; Quadrupole ion energy 5 eV, Quadrupole low mass 250 m/z; collision energy 15 eV, collision RF 600 Vpp, transfer time 90 µs, pre pulse storage 12 µs. The instrument was calibrated with Sodium formate prior to measurement of the samples. The accuracy of the calibration masses was rechecked by measuring Sodium formate after the sample measurements. The spectra were recorded with the Compass Software (Bruker Daltonics) containing the OTOF Control 3.4 and Hystar 3.2 software for controlling the MS instrument and the HPLC. For spectra deconvolution and data evaluation the Data Analysis software DA 4.2 (Bruker Daltonics) was used.

Liquid chromatography – mass spectrometry (LC-MS)

LC-MS analysis was performed on a Single Quadrupole system consisting of a LC20AB liquid chromatograph, a SPD-20A UV/Vis detector and a LC-MS 2020 (Shimadzu Scientific Instruments, Columbia, MD, USA). To separate samples by LC a Synergi 4 µm fusion-RP column (4.6 x 150 mm) (Phenomenex lnc., Torrance, CA) was used with eluent A 0.1 % (v/v) formic acid in water and eluent B 0.1 % (v/v) formic acid in methanol. The detection range was set from 60 – 1000 m/z or from 500 – 2000 m/z depending on the samples mass and charge. The injection volume of 20 µL sample was loaded onto the column and a stepwise methanol gradient was used with a (i) linear gradient from 5 to 90 % eluent B in 8 min, (ii) washing at 90 % eluent B for 5 min, (iii) a linear gradient to from 95 – 5 % eluent B in 1 min, and (iv) equilibration of the column with 5 % of eluent B for 4 min.

High-performance liquid chromatography

Purity of peptides was analyzed using an Agilent HPLC system (Agilent, Santa Clara, CA, USA) consisting of a flexible pump (G7104C), a vial sampler (G7129C), a multi column thermostat (G7166A) with Quick-connect heat exchanger (G7116-60051) and a VWD detector (G7114A). Separation was performed on a Zorbax® 300SB CN column (150×4.6 mm) at 22 °C with an ACN gradient increasing from 5 % to 60 % ACN over 18 minutes at a flow rate of 1.0 mL/min. Then, initial conditions were set to wash and equilibrate the column. Peptides were detected at $\lambda = 214$ nm.

MMP digest of protease-sensitive peptide sequences

The incubation of MMP sensitive peptide sequences with MMPs was performed by dissolving the lyophilized 'MMP sensitive peptide sequence 1' (GPQGIAGQK(N_3)Q) and 'MMP sensitive peptide sequences 2' (GPSGLLAHK(N_3)Q) in MMP buffer (50 mM Tris, 150 mM, NaCl, 1 µM$ZnCl_2$, 10 mM $CaCl_2$, pH 7.4) to a final concentration of 1 mM. For time-dependent release experiment, 30 µl of each peptide were mixed with MMP-1, MMP-8 or MMP-9 with a final concentration of 35.1 nM, 13.2 nM or 10.6 nM, respectively (according to MMP concentrations from patients with RA[8]). The reaction mixtures were incubated at 37 °C with gentle agitation for defined periods of time (30 minutes, 2, 4, 6, 24 and 48 hours). The enzyme activity was stopped by adding EDTA to a final concentration of 1 mM and by heating the mixture to 95 °C for 5 minutes. Experiments were performed in triplicates.

For concentration-dependent release, 40 µl of peptide solution was mixed with different concentration of an MMP-Mix, consisting of MMP-1, -8, -9. The concentration range is from 0.16 nM to 16 nM. The mix of MMP-1, -8 and -9 with a final concentration of 16 nM was prepared by mixing 5.33 nM MMP-1, -8 and -9. The lower concentrations were prepared by diluting the 16 nM solution by factor 2, 5, 20 and 100. The reaction mixtures were incubated at 37 °C for 24 hours and the protease activity was stopped by adding EDTA to a final concentration of 1 mM and by heating up to 95 °C for 5 minutes. Experiments were performed in triplicates.

Cleavage efficiency was assessed on a LaChromUltra UPLC system equipped with a Hitachi L-2455U diode array detector and two L-2160U pumps (VWR Hitachi, Tokyo, Japan). 20 µL MMP sensitive peptide sequence sample was applied on a ZORBAX Eclipse XDB-C18 column (4.6 mm× 150 mm, Agilent, Santa Clara, CA) equilibrated with a

solution of 95% water containing 0.1% TFA and 5% acetonitrile (ACN) containing 0.1% TFA. The MMP sensitive peptide sequences and their cleaved fragments were eluted by a linear gradient of 5–65% ACN containing 0.1% TFA with a flow rate of 1 mL/min. Column temperature was kept at 22°C by a L-2300 column oven and absorbance was monitored at $\lambda = 214$ nm.

Photocleavage

100 µL L-reporter 2 (0.5 mg/mL) were prepared in an Eppendorf tube and placed under a CAMAG UV lamp in 10 cm distance. The sample was irradiated for 6 hours and the experimental setting was covered with a cardboard box. 37.5 µL magnetic streptavidin-beads were prepared and washed and equilibrated with phosphate-buffered saline (PBS) and tris-buffered saline (TBS), respectively. Sample volume was diluted to minimum 300 µL with TBS and beads were added and incubated for at least 30 minutes on a benchtop shaker at room temperature. The supernatant was transferred to a new Eppendorf tube and the beads were washed with wash buffer (2 M urea, TBS, pH 7.5). Biotinylated peptide fragment was eluted by adding elution buffer (2 % SDS) and heating up to 95 °C. The eluted fraction and the supernatant were ziptipped and MALDI measurements were performed.

Cell culture

NIH3T3 fibroblasts (CRL-1658; ATCC, Manassas, VA) were cultured in growth medium (DMEM, high glucose containing 10 % BCS, 100 U/mL penicillin G and 100 µg/µL streptomycin) in 75 cm^2 culture flasks at 37 °C and 5 % CO_2.

Preparation and isolation of extracellular matrix

Cultivation of NIH 3T3 fibroblasts and cell-derived extracellular matrix was performed according to.[64] In short: 8-Well NuncTM Lab-TekTM II Chamber SlideTM System surfaces were pre-treated with a 2 % aqueous solution of 3-aminopropyldimethylmethoxysilane (APTES) for 15 minutes and washed three times with ultrapure water followed by 30 minutes incubation with 0.125 % glutaraldehyde solution and four washing steps with dH_2O and sterilization by UV irradiation for 60 minutes. Finally, the 8-Well NuncTM Lab-TekTM II Chamber SlideTM System and 96-well plates were incubated with a 2 % gelatin solution in PBS for 60 minutes and washed three times with PBS prior to use. NIH3T3 fibroblasts were maintained in a culture flask (75mm^2) in Dulbecco's Modified Eagle's Medium, high-glucose (DMEM, containing 10 % BCS,

penicillin G (100 U mL-1) and streptomycin (100 µg µL-1)) at 37 °C under CO_2 (5 %). For ECM production the cells were seeded in 8-Well NuncTM Lab-TekTM II Chamber SlideTM System ($16.7x10^4$ cells mL-1, 300 µL growth medium per well) or in 96-well plates ($20x10^4$ cells mL-1, 150 µL growth medium per well) and grown for 24 hours at 37 °C under CO_2 (5 %). The growth medium was exchanged every 24 hours to Dulbecco's Modified Eagle's Medium, high-glucose (DMEM, containing 10 % BCS, penicillin G (100 U mL-1) and streptomycin (100 µg µL-1)) with additional sodium ascorbate (16.8 mg/mL) over an incubation period of 6 days. After culture, extracellular matrix components were isolated following existing protocols [64]. The medium was carefully aspirated, and the cells were washed with PBS twice and subsequently incubated with ultrapure water for 15 minutes and a second time for 30 minutes followed by three additional washing steps with PBS. After water incubation, the cells were extracted using a triton-x-ammonia buffer (0.5 % (v/v) triton-X and 20 mM NH4OH in PBS pH 7.4) for 10 minutes at 37°C. Finally, extraction buffer was removed by washing with PBS for five times.

Coupling of peptides to extracellular matrix

The lyophilized isotopically labelled peptides were reconstituted in TG buffer (buffer (50 mM Tris-HCl buffer, 150 mM NaCl, 2.5 mM $CaCl_2$, pH 7.4) and the concentration was determined by bichinchoninic acid (BCA) assay and adjusted to a final concentration of 7.5 nmol/mL. 100 µL of peptide solution was added to isolated ECM in 96-well plates and incubated with 20U/mL FXIIIa (182 U/mL, Zedira) for 30 minutes at 37 °C. Mass tag constructs were also coupled in absence of transglutaminase as negative control. After supernatant removal, ECM was washed three times with TBST, and three times with PBS.

Bioresponsive release of mass reporters from ECM

Bioresponsive release of mass reporters from ECM was performed by incubating immobilized peptides on ECM with 8 nM MMP-9. Immobilized peptides were incubated with MMP-9 at 37 °C and 5% CO_2 for 48 hours. Peptide quantification was performed via HRP-TMB detection system. All wells were incubated with Streptavidin-HRP conjugate (1:5000 in PBS) at RT for 1 hour followed by addition of TMB solution (TMB : H_2O_2, 1 : 1) for 15 minutes. The reaction was stopped by adding 50 µL 2 M sulfuric acid and absorbance was measured at λ = 450 nm on an absorbance microplate reader.

Purification steps of mass tags after bioresponsive release from ECM

Mass reporters were released from ECM by incubation with MMP, which cleave the incorporated MMP sensitive peptide sequence. Subsequently mass tags were purified by following three steps: (1) irradiation with UV light λ = 366 nm for 6 hours, (2) affinity purification by binding biotinylated peptides to magnetic streptavidin-coated beads for 30 minutes and (3) enzymatic cleavage from streptavidin beads by AcTEV protease (10 U/mL, Invitrogen): After incubation with MMP-9 the supernatant was transferred to new Eppendorf tubes. The samples were placed under an UV lamp (8W) and were irradiated with λ = 366 nm for 6 hours. Afterwards the samples were added to the appropriate amount of magnetic streptavidin beads (4 nmol/mg peptide) and were incubated for 30 minutes at room temperature on a roller mixer. The supernatant was discarded, and beads were washed with TBS twice. The beads were re-suspended in TEV buffer (50 mM Tris-HCl, pH 8.0, 10 mM EDTA, 10 mM DTT) and 10 U/20 µg peptide AcTEV protease was added and incubated at 30 °C for 6 hours. Supernatant was collected and for analysis by LC-MS/MS.

LC-MS/MS measurements

Peptides were cleaned up using C-18 Stage Tips.[65] Each Stage Tip was prepared with three discs of C-18 Empore SPE Discs (3M) in a 200 µl pipet tip. Samples were acidified with formic acid to a final conc. of 0.5% formic acid. Peptides were eluted from Stage Tip with 60 % acetonitrile in 0.3 % formic acid, dried in a vacuum concentrator (Eppendorf), and stored at -20 °C. Peptides were dissolved in 2% acetonitrile / 0.1 % formic acid prior to nanoLC-MS/MS analysis.

For the LC-MS/MS measurements of mass tag sequences S1-3, the NanoLC-MS/MS analyses were performed on a LTQ-Orbitrap Velos Pro (Thermo Scientific) equipped with a PicoView Ion Source (New Objective) and coupled to an EASY-nLC 1000 (Thermo Scientific). Peptides were loaded on capillary columns (PicoFrit, 30 cm x 150 µm ID, New Objective) self-packed with ReproSil-Pur 120 C18-AQ, 1.9 µm (Dr. Maisch) and separated with a 30-minute linear gradient from 3 % to 30 % acetonitrile and 0.1 % formic acid and a flow rate of 500 nl/min. MS scans were acquired in the Orbitrap analyzer with a resolution of 30000 at m/z 400, MS/MS scans were acquired in the Orbitrap analyzer with a resolution of 7500 at m/z 400 using HCD fragmentation with 20 % normalized collision energy. A TOP5 data-dependent MS/MS method was used; dynamic exclusion was applied with a repeat count of 1 and an exclusion duration of 30 seconds; singly charged precursors were

excluded from selection. Minimum signal threshold for precursor selection was set to 50000. Predictive AGC was used with AGC target a value of 1e6 for MS scans and 5e4 for MS/MS scans. Lock mass option was applied for internal calibration in all runs using background ions from protonated decamethylcyclopentasiloxane (m/z 371.10124).

The NanoLC-MS/MS measurements of reporter pair 1 and 2 and of the mass tag release experiments from ECM were performed on an Orbitrap Fusion (Thermo Scientific) equipped with a PicoView Ion Source (New Objective) and coupled to an EASY-nLC 1000 (Thermo Scientific). Peptides were loaded on capillary columns (PicoFrit, 30 cm x 150 µm ID, New Objective) self-packed with ReproSil-Pur 120 C18-AQ, 1.9 µm (Dr. Maisch) and separated with a 30-minute linear gradient from 3 % to 30 % acetonitrile and 0.1 % formic acid and a flow rate of 500 nl/min. Both MS and MS/MS scans were acquired in the Orbitrap analyzer with a resolution of 60,000 for MS scans and 15,000 for MS/MS scans. A data-dependent targeted MS/MS method with a fixed cycle time of 3 seconds was used with a target mass of m/z 413.2144 (corresponding to the doubly charged mass tag construct). For the target mass HCD collision energy was set to 20 % normalized collision energy and the isolation window was set to 0.5 m/z to minimize peak overlapping from isotopic peaks. Mass tolerance was set to 22 ppm. Nontarget masses were measured using standard parameters (35 % normalized collision energy, isolation window 2.5 m/z, dynamic exclusion with repeat count of 1 and an exclusion duration of 30 seconds). Singly charged precursors were excluded from selection. Injection time was increased from 50 ms for nontarget masses to 500 ms for target mass. Minimum signal threshold for precursor selection for nontarget masses was set to 50,000. For target mass no threshold was set. Predictive AGC was used with an AGC target value of 2e5 for MS scans and 5e4 for MS/MS scans. EASY-IC was used for internal calibration. The Xcalibur™ software (Thermo Fisher Scientific Inc., MA) was used for data analysis.

Imaging of immobilized mass tag constructs on ECM

The lyophilized mass tag constructs were reconstituted in TG buffer (50 mM Tris-HCl buffer, 150 mM NaCl, 2.5 mM $CaCl_2$, pH 7.4) and the concentration was determined by BCA assay and then adjusted to a final concentration of 7.5 nmol/mL. 300 µL of 7.5 nmol/mL were added to isolated ECM in 8-Well NuncTM Lab-TekTM II Chamber SlideTM System and incubated with 20 U/mL FXIIIa (182 U/mL, CSL Behring) for 30 minutes at 37 °C and 5% CO_2. Mass tag constructs were also coupled in absence of transglutaminase as negative control. 1x Roti®-Block solution for 60 minutes at RT was

used to block ECM. After three washing steps with PBS the primary rabbit anti-fibronectin antibody (1:400 in PBS, overnight at 4 °C) was added. Goat anti-rabbit IgG Alexa Fluor® 488 conjugate (1:500 in PBS, 1 hour, RT) was used as a secondary antibody and the immobilized biotinylated isotopically labelled peptides were stained by using Streptavidin-Cy5 (1:1000 in PBS, 1 hour, RT). After three washing steps each with TBST and PBS, ECM was analyzed on a high resolution AOBS SP2 confocal laser scanning microscope (Leica microsystem, Wetzlar, Germany) with a 63x N.A. 1.4-0.60 Oil I BL HCX PL APO I objective. To avoid crosstalk the emission signals were collected independently. To confirm the cleavage of MMP sensitive peptide sequences, ECM was incubated with 300µL 9.6 nM MMP-Mix (MMP-1,-8,-9; 3.2 nM each) and MMP buffer only as negative control for 48 hours at 37 °C. Wells were analyzed again with a high resolution AOBS SP2 confocal laser scanning microscope (Leica microsystem, Wetzlar, Germany) with a 63x N.A. 1.4-0.60 Oil I BL HCX PL APO I objective to determine cleavage of peptide from ECM. Image processing was performed in ImageJ (http://imagej.nih.gov/ij/).

Quantification of binding efficiency of L-reporter2 to ECM catalyzed by FXIIIa or rhTG2

The lyophilized model peptide was reconstituted in TG buffer (buffer (50 mM Tris-HCl buffer, 150 mM NaCl, 2.5 mM $CaCl_2$, pH 7.4) and the concentration was determined by BCA assay and adjusted to a final concentration of 0.75, 7.5, 15, 30 and 60 nmol/mL. 100 µL of peptide solution was added to isolated ECM in 96-well plates and incubated with 20 U/mL rhTG2 (2957 U/mL, Zedira) or with 20 U/mL FXIIIa (182 U/mL, Zedira) for 30 minutes at 37 °C. The same conditions were tested in absence of transglutaminase as negative control and to determined unspecific adsorption. After supernatant removal, the ECM was washed with PBS twice and three times with TBST, followed by a 1-hour incubation with Streptavidin-HRP conjugate (1:5000 in PBS) at RT. For peptide quantification on ECM wells were incubated with TMB solution (TMB : H_2O_2, 1 : 1) for 15 minutes and reaction was stopped by adding 50 µL 2 M sulfuric acid. Absorbance was measured at λ = 450 nm on an absorbance microplate reader.

Statistical analysis

Data were analyzed using Student's t-test or one-way ANOVA with pair-wise comparison by Tukey *post-hoc* test using Origin (OriginLab Corporation, MA). Results were

considered statistically significant at $p \leq 0.05$ (*). Results are shown as mean with standard deviation (SD).

Acknowledgments

Technical support is kindly acknowledged for Matthias Beudert and Niklas Hauptstein regarding CLSM and for Dr. Büchner and his team regarding MALDI and ESI-MS measurements. Financial support is kindly acknowledged by the German Research Foundation (DFG) through the Sino-German Center (Grant # ME3820/3-1).

References

1. Choi, Y. C.; Dalakas, M. C., Expression of matrix metalloproteinases in the muscle of patients with inflammatory myopathies. *Neurology* **2000,** *54* (1), 65-71.
2. Vernooy, J. H.; Lindeman, J. H.; Jacobs, J. A.; Hanemaaijer, R.; Wouters, E. F., Increased activity of matrix metalloproteinase-8 and matrix metalloproteinase-9 in induced sputum from patients with COPD. *Chest* **2004,** *126* (6), 1802-10.
3. Tchetverikov, I.; Lohmander, L. S.; Verzijl, N.; Huizinga, T. W.; TeKoppele, J. M.; Hanemaaijer, R.; DeGroot, J., MMP protein and activity levels in synovial fluid from patients with joint injury, inflammatory arthritis, and osteoarthritis. *Ann Rheum Dis* **2005,** *64* (5), 694-8.
4. Murphy, G.; Knauper, V.; Atkinson, S.; Butler, G.; English, W.; Hutton, M.; Stracke, J.; Clark, I., Matrix metalloproteinases in arthritic disease. *Arthritis research* **2002,** *4 Suppl 3*, S39-49.
5. Zwerina, J.; Redlich, K.; Polzer, K.; Joosten, L.; Kronke, G.; Distler, J.; Hess, A.; Pundt, N.; Pap, T.; Hoffmann, O.; Gasser, J.; Scheinecker, C.; Smolen, J. S.; van den Berg, W.; Schett, G., TNF-induced structural joint damage is mediated by IL-1. *Proc Natl Acad Sci U S A* **2007,** *104* (28), 11742-7.
6. Migita, K.; Eguchi, K.; Kawabe, Y.; Ichinose, Y.; Tsukada, T.; Aoyagi, T.; Nakamura, H.; Nagataki, S., TNF-alpha-mediated expression of membrane-type matrix metalloproteinase in rheumatoid synovial fibroblasts. *Immunology* **1996,** *89* (4), 553-7.
7. Liacini, A., Induction of matrix metalloproteinase-13 gene expression by TNF-α is mediated by MAP kinases, AP-1, and NF-κB transcription factors in articular chondrocytes. *Experimental Cell Research* **2003,** *288* (1), 208-217.
8. Yoshihara, Y.; Nakamura, H.; Obata, K.; Yamada, H.; Hayakawa, T.; Fujikawa, K.; Okada, Y., Matrix metalloproteinases and tissue inhibitors of metalloproteinases in synovial fluids from patients with rheumatoid arthritis or osteoarthritis. *Ann Rheum Dis* **2000,** *59* (6), 455-461.
9. Sun, L.; Wang, X.; Kaplan, D. L., A 3D cartilage - inflammatory cell culture system for the modeling of human osteoarthritis. *Biomaterials* **2011,** *32* (24), 5581-9.
10. Rai, M. F.; Rachakonda, P. S.; Manning, K.; Vorwerk, B.; Brunnberg, L.; Kohn, B.; Schmidt, M. F., Quantification of cytokines and inflammatory mediators in a three-dimensional model of inflammatory arthritis. *Cytokine* **2008,** *42* (1), 8-17.
11. Samavedi, S.; Diaz-Rodriguez, P.; Erndt-Marino, J. D.; Hahn, M. S., A Three-Dimensional Chondrocyte-Macrophage Coculture System to Probe Inflammation in Experimental Osteoarthritis. *Tissue Eng Part A* **2017,** *23* (3-4), 101-114.
12. Ritzer, J.; Luhmann, T.; Rode, C.; Pein-Hackelbusch, M.; Immohr, I.; Schedler, U.; Thiele, T.; Stubinger, S.; Rechenberg, B. V.; Waser-Althaus, J.; Schlottig, F.; Merli, M.; Dawe, H.; Karpisek, M.; Wyrwa, R.; Schnabelrauch, M.; Meinel, L., Diagnosing peri-implant disease using the tongue as a 24/7 detector. *Nat Commun* **2017,** *8*.
13. Braun, A. C.; Gutmann, M.; Ebert, R.; Jakob, F.; Gieseler, H.; Luhmann, T.; Meinel, L., Matrix Metalloproteinase Responsive Delivery of Myostatin Inhibitors. *Pharmaceutical research* **2017,** *34* (1), 58-72.
14. Braun, A. C.; Gutmann, M.; Mueller, T. D.; Luhmann, T.; Meinel, L., Bioresponsive release of insulin-like growth factor-I from its PEGylated conjugate. *J Control Release* **2018,** *279*, 17-28.
15. Mi, Y.; Wolfram, J.; Mu, C.; Liu, X.; Blanco, E.; Shen, H.; Ferrari, M., Enzyme-responsive multistage vector for drug delivery to tumor tissue. *Pharmacol Res* **2016,** *113* (Pt A), 92-99.
16. Liu, S.; Netzel-Arnett, S.; Birkedal-Hansen, H.; Leppla, S. H., Tumor Cell-selective Cytotoxicity of Matrix Metalloproteinase-activated Anthrax Toxin. *Cancer Research* **2000,** *60* (21), 6061-6067.
17. Wythe, S. E.; DiCara, D.; Taher, T. E.; Finucane, C. M.; Jones, R.; Bombardieri, M.; Man, Y. K.; Nissim, A.; Mather, S. J.; Chernajovsky, Y.; Pitzalis, C., Targeted delivery of cytokine therapy to rheumatoid tissue by a synovial targeting peptide. *Ann Rheum Dis* **2013,** *72* (1), 129-35.

18. Adams, G.; Vessillier, S.; Dreja, H.; Chernajovsky, Y., Targeting cytokines to inflammation sites. *Nature biotechnology* **2003,** *21* (11), 1314-20.
19. Guarnieri, D.; Biondi, M.; Yu, H.; Belli, V.; Falanga, A. P.; Cantisani, M.; Galdiero, S.; Netti, P. A., Tumor-activated prodrug (TAP)-conjugated nanoparticles with cleavable domains for safe doxorubicin delivery. *Biotechnol Bioeng* **2015,** *112* (3), 601-11.
20. Savariar, E. N.; Felsen, C. N.; Nashi, N.; Jiang, T.; Ellies, L. G.; Steinbach, P.; Tsien, R. Y.; Nguyen, Q. T., Real-time in vivo molecular detection of primary tumors and metastases with ratiometric activatable cell-penetrating peptides. *Cancer Res* **2013,** *73* (2), 855-64.
21. Lee, S.; Cha, E. J.; Park, K.; Lee, S. Y.; Hong, J. K.; Sun, I. C.; Kim, S. Y.; Choi, K.; Kwon, I. C.; Kim, K.; Ahn, C. H., A near-infrared-fluorescence-quenched gold-nanoparticle imaging probe for in vivo drug screening and protease activity determination. *Angew Chem Int Ed Engl* **2008,** *47* (15), 2804-7.
22. Lee, S.; Ryu, J. H.; Park, K.; Lee, A.; Lee, S. Y.; Youn, I. C.; Ahn, C. H.; Yoon, S. M.; Myung, S. J.; Moon, D. H.; Chen, X.; Choi, K.; Kwon, I. C.; Kim, K., Polymeric nanoparticle-based activatable near-infrared nanosensor for protease determination in vivo. *Nano Lett* **2009,** *9* (12), 4412-6.
23. Kwong, G. A.; von Maltzahn, G.; Murugappan, G.; Abudayyeh, O.; Mo, S.; Papayannopoulos, I. A.; Sverdlov, D. Y.; Liu, S. B.; Warren, A. D.; Popov, Y.; Schuppan, D.; Bhatia, S. N., Mass-encoded synthetic biomarkers for multiplexed urinary monitoring of disease. *Nature biotechnology* **2013,** *31* (1), 63-70.
24. Warren, A. D.; Kwong, G. A.; Wood, D. K.; Lin, K. Y.; Bhatia, S. N., Point-of-care diagnostics for noncommunicable diseases using synthetic urinary biomarkers and paper microfluidics. *Proc Natl Acad Sci U S A* **2014,** *111* (10), 3671-6.
25. Ehrbar, M.; Rizzi, S. C.; Hlushchuk, R.; Djonov, V.; Zisch, A. H.; Hubbell, J. A.; Weber, F. E.; Lutolf, M. P., Enzymatic formation of modular cell-instructive fibrin analogs for tissue engineering. *Biomaterials* **2007,** *28* (26), 3856-66.
26. Ehrbar, M.; Rizzi, S. C.; Schoenmakers, R. G.; Miguel, B. S.; Hubbell, J. A.; Weber, F. E.; Lutolf, M. P., Biomolecular hydrogels formed and degraded via site-specific enzymatic reactions. *Biomacromolecules* **2007,** *8* (10), 3000-7.
27. Sala, A.; Ehrbar, M.; Trentin, D.; Schoenmakers, R. G.; Voros, J.; Weber, F. E., Enzyme mediated site-specific surface modification. *Langmuir* **2010,** *26* (13), 11127-34.
28. Schense, J. C.; Hubbell, J. A., Cross-linking exogenous bifunctional peptides into fibrin gels with factor XIIIa. *Bioconjug Chem* **1999,** *10* (1), 75-81.
29. Schmoekel, H. G.; Weber, F. E.; Schense, J. C.; Gratz, K. W.; Schawalder, P.; Hubbell, J. A., Bone repair with a form of BMP-2 engineered for incorporation into fibrin cell ingrowth matrices. *Biotechnol Bioeng* **2005,** *89* (3), 253-62.
30. Zisch, A. H.; Schenk, U.; Schense, J. C.; Sakiyama-Elbert, S. E.; Hubbell, J. A., Covalently conjugated VEGF–fibrin matrices for endothelialization. *Journal of Controlled Release* **2001,** *72* (1-3), 101-113.
31. Yamada, K. M., Extracellular Matrix. *Current Protocols in Cell Biology* **2009,** *45* (1), 10.0.1-10.0.3.
32. Schlie-Wolter, S.; Ngezahayo, A.; Chichkov, B. N., The selective role of ECM components on cell adhesion, morphology, proliferation and communication in vitro. *Exp Cell Res* **2013,** *319* (10), 1553-61.
33. Cukierman, E.; Pankov, R.; Stevens, D. R.; Yamada, K. M., Taking cell-matrix adhesions to the third dimension. *Science* **2001,** *294* (5547), 1708-12.
34. Ross, P. L.; Huang, Y. L. N.; Marchese, J. N.; Williamson, B.; Parker, K.; Hattan, S.; Khainovski, N.; Pillai, S.; Dey, S.; Daniels, S.; Purkayastha, S.; Juhasz, P.; Martin, S.; Bartlet-Jones, M.; He, F.; Jacobson, A.; Pappin, D. J., Multiplexed protein quantitation in Saccharomyces cerevisiae using amine-reactive isobaric tagging reagents. *Mol Cell Proteomics* **2004,** *3* (12), 1154-1169.

35. Braun, A. C.; Gutmann, M.; Luhmann, T.; Meinel, L., Bioorthogonal strategies for site-directed decoration of biomaterials with therapeutic proteins. *J Control Release* **2018,** *273*, 68-85.
36. Sivaramakrishnan, M.; Croll, T. I.; Gupta, R.; Stupar, D.; Van Lonkhuyzen, D. R.; Upton, Z.; Shooter, G. K., Lysine residues of IGF-I are substrates for transglutaminases and modulate downstream IGF-I signalling. *Biochim Biophys Acta* **2013,** *1833* (12), 3176-3185.
37. Wu, F.; Braun, A.; Luhmann, T.; Meinel, L., Site-Specific Conjugated Insulin-like Growth Factor-I for Anabolic Therapy. *Acs Biomaterials Science & Engineering* **2018,** *4* (3), 819-825.
38. Nagase, H.; Fields, G. B., Human matrix metalloproteinase specificity studies using collagen sequence-based synthetic peptides. *Biopolymers* **1996,** *40* (4), 399-416.
39. Holmes, C. P.; Jones, D. G., Reagents for Combinatorial Organic-Synthesis - Development of a New O-Nitrobenzyl Photolabile Linker for Solid-Phase Synthesis. *Journal of Organic Chemistry* **1995,** *60* (8), 2318-2319.
40. Mikkelsen, R. J. T.; Grier, K. E.; Mortensen, K. T.; Nielsen, T. E.; Qvortrup, K., Photolabile Linkers for Solid-Phase Synthesis. *Acs Combinatorial Science* **2018,** *20* (7), 377-399.
41. Thompson, A.; Schäfer, J.; Kuhn, K.; Kienle, S.; Schwarz, J.; Schmidt, G.; Neumann, T.; Hamon, C., Tandem Mass Tags: A Novel Quantification Strategy for Comparative Analysis of Complex Protein Mixtures by MS/MS. *Analytical Chemistry* **2003,** *75* (8), 1895-1904.
42. Bochet, C. G., Photolabile protecting groups and linkers. *J Chem Soc Perk T 1* **2002,** (2), 125-142.
43. Brown, B. B.; Wagner, D. S.; Geysen, H. M., A single-bead decode strategy using electrospray ionization mass spectrometry and a new photolabile linker: 3-amino-3-(2-nitrophenyl)propionic acid. *Mol Divers* **1995,** *1* (1), 4-12.
44. Vaisar, T.; Urban, J., Probing the proline effect in CID of protonated peptides. *J Mass Spectrom* **1996,** *31* (10), 1185-7.
45. Huang, Y.; Tseng, G. C.; Yuan, S.; Pasa-Tolic, L.; Lipton, M. S.; Smith, R. D.; Wysocki, V. H., A data-mining scheme for identifying peptide structural motifs responsible for different MS/MS fragmentation intensity patterns. *J Proteome Res* **2008,** *7* (1), 70-9.
46. Gilbert, T. W.; Sellaro, T. L.; Badylak, S. F., Decellularization of tissues and organs. *Biomaterials* **2006,** *27* (19), 3675-83.
47. Cavalcante, F. S.; Ito, S.; Brewer, K.; Sakai, H.; Alencar, A. M.; Almeida, M. P.; Andrade, J. S., Jr.; Majumdar, A.; Ingenito, E. P.; Suki, B., Mechanical interactions between collagen and proteoglycans: implications for the stability of lung tissue. *J Appl Physiol (1985)* **2005,** *98* (2), 672-9.
48. Tchetverikov, I.; Lard, L. R.; DeGroot, J.; Verzijl, N.; TeKoppele, J. M.; Breedveld, F. C.; Huizinga, T. W.; Hanemaaijer, R., Matrix metalloproteinases-3, -8, -9 as markers of disease activity and joint damage progression in early rheumatoid arthritis. *Ann Rheum Dis* **2003,** *62* (11), 1094-9.
49. Yamanaka, H.; Matsuda, Y.; Tanaka, M.; Sendo, W.; Nakajima, H.; Taniguchi, A.; Kamatani, N., Serum matrix metalloproteinase 3 as a predictor of the degree of joint destruction during the six months after measurement, in patients with early rheumatoid arthritis. *Arthritis & Rheumatism* **2000,** *43* (4).
50. Rohani, M. G.; Parks, W. C., Matrix remodeling by MMPs during wound repair. *Matrix Biol* **2015,** *44-46*, 113-21.
51. Giannandrea, M.; Parks, W. C., Diverse functions of matrix metalloproteinases during fibrosis. *Dis Model Mech* **2014,** *7* (2), 193-203.
52. Ravanti, L.; Kähäri, V. M., Matrix metalloproteinases in wound repair (review). *International Journal of Molecular Medicine* **2000**.
53. Nwomeh, B. C.; Liang, H. X.; Cohen, I. K.; Yager, D. R., MMP-8 is the predominant collagenase in healing wounds and nonhealing ulcers. *J Surg Res* **1999,** *81* (2), 189-95.
54. Gutierrez-Fernandez, A.; Inada, M.; Balbin, M.; Fueyo, A.; Pitiot, A. S.; Astudillo, A.; Hirose, K.; Hirata, M.; Shapiro, S. D.; Noel, A.; Werb, Z.; Krane, S. M.; Lopez-Otin, C.; Puente, X.

S., Increased inflammation delays wound healing in mice deficient in collagenase-2 (MMP-8). *FASEB J* **2007,** *21* (10), 2580-91.
55. Ramon, J.; Saez, V.; Baez, R.; Aldana, R.; Hardy, E., PEGylated interferon-alpha2b: a branched 40K polyethylene glycol derivative. *Pharmaceutical research* **2005,** *22* (8), 1374-86.
56. Lee, S. H.; Lee, S.; Youn, Y. S.; Na, D. H.; Chae, S. Y.; Byun, Y.; Lee, K. C., Synthesis, characterization, and pharmacokinetic studies of PEGylated glucagon-like peptide-1. *Bioconjug Chem* **2005,** *16* (2), 377-82.
57. Gregoriadis, G.; Fernandes, A.; Mital, M.; McCormack, B., Polysialic acids: potential in improving the stability and pharmacokinetics of proteins and other therapeutics. *Cell Mol Life Sci* **2000,** *57* (13-14), 1964-9.
58. Irwin, N.; Green, B. D.; Gault, V. A.; Greer, B.; Harriott, P.; Bailey, C. J.; Flatt, P. R.; O'Harte, F. P., Degradation, insulin secretion, and antihyperglycemic actions of two palmitate-derivitized N-terminal pyroglutamyl analogues of glucose-dependent insulinotropic polypeptide. *J Med Chem* **2005,** *48* (4), 1244-50.
59. Basel, M. T.; Shrestha, T. B.; Troyer, D. L.; Bossmann, S. H., Protease-sensitive, polymer-caged liposomes: a method for making highly targeted liposomes using triggered release. *ACS Nano* **2011,** *5* (3), 2162-75.
60. Park, C.; Kim, H.; Kim, S.; Kim, C., Enzyme responsive nanocontainers with cyclodextrin gatekeepers and synergistic effects in release of guests. *J Am Chem Soc* **2009,** *131* (46), 16614-5.
61. Lee, E. S.; Na, K.; Bae, Y. H., Super pH-sensitive multifunctional polymeric micelle. *Nano Lett* **2005,** *5* (2), 325-9.
62. Choi, S. W.; Zhang, Y.; Xia, Y., A temperature-sensitive drug release system based on phase-change materials. *Angew Chem Int Ed Engl* **2010,** *49* (43), 7904-8.
63. de Gracia Lux, C.; Joshi-Barr, S.; Nguyen, T.; Mahmoud, E.; Schopf, E.; Fomina, N.; Almutairi, A., Biocompatible polymeric nanoparticles degrade and release cargo in response to biologically relevant levels of hydrogen peroxide. *J Am Chem Soc* **2012,** *134* (38), 15758-64.
64. Gutmann, M.; Bechold, J.; Seibel, J.; Meinel, L.; Lühmann, T., Metabolic Glycoengineering of Cell-Derived Matrices and Cell Surfaces: A Combination of Key Principles and Step-by-Step Procedures. *ACS Biomaterials Science & Engineering* **2018**.
65. Rappsilber, J.; Mann, M.; Ishihama, Y., Protocol for micro-purification, enrichment, pre-fractionation and storage of peptides for proteomics using StageTips. *Nat Protoc* **2007,** *2* (8), 1896-906.

Supporting Information

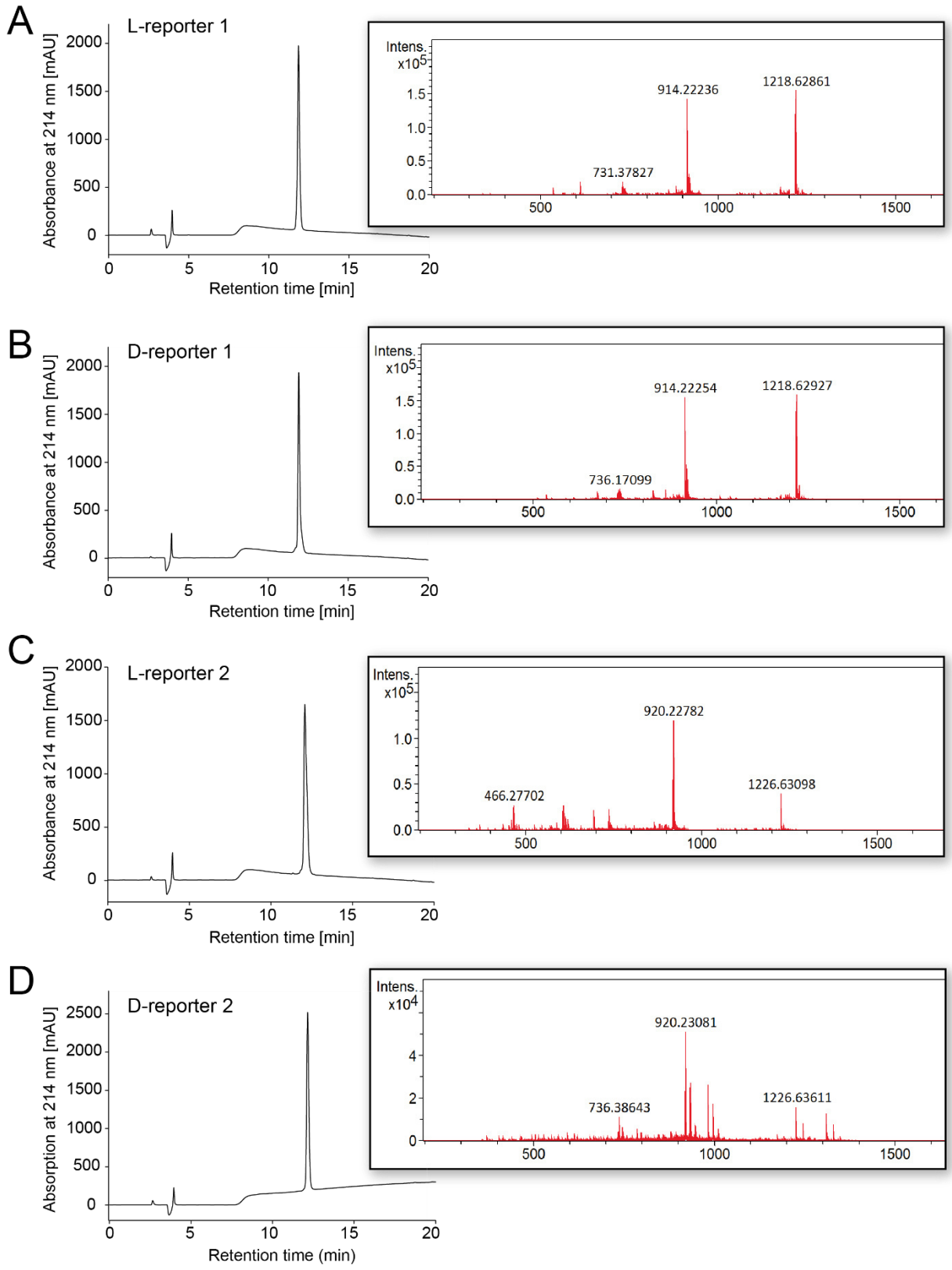

Figure S 1 Peptide purity was analyzed by RP-HPLC and peptide identification was performed by ESI for (A) L-mass reporter 1, (B) D-mass reporter 1, (C) L-mass reporter 2 and (D) D-mass reporter 2.

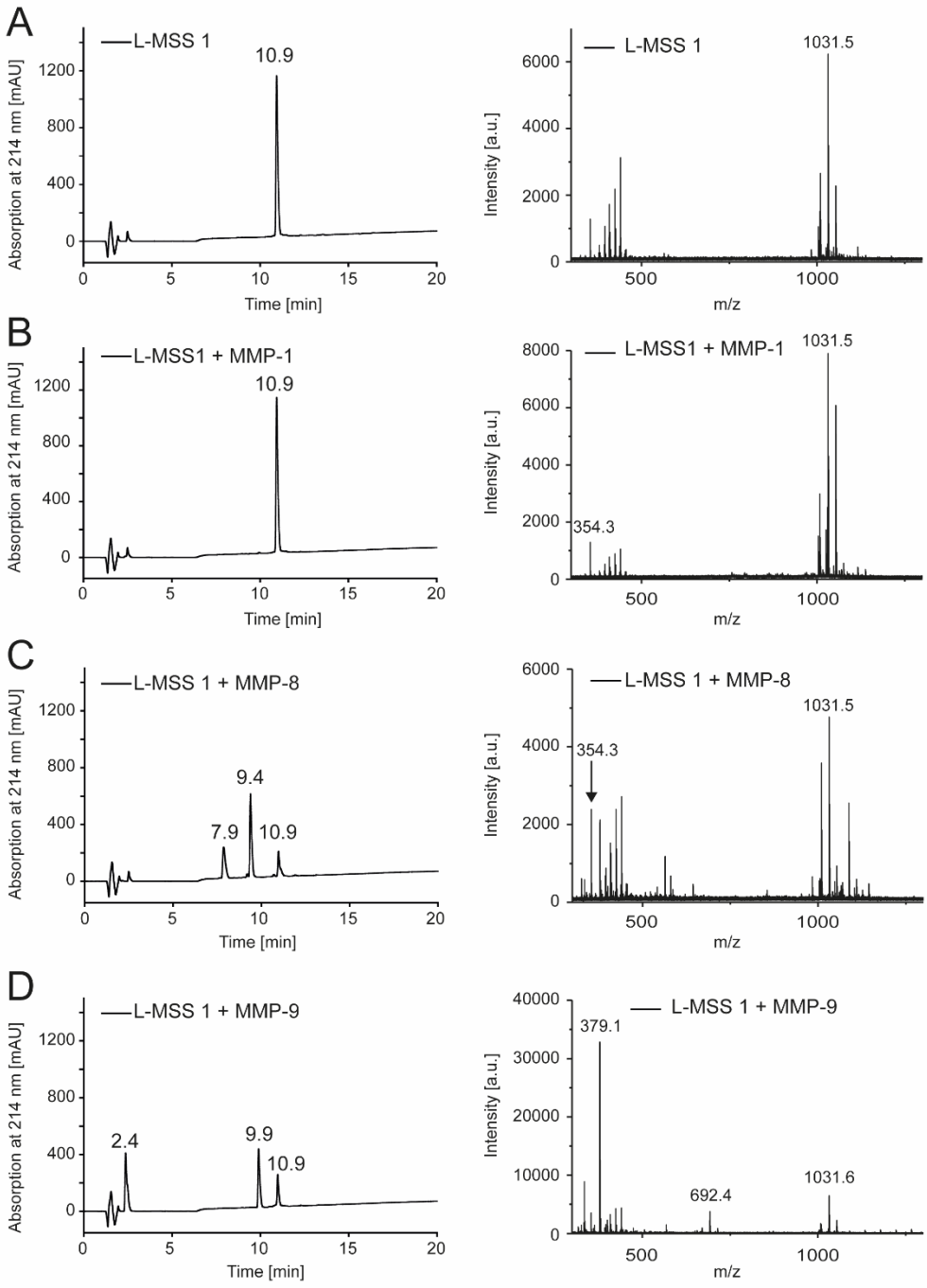

Figure S 2 RP-HPLC analysis and MALDI measurements of the synthesized protease-sensitive sequences incubated with MMP-1, -8 and -9 as function of time to assess peptide purity and the cleavage kinetics. (A) 'L-MMP sensitive peptide sequence 1' synthesized with natural L-amino acids. (B) 'L-MMP sensitive peptide sequence 1' + 35.1 nM MMP-1, (C) 'L-MMP sensitive peptide sequence 1' + 13.2 nM MMP-8 and (D) 'L-MMP sensitive peptide sequence 1' +10.6 nM MMP-9.

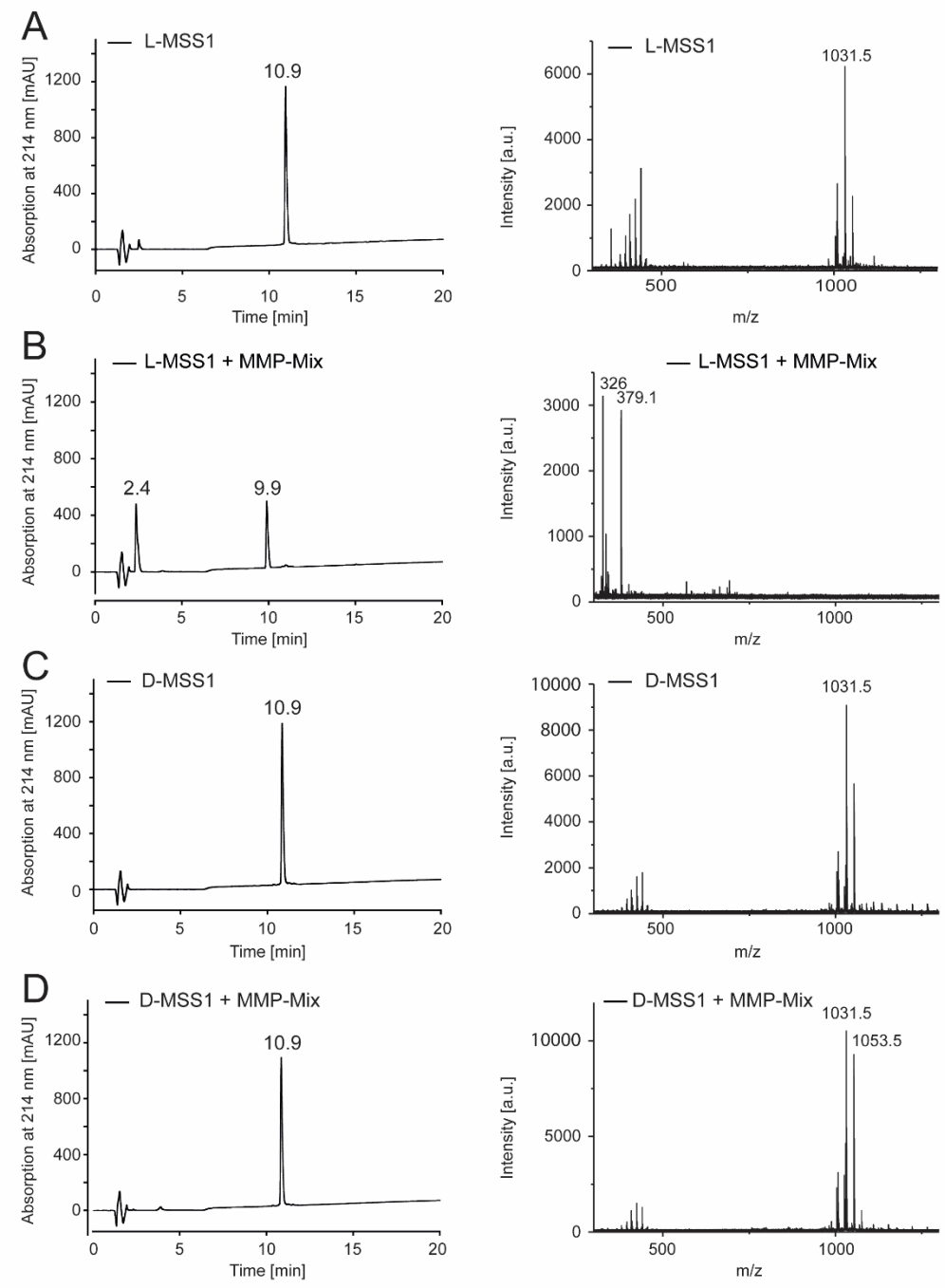

Figure S 3 RP-HPLC analysis and MALDI measurements of L- and D-matrix metalloproteinase reporter 1 incubated with a mix of MMP-1, -8 and -9 for 24 h at 37 °C. (A) 'L-MMP sensitive peptide sequence 1' was incubated without (A) and with (B) MMP-1, -8 and -9 and the results show complete cleavage of 'L-MMP sensitive peptide sequence 1' after 24 h. 'D-MMP sensitive peptide sequence 1' was incubated without (C) and with (D) MMP-Mix and showed no cleavage after 24 h.

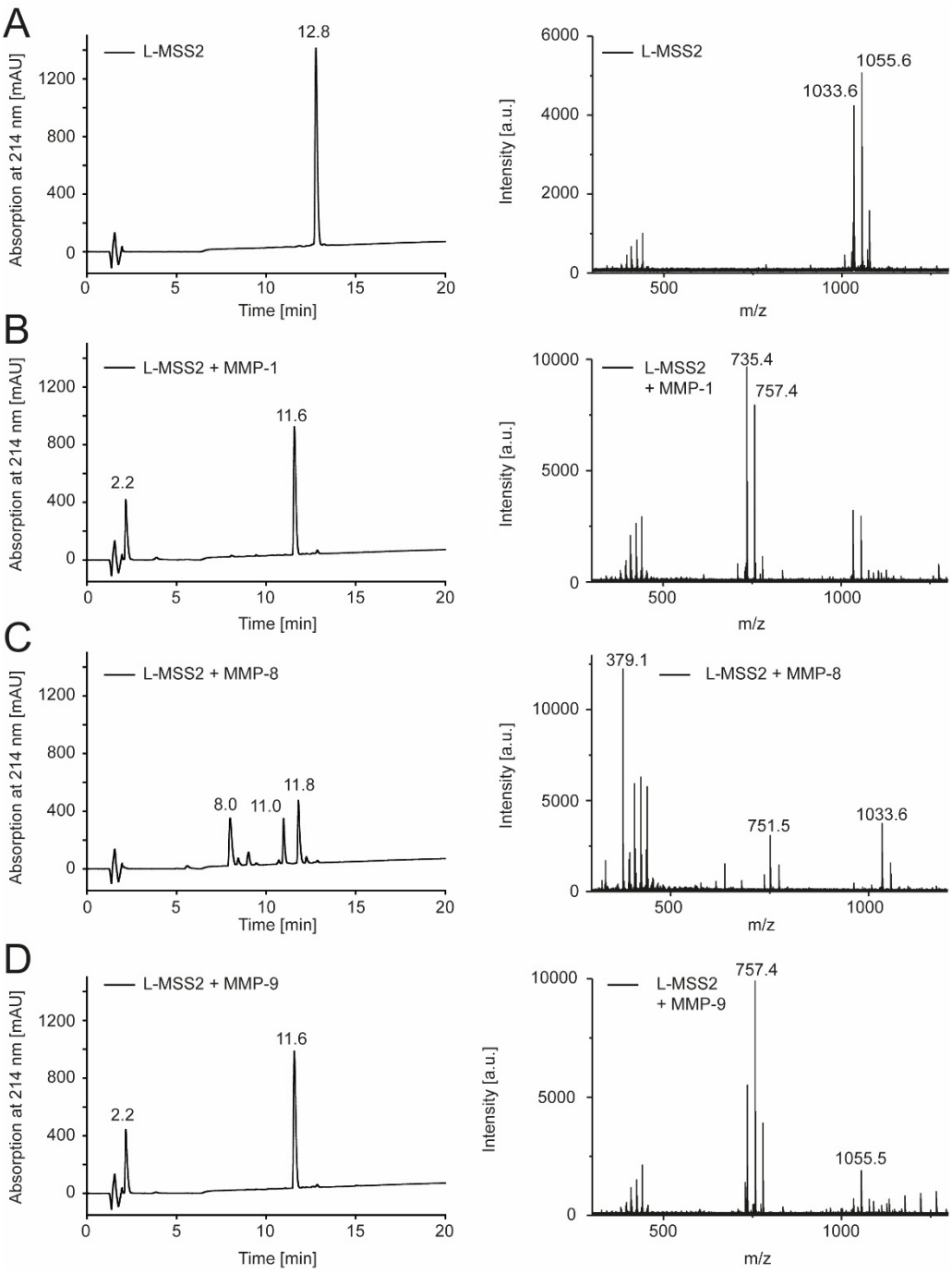

Figure S 4 RP-HPLC analysis and MALDI measurements of the synthesized protease-sensitive sequences incubated with MMP-1, -8 and -9 as function of time to assess peptide purity and the cleavage kinetics, here after 48 hours. (A) 'L-MMP sensitive peptide sequence 2' synthesized with natural L-amino acids. (B) 'L-MMP sensitive peptide sequence 2' + 35.1 nM MMP-1, (C) 'L-MMP sensitive peptide sequence 2' + 13.2 nM MMP-8 and (D) 'L-MMP sensitive peptide sequence 2' +10.6 nM MMP-9.

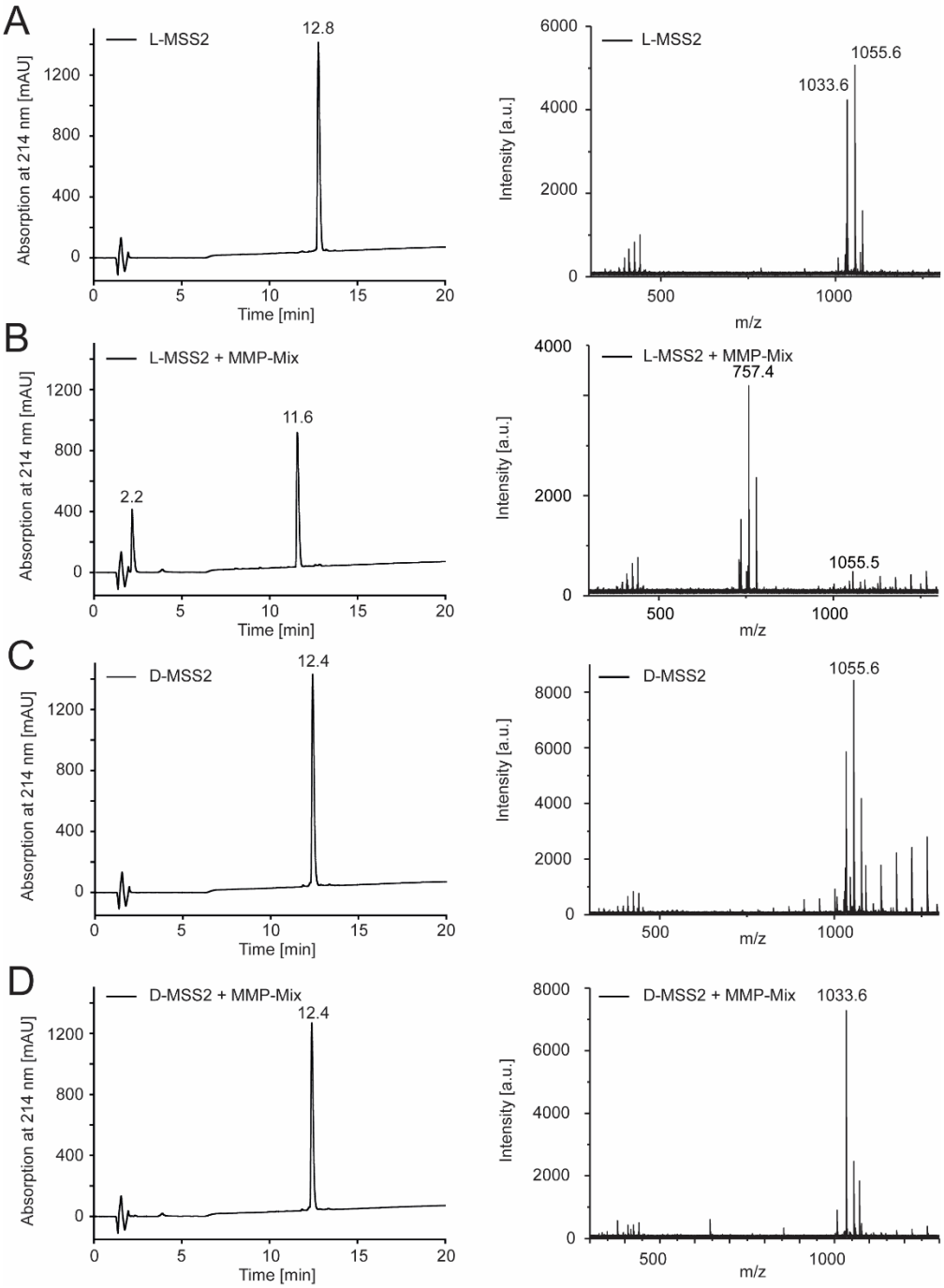

Figure S 5 RP-HPLC analysis and MALDI measurements of L- and D-matrix metalloproteinase reporter 2 incubated with a mix of MMP-1, -8 and -9 for 24 hours at 37 °C. (A) 'L-MMP sensitive peptide sequence 2' was incubated without (A) and with (B) MMP-1, -8 and -9 and the results show complete cleavage of 'L-MMP sensitive peptide sequence 2' after 24 h. 'D-MMP sensitive peptide sequence 2' was incubated without (C) and with (D) MMP-Mix and showed no cleavage after 24 h.

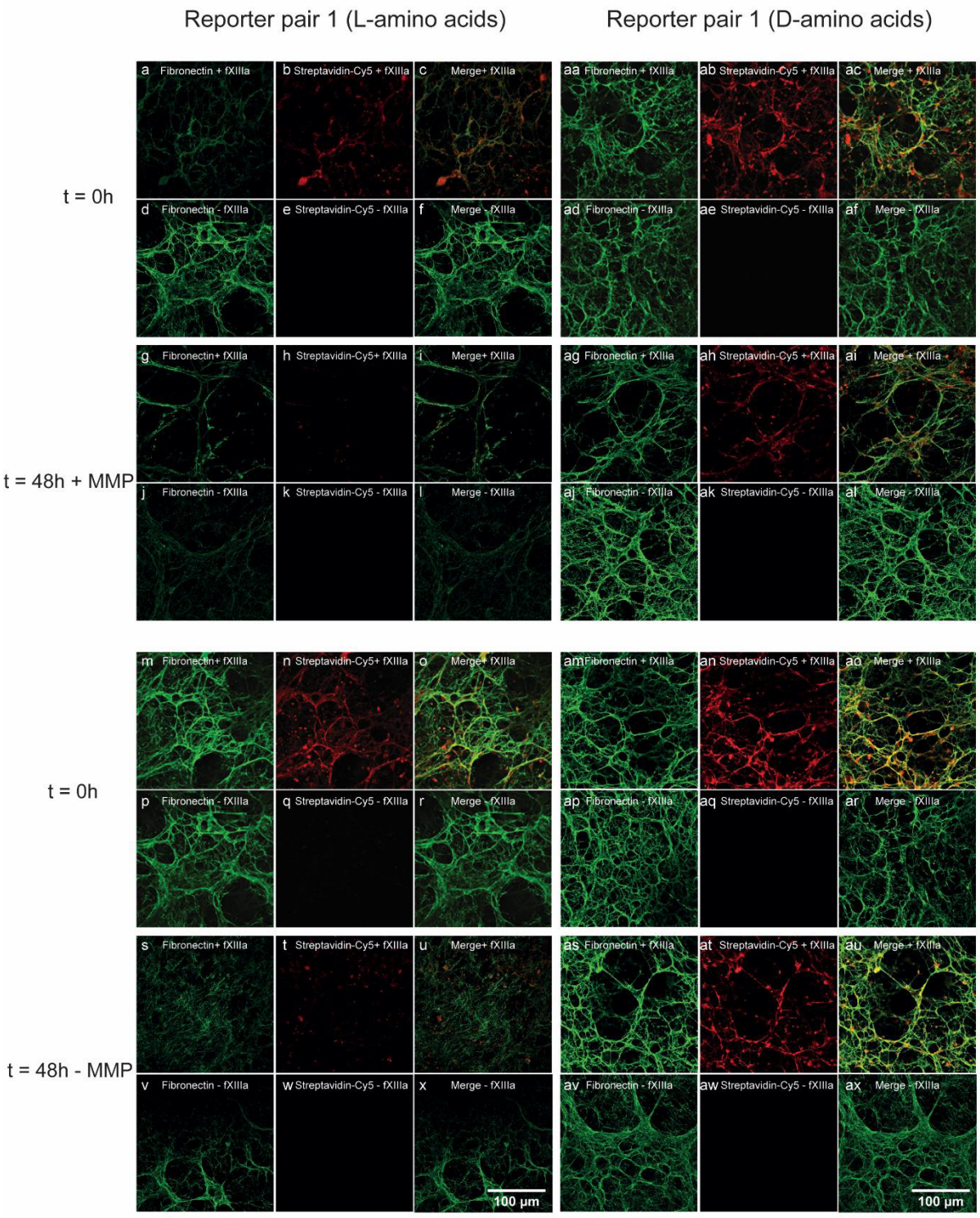

Figure S 6 Confocal laser scanning images of reporter pair 1 in L- and D-version. Images were taken immediately after incubating peptides on ECM with and without transglutaminase (t = 0 h), after 48 hours of incubation with MMP-9 (t = 48 h + MMP) and after 48 hours incubation with buffer (t = 48 h – MMP). Fibronectin was stained with AF488 (green), biotinylated peptides immobilized on ECM were stained with Cy5 (red) and the pictures were merged in the third column (yellow).

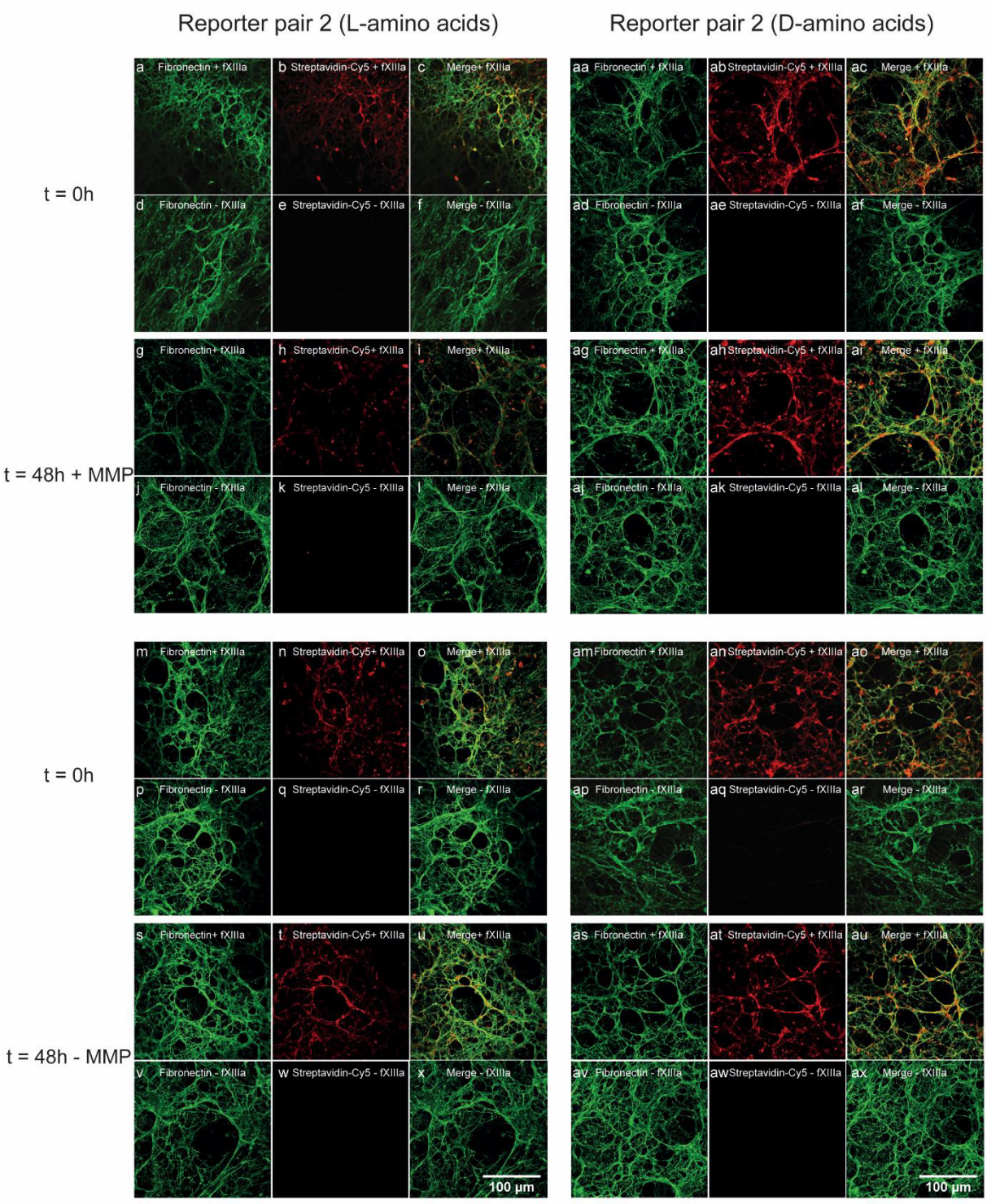

Figure S 7 Confocal laser scanning images of reporter pair 2 in L- and D-version. Images were taken immediately after incubating peptides on ECM with and without transglutaminase (t = 0 h), after 48 hours of incubation with MMP-9 (t = 48 h + MMP) and after 48 hours incubation with buffer (t = 48 h – MMP). Fibronectin was stained with AF488 (green), biotinylated peptides immobilized on ECM were stained with Cy5 (red) and the pictures were merged in the third column (yellow).

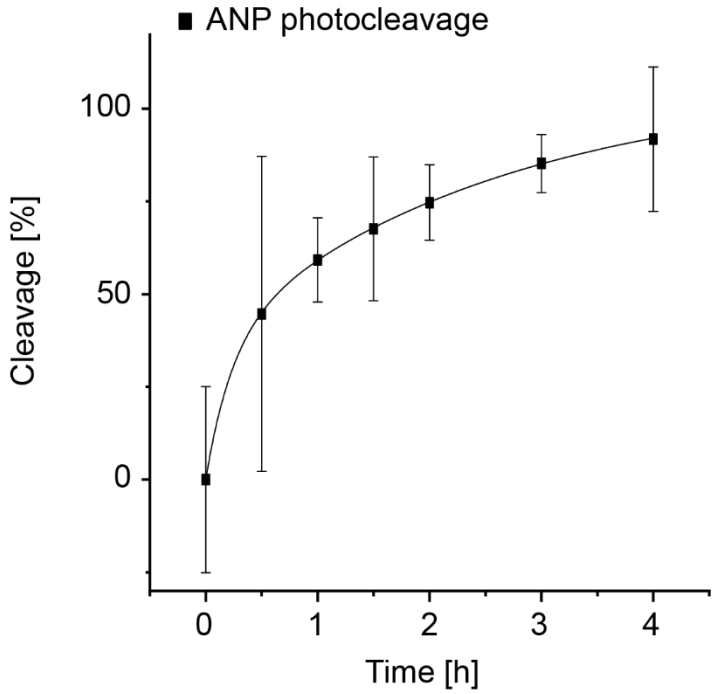

Figure S 8 RP-HPLC analysis of ANP photo-cleavage with UV light of 366 nm. After 4 h of UV irradiation the ANP molecule was almost completely cleaved.

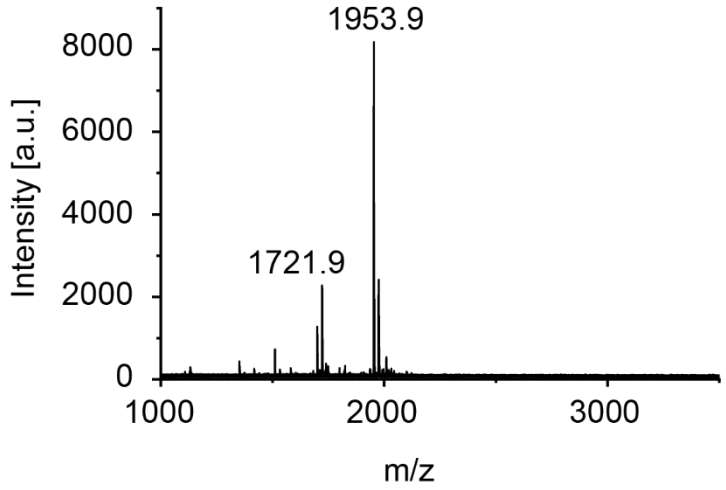

Figure S 9 MALDI spectrum of N-terminal part of L-reporter 2 after photolysis with 366 nm.

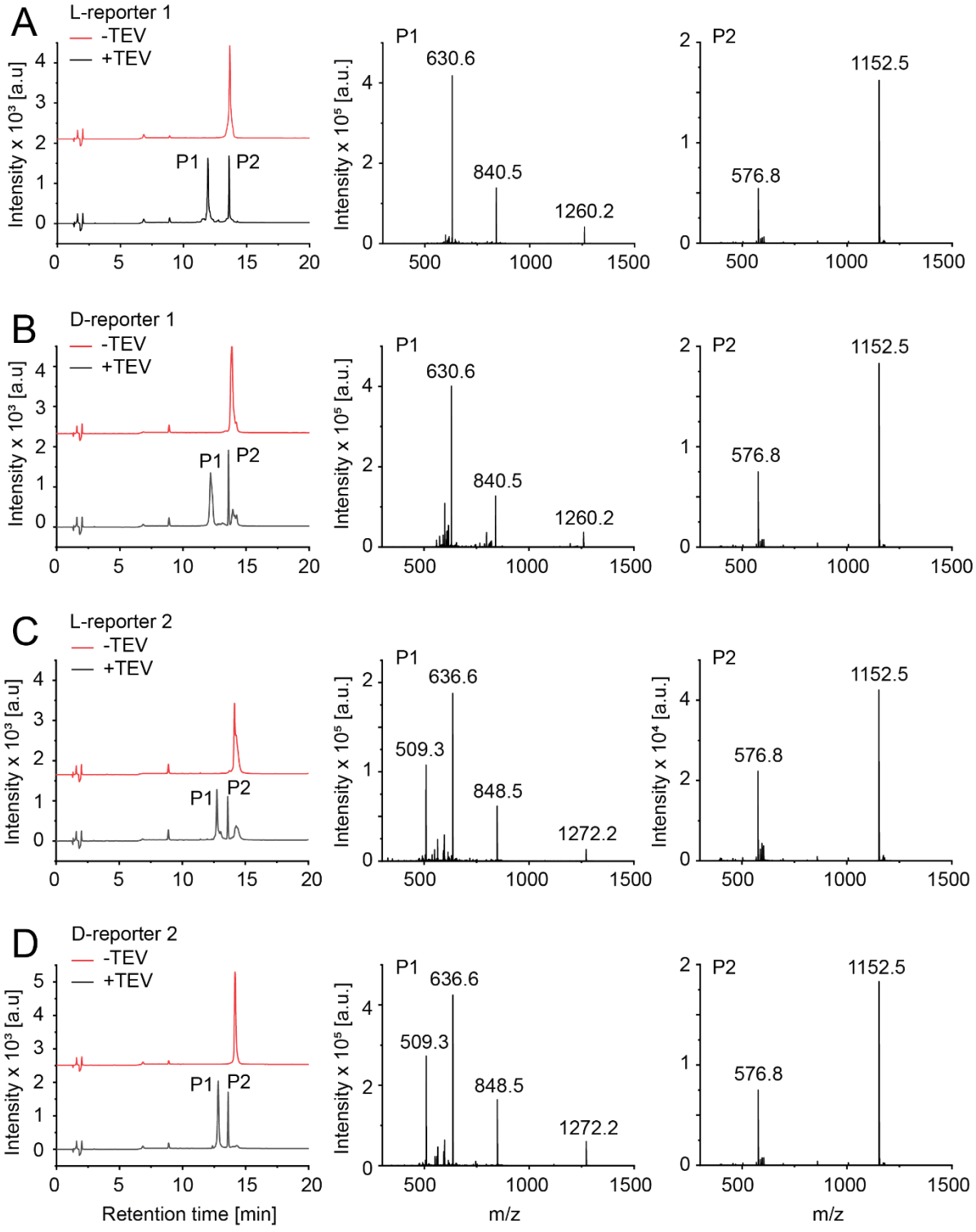

Figure S 10 RP-HPLC analysis and ESI spectra of reporter pair 1 and 2 after incubation with TEV protease. The four mass reporters were dissolved in TEV buffer (50 mM Tris-HCl, pH 8.0, 10 mM EDTA, 10 mM DTT) to reach a final concentration of 0.5 mM. 10 U / 20 µg peptide of AcTEV protease was added and samples were incubated at 30 °C for 6 hours. Supernatant was collected and analyzed by RP-HPLC and ESI. n=3 (A) L-reporter 1, (B) D-reporter 1, (C) L-reporter 2 and (D) D-reporter 2 were completely cleaved by TEV protease and cleavage was confirmed by ESI. Reporter pair 1 is cleaved in two peptide fragment with a calculated mass of $[M+H]^+$ = 1151.35 and $[M+H]^+$ = 2519.77 g/mol and reporter pair 2 resulted in two peptide fragments after TEV incubation with a calculated mass of $[M+H]^+$ = 1151.35 and $[M+H]^+$ = 2543.83 g/mol.

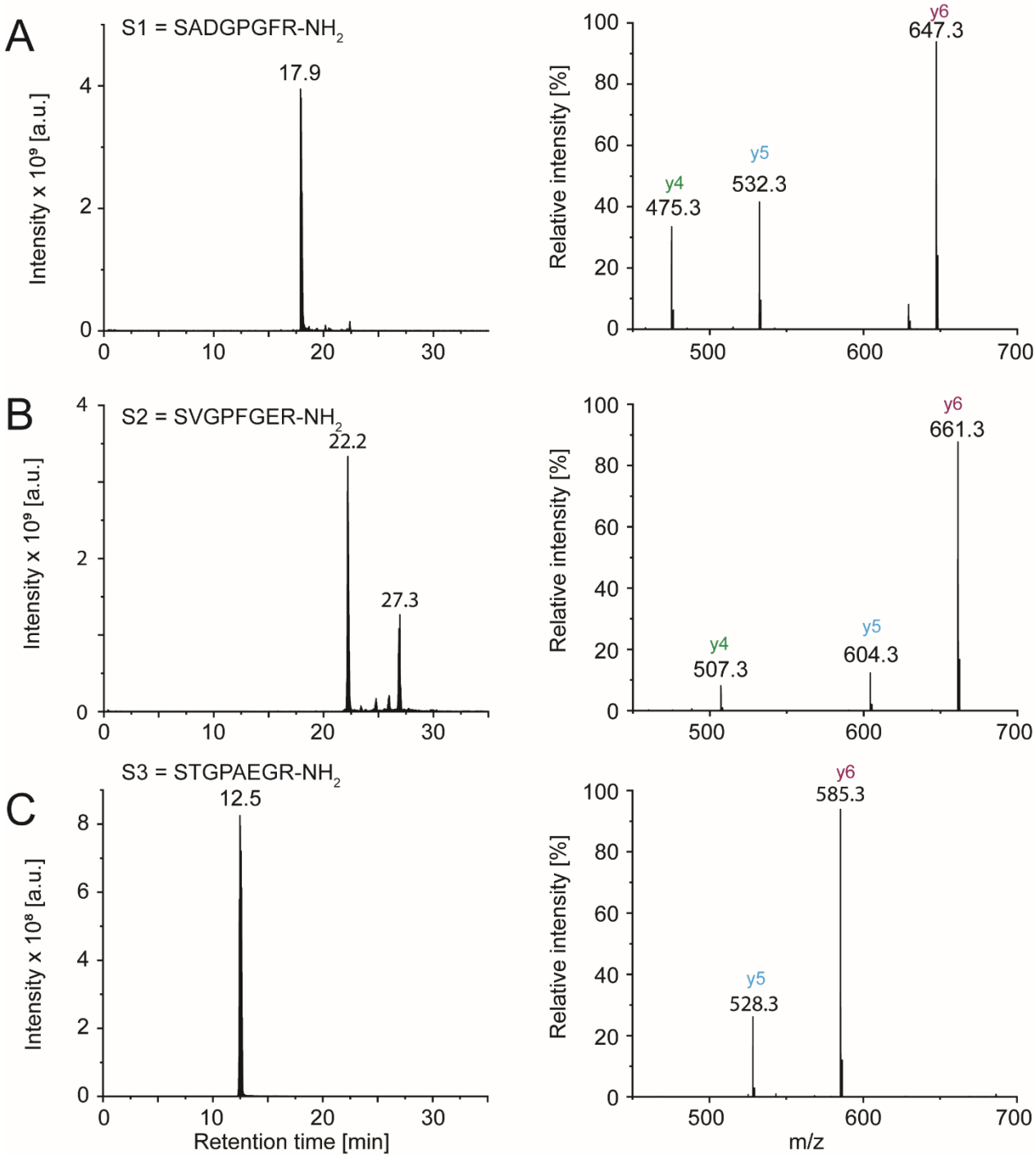

Figure S 11 Base peak chromatograms and MS² spectra of the three initially designed mass tag sequences S1-S3 obtained with 20 % normalized collision energy and the precursor ions m/z 403.2010, m/z 424.2242, and m/z 387.1980 for S1, S2, and S3, respectively.

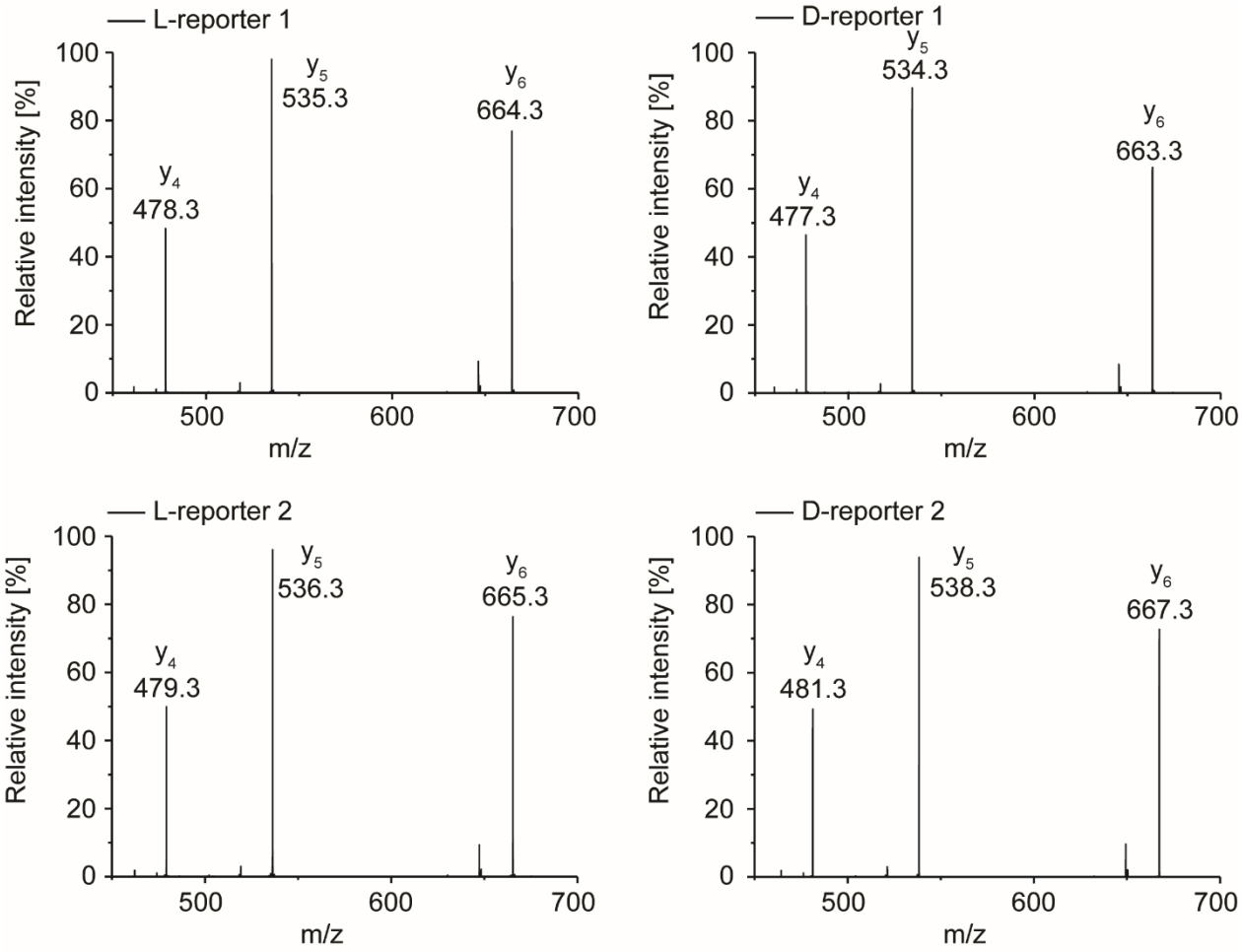

Figure S 12 MS² spectra of mass reporter pairs 1 and 2 in L- and D-version using 413.2144 ± 22 ppm as precursor ion and 20 % of normalized collision energy. The spectra show y_4, y_5 and y_6 fragment ions. The reporters were produced by enriching the mass tag with heavy amino acids during peptide synthesis producing variants differentiated by 1 Da for the reporter pair 1 and by 2 Da for the reporter pair 2.

CHAPTER 3: SOLUBLE MASS REPORTERS FOR DETECTION OF ENZYME ACTIVITY AND MULTIPLEXED ANALYSIS

Katharina Dodt[1], Yejun Hu[2], Stephanie Lamer[3], Andreas Schlosser[3], Tessa Lühmann[1], Hongwei Ouyang[2], Lorenz Meinel[1]

[1] Institute of Pharmacy and Food Chemistry, University of Würzburg, 97074 Würzburg, Germany

[2] Center for Stem Cell and Tissue Engineering, School of Medicine, Zhejiang University, Hangzhou 310058, China

[3] Rudolf-Virchow-Center for Experimental Biomedicine, University of Wuerzburg, Josef-Schneider-Str. 2, 97080 Wuerzburg, Germany

Unpublished manuscript

Abstract

Many osteoarthritis (OA) or rheumatoid arthritis (RA) diagnostic systems are systemically injected and analyzed by *in vivo* imaging. Inflammation in the knee joint can be monitored by measuring enzyme activity in synovial fluid (SF) collected during arthrocentesis, but visits to the joint are limited. In order to overcome these limitations, we designed a soluble mass reporter system consisting of seven modules with different functions monitoring enzyme activity in SF. It was adapted from a previously presented mass reporter system with immobilizing ability, which is already characterized in terms of responsiveness to matrix metalloproteinases (MMPs) and TEV protease (TEVp), ultraviolet (UV)-sensitivity, and multiplexing. In this study the soluble system is further characterized and its feasibility in an *in vivo* osteoarthritic mouse model was tested. The system is bio-orthogonally clicked with its azide-residue to a 10 kDa dibenzocyclooctyne (DBCO)-4-arm-polyethylene glycol (PEG) to retain the mass reporters in the joint cavity. The core module is the isotopically labelled mass tag sequence, which allows for multiplexed analysis due to the applied isobaric mass encoding strategy. The mass tags are released from the 10 kDa polymer in response to elevated levels of MMPs which cleave an incorporated protease-sensitive sequence (PSS). The stability of mass reporter peptide fragments (apart from their designated cleavage sites) against MMP cleavage, UV irradiation and TEVp cleavage was tested to ensure the peptide's integrity during purification before tandem mass spectrometry (LC-MS/MS). The *in vivo* study showed biocompatibility of mass reporters in mice.

Introduction

Enzyme activity in synovial fluid can be measured by ELISA when SF is withdrawn by arthrocentesis (joint aspiration). Such intra-articular visits, however, are limited to three times per year in many contries[1], body fluids like blood (in small volumes) and urine can be collected daily. Therefore, soluble detection systems with diagnostic value are often systemically injected, fulfill a targeting strategy and are monitored by *in vivo* imaging or near infrared fluorescence (NIR)[2-4]. The aforementioned diagnostic systems share a systemic administration and remain in the body for detection. The principles of mass-encoded peptides were developed in previous studies,[5] in which iron oxide nanoworms were modified with mass-encoded peptides with a disease-associated protease sensitive sequence and a urine targeting sequence. The nanoworms passively accumulate in liver tissue[6] where proteases cleave the peptide sequence and the cleaved peptide fragments are directed to the kidney by Glu-fib, a modified derivative of the endogenous fibrinopeptide B[7], and are secreted into the urine from where they are detected by tandem mass spectrometry.

In order to overcome the limitations of intra-articular visits we designed a soluble diagnostic system to detect enzyme (MMP) activity in an inflammatory environment after a single intra-articular injection. We developed a soluble diagnostic mass reporter system, that was modified from a previously inflammation-sensing mass reporter system being immobilized on ECM and was tested in an *in vitro* setting.[8, 9] Compared to the previous system the N-terminal affinity tag was changed from biotin to Strep-tag II, coupled to a 2.5 kDa PEG-chain to increase the system's plasma half-life. The following modules: TEV protease sequence (TEVs), isotopically labelled mass tag, photolabile linker and the protease-sensitive sequence are similar in both systems and were already characterized. But instead of the immobilization tag (transglutaminase (TG) sequence) the PSS was C-terminally extended by azidolysine as a prerequisite for strain-promoted azide-alkyne cycloaddition to a 10 kDa-DBCO-4-arm-PEG. The purpose of this study was to further characterize the mass reporter system and to test the system's feasibility in an *in vivo* osteoarthritis mouse model. It was expected to determine the MMP activity in SF from osteoarthritic mouse knee joints and identify different protease patterns in each mouse as MMP activity has been proven to be linked with cartilage degradation and joint destruction[10-12]. In analogy to the nanoworm study, in this system the isotopically labelled peptides were released in response to elevated protease levels and detected by LC-MS/MS.

To avoid disadvantages of targeting, like off-site peptide cleavage after systemic administration and the fact, that the passage of molecules from the blood to the synovial space is affected of the molecule's size, its concentration in blood and the state of synovial inflammation[13], we chose the local application route of intra-articular injection. The injection results in a diagnostic depot and ensured that the mass reporter concentration in the synovial gap was constant with each injection in each individual. Due to the 4-arm-PEG module the mass reporters' size (~26 800 Da, **table 2**) is increased with the aim to retain them in the joint cavity. Diffusion into the blood stream through synovial capillary, synovial interstitium and lymphatic drainage system[14] probably takes place anyway, but due to the reporters' size the diffusion rate may be strongly decreased.

Results

Soluble mass reporter system

The soluble mass reporters consist of seven modules with individual functions. Module #1 comprised of a N-terminal 2.5 kDa PEG to adapt the pharmacokinetic profile (prolongation of half-life), followed by the Strep-tag II sequence, an improved artificial peptide ligand of streptavidin[15] for affinity purification containing an N-terminal cysteine for the thiol-iodoacetamide coupling strategy to 2.5 kDa PEG. The TEV protease substrate sequence was chosen as module #3 and functioned as enzymatic cleavage site to separate PEG/Strep-tag II/TEVs from the mass tag during the purification process and before LC-MS/MS analysis. Module #4 consists of the isotopically labelled mass tag, that is used for multiplexed detection in tandem mass spectrometry, followed by a photo-labile molecule (3-amino-3-(2-nitrophenyl)propionic acid), that was incorporated to separate the mass tag from the following protease-sensitive sequence. This module #6 is used in two different matrix metalloproteinase substrate sequences (MSS) having different sensitivity to MMPs. Moreover, MSS1 and 2 were synthesized in a cleavable L-amino acid version and a non-cleavable D-amino acid version, which served as internal, negative control. The MSSs were synthesized with a C- terminal azidolysine residue to click the peptide to module #7, a high molecular weight 4-arm-DBCO-PEG (**Figure 1**). As the mass reporter system should be applied in a mouse model of OA, the strain-promoted azide-alkyne cycloaddition (SPAAC) was chosen, because it does not require cytotoxic copper as a catalyst.

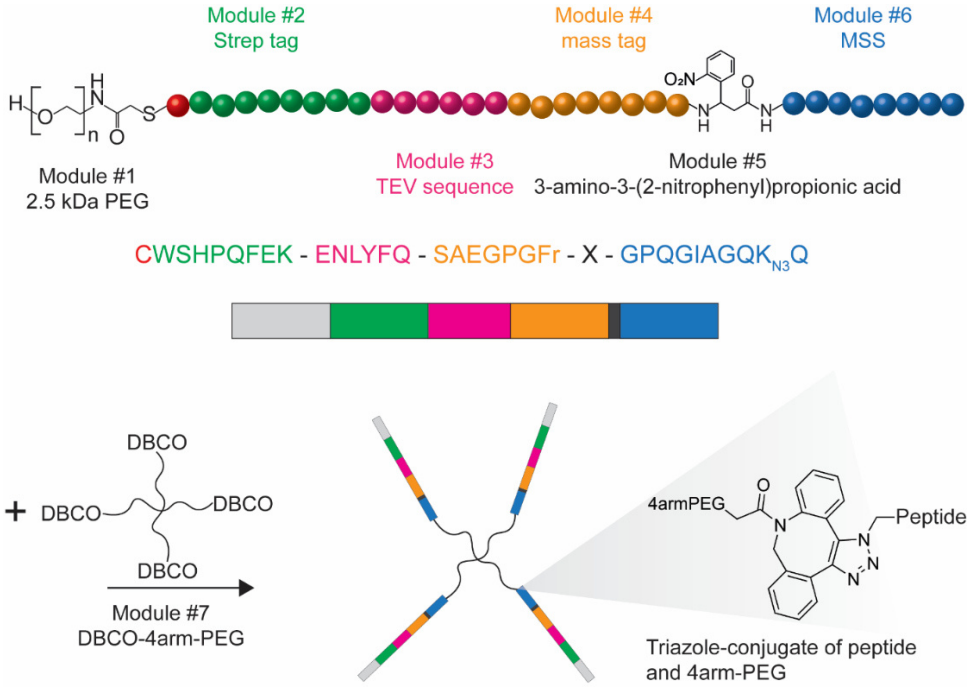

Figure 4 Overview of soluble mass reporters assembled from seven modules, each with a unique function.

The amino acid sequence consists of 34 amino acids and was synthesized by solid phase peptide synthesis (SPPS), purified via fast protein liquid chromatography (FPLC, Äkta) and characterized by reversed-phase high performance liquid chromatography (RP-HPLC) and matrix-assisted laser desorption/ionization (MALDI) (**Figure S1**).

Table 1 shows the mass reporter's name, acronym, amino acid sequence, and their molecular weight.

Table 3 Information on mass reporter peptides

Name	Acronym	Sequence	Molecular weight [g/mol]
soluble L-MSS1 - mass reporter 1	sL-reporter 1	CWSHPQFEK-ENLYFQ-SAEGPG^{+6}Fr-X-GPQGIAGQK$_{N3}$Q	3989.31
soluble D-MSS1 - mass reporter 1	sD-reporter 1	CWSHPQFEK-ENLYFQ-S^{+1}AEG^{+1}P^{+3}G^{+1}Fr-X-GpqGiaGqK$_{N3}$Q	3989.31
soluble L-MSS2 - mass reporter 2	sL-reporter 2	CWSHPQFEK-ENLYFQ-S^{+4}AEGP^{+2}GFr-X-GPSGLLAHK$_{N3}$Q	4013.88
soluble D-MSS2 - mass reporter 2	sD-reporter 2	CWSHPQFEK-ENLYFQ-$^{+1}$S^{+4}AEGP^{+1}GFr-X-GpsGllahK$_{N3}$Q	4013.88
Soluble pre-cleaved reporter	s-pc-reporter	CWSHPQFEK-ENLYFQ-S^{+3}AEGP^{+3}GFr-X-GPQG	3331.59

The N-terminal cysteine was used to increase the peptides' molecular weight by coupling it to a ~2.5 kDa PEG chain. The used PEG was functionalized with iodoacetamide to perform an iodoacetamide-thiol reaction to couple it to the cysteine's thiol (**Figure S2**). By the introduction of a 10 kDa 4-arm-DBCO-PEG, which was synthesized from the two educts 4-arm-PEG-NH_2 and DBCO-PEG-N-hydroxysuccinimide (NHS), the peptides' molecular weight and their hydrodynamic radius was further increased with the aim to prevent/restrain diffusion from the site of injection. The 4-arm-DBCO-PEG was coupled to the peptide by the bio-orthogonal SPAAC. The SPAAC was chosen as coupling strategy over the copper-catalyzed azide-alkyne cycloaddition (CuAAC) because it proceeds rapidly under mild reaction conditions and function in absence of a cytotoxic copper (Cu(I)) catalyst[16, 17]. **Table 2** details the characteristics of the soluble mass reporters.

Table 4 Amino acid sequence and molecular weight of a4arm-PEG mass reporters

Acronym	**Sequence**	**MW [g/mol]**	**Concentration [mM]**
PEG-sLr1-4armPEG	[PEG - CWSHPQFEK-ENLYFQ-SAEGPG^{+6}Fr-X-GPQGIAGQK$_{N3}$Q]$_4$ – 4-arm-PEG	~ 26800	0.784
PEG-sDr1-4armPEG	[PEG - CWSHPQFEK-ENLYFQ-S^{+1}AEG^{+1}P^{+3}G^{+1}Fr-X-GpqGiaGqK$_{N3}$Q]$_4$ – 4-arm-PEG	~ 26800	1.764
PEG-sLr2-4armPEG	[PEG - CWSHPQFEK-ENLYFQ-S^{+4}AEGP^{+2}GFr-X-GPSGLLAHK$_{N3}$Q]$_4$ – 4-arm-PEG	~ 26800	1.635
PEG-sDr2-4armPEG	[PEG - CWSHPQFEK-ENLYFQ-$^{+1}$S^{+4}AEGP^{+1}GFr-X-GpsGllahK$_{N3}$Q]$_4$ – 4-arm-PEG	~ 26800	1.384
Validation reporter	PEG - CWSHPQFEK-ENLYFQ-SAEGPGFr-X-GPQG	7417.45	0.256

Compared to the soluble mass reporters the validation reporter has an already pre-cleaved MSS and was not coupled to a 10 kDa 4-arm-PEG, so that it resembled the mass reporter peptides after MMP cleavage which allowed the diffusion from the injection site. It was applied in order to validate the systems function and to make sure, that the diffusion route from SF to blood (or other collected body fluid) really worked.

After sample collection, the cleaved mass reporters undergo a three-step purification procedure to purify the peptide from the body fluid and to isolate the mass tag from the

attached modules. Step #1 is the UV irradiation with 365 nm for 6 hours to cleavage the photolabile linker between mass tag and the four remaining amino acids from the MSS. The second step is affinity purification by using the Strep-tag II complexing ability to bind to Strep-Tactin® coated magnetic beads. In doing so the mass tag containing peptides are separated from the photo-cleaved amino acid residues. The treated mass reporters are now immobilized on beads and to release the mass tag, the beads are incubated with TEVp for 6 hours. The mass tags are now located in the supernatant, which is cleaned-up by StageTips and analysed by LC-MS/MS.

MMP-substrate sequences

Two PSS also named MMP-substrate sequences (as they are cleaved by MMPs) were chosen for the diagnostic system: MSS1 and MSS2 possess the amino acid sequences of GPQGIAGQK$_{N3}$Q and GPSGLLAHK$_{N3}$Q, respectively (**Table 3**). According to previous experiments, they possess different cleavage kinetics while the cleavage efficiency increased from MSS1 to MSS2 (for MMP-1 and -9).[8] The MSS1 and 2 were synthesized in two versions: on the one hand with natural occurring L-amino acids and on the other hand with non-natural D-amino acids. The D-versions were not cleaved by MMPs and served as internal standard. L- and D-sequences were used as pairs. The four peptides were synthesized with a C-terminal glutamine (Q), which was added because in prior studies an increased cleavage efficiency with glutamine was postulated[18]. The four amino acid sequences were synthesized by solid phase peptide synthesis, purified by FPLC and identified with RP-HPLC and LC-MS (**Figure S3).**

Table 5 Amino acid sequence and molecular weight of matrix metalloproteinase substrate sequences (MSS)

Name	**Sequence***	**Molecular Weight**
L-MSS1	GPSGIAGQK$_{N3}$Q	1008.51
D-MSS1	GpsGiaGqK$_{N3}$Q	1008.51
L-MSS2	GPSGLLAHK$_{N3}$Q	1032.55
D-MSS2	GpsGllahK$_{N3}$Q	1032.55

*Small letters indicate D-amino acids

MMP responsiveness of MSS

The methods and results of MMP cleavage experiments of MSS1 and 2 in L- and D-version are shown in chapter 2, Figure 2.

Stability of peptide fragments against MMPs

The following peptide fragments (**Table 4**) were synthesized to characterize the whole peptide construct in terms of protease- (MMP and TEVp) and light-sensitivity. The fragments were used, because if another cleavage site was found, it would be easier to locate the site of cleavage in a smaller fragment than in the whole peptide construct. The peptide fragments were synthesized by solid phase peptide synthesis, purified by FPLC and analysed by RP-HPLC and LC-MS (**Figure S4**).

Table 6 Amino acid sequence and molecular weight of peptide fragments

Name	**Sequence**	**Molecular weight [g/mol]**	**$[M+H]^{2+}$**
SeqKD1	FEKENLY	984.06	493.03
SeqKD2	PGFrGPQ	799.87	400.94
Cys-Ala	CWSHPQFEKENLYFQSA	2156.34	1079.17
ST	CWSHPQFEK	1202.34	602.17
TEVs	ENLYFQS	899.94	450.97
Mass tag	SAEGPGFr	861.89	431.95

The peptide fragments were dissolved in MMP buffer (50 mM Tris-HCl, 200 mM NaCl, 5 mM $CaCl_2$, 1 µM $ZnCl_2$, pH 7.4) and diluted to a final concentration of 1 mg/ml. As the cysteine's sulfhydryl group can block MMPs activity by coordinating the catalytic zinc ion in the catalytic domain, both peptides, Cys-Ala and Strep-tag II, were incubated with iodoacetamide to alkylate the N-terminal cysteine and to prevent the formation of a complex with the zinc ion[19, 20]. A 10-fold MMP-Mix stock solution was prepared and was added to the peptides to reach a final concentration of 35.1 mM for MMP-1, 13.2 mM for MMP-8, 10.6 mM for MMP-9 and 4 nM for MMP-13 and they were incubated for 15 hours at 37 °C. After the reaction was stopped by heating the reaction mix to 95 °C for 15 minutes the peptides were analysed by RP-HPLC. For five of the six peptide fragments no MMP responsiveness was detected as peak shape and retention time remained unchanged before and after MMP incubation (**Figure 2A, B, C, E, F**). After MMP incubation of Cys-Ala a small new peak appeared next to the main peptide peak. LC-MS measurements revealed that the C-terminal tripeptide Gln-Ser-Ala (QSA) was cleaved (**Figure 2D**).

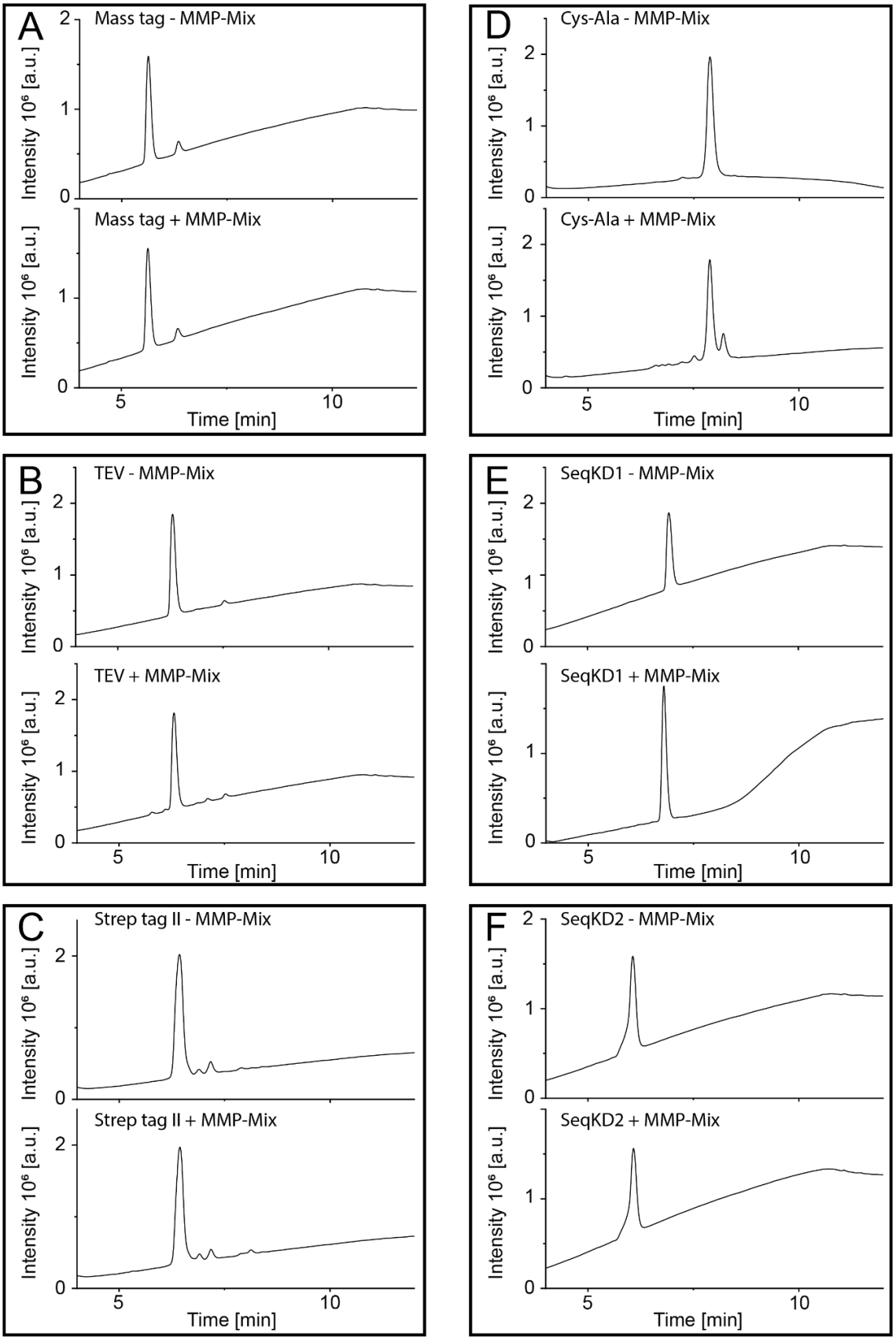

Figure 5 MMP incubation of (A) mass tag, (B) TEVs, (C) Strep-tag II, (D) Cys-Ala peptide, (E) SeqKD1 and (F) SeqKD2. Peptide fragments A-C and E and F show no sensitivity to MMP-1, -8, -9 and -13.

Mass tag family design

The basics for designing the mass tag family were explained previously.[8, 9] In short: the mass tag consisted of eight amino acids and should fragment into 2-3 y-type fragment ions. Proline in the middle of an amino acid sequence induce bond cleavage N-terminal to the proline residue[21] or the cleavage C-terminal to an acidic amino acid dominate the fragmentation pattern when a N-terminal arginine is present and aspartic acid is at least in a distance of one amino acid or glutamic acid has at least a distance of three amino acids to arginine[22]. The sequences S1-3 were synthesized as initial mass tag and characterized based on their retention time and fragmentation pattern in LC-MS/MS.[8] Due to the elution with moderate acetonitrile concentration and the fragmentation pattern with three y-fragment ions with moderate to high intensity, the S1 peptide sequence was assigned as mass tag. Over time we encountered problems during SPPS due to aspart-imide formation despite the fact that 0.1 M hydroxybenzotriazole (HOBt) solution was used for Fmoc-deprotection to scavenge piperidine as it tends to react with the peptide-imide and forms an irreversible peptide-piperidide[23] (**Figure S5**). That was the reason why aspartic acid was changed to glutamic acid, which is less susceptible to that side reaction (**Table 5**).

Table 7 Characteristics of final mass tag.

Name	Sequence	MW	$[M + 2H^+]^{2+}$
S4 = mass tag	SAEGPGFr	819.86, N-Ac: 861.88	410.93; 431.94
*S4	SAEGPGFr $^{+6}$	825.42;	413.21

The amino acid exchange from aspartic acid (Asp, D) in S1 to glutamic acid (Glu, E) in the final mass tag sequence led to a retention time shift of 0.5 minutes and a slightly change in the fragmentation pattern in MS^2. The S1 sequence fragmented in y_4-, y_5- and y_6-fragment ions with y_6 being the most intensive fragment and the y_4- and y_5-ions occurred with only half the intensity. For the final mass tag, the y_5-fragment ion, which means the bond breakage between E and G, is favored and the y_4- and y_6-fragment ions occurred with lower intensity than y_5 but more intensive than the two remaining fragment ions of S1 (viewed relatively to the highest fragment ion, **Figure 3**).

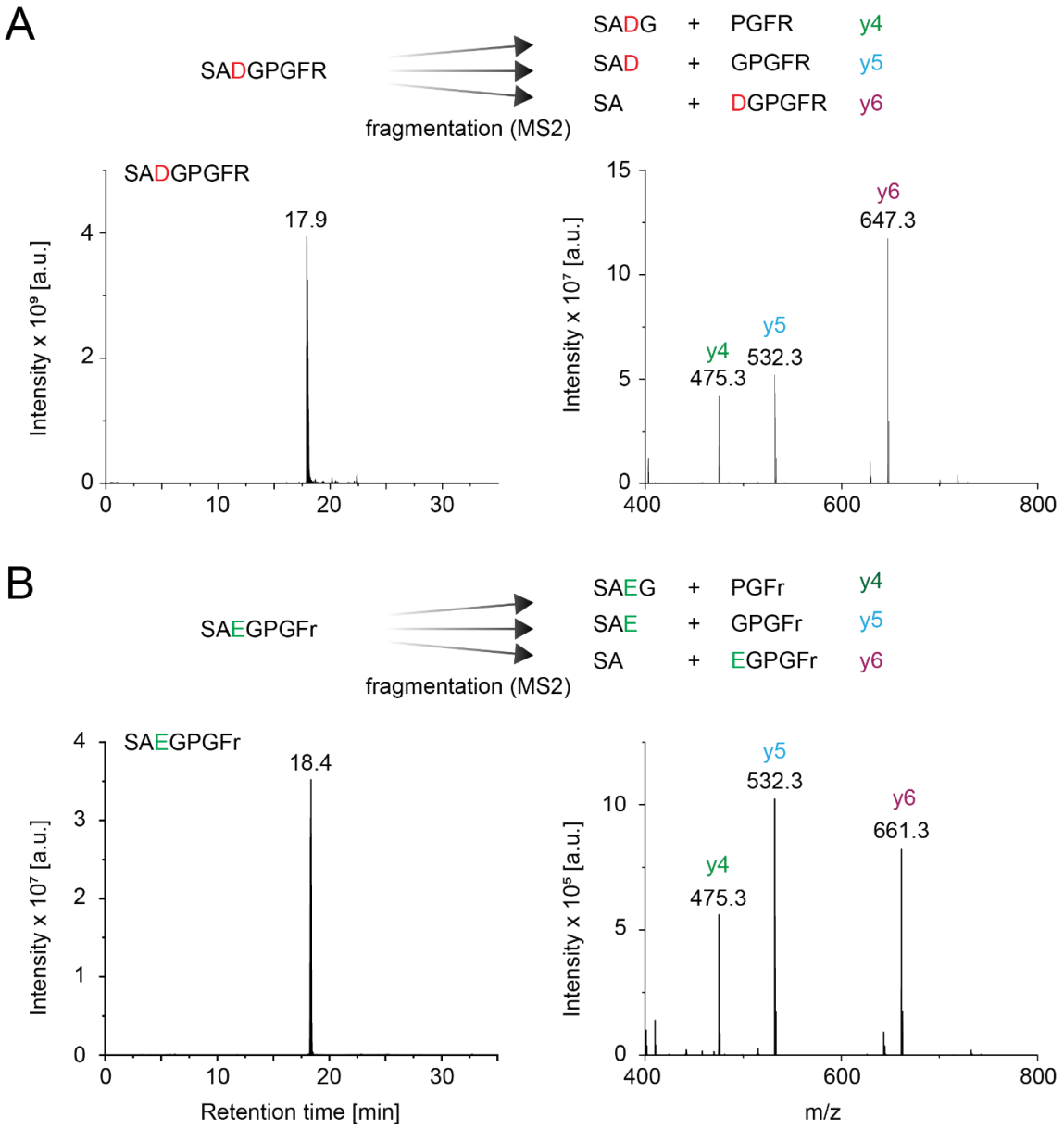

Figure 6 RP-HPLC chromatogram and MS² spectra of (A) mass tag sequence S1 and (B) the final mass tag sequence with glutamine instead of asparagine.

To develop our mass tag library, the principles of isobaric mass encoding were adapted[5] as already described in chapter 1 and 2. In short: the individual members of our reporter family share the same parent mass but show unique and distinguishable ions after fragmentation by tandem mass spectrometry. The five produced mass reporters were centered on the y_4-, y_5- and y_6-fragment ions by isotopically labelling the tripeptide Pro-Gly-Phe (PGF). The introduced mass shift was balanced by enriching the balancing ion (SA or SAE or SAEG) with isotopically labelled amino acids. In the end a peptide library resulted with five mass tag sequences that possess the same parent mass but have distinct y-type fragment ions after fragmentation in MS^2. Each mass tag sequence is assigned to a specific MSS (**Figure 4A**).

In LC-MS for all mass tags the same retention time is detected, due to the similar amino acid sequence (**Figure 4B**). But in MS^2 the five different mass tags were fragmented in y_4-, y_5- and y_6-fragment ions that differ by 1 or 2 Da each. The five mass tags were analyzed in a mixture and in LC-MS^1 they were indistinguishable and are selected as precursor ions, whereas in MS^2 five y-fragment ions were created and confirmed that they can be detected simultaneously (**Figure 4C**). The fragmentation pattern of y_4-, y_5- and y_6-ions is magnified in figure 6D and showed that their overall intensities differ among them but their relative intensity within the group of a specific y-type ion remained the same (**Figure 4D**).

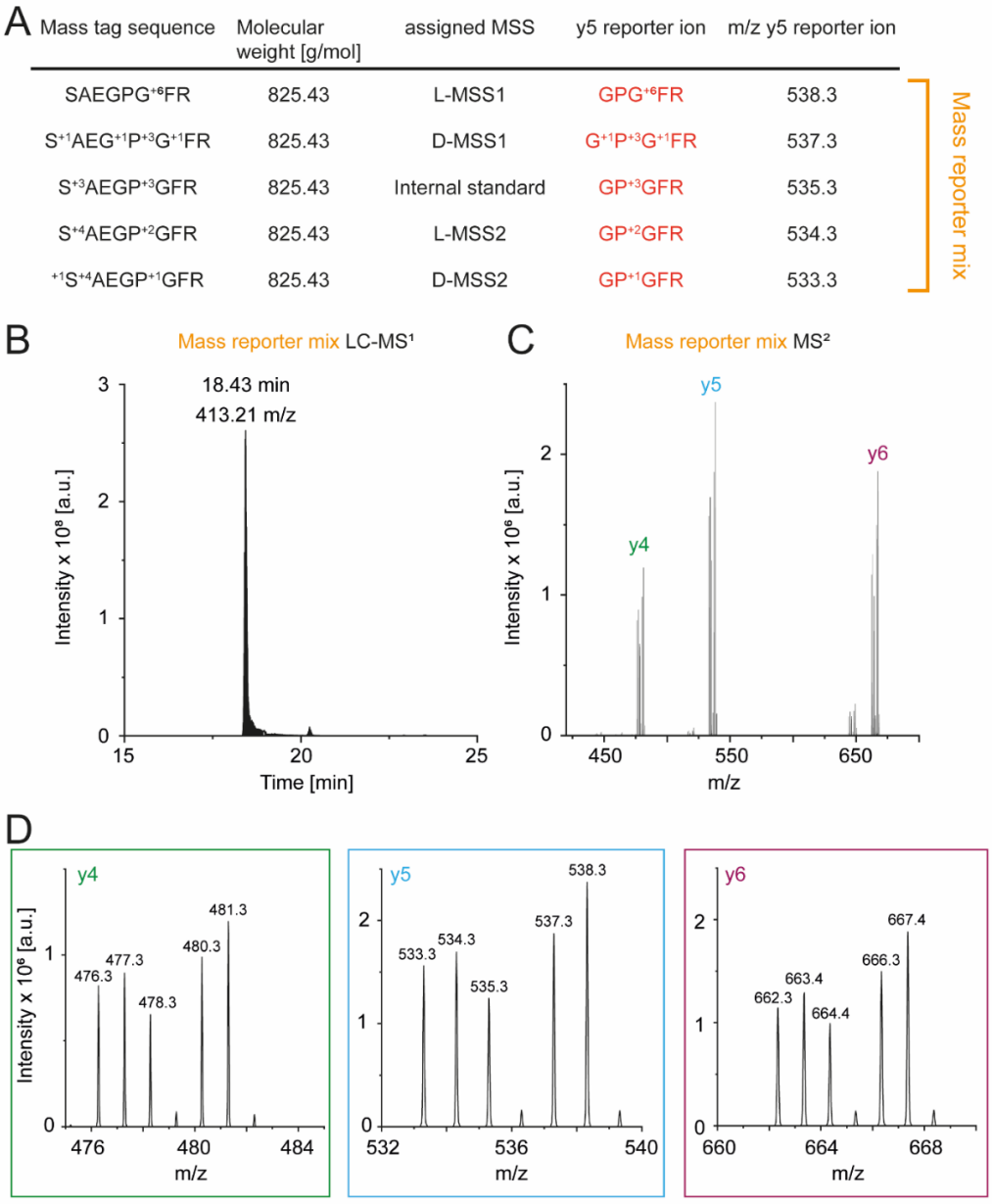

Figure 7 (A) Overview of five mass tag family members. LC-MS/MS measurements were performed with the mass reporter mix consisting of five mass reporters. (B) The different reporters are undistinguishable in LC-MS^1 but (C) showed distinct fragmentation in MS^2. In (D) the fragmentation pattern of y4-, y5-, and y6-fragment ions are zoomed in.

To determine the detection limit of mass tags in LC-MS/MS a dilution series of the non-isotopically labelled mass tag was prepared with a concentration range from 5 pM to 5 nM. The intensity of signals was plotted against the concentration and a linear curve fit was applied. The signals follow a linear course ((A) $r^2 = 0.978$ and (B) $r^2 = 0.980$) and even the lowest concentration of 5 pM was detectable (**Figure 5**).

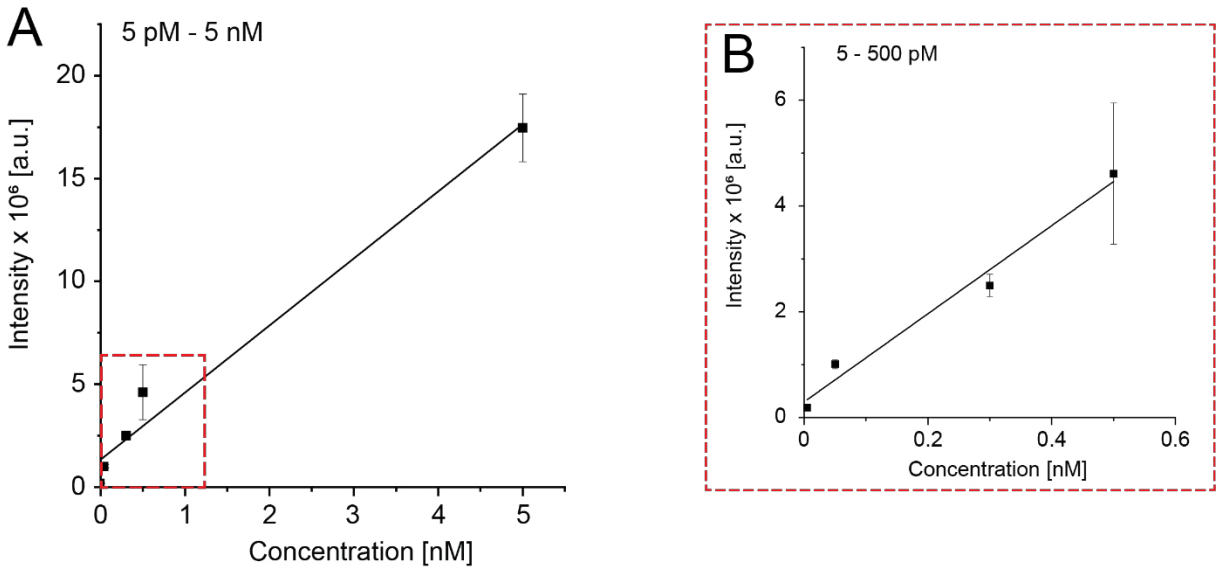

Figure 8 Dilution series of (A) mass tag measured by LC-MS in the range of 5 pM - 5 nM. In (B) the concentration range of 5 pM - 500 pM is enlarged.

Photo-sensitive linker

(S)-3-amino-3-(2-nitrophenyl)propionic acid (ANP) is a light-sensitive molecule, that undergoes a radical reaction when irradiated with UV light > 350 nm wavelength[24]. As it is stable in acidic and basic environment[25], it is widely used for organic synthesis, as resin for peptide synthesis[26, 27] or incorporated in amino acid sequences (peptides) and used as photo-sensitive cleavage site[5, 28].

Photocleavage

For the first photocleavage experiments the UV-LED Solo P lamp (~ 2000 mW/cm^2 in 15 cm distance, Opsytec Dr. Gröbel) was used but even when its intensity was reduced by 50 % the irradiance was too strong and caused side reactions, like the formation of disulfide bonds between Strep-tag II peptides with N-terminal cysteine (**Figure S6**). But as the cysteine's thiol group is used to couple the peptide to a 2.5 kDa PEG moiety to increase the peptides half-life during circulation there is no free thiol group during the purification

process. In addition, the use of the CAMAG UV lamp (1.1 mW/cm^2 in 17 cm distance) with a lower irradiance circumvented the disulfide bond formation.

Peptide fragments were irradiated with UV-LED Solo P 365 nm lamp (50 % intensity) with 5 cm distance to light source and placed in a Thermoshaker at 22 °C to avoid sample heating during irradiation. Before exposure to light and after 30 minutes of irradiation peptide fragments were analyzed by RP-HPLC. The chromatograms showed that the UV light has no influence on the peptides' stability of mass tag, TEVs, SeqKD1 and 2 (**Figure 6A, B, E, F**), but for Strep-tag II (**Figure 6C**) and Cys-Ala peptide (**Figure 6D**), that encountered disulfide bond formation when irradiated with UV-LED Solo P lamp. 30 minutes irradiation with the CAMAG UV lamp did not lead to disulfide bond formation for Strep-tag II (**Figure S7**).

TEV protease substrate sequence

The tobacco etch virus is a potyvirus, member of the picornaviridiae superfamily and infects plants. The virus has a single-stranded, plus RNA that can encode a 346 kDa polyprotein and forms a nuclear inclusion body in the nucleus of infected cells[29, 30]. The inclusion body consists of two viral-encoded proteins, of which one is a 49 kDa protein with proteolytic activity[31]. In an autocatalytic process the carboxy-terminal 27 kDa-protein is formed by cleaving its consensus sequence ENLYFQ/S (cleavage between Q and S) and is called TEV protease further on. It has a catalytic triad of histidine, aspartic acid and cysteine and possesses a stringent substrate sequence[29, 32]. Its physiological function in the tobacco etch virus is the cleavage of the polyprotein[33]. TEVp is commonly used to separate a protein from its fusion tag, which was used to improve recombinant protein expression, protein detection, or for protein purification processes[34]. As no protease with similar substrate sequence endogenously exist in humans, it was a good strategy to use it as a cleavage site, as future *in vivo* applications of our mass reporters were planned.

TEV protease activity

The recombinant TEVp was purchased from Invitrogen (AcTEV) and different batches were used. AcTEV is an enhanced protease version, as it is more active and stable as the wild-type enzyme. It possesses an N-terminal polyhistidine tag for purification reasons and a mutation at amino acid 219 (S219V) to prevent autoinactivation[35]. To compare AcTEV protease activity from different batches, the protease activity was determined by Abcam

TEV activity kit. The activity test showed no significant difference in activity of batch 1 compared to the batches 2 -5, so they were used without adaptation of applied units after batch 1 was empty (**Figure 7**).

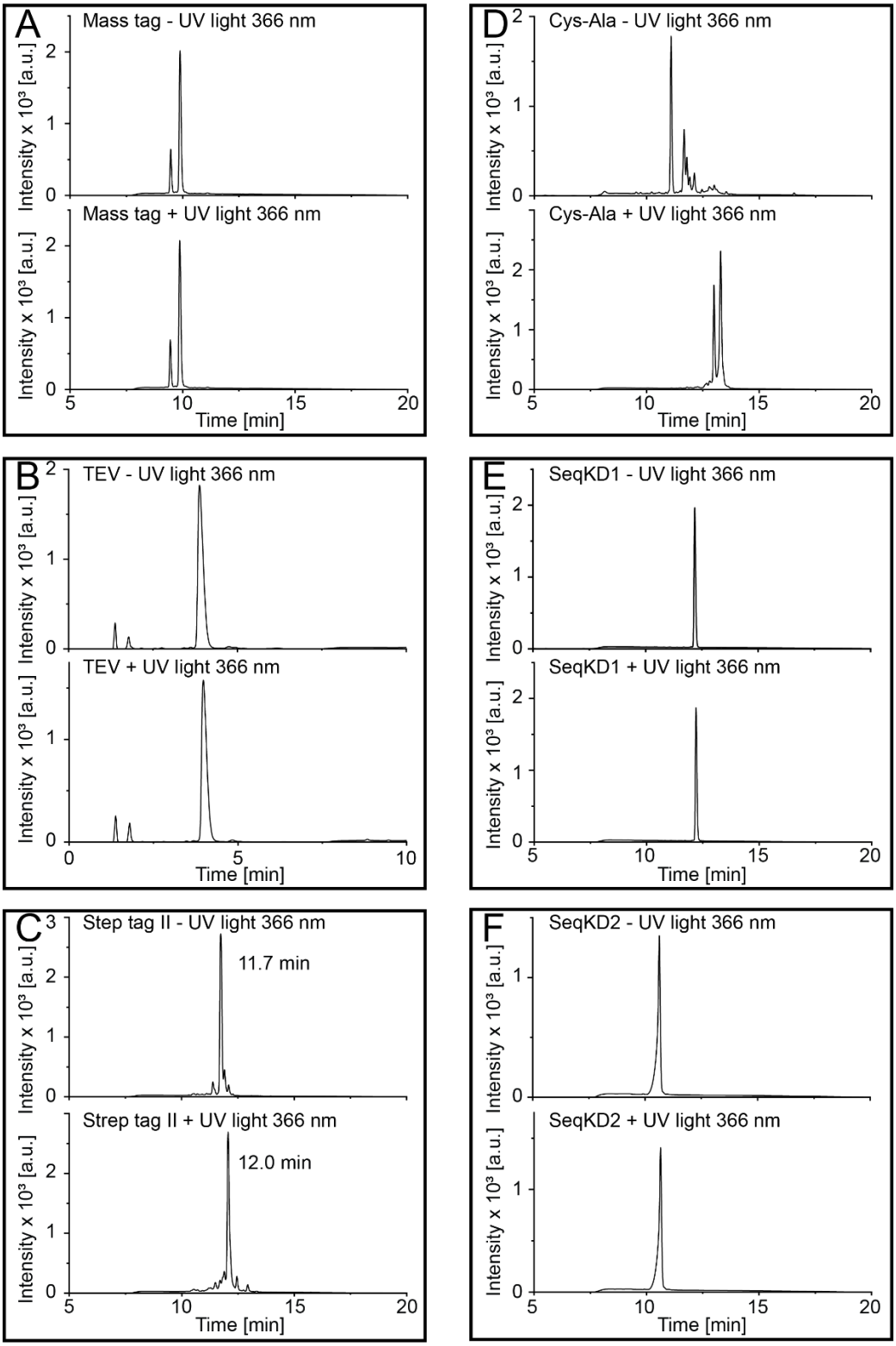

Figure 9 Exposure of peptide fragments to UV light of 366 nm wavelength. (A) Mass tag, (B) TEVs, (E) SeqKD1 and (F) SeqKD2 were not affected by UV irradiation but (C) Strep-tag II and (D) Cys-Ala showed the appearance of new peaks. Due to disulphide bond formation the retention time shifted.

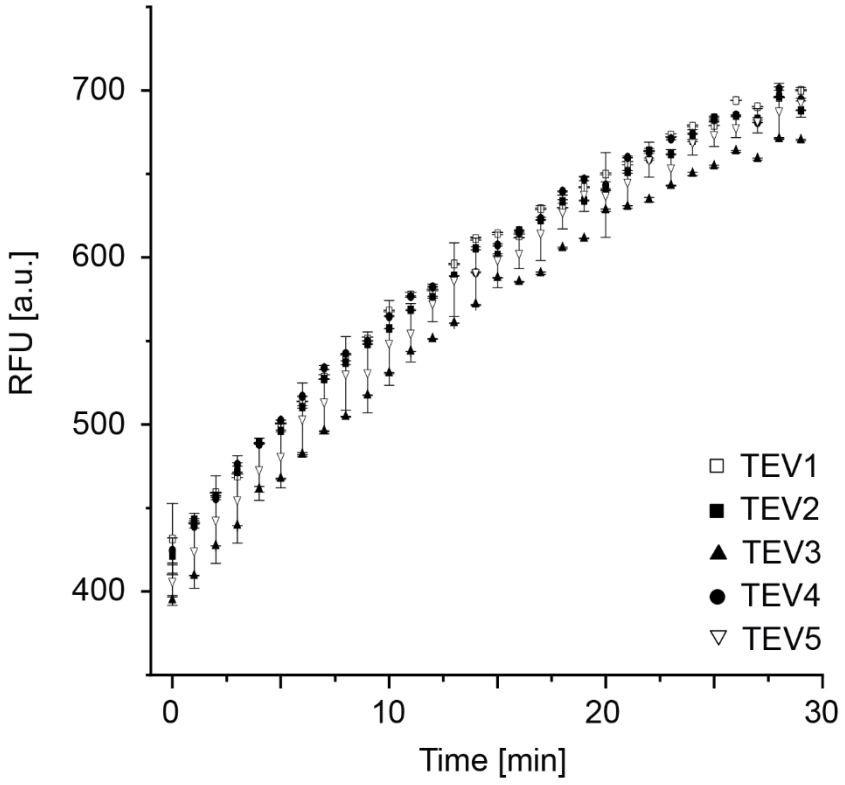

Figure 10 Protease activity of different TEV batches. The difference in protease activity is not significant between batch 1 and batches 2-5 after 30 minutes.

TEV protease cleavage

Peptide fragments were diluted in TEV buffer and incubated with 50 U (10 U/20 µg peptide) AcTEV protease at 30 °C for 6 hours. The negative control was incubated in absence of TEVp. Peptide analysis was performed by RP-HPLC showing that peptide fragments are not susceptible to TEVp except as expected the TEVs ENLYFQS with the cleavage site between glutamine and serine (**Figure 8**).

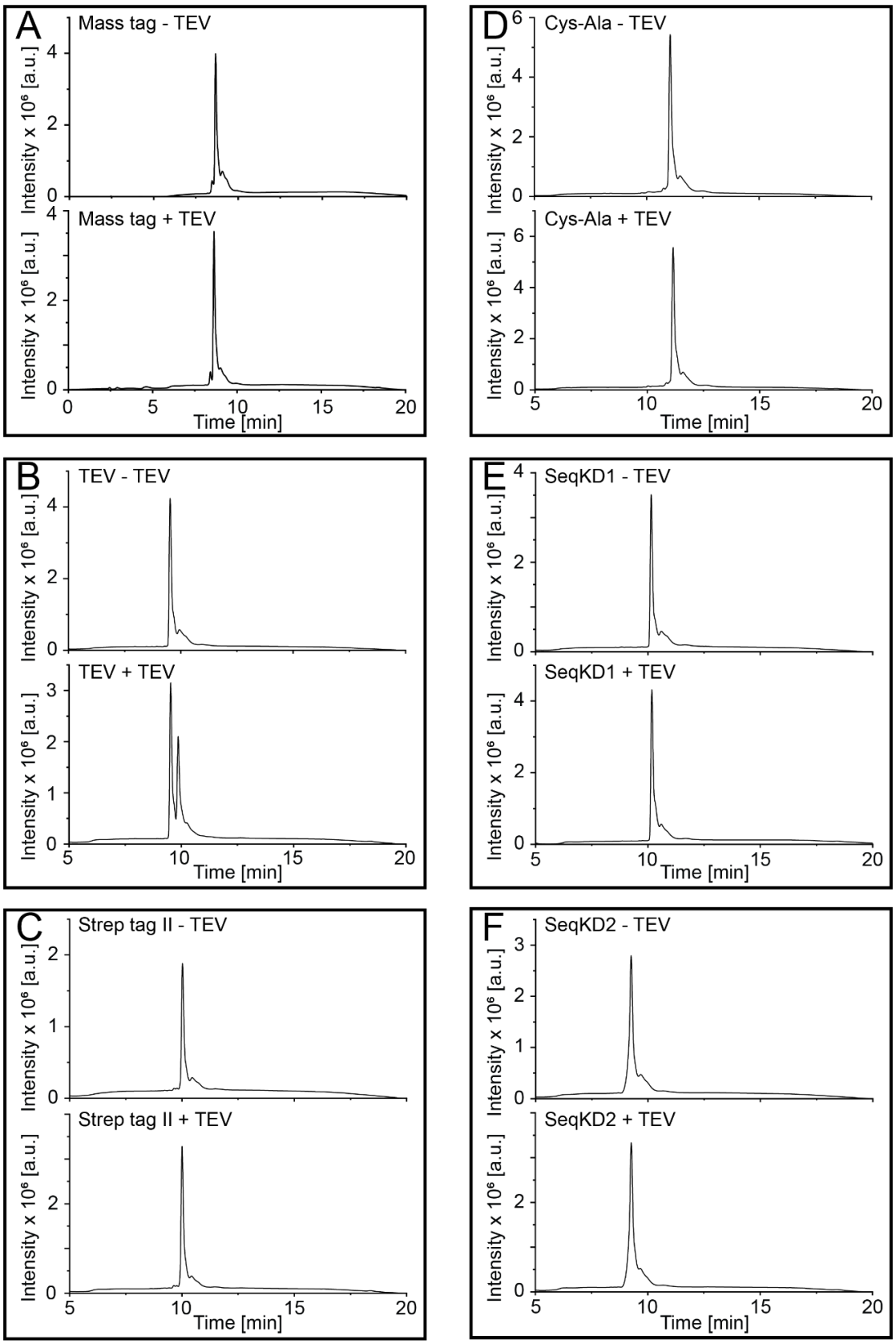

Figure 11 Incubation of peptide fragments with TEVp. The peptide fragment of (A) mass tag, (C) Strep-tag II, (D) Cys-Ala, (E) SeqKD1 and (F) SeqKD2 were not cleaved by AcTEV. The TEVs ENLYFQS (B) was cleaved as expected between Q and S, which is seen in RP-HPLC as two peaks are present. The smaller second peak originate from the TEVs without serine.

Proof of concept in an *in vivo* mouse model of osteoarthritis

The *in vivo* proof of concept of mass reporters and their biocompatibility was tested in an osteoarthritic mouse model at Zhejiang University, Hangzhou. The ethic commission of the Zhejiang University confirmed the experiment (ZJU20170298). 6 mice were randomly assigned to the OA-group, where the destabilization of medial meniscus (DMM) was performed in a surgical operation and 6 mice were assigned to the sham group, were the meniscotibial ligament was exposed but not transected.

The aim of the *in vivo* DMM mouse model was to demonstrate the system's feasibility regarding MSS cleavage, mass tag detection from blood samples, sample purification from body fluids and it was expected to observe a higher cleavage rate for L-reporters in DMM group than in sham group compared to their D-equivalent. The strategy was to inject a mix of four mass reporters plus the validation reporter into the synovial gap of the knee joint after osteoarthritis was induced in the OA DMM mouse model (**Figure 9A**). In a healthy environment with no MMPs present the mass reporters should remain in the joint cavity due to their size (**Figure 9B**). But in inflammatory tissue with elevated MMP levels, the MSS was expected to be cleaved and released mass reporter peptides, which have now an average molecular weight of ~7000 Da, are able to diffuse faster into the blood stream or lymphatic drainage system than those still bound to 4-arm-PEG (**Figure 9C**). After certain time intervals blood was collected and samples should have been processed and analyzed by tandem mass spectrometry (**Figure 9D**).

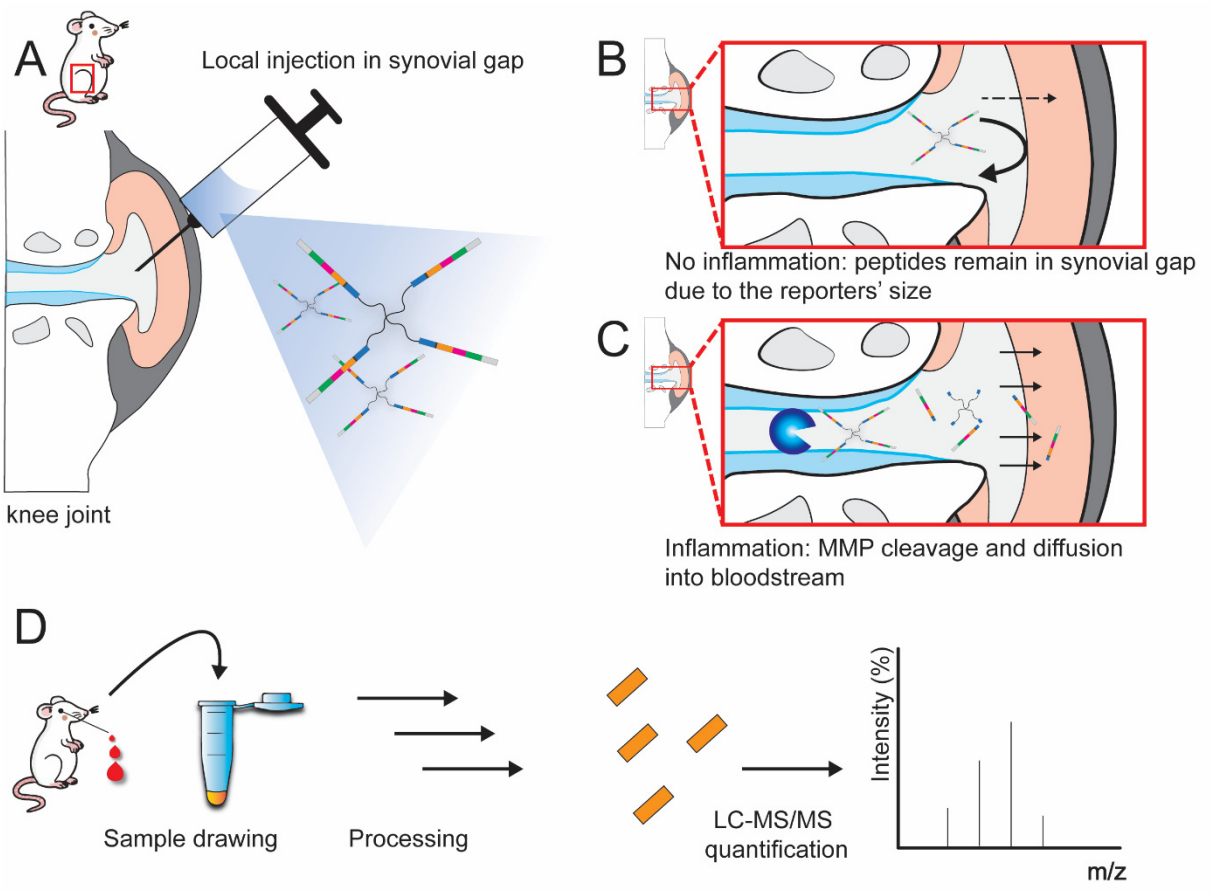

Figure 12 (A) Intra-articular injection of mass reporter mix in knee joint of DMM and sham mice. (B) When no inflammation is present, the mass reporter peptides are not released from their 10 kDa-4-arm-PEG and remain inside the synovial gap. (C) During inflammation with elevated levels of MMP the mass reporter peptides are cleaved from the high molecular weight PEG and diffuse into the blood stream. (D) Blood samples were collected and processed, and the isolated mass tags analysed by LC-MS/MS.

To evaluate the inflammatory status and to verify if the DMM mouse model successfully introduced OA, the medial femoral condyle was stained with HE and Safranin O. It is visible that both sham group and normal group showed complete meniscus and smooth cartilage tissue. But for the DMM group, the meniscus was replaced by fibrous tissue, the ECM of cartilage was degraded, and an erosion of surface cartilage down to the calcified cartilage below the tidemark can be seen. The tissue sections of the DMM group showed a focal loss of Safranin O staining which is indicative for proteoglycan loss (**Figure 10A**). The International cartilage Repair Society (ICRS) score is a validated score for macroscopic evaluation of cartilage repair.[36, 37] The cartilage was evaluated and an ICRS score of 14.17 ± 1.47 and 17.60 ± 0.55 was found for DMM and sham group, respectively, showing a significant difference between both scores (**Figure 10B**).

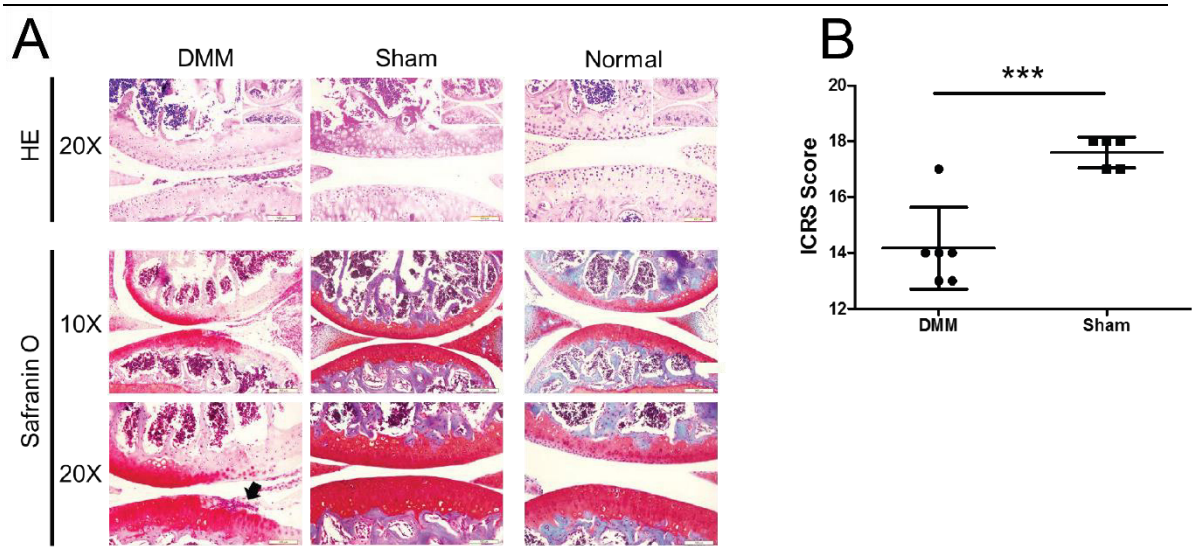

Figure 13 Degeneration of cartilage by HE and safranin O staining after 8 days. (A) Histologic sections of medial femoral condyle of DMM group (n=6), sham group (n=5) and one untreated mouse (normal) were subjected to HE and SO staining and (B) the ICRS score was assessed to evaluate cartilage injury.

Furthermore, histological staining showed that the DMM model also induced inflammation in non-articular tissue, whereas the sham operated group showed no injury resulting in a mild biocompatibility of injected mass reporters (**Figure 11A).** The inflammation score for the fat pad demonstrated a significant difference between DMM and sham group as did the synovial score for the synovium, which depend on layer thickness and lymphocytes. Whereas the cruciate ligament was evaluated with the Mankin's score according to[38]. The score showed no histologic difference between DMM and sham group (**Figure 11B**).

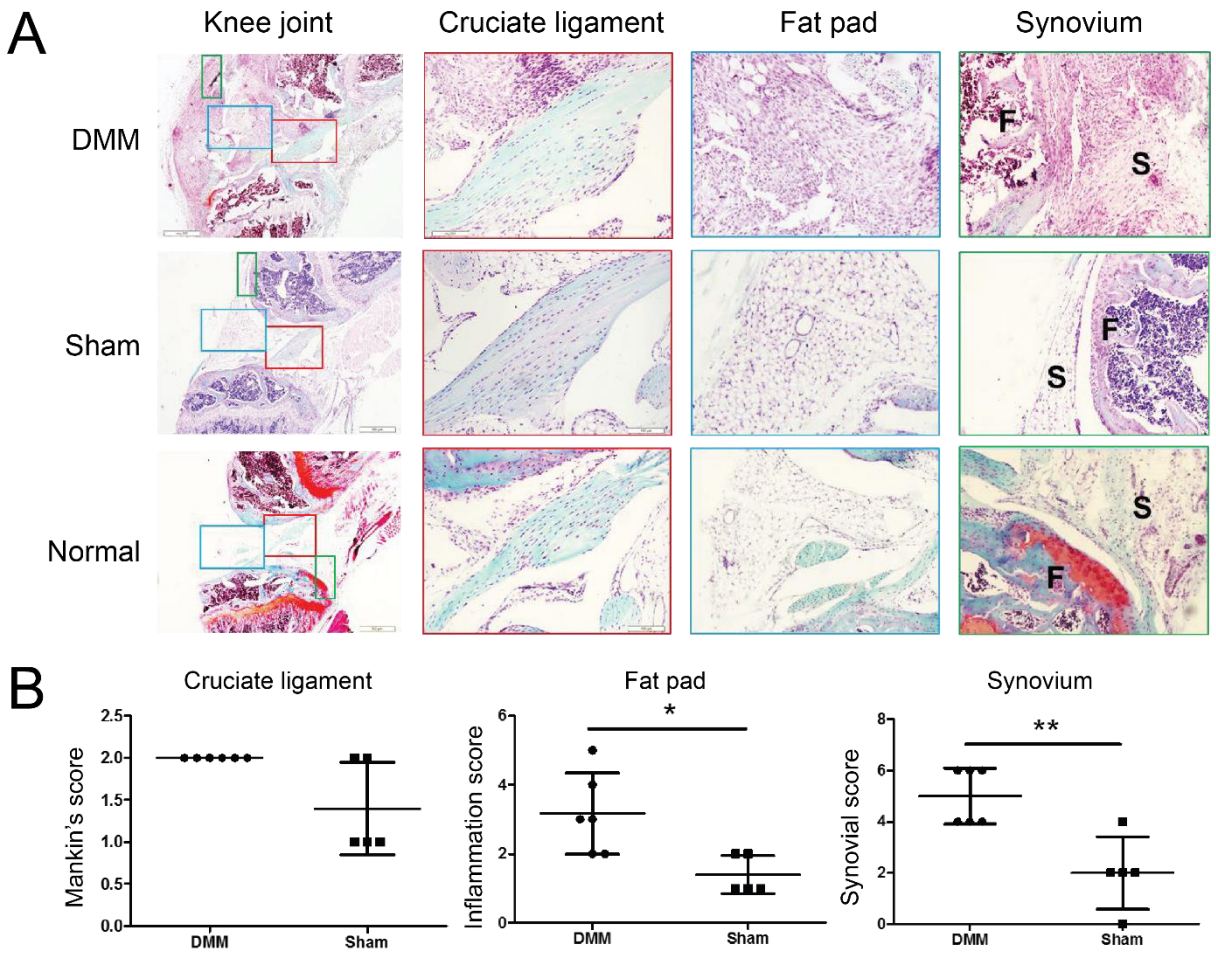

*Figure 14 (A) SO staining of non-articular cartilage joint tissue: cruciate ligament, fat pad and synovium of an osteoarthritic mouse, a sham-operated mouse and an untreated mouse (normal). In the synovium sections the synovium and femur are marked with bold letters **S** and **F**, respectively. (B) Evaluation of the histology by applying the Mankin's score for cruciate ligament, the inflammation score for the fat pad and the synovial score for synovium.*

The blood samples should be shipped to Germany. But due to export restrictions and customs problems in China the samples did not arrive in Würzburg and could not be analyzed with respect to the release of mass reporters.

Discussion

A soluble mass reporter system with seven functional modules was developed, characterized, and was tested *in vivo*. By using a high molecular weight polymer, we aimed to create a local depot in the joint cavity to observe enzyme activity in SF. By adapting the principles of isobaric mass encoding, a mass reporter family consisting of five family members was created by enriching the mass tag octamer with heavy amino acids and their multiplexing ability in LC-MS/MS was verified. The characterization experiments of mass reporter peptides regarding protease- and UV light-sensitivity showed that the MSSs were cleaved by MMPs at the predicted cleavage site, as well as the TEVs by TEVp, while other peptide fragments are stable during protease incubation and UV irradiation. The *in vivo* animal studies showed biocompatibility of mass reporters after an application period of five days and no triggered immune response. But due to customs problems the purification of mass tags from blood and their detection by LC-MS/MS could not be performed but should be in the future to demonstrate the system's feasibility.

The DMM mouse model for surgical OA induction has been chosen as this procedure more reliably represented cartilage degradation and subchondral bone changes than the type-II collagenase induced OA mouse model.[39] Previous studies demonstrated that the severity of articular cartilage lesions progressively increased by 10-16 weeks.[40, 41] We chose the mass reporter injection at day three after surgery to evaluate the sensitivity of our system in the early phase of disease. Since the blood samples were not analysed as of shipment issues from China to Germany a final discussion on reporter performances is unfortunately impossible. Further, the read out of enzyme activity may be restricted by the stability of mass reporters in SF or plasma and the diffusion of mass reporters out of the joint cavity. In order to make a precise proposition about the observation period further experiments have to be conducted, like the determination of mass reporter's stability in body fluids.

The number of mass tag family members is not restricted to 5 members, as was used here. Depending on the total mass shift that is introduced to the amino acid sequence, the mass reporter family can be extended to more than ten members and the acquisition of information from only one sample can be increased by this multiplexing approach. It is important to emphasize that only isotopically labelled sequences are included in the mass reporter family. The non-isotopically labelled mass tag cannot be a member of the mass tag family despite its ability of fragmenting into distinct y-type fragment ions in MS^2, because

its parent mass differentiates from that of the other members and so it is not indistinguishable in LC-MS[1]. Furthermore, the non-labelled mass tag is not selected as precursor ion together with the other family members for further fragmentation. As a result, it is not able to be simultaneously detected with other mass tags that possess a mass shift, here +6 Da.

Moreover, it is possible to extend the mass reporter peptide by a therapeutic agent, like cytokines, growth factors, or chemical drugs, that are released in response to a certain stimulus. Instead of the N-terminal 2.5 kDa PEG used here, a cytokine may be linked to Strep-tag II by the same PSS that is already used in the system between 4-arm-PEG and mass tag. With this strategy in response to the same stimuli not only the cytokine is released but also the mass reporter peptides are cleaved off the high molecular weight polymer with their modules for purification and mass tag isolation. Hence, monitoring of the cytokine release via the mass tags by LC-MS/MS would be achieved. Furthermore, the exchange of the N-terminal PEG by a targeting residue holds potential to lead the cleaved mass reporter peptide to the body fluid they are collected from, like urine. Urinary excreted substances, like urea, creatinine or fibrinopeptide B, who all filter freely into the urine[5] may be selected. The used PSSs were cleaved by MMPs and released the mass reporter peptides with distinct kinetics. As a future strategy, faster- or slower-releasing PSS may be incorporated into the peptide sequence to modulate the observation period of enzyme activity in inflammatory environment or linkers that are sensitive to other proteases,[42] pH,[43] temperature,[44] or ROS[45] may be used. As the mass reporter system is built of modules, it presents a flexible system, that may be adjusted to the patients need. For example, any other alkyne-bearing molecule or polymer that support the local remain in the joint cavity, e.g. bio-degradable nanoparticles,[46] higher-branched PEGs,[47] or quantum dots[48, 49] feature a good alternative for the C-terminal DBCO-4-arm-PEG.

In conclusion, this study presents a soluble mass reporter system, that release isotopically labelled mass tags in response to MMPs. The multiplexing ability of mass tags was demonstrated and may provide a new possibility to monitor enzyme activity from inflammatory environment. The system's biocompatibility was verified but its *in vivo* feasibility remains to be tested.

Materials & Methods

Materials

The following chemicals were purchased from Sigma Aldrich (Taufkirchen, Germany): N, N-diisopropylcarbodiimide (DIC), hydroxybenzotriazole (HOBt), dimethyl sulfoxide (DMSO), iodoacetamide, trifluoroacetic acid (TFA), acetic anhydride, ethylenediaminetetraacetic acid (EDTA), thioanisole, anisole, and ethanedithiol (edt). Diethyl ether was purchased from Jäklechemie, polyethylene frit and Luer stopper from MultiSynTech GmbH (Witten, Germany), and Ziptip pipette tips from Merck Millipore (Darmstadt, Germany). Piperidine was purchased from Alfa Aesar (Haverhill, USA), AcTEV Protease from Invitrogen (Carlsbad, USA) and N, N-diisopropylethylamine (DIPEA) was purchased from Carl Roth GmbH + Co. KG (Karlsruhe, Germany). All Fluorenylmethoxycarbonyl-protected (Fmoc) amino acids and rink-amide resin were purchased from Iris Biotech (Marktredwwitz, Germany) and isotopically labelled amino acids were purchased from Cambridge Isotope Laboratories Inc (Tewksbury, USA), except for Fmoc-Phenylalanine (Ring$^{13}C_6$) which was purchased from Anaspec (Seraing, Belgium). Matrix metalloproteinases (MMP-1, MMP-8, MMP-9), acetonitrile (ACN), and methanol were purchased from VWR (Darmstadt, Germany). Fmoc-(S)-3-amino-3-(2-nitrophenyl)propionic acid was purchased from ChemImpex (Wood Dale, USA). The following kits and chemicals were purchased from Thermo Fisher Scientific (Waltham, USA): Pierce™ BCA Protein Assay Kit, Peptide Digest Assay Standard N, N-dimethylformamide (DMF) and dichloromethane (DCM). DBCO-PEG-NHS was purchased from Jena Bioscience (Jena, Germany), 4-arm- PEG-NH_2 (10 kDa) from Advanced BioChemicals (Lawrenceville, USA) and iodoacetamide-PEG-COOH from Nanocs (New York, USA).

Methods

Peptide synthesis

1. Isotopically labelled peptides were synthesized manually or semi-automated with the SP wave (Biotage).

Manually

Fmoc-based solid phase peptide synthesis was performed with DIC/DIPEA in DMF as coupling reagents, and 20 %, and 40 % piperidine in DMF as Fmoc-deprotection reagent. The resin was transferred to a 20 mL syringe with polyethylene frit and plastic fit (MultiSynTech GmbH, Witten, Germany) and was swollen in DMF for 30-60 minutes and subsequently Fmoc-group was removed with 40 % piperidine in DMF for 3 minutes and 20 % piperidine in DMF for 12 minutes. Amino acids (AA) were used in a 5-fold molar excess compared to used resin. AA were dissolved in 0.5 M HOBt in DMF and then 80 µL DIC was added. The mixture was mixed on an orbital shaker for 5 minutes before 88 µL DIPEA were added and then the reaction mix was filled in the reaction vessel with resin. The coupling time was two hours on an orbital shaker, except for glycines following prolines the reaction time was extended to eight hours or overnight. Between deprotection and coupling five washing steps with 2 mL DMF were performed. To avoid aspart-imide formation the deprotection-reagent for Asp and all following AA was extended with 0.1 M HOBt in 20 % and 40 % piperidine in DMF. Double coupling was performed for AA number 25 and all followings. The resin was dried by washing three times with DCM and three times with diethyl ether and then the resin is stored for at least one hour under the hood. The peptide cleavage from the solid support was performed with a cleavage mixture of 90:5:3:2 TFA:Thioanisol:edt:anisol. Incubation time was 1.5 hours twice. Cleaved peptide was collected in ice-cold diethyl ether. For precipitation peptide solution was stored on ice and then washed three times with diethyl ether. Supernatant was discarded and pellet was dried under the hood.

Manually synthesized peptides were:

a. GPGQIAGQ
b. GPSGLLAH
c. PTLGLLAA
d. GpGqiaGq
e. GpsGllah
f. ptlGllaa

g. SADGPGFr
h. WSHPQFEK with C-termina Cys

Semi-automated with SP wave (Biotage)

Fmoc-based solid phase peptide synthesis was performed in SP wave synthesizer with microwave heating and an incorporated shaker with 900 rpm. The resin was transferred to a 10 mL syringe with a central outlet and a polyethylene frit. The resin was swollen for 30 – 60 minutes in DMF. The Fmoc-group was removed by incubating the peptide with 25 % piperidine in DMF for 3 minutes at 75 C followed by three washing steps with 2.5 mL DMF. AA- reagent mix had to be prepared manually according to the manual peptide synthesis and added to the resin. The coupling program was set to 50 °C for 10 minutes, followed by three washing steps with 2.5 mL DMF. If N-acetylation was needed it was performed with an acetylation mixture that was prepared manually: 75 µL acetic anhydride and 150 µL DIPEA in 3 mL DMF for 25 minutes at room temperature. Peptide was dried by washing three times with 2 mL DCM and three times with 2 mL diethyl ether. Peptide cleavage was performed according to manual peptide synthesis. The following peptides were synthesized semi-automatically:

a. ENLYFQS
b. SAEGPGFr
c. Cys-Ala
d. SeqKD1
e. SeqKD2
f. sL-reporter 1
g. sD-reporter 1
h. sL-reporter 2
i. sD-reporter 2

Peptide purification with preparative HPLC

Peptide purification was performed by preparative HPLC (GE Äkta Pure 25 or Äkta Explorer). The Äkta Pure was equipped with a faction collector F9R and detector U9-D. The Äkta Explorer was equipped with fraction collector Frac-950, pump system P-900 and a UV detector UV-900.

A preparative reversed phase C18 column (Phenomenex Jupiter 15u, C18; 250 x 21.2 mm; particle size 800 Å or Phenomenex Luna 5 µm, c18(2), 250 x 21.2 mm, 100 Å) served as the stationary phase. The mobile phase consisted of eluent A (0.1% (v/v) TFA in water) and eluent B (0.1% (v/v) TFA in acetonitrile). The samples were dissolved in acetonitrile/water mixtures with different acetonitrile concentrations according to the sample's solubility. The column was equilibrated with 5 CV of the acetonitrile/water mixture in which the sample was diluted. Sample application was performed with a superloop (10 or 150 mL, Ge Healthcare) and unbound impurities were washed off the column with 2 CV before the stepwise or linear acetonitrile gradient started up to 95 % eluent B. 2 mL fractions were collected with fraction collector. The column was washed with 95 % eluent B and equilibrated for the next purification. The fractions' purity was analyzed by analytical HPLC and by MALDI-TOF or LC-MS.

Analytical reversed-phase high-performance liquid chromatography (RP-HPCL)

RP-HPLC analysis was performed using a VWR Hitachi Elite LaChrom HPLC (Autosampler L-2200; Pump L-2130; Column Oven L-2300; UV detector L-2400) or an Hitachi LaChrom Ultra UHPLC system (Autosampler L-2200U; Pump L-2160U; Column Oven L-2300; Diode Array Detector L-2455U) (both VWR International GmbH, Darmstadt, Germany) or an Agilent 1260 Infinity II system equipped with 1260 flexible pump, 1260 vialsampler, 1260 multicolumn thermostat (MCT) and a 1260 variable wavelength detector (VWD). A ZORBAX Eclipse XDB-C18 column (4.6 ID x 150 mm, 80 Å, 5 µm) or a ZORBAX 300-SB CN column (4.6 ID x 150 mm, 5 µm) (Agilent, Santa Clara, CA) was utilized. The mobile phase consisted of eluent A (0.1% (v/v) TFA in water) and eluent B (0.1% (v/v) TFA in acetonitrile). Column oven temperature was kept at ambient temperature and the absorbance was monitored at a wavelength of λ = 214 nm, unless specified otherwise.

The columns' function was tested by injection of 10 µL of HPLC peptide standard mixture (Sigma Aldrich, H2016) before columns were first used.

Liquid chromatography – mass spectrometry (LC-MS)

Mass spectrometry was performed with a LC-MS 2020 system from Shimadzu. The Shimadzu Single Quadrupole Liquid Chromatograph Mass Spectrometer system is

equipped with a DGU-20A3R degassing unit, a LC20AB liquid chromatograph, a SPD-20A UV/Vis detector and a LC-MS 2020 (Shimadzu Scientific Instruments, Columbia, MD, USA). To separate samples by LC a Synergi 4u fusion-RP column (4.6 x 150 mm) (Phenomenex lnc., Torrance, CA) was used with eluent A 0.1 % (v/v) formic acid in water and eluent B 0.1 % (v/v) formic acid in methanol. The detection range was set from 60 – 1000 m/z or from 500 – 2000 m/z depending on the samples mass and charge. The injection volume of 20 µL sample was loaded onto the column and a stepwise methanol gradient was used with a (i) linear gradient from 5 to 90 % eluent B in 8 min, (ii) washing at 90 % eluent B for 5 min, (iii) a linear gradient to from 95 – 5 % eluent B in 1 min, and (iv) equilibration of the column with 5 % of eluent B for 4 min.

MALDI

The MALDI mass spectra were performed with an ultrafleXtreme mass spectrometer (Bruker Daltonics, Bremen), equipped with a 355 nm smartbeam-II™ laser. All MALDI-TOF spectra were acquired in the positive reflectron mode.

For the external calibration 1 µL of a CsI_3 solution (40 mg/mL in acetonitrile) was mixed with 1 µL of a DCTB (*trans*-2-[3-(4-tert-Butylphenyl)-2-methyl-2-propenylidene]malononitrile) solution (20 mg/mL in acetonitrile) and 0.5 µL of the mixture were dropped onto the stainless steel target. For peptide analysis 1 µl of the sample solution (1 mg/ml in H_2O/ACN/0.1 %TFA) and 1 µl of a sinapic acid solution (20 mg/mL in 40 % ACN/H_2O/0.1 % TFA) were mixed and 0.5 µl of the mixture were dropped onto the stainless steel target (MTP 384 target plate ground steel, Bruker Daltonics #8280784). Depending on the sample's properties e.g. for PEG-containing molecules SDHB solution (20 mg/mL in MeOH) or α-cyano-4-hydroxycinammic acid solution (saturated in 40% ACN/H_2O/ 0.1 % TFA) were used instead of sinapinic acid solution. 2000 shots were accumulated for the spectrum.

Lyophilization

To evaporate acetonitrile from Äkta peptide fractions, samples were stored in a current of nitrogen in TurboVap LV Evaporator for at least 1.5 hours. Then samples were frozen at -80 °C for at least 30 minutes and three holes were punched in the falcon tube lid. The lyophilization was performed with Freeze Dryer Alpha 1-4 (Martin Christ

Gefriertrocknungsanlagen GmbH, Osterode, Germany) with -53 °C for the primary drying process and 3,010 mbar. A second freeze drying process is performed with VirTis Benchtop K Freeze dryer (SP Scientific, USA) with a condenser temperature of -79.0 °C and 14 µbar after primary lyophilized peptides were dissolved in ultrapure water and frozen at -80 °C. Lyophilized peptides are stored at -80 °C until use.

Bicinchoninic acid (BCA) assay

The BCA assay was performed with a "Peptide Digest Assay Standard" (Thermo Fisher, 23295) to determine the concentrations of mass reporter peptides. The appropriate volume of working reagent (WR) was prepared by mixing BCA Reagent A and B 50:1 and a clear, greenish solution resulted. 10 µL of mas reporter peptides as triplicate and of peptide standard (each in duplicate) was pipetted in a microplate well and 200 µL WR was added and mixed thoroughly. After incubation at 37 °C for 30 minutes, the absorbance was measured at 562 nm on a plate reader.

N-hydroxysuccinimide (NHS) reaction

Since a 4-arm-DBCO-PEG is not commercially available it was synthesized in an NHS-amine reaction by using the educts: DBCO-PEG$_4$-NHS ester (649.69 g/mol) and 4-arm-PEG-NH$_2$ (10 kDa). Initially a 10 mM stock solution of DBCO-PEG$_4$-NHS in DMSO was prepared. 50 mg 4-arm-PEG-NH$_2$ were dissolved in 10 mL PBS on a 50 mL falcon tube and mixed with 250 µL of DBCO-PEG$_4$-NHS stock solution and incubated on a roller mixer at room temperature for 16 hours. The reaction was purified via fast protein liquid chromatography (Phenomenex Jupiter C18 column) with a stepwise 0.1 % TFA in acetonitrile gradient (i) from 10 to 40 % in 10 minutes, (ii) from 40 to 70 % in 50 minutes, (iii) from 70 to 100 % in 4.5 minutes, and (iv) column wash with 100 % acetonitrile in 12.5 minutes. MALDI measurements were performed to analyze the 4-arm-PEG-DBCO's mass. A mass shift was observed, and the mean mass difference was used to calculate the mean loading for each 4-arm-PEG molecule.

Strain-promoted alkyne-azide cycloaddition (SPAAC)

The DBCO-4-arm-PEG was dissolved in PBS and was added to the alkyne-modified mass reporter peptide in a molar ration of 1.5:1. The reaction was carried out in an Eppendorf

cap and was equipped with an agitator and placed on a magnetic stirrer over night at room temperature. The reaction must be protected from light.

Thiol – iodoacetamide (IA) reaction

The unpurified reaction mixture of the copper-free click reaction was used for N-terminal PEGylation of the peptide via the thiol-iodoacetamide reaction. The components were used in a ratio of 1:1.5 of 4-arm-PEG-peptide-conjugate : iodoacetamide-PEG-COOH. The reaction was carried out in an Eppendorf cap and was equipped with an agitator and placed on a magnetic stirrer over night at room temperature. The reaction must be protected from light. Purification was performed by size exclusion purification with Vivaspin 500 (10000 MWCO). First the membrane was wetted by 500 µL PBS. Then the reaction mix was filled into the Vivaspin and spun at 9000 g at 4 °C until volume is reduced to approximately 100 µL. The Vivaspin was refilled with PBS up to 500 µL until a total of five volume exchanges took place. The mass was analyzed by MADLI after samples were desalted by ZipTip pipett tips according to the manufacturer's instructions.

Enzyme reactions

MMP digest of peptide fragments

Lyophilized peptide fragments were diluted in MMP buffer (50 mM Tris, 150 mM, NaCl, 1 µM$ZnCl_2$, 10 mM $CaCl_2$, pH 7.4) to a final concentration of 1 mg/mL and the pH was adjusted to 7.5 with 0.1 M NaOH. For alkylation of N-terminal thiol groups in Strep-tag II and Cys-Ala peptide, a 0.5 M iodoacetamide solution in ultrapure water was prepared and 5 µL of stock solution was added to 45 µL peptide solution and was incubated on a roller mixer for 1 hour in the dark. The pH was controlled after the reaction and if necessary adjusted to 7.5 again. A 10-fold molar MMP-Mix was prepared with 351 nM MMP-1, 132 nM MMP-8, 106 nM MMP-9 and 40 nM MMP-13. Peptide solution and MMP-Mix were mixed 10:1 and were incubated at 37 °C for 15 hours. The negative control consisted of peptide solution incubated with MMP buffer at 37 °C for 15 hours. Experiment was performed in triplicates. The enzyme activity was stopped by heating the mixture to 95 °C for 15 minutes. Cleavage efficiency was assessed on a LaChromUltra UPLC system equipped with a Hitachi L-2455U diode array detector and two L-2160U pumps (VWR

Hitachi, Tokyo, Japan). 20 µL PSL sample was applied on a ZORBAX Eclipse XDB-C18 column (4.6 mm× 150 mm, Agilent, Santa Clara, CA) equilibrated with a solution of 95% water containing 0.1% TFA and 5% acetonitrile (ACN) containing 0.1% TFA. PSL and cleaved fragments were eluted by a linear gradient of 5–65% ACN containing 0.1% TFA with a flow rate of 1 mL/min. Column temperature was kept at 22°C by a L-2300 column oven and absorbance was monitored at λ = 214 nm.

TEV protease incubation of peptide fragments

Peptide fragments were dissolved in TEV buffer (50 mM Tris-HCl, pH 8.0, 10 mM EDTA, 10 mM DTT) to reach a final concentration of 1 mg/mL. The peptides were incubated in absence and in presence of 50 units TEVp at 30 °C for one hour in triplicates. The enzyme activity was stopped by heating the reaction mixture to 95 °C for 5 minutes. Cleavage efficiency was analyzed by RP-HPLC analog to the analysis of MMP digest of peptide fragments.

UV irradiation of peptide fragments

The peptide fragments (n=3) were dissolved in ultrapure water to reach a final concentration of 1 mg/mL and filled in Eppendorf tubes. The tubes were places in 5 cm distance to the light source in a Thermoshaker at 22 °C to avoid sample heating during irradiation. The samples were irradiated with UV-LED Solo P 365 nm lamp (~ 2000 mW/cm^2 in 15 cm distance, Opsytec Dr. Gröbel) with a reduced intensity by 50 %. Strep-tag II was also irradiated with CAMAG UV lamp (1.1 mW/cm^2 in 17 cm distance) in a distance of 10 cm for 30 minutes. Before exposure to light and after 30 minutes of irradiation peptides were analyzed by RP-HPLC. For the chromatographical analysis an Agilent 1200 device was used equipped with a degaser (G1322A), a quaternary pump (G1311A), an autosampler (G1329A), a thermostatted column compartment (TCC, G1316A) and a variable wavelength detector (VWD, G1314B).

LC-MS/MS of mass reporter mix

An equal amount of all five mass reporters was mixed and purified in three steps: UV irradiation, affinity purification and cleavage by TEVp. Before measurements the sample was cleaned up using C-18 Stage Tips[50] as described before.

NanoLC-MS/MS analyses were performed on an Orbitrap Fusion (Thermo Scientific) equipped with a PicoView Ion Source (New Objective) and coupled to an EASY-nLC 1000 (Thermo Scientific). Peptides were loaded on capillary columns (PicoFrit, 30 cm x 150 µm ID, New Objective) self-packed with ReproSil-Pur 120 C18-AQ, 1.9 µm (Dr. Maisch) and separated with a 30-minute linear gradient from 3 % to 30 % acetonitrile and 0.1 % formic acid and a flow rate of 500 nl/min.

Both MS and MS^2 scans were acquired in the Orbitrap analyzer with a resolution of 60,000 for MS scans and 15,000 for MS^2 scans. A data dependent targeted MS^2 method with a fixed cycle time of 3 seconds was used with a target mass of m/z 413.2144 (corresponding to the doubly charged mass tag construct). For the target mass HCD collision energy was set to 20 % normalized collision energy and the isolation window was set to 0.5 m/z to minimize peak overlapping from isotopic peaks. Mass tolerance was set to 22 ppm. Nontarget masses were measured using standard parameters (35 % normalized collision energy, isolation window 2.5 m/z, dynamic exclusion with repeat count of 1 and an exclusion duration of 30 seconds). Singly charged precursors were excluded from selection. Injection time was increased from 50 ms for nontarget masses to 500 ms for target mass. Minimum signal threshold for precursor selection for nontarget masses was set to 50,000. For target mass no threshold was set. Predictive AGC was used with a AGC target value of 2e5 for MS scans and 5e4 for MS^2 scans. EASY-IC was used for internal calibration.

Mass tag dilution series and detection by tandem mass spectrometry

Lyophilized N-acetylated mass tag (MW = 862.4 g/mol) was dissolved in PBS and a concentration series of 5 pM, 50 pM, 0.3 nM, 0.5 nM and 5 nM was prepared.

Peptides were cleaned up using C-18 Stage Tips[50] before LC-MS/MS measurements. Each Stage Tip was prepared with three discs of C-18 Empore SPE Discs (3M) in a 200 µl pipet tip. Samples were acidified with formic acid to a final conc. of 0.5% formic acid. Peptides were eluted from Stage Tip with 60 % acetonitrile in 0.3 % formic acid, dried in a vacuum

concentrator (Eppendorf), and stored at -20 °C. Peptides were dissolved in 2% acetonitrile / 0.1 % formic acid prior to nanoLC-MS/MS analysis. NanoLC-MS/MS analyses were performed on a LTQ-Orbitrap Velos Pro (Thermo Scientific) equipped with a PicoView Ion Source (New Objective) and coupled to an EASY-nLC 1000 (Thermo Scientific). Peptides were loaded on capillary columns (PicoFrit, 30 cm x 150 µm ID, New Objective) self-packed with ReproSil-Pur 120 C18-AQ, 1.9 µm (Dr. Maisch) and separated with a 30-minute linear gradient from 3% to 30% acetonitrile and 0.1% formic acid and a flow rate of 500 nl/min. MS scans were acquired in the Orbitrap analyzer with a resolution of 30000 at m/z 400, MS^2 scans were acquired in the Orbitrap analyzer with a resolution of 7500 at m/z 400 using HCD fragmentation with 30% normalized collision energy. A TOP5 data dependent MS^2 method was used; dynamic exclusion was applied with a repeat count of 1 and an exclusion duration of 30 seconds; singly charged precursors were excluded from selection. Minimum signal threshold for precursor selection was set to 50000. Predictive AGC was used with AGC target a value of 1e6 for MS scans and 5e4 for MS^2 scans. Lock mass option was applied for internal calibration in all runs using background ions from protonated decamethylcyclopentasiloxane (m/z 371.10124). The Xcalibur™ software (Thermo Fisher Scientific Inc., MA) was used for data analysis.

Animal experiments

The animal experiments were conducted in consensus with a positive ethic vote from the ethics committee from the Zhejiang University, Hangzhou, China (ZJU20170298).

Mouse model of surgical destabilization of medial meniscus (DMM)

Thirteen C57BL/6 male mice at 8 weeks of age were used. Mice were anesthetized with 10 mg/kg pentobarbital and knees were prepared for aseptic surgery. Six mice were randomly assigned to the DMM group, and six mice to the sham group and one back-up mouse. Under anesthesia, a straight incision was made on the anterior side of knee, the anteromedial side of the joint capsule was cut, and the anterior horn of the medial meniscus was dislocated anteriorly with forceps. Meniscectomy was performed by resecting about 2/3 of the meniscus and then the articular cavity was closed by normal surgery. A sham operation procedure was also performed in which the meniscotibial ligament was exposed but not transected. Intra-articular injections (10 µl) of 250 µM mass reporter mix in PBS (50 µM PEG-sLr1-4armPEG, 50 µM PEG-sDr1-4armPEG, 50 µM PEG-sLr2-4armPEG,

50 µM PEG-sDr2-4armPEG and 50 µM validation reporter) were conducted three days after surgery. Sham-operated group, also receiving the mass reporters, served as control. The mice were kept in a group of three per cage and were allowed to walk freely and were sacrificed at day 8 post-surgery.

Blood was collected retrobulbar from the jugular vein 1, 3, 6, 12, 24, 48, 72 and 120 hours after mass reporter injection and was snap frozen in liquid nitrogen and stored at -80 °C.

Macroscopic and histological assessment

Specimens were fixed, decalcified in 0.5 M EDTA, dehydrated and embedded within paraffin blocks. Histological sections (6 µm) were prepared using a microtome, and subsequently deparaffinized with xylene, hydrated using decreasing concentrations of ethanol, and then subjected to hematoxylin and eosin (HE) staining and safranin O staining for the evaluation of cartilage degradation. Macroscopic pictures were taken using a digital camera (Olympus IX71) on a dedicated medical photography platform.

OA histopathology was evaluated by using the Osteoarthritis Research Society International cartilage OA histopathology scoring system, as described before[51].

Histological score evaluation was performed using the modified Mankin's score: the quantity of fibroblast-like cells, immunological cells and blood vessels was assessed by a modification of techniques utilized as described previously[52]. Inflammation score evaluation was performed using the area percentage of inflammatory cell infiltration[38] and synovial score evaluation was performed using thickness (cell layer) and the area percentage of inflammatory cell infiltration in synovium. Investigators were blinded to group identity, from group assignment through histologic scoring.

Acknowledgments

Technical support is kindly acknowledged for Dr. Büchner and his team from the Organic Chemistry Department for MALDI and ESI-MS measurements. Financial support is kindly acknowledged by the German Research Foundation (DFG) through the Sino-German Center (Grant # ME3820/3-1). The animal experiments were performed under the guidance of Yejun Hu and Prof. Ouyang's lab. Mr. Hu's support for the histological assessment is kindly acknowledged.

References

1. Zuber, T. J., Knee joint aspiration and injection. *Am Fam Physician* **2002,** *66* (8), 1497-500, 1503-4, 1507.
2. Lai, W. F.; Chang, C. H.; Tang, Y.; Bronson, R.; Tung, C. H., Early diagnosis of osteoarthritis using cathepsin B sensitive near-infrared fluorescent probes. *Osteoarthritis and cartilage* **2004,** *12* (3), 239-44.
3. Lee, H.; Lee, K.; Kim, I. K.; Park, T. G., Synthesis, characterization, and in vivo diagnostic applications of hyaluronic acid immobilized gold nanoprobes. *Biomaterials* **2008,** *29* (35), 4709-18.
4. Zhang, H.; Fan, J.; Wang, J.; Zhang, S.; Dou, B.; Peng, X., An off-on COX-2-specific fluorescent probe: targeting the Golgi apparatus of cancer cells. *J Am Chem Soc* **2013,** *135* (31), 11663-9.
5. Kwong, G. A.; von Maltzahn, G.; Murugappan, G.; Abudayyeh, O.; Mo, S.; Papayannopoulos, I. A.; Sverdlov, D. Y.; Liu, S. B.; Warren, A. D.; Popov, Y.; Schuppan, D.; Bhatia, S. N., Mass-encoded synthetic biomarkers for multiplexed urinary monitoring of disease. *Nature biotechnology* **2013,** *31* (1), 63-70.
6. Park, J. H.; von Maltzahn, G.; Zhang, L.; Schwartz, M. P.; Ruoslahti, E.; Bhatia, S. N.; Sailor, M. J., Magnetic Iron Oxide Nanoworms for Tumor Targeting and Imaging. *Adv Mater* **2008,** *20* (9), 1630-1635.
7. Morris, T. A.; Marsh, J. J.; Burrows, C. M.; Chiles, P. G.; Konopka, R. G.; Pedersen, C. A., Urine and plasma levels of fibrinopeptide B in patients with deep vein thrombosis and pulmonary embolism. *Thrombosis Research* **2003,** *110* (2-3), 159-165.
8. Dodt, K.; Lamer, S.; Drießen, M.; Bölch, S.; Schlosser, A.; Lühmann, T.; Meinel, L., Mass-Encoded Reporters Reporting Proteolytic Activity from within the Extracellular Matrix. *ACS Biomaterials Science & Engineering* **2020,** *6* (9), 5240-5253.
9. Dodt, K.; Driessen, M. D.; Lamer, S.; Schlosser, A.; Lühmann, T.; Meinel, L., A Complete and Versatile Protocol: Decoration of Cell-Derived Matrices with Mass-Encoded Peptides for Multiplexed Protease Activity Detection. *ACS Biomaterials Science & Engineering* **2020**.
10. Tetlow, L. C.; Woolley, D. E., Comparative immunolocalization studies of collagenase 1 and collagenase 3 production in the rheumatoid lesion, and by human chondrocytes and synoviocytes in vitro. *Br J Rheumatol* **1998,** *37* (1), 64-70.
11. Billinghurst, R. C.; Dahlberg, L.; Ionescu, M.; Reiner, A.; Bourne, R.; Rorabeck, C.; Mitchell, P.; Hambor, J.; Diekmann, O.; Tschesche, H.; Chen, J.; Van Wart, H.; Poole, A. R., Enhanced cleavage of type II collagen by collagenases in osteoarthritic articular cartilage. *The Journal of clinical investigation* **1997,** *99* (7), 1534-45.
12. Lindy, O.; Konttinen, Y. T.; Sorsa, T.; Ding, Y.; Santavirta, S.; Ceponis, A.; Lopez-Otin, C., Matrix metalloproteinase 13 (collagenase 3) in human rheumatoid synovium. *Arthritis and rheumatism* **1997,** *40* (8), 1391-9.
13. Kushner, I.; Somerville, J. A., Permeability of human synovial membrane to plasma proteins. Relationship to molecular size and inflammation. *Arthritis and rheumatism* **1971,** *14* (5), 560-70.
14. Levick, J. R.; McDonald, J. N., Fluid movement across synovium in healthy joints: role of synovial fluid macromolecules. *Ann Rheum Dis* **1995,** *54* (5), 417-23.
15. Skerra, A.; Schmidt, T. G. M., Applications of a peptide ligand for streptavidin: the Strep-tag. *Biomolecular Engineering* **1999,** *16* (1-4), 79-86.
16. Braun, A. C.; Gutmann, M.; Luhmann, T.; Meinel, L., Bioorthogonal strategies for site-directed decoration of biomaterials with therapeutic proteins. *J Control Release* **2018,** *273*, 68-85.
17. Agard, N. J.; Prescher, J. A.; Bertozzi, C. R., A strain-promoted [3 + 2] azide-alkyne cycloaddition for covalent modification of biomolecules in living systems. *J Am Chem Soc* **2004,** *126* (46), 15046-7.

18. Ritzer, J.; Luhmann, T.; Rode, C.; Pein-Hackelbusch, M.; Immohr, I.; Schedler, U.; Thiele, T.; Stubinger, S.; Rechenberg, B. V.; Waser-Althaus, J.; Schlottig, F.; Merli, M.; Dawe, H.; Karpisek, M.; Wyrwa, R.; Schnabelrauch, M.; Meinel, L., Diagnosing peri-implant disease using the tongue as a 24/7 detector. *Nat Commun* **2017,** *8*.
19. Nagase, H.; Visse, R.; Murphy, G., Structure and function of matrix metalloproteinases and TIMPs. *Cardiovasc Res* **2006,** *69* (3), 562-73.
20. Van Wart, H. E.; Birkedal-Hansen, H., The cysteine switch: a principle of regulation of metalloproteinase activity with potential applicability to the entire matrix metalloproteinase gene family. *Proc Natl Acad Sci U S A* **1990,** *87* (14), 5578-82.
21. Vaisar, T.; Urban, J., Probing the proline effect in CID of protonated peptides. *J Mass Spectrom* **1996,** *31* (10), 1185-7.
22. Huang, Y.; Tseng, G. C.; Yuan, S.; Pasa-Tolic, L.; Lipton, M. S.; Smith, R. D.; Wysocki, V. H., A data-mining scheme for identifying peptide structural motifs responsible for different MS/MS fragmentation intensity patterns. *J Proteome Res* **2008,** *7* (1), 70-9.
23. Palasek, S. A.; Cox, Z. J.; Collins, J. M., Limiting racemization and aspartimide formation in microwave-enhanced Fmoc solid phase peptide synthesis. *J Pept Sci* **2007,** *13* (3), 143-8.
24. Pillai, V. R., Photoremovable protecting groups in organic synthesis. *Synthesis* **1980,** *1980* (01), 1-26.
25. Sternson, S. M.; Schreiber, S. L., An acid- and base-stable o-nitrobenzyl photolabile linker for solid phase organic synthesis. *Tetrahedron Lett* **1998,** *39* (41), 7451-7454.
26. Brown, B. B.; Wagner, D. S.; Geysen, H. M., A single-bead decode strategy using electrospray ionization mass spectrometry and a new photolabile linker: 3-amino-3-(2-nitrophenyl)propionic acid. *Mol Divers* **1995,** *1* (1), 4-12.
27. Kim, J.; Kyeong, S.; Shin, D.-S.; Yeo, S.; Yim, J.; Lee, Y.-S., Facile Synthesis of N-(9-Fluorenylmethyloxycarbonyl)-3-amino-3-(4,5-dimethoxy-2-nitrophenyl)propionic Acid as a Photocleavable Linker for Solid-Phase Peptide Synthesis. *Synlett* **2013,** *24* (06), 733-736.
28. Bosques, C. J.; Imperiali, B., Photolytic control of peptide self-assembly. *J Am Chem Soc* **2003,** *125* (25), 7530-1.
29. Parks, T. D.; Howard, E. D.; Wolpert, T. J.; Arp, D. J.; Dougherty, W. G., Expression and purification of a recombinant tobacco etch virus NIa proteinase: biochemical analyses of the full-length and a naturally occurring truncated proteinase form. *Virology* **1995,** *210* (1), 194-201.
30. Dougherty, W. G.; Dawn Parks, T., Post-translational processing of the tobacco etch virus 49-kDa small nuclear inclusion polyprotein: Identification of an internal cleavage site and delimitation of VPg and proteinase domains. *Virology* **1991,** *183* (2), 449-456.
31. Carrington James, D. W., A viral cleavage site casette: identification of amino acid sequences required for tobacco etch virus polyprotein processing. *Proc Natl Acad Sci U S A* **1988,** *85*, 3391-3395.
32. Dougherty, W. G.; Parks, T. D.; Cary, S. M.; Bazan, J. F.; Fletterick, R. J., Characterization of the catalytic residues of the tobacco etch virus 49-kDa proteinase. *Virology* **1989,** *172* (1), 302-310.
33. Carrington, J. C.; Dougherty, W. G., Small nuclear inclusion protein encoded by a plant potyvirus genome is a protease. *Journal of Virology* **1987,** *61* (8), 2540-2548.
34. Young, C. L.; Britton, Z. T.; Robinson, A. S., Recombinant protein expression and purification: a comprehensive review of affinity tags and microbial applications. *Biotechnol J* **2012,** *7* (5), 620-34.
35. Kapust, R. B.; Tozser, J.; Fox, J. D.; Anderson, D. E.; Cherry, S.; Copeland, T. D.; Waugh, D. S., Tobacco etch virus protease: mechanism of autolysis and rational design of stable mutants with wild-type catalytic proficiency. *Protein Eng* **2001,** *14* (12), 993-1000.
36. van den Borne, M. P.; Raijmakers, N. J.; Vanlauwe, J.; Victor, J.; de Jong, S. N.; Bellemans, J.; Saris, D. B.; International Cartilage Repair, S., International Cartilage Repair Society (ICRS) and

Oswestry macroscopic cartilage evaluation scores validated for use in Autologous Chondrocyte Implantation (ACI) and microfracture. *Osteoarthritis and cartilage* **2007,** *15* (12), 1397-402.
37. Moriya, T.; Wada, Y.; Watanabe, A.; Sasho, T.; Nakagawa, K.; Mainil-Varlet, P.; Moriya, H., Evaluation of reparative cartilage after autologous chondrocyte implantation for osteochondritis dissecans: histology, biochemistry, and MR imaging. *J Orthop Sci* **2007,** *12* (3), 265-73.
38. Hu, Y.; Ran, J.; Zheng, Z.; Jin, Z.; Chen, X.; Yin, Z.; Tang, C.; Chen, Y.; Huang, J.; Le, H.; Yan, R.; Zhu, T.; Wang, J.; Lin, J.; Xu, K.; Zhou, Y.; Zhang, W.; Cai, Y.; Dominique, P.; Heng, B. C.; Chen, W.; Shen, W.; Ouyang, H. W., Exogenous stromal derived factor-1 releasing silk scaffold combined with intra-articular injection of progenitor cells promotes bone-ligament-bone regeneration. *Acta Biomater* **2018,** *71*, 168-183.
39. Kim, B. J.; Choi, B. H.; Jin, L. H.; Park, S. R.; Min, B.-H., Comparison between subchondral bone change and cartilage degeneration in collagenase- and DMM- induced osteoarthritis (OA) models in mice. *Tissue Engineering and Regenerative Medicine* **2013,** *10* (4), 211-217.
40. Loeser, R. F.; Olex, A. L.; McNulty, M. A.; Carlson, C. S.; Callahan, M.; Ferguson, C.; Fetrow, J. S., Disease progression and phasic changes in gene expression in a mouse model of osteoarthritis. *PLoS One* **2013,** *8* (1), e54633.
41. Fang, H.; Huang, L.; Welch, I.; Norley, C.; Holdsworth, D. W.; Beier, F.; Cai, D., Early Changes of Articular Cartilage and Subchondral Bone in The DMM Mouse Model of Osteoarthritis. *Sci Rep* **2018,** *8* (1), 2855.
42. Law, B.; Weissleder, R.; Tung, C. H., Peptide-based biomaterials for protease-enhanced drug delivery. *Biomacromolecules* **2006,** *7* (4), 1261-5.
43. Lee, E. S.; Na, K.; Bae, Y. H., Super pH-sensitive multifunctional polymeric micelle. *Nano Lett* **2005,** *5* (2), 325-9.
44. Choi, S. W.; Zhang, Y.; Xia, Y., A temperature-sensitive drug release system based on phase-change materials. *Angew Chem Int Ed Engl* **2010,** *49* (43), 7904-8.
45. de Gracia Lux, C.; Joshi-Barr, S.; Nguyen, T.; Mahmoud, E.; Schopf, E.; Fomina, N.; Almutairi, A., Biocompatible polymeric nanoparticles degrade and release cargo in response to biologically relevant levels of hydrogen peroxide. *J Am Chem Soc* **2012,** *134* (38), 15758-64.
46. Repenko, T.; Rix, A.; Ludwanowski, S.; Go, D.; Kiessling, F.; Lederle, W.; Kuehne, A. J. C., Bio-degradable highly fluorescent conjugated polymer nanoparticles for bio-medical imaging applications. *Nat Commun* **2017,** *8* (1), 470.
47. Veronese, F. M.; Schiavon, O.; Pasut, G.; Mendichi, R.; Andersson, L.; Tsirk, A.; Ford, J.; Wu, G.; Kneller, S.; Davies, J.; Duncan, R., PEG-doxorubicin conjugates: influence of polymer structure on drug release, in vitro cytotoxicity, biodistribution, and antitumor activity. *Bioconjug Chem* **2005,** *16* (4), 775-84.
48. Wang, X.; Sun, X.; Lao, J.; He, H.; Cheng, T.; Wang, M.; Wang, S.; Huang, F., Multifunctional graphene quantum dots for simultaneous targeted cellular imaging and drug delivery. *Colloids Surf B Biointerfaces* **2014,** *122*, 638-644.
49. Yuan, Q.; Hein, S.; Misra, R. D., New generation of chitosan-encapsulated ZnO quantum dots loaded with drug: synthesis, characterization and in vitro drug delivery response. *Acta Biomater* **2010,** *6* (7), 2732-9.
50. Rappsilber, J.; Mann, M.; Ishihama, Y., Protocol for micro-purification, enrichment, pre-fractionation and storage of peptides for proteomics using StageTips. *Nat Protoc* **2007,** *2* (8), 1896-906.
51. Hayashi, S.; Fujishiro, T.; Hashimoto, S.; Kanzaki, N.; Chinzei, N.; Kihara, S.; Takayama, K.; Matsumoto, T.; Nishida, K.; Kurosaka, M.; Kuroda, R., p21 deficiency is susceptible to osteoarthritis through STAT3 phosphorylation. *Arthritis Res Ther* **2015,** *17*, 314.
52. Shen, W.; Chen, X.; Hu, Y.; Yin, Z.; Zhu, T.; Hu, J.; Chen, J.; Zheng, Z.; Zhang, W.; Ran, J.; Heng, B. C.; Ji, J.; Chen, W.; Ouyang, H. W., Long-term effects of knitted silk-collagen sponge

scaffold on anterior cruciate ligament reconstruction and osteoarthritis prevention. *Biomaterials* **2014,** *35* (28), 8154-63.

Supporting information

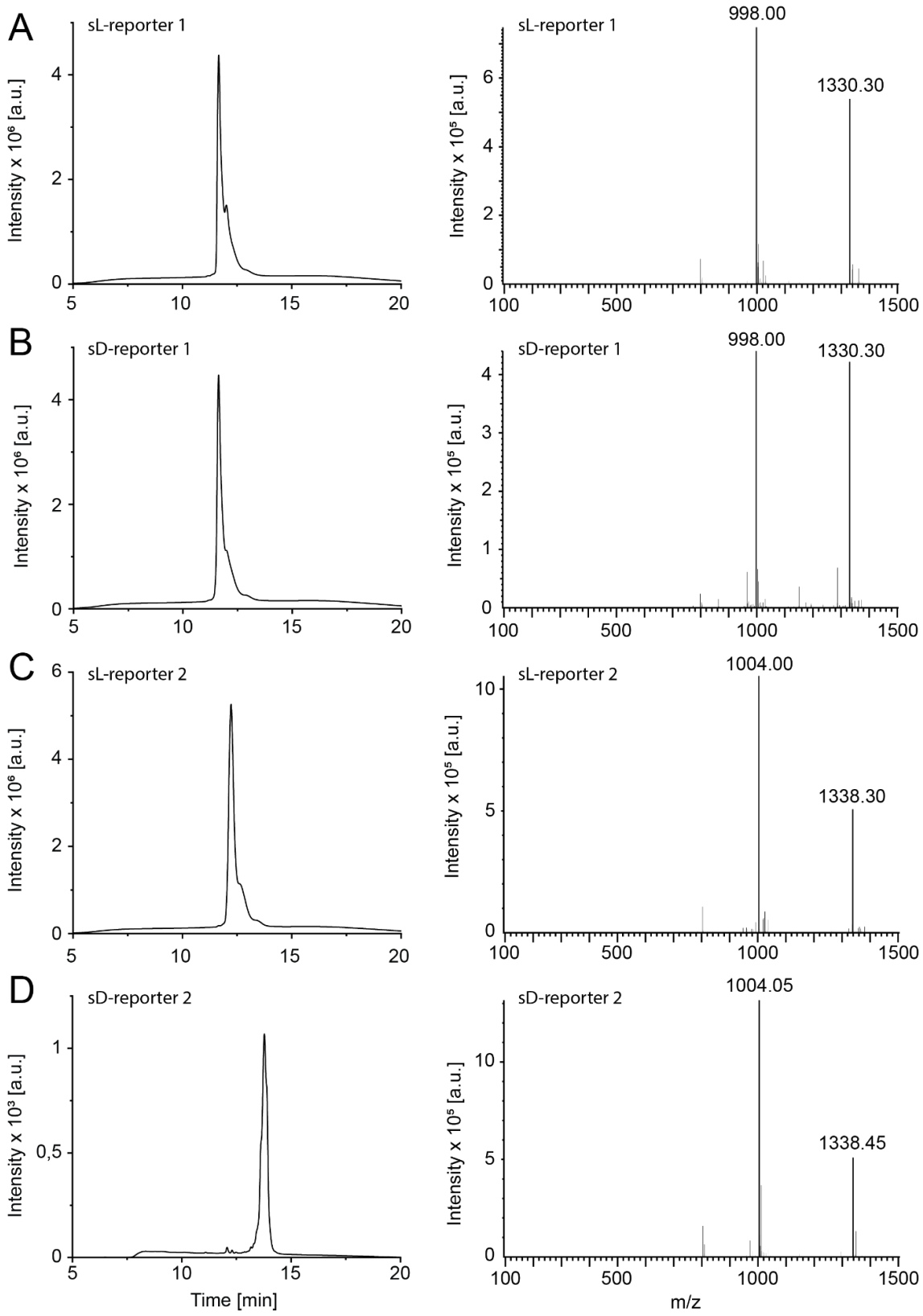

Figure S 13 RP-HPLC analysis and MALDI spectra of mass reporter peptides: (A) sL-reporter 1, (B) SD-reporter 1, (C) SL-reporter 2, and (D) SD-reporter 2.

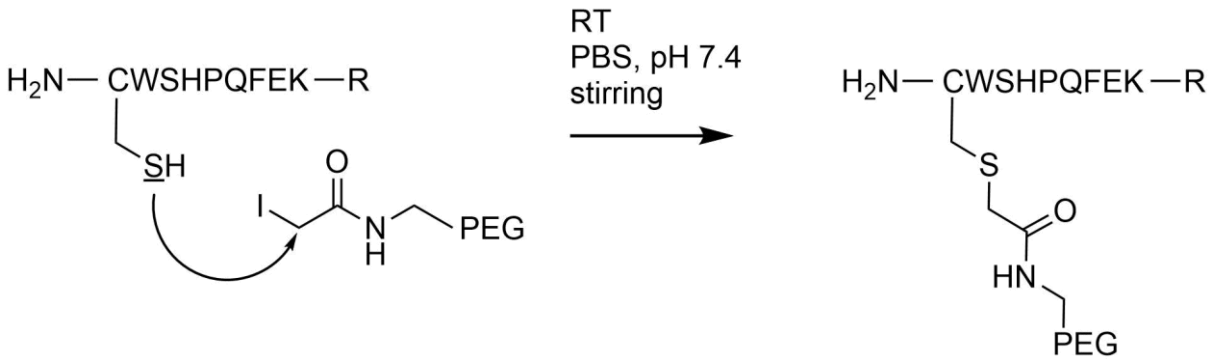

Figure S 14 Iodoacetamide-thiol reaction of N-terminal cysteine residue with iodoacetamide-PEG.

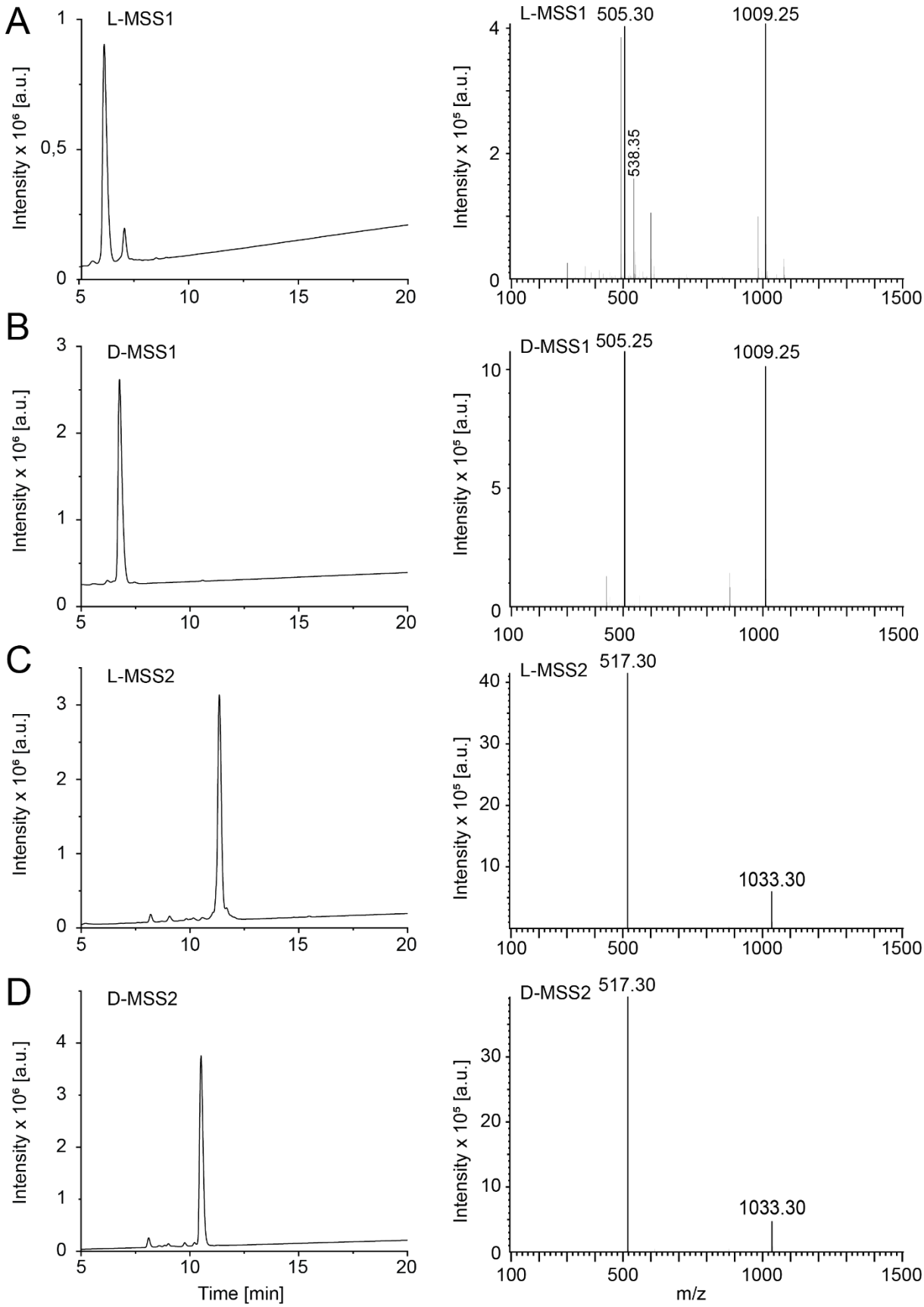

Figure S 15 RP-HPLC chromatograms and ESI spectra of matrix metalloproteinase substrate sequences 1 and 2 in L- and D-version: (A) L-MMS1, (B) D-MSS1, (C) L-MSS2, and (D) D-MSS2.

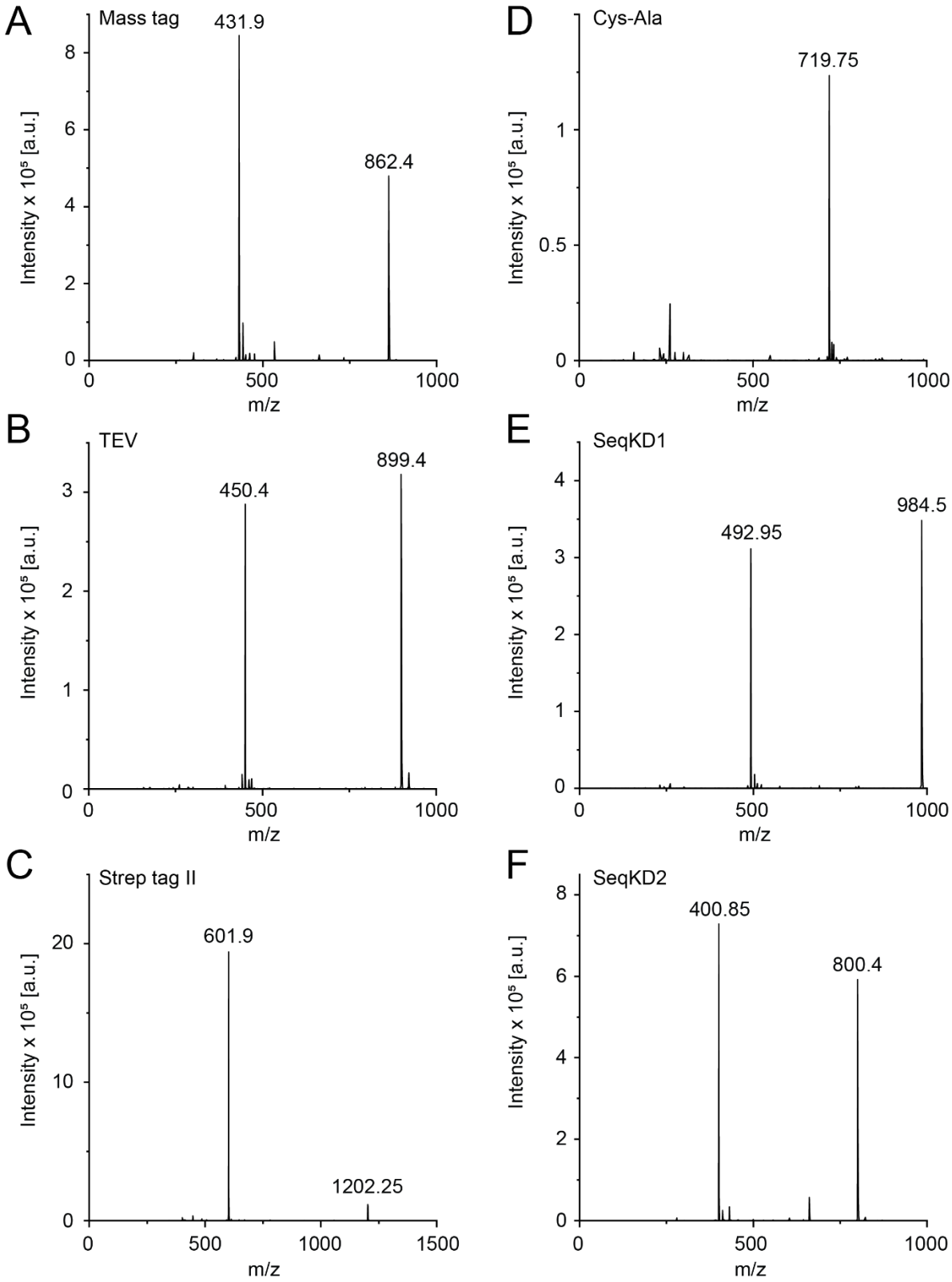

Figure S 16 ESI spectra of the following peptide fragments: (A) mass tag (calculated mass = 861.89 Da, double charged calculated mass = 431.95 Da), (B) TEVs (calculated mass = 899.94 Da, double charged calculated mass = 450.97 Da), (C) Strep tag II (calculated mass = 1202.34 Da, double charged calculated mass = 602.17 Da), (D) Cys-Ala (calculated mass = 2156.34 Da, triple charged calculated mass = 719.78 Da), (E) SeqKD1(calculated mass = 984.06 Da, double charged calculated mass = 493.03 Da), and (F) SeqKD2(calculated mass = 799.87 Da, double charged calculated mass = 400.94 Da).

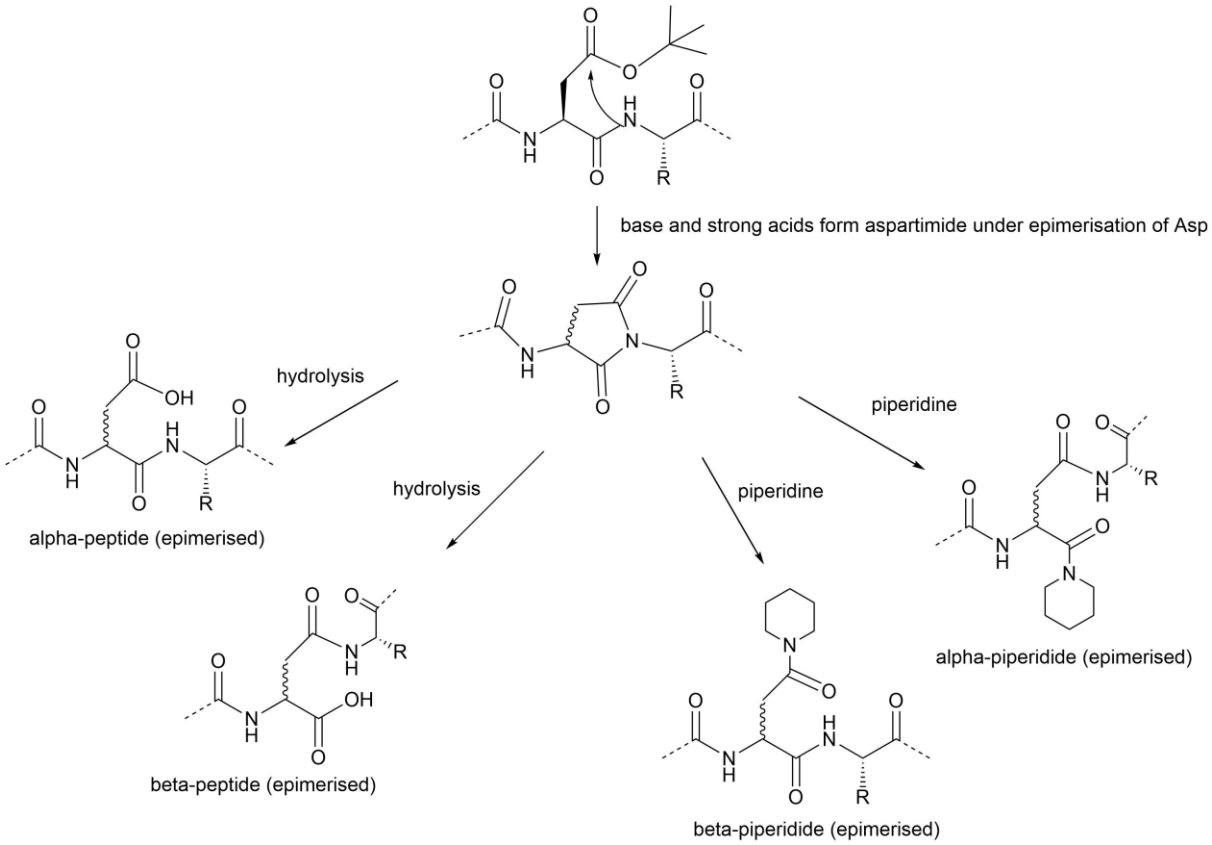

Figure S 17 Aspartimide formation of asparagine residue during peptide synthesis.

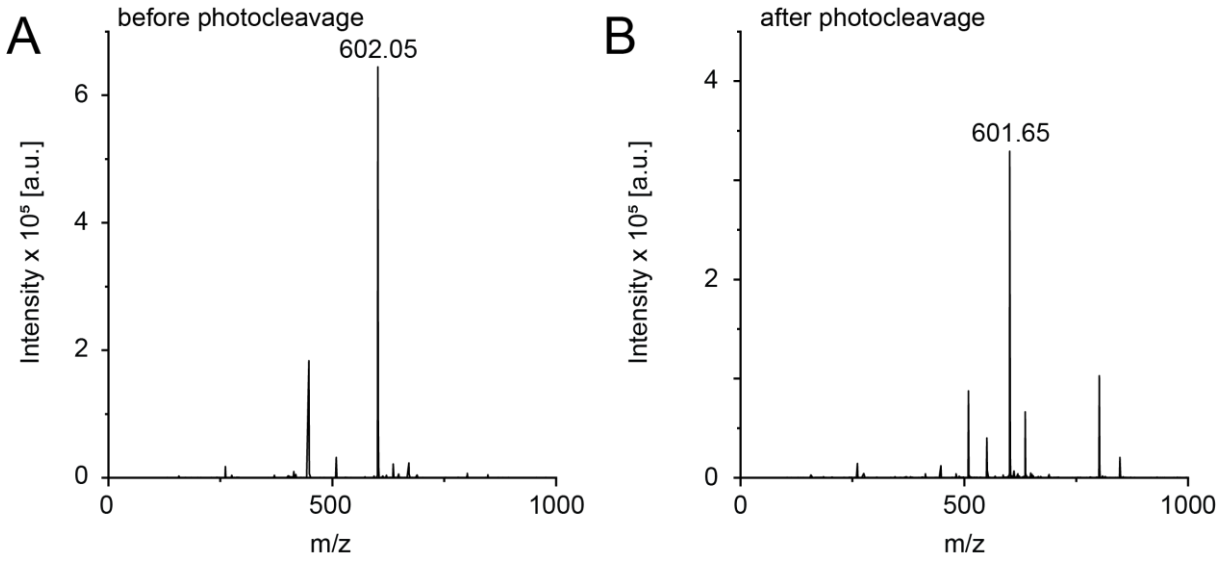

Figure S 18 ESI spectra of Strep-tag II peptide (A) before and (B) after UV irradiation. The disulfide bond formation is shown by a mass reduction of 0.5 from 602.05 to 601.65 m/z.

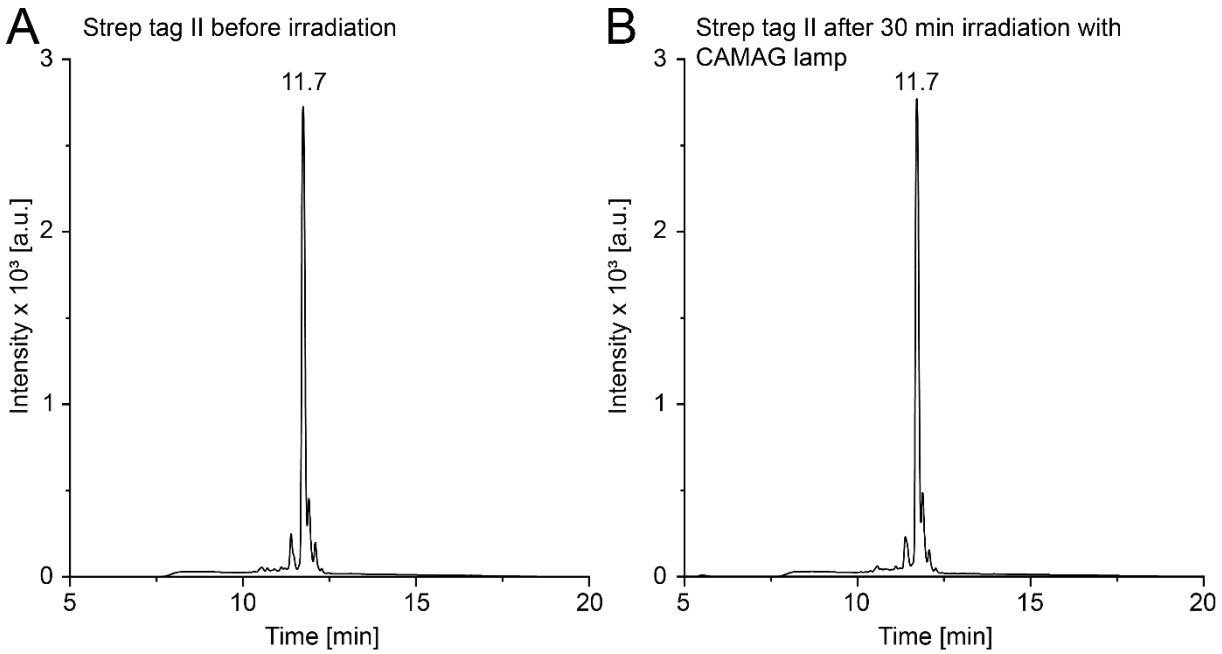

Figure S 19 RP-HPLC chromatograms of Strep-tag II (A) before irradiation and (B) after UV irradiation with CAMAG UV lamp for 30 minutes. When irradiated with a UV lamp with lower irradiance no disulfide bond formation was shown as no retention time shift is observed.

CONCLUSION AND OUTLOOK

Inflammatory disease, such as rheumatoid arthritis, inflammatory bowel disease, asthma, and arteriosclerosis were linked with elevated enzyme levels, especially matrix metalloproteinases (MMPs).[1-4] Many studies were performed to correlate MMP activity to the diagnosis of inflammatory diseases, to medicinal strategies, or to the response to therapy.[5-7] In a study on dry eye a point-of-care test identified patients with elevated MMP-9 levels and directed anti-inflammatory therapy with the result of symptomatic improvement and reduced inflammation.[8, 9] The use of MMPs as diagnostic biomarkers was already translated into clinic. For example, in dental medicine there are two commercially available diagnostic tests based on MMP-8 activity measurements. These are used to monitor the inflammatory status in the oral cavity post-implantation, to screen periodontitis patients, to predict disease progression, or to monitor the response to treatment.[10, 11] Using MMPs as diagnostic markers for rheumatoid arthritis (RA) revealed inconsistent results. One study evaluated the effects of anti-tumor necrosis factor-α (TNF-α, golimumab) therapy on inflammatory markers, such as MMP-3. Serum concentrations decreased already after 24 hours and low levels persisted through 24 weeks after periodic subcutaneous (s.c.) TNF-α application but no significant correlation between MMP-3 and clinical assessment was observed.[12] Another study evaluated anti-TNF-α therapy (etanercept) and its modulation of serum and synovial MMP levels. MMP-1 and -3 serum levels were decreased and the baseline MMP-3 levels correlated with the clinical assessment after 12 weeks anti- TNF-α therapy, which may indicate that a prediction of clinical assessment might be possible.[13] These results are contradictious because increased MMPs levels may be spatiotemporal limited in disease[1] or MMP levels alone may not give sufficient diagnostic or predictive information.[14-17] To clarify MMP-3's potential biomarker ability in RA patients and to draw important information from MMP activity further studies and a better understanding of e.g. MMP activity pattern are necessary. Until today MMP activity was detected in a multitude of pathologies with various methods. For example, a MMP-9 specific immunocapture activity assay for Sjögren's syndrome was established[18] or in another study a radiometric assay for MMP activity was developed by designing a synthetic ^{14}C-labelled peptide substrate[19] or extracellular matrix turnover was observed by measuring MMP activity with ^{14}C-radiolabelled type I collagen.[20] Most commonly zymography[21-23] or colorimetric assays were applied for the determination of MMP activity. While some colorimetric assays are based on the change of color shift by

the assembly or breakdown of gold nanoparticles,[24, 25] others are chromogenic peptide probes or Förster resonance energy transfer (FRET) substrates specific for distinct MMP isoforms or for the entire MMP family, which consist of a fluorogenic substrate that is chemically conjugated to polymers, nanoparticles or other scaffolds via a MMP-sensitive peptide linker and cleavage thereof lead to emittance of a fluorescence signal.[26-30] The aforementioned methods display an absolute value for enzyme activity obtained by comparing measured values to standard values. In zymographic assays often not only active but also pro-enzymes are detected because they are presumably activated *in situ* by denaturation/renaturation.[22, 31]

This thesis established a cornerstone in diagnostic systems being able to monitor enzyme activity and serve to further characterize inflammatory disease models with MMP involvement based on multiplexed detection of mass-encoded peptides by tandem mass spectrometry (LC-MS/MS). Two advanced strategies were developed (i) a mass reporter system that is covalently coupled to fibronectin in cell-derived extracellular matrix (ECM) and monitor enzyme activity from within ECM and (ii) a soluble mass reporter system that was intended for the application in the synovial gap of arthritic joints and report enzyme activity from synovial fluid.

For both systems the isotopically labelled mass tag sequence presented the core element, as it allowed multiplexed detection by LC-MS/MS. The use of isotopes to quantify or identify protein or peptide mixtures was developed earlier using the very well characterized methods of isotope-coding affinity tags (ICAT), tandem mass tags (TMT), isobaric tags for relative and absolute quantitation (iTRAQ) or variation of these.[32] These methods were developed to quantify proteins and peptides from an unknown protein pool and further identify them by correlating the MS^2 spectra with sequence databases.[33-35] Our mass reporters are not designed for identification reasons but for (relative) quantification of a known proteinase by using the appropriate protease-sensitive sequence as previously reported.[36] The ICATs are used in pairs, one light tag and one heavy tag enriched with ^{2}H, ^{13}C, or ^{15}N, used to label two different cell states. The quantification is performed by comparing MS signal intensities of proteins with a mass difference of the light and heavy tag. The MS spectra are quite complex since all labelled proteins are detected at once and the accuracy of quantification is reduced compared to our method as protein 1 with the light tag might co-elute with protein 2 labelled with the heavy tag. Our isobaric mass-encoding strategy overcomes the problem of sample complexity, as the mass tags themselves are

isolated from the sample fluid by three purification and isolation steps (i) cleavage by UV light, (ii) affinity purification with streptavidin-coated beads using the biotin affinity tag and (iii) incubation with TEVp to receive a mixture of pure mass tags all having the same parent mass but fragment in distinct fragment ions in MS^2. The mass tags are chromatographically indistinguishable in LC-MS^1 due to their identical parent mass, which is a characteristic that enhance sensitivity compared to mass-difference labelling.[37] Moreover, more than two cell states/samples at once can be investigated with the mass tag family because the multiplexed set can be highly increased: if the isotopically labelling is only focused on the y_5-fragment ions, the fragment ions with the highest intensity in MS^2, it would be possible to develop 14 different mass tags with heavy amino acids commercially available from Cambridge isotope laboratories (CIL), 17 and 8 mass tag versions if the fragment ions are centered on y_4 or y_6, respectively. If the amino acid sequence of our mass tags (SAEGPGFr) was varied, there are almost no multiplexing limits as long as suitable mass-encoded amino acids are available. The quantification with TMTs[38, 39] and iTRAQs[37, 40] is based on a MS^2 method where quantity of labelled peptides is revealed by the relative abundance of released fragment ion from the tag after MS^2. The tags' structure is similar to our developed mass tag family because they consist of a fragment region labelled with heavy amino acids and a neutralization region to balance the introduced mass shift. A reactive group, like N-hydroxysuccinimide (NHS) or iodoacetamide, is used to selectively couple the tags to a peptide's amine or thiol group. If our mass reporters hold a reactive functionality instead of the MMP substrate sequences (MSS) and immobilization sequence, they might as well be used as multiplexed sets to quantify and identify unknown proteins just as TMTs and iTRAQs do. The mandatory MS^2 measurements increase analysis time, but the gained reduced sample complexity and higher signal-to-noise ratio diminish this drawback.[38]

The development of two mass reporter systems – one soluble with a high molecular weight polymer and one immobilized to ECM with the transglutaminase (TG) peptide sequence – was performed to use the systems in different environments. The soluble and the immobilizing system, both comprise the same two matrix metalloproteinase substrate sequences with different MMP sensitivity. The cleavage efficiency of the incorporated MSSs might be different for the two systems despite using the same amino acid sequence, because of the different accessibility of the MSSs in both systems. The mass reporters immobilized onto ECM by FXIIIa report MMP activity directly from ECM and the MMP

cleavage might be affected due to steric hindrance of ECM components. The soluble mass reporters may report MMP activity more accurately from synovial fluid (SF) and might have a slightly higher cleavage efficiency as they are in solution and statistically "meet" MMPs (also in solution) more often than the immobilized reporters. The applied MSSs are sensitive to several MMPs reflecting overall MMP activity. Due to the overlapping substrate specificity of MMPs, phage display strategies were applied to identify specific substrate sequences for a single MMP and the recognition sequence could be adopted for our system.[41, 42] Both systems possess an affinity tag, but only the mass reporters with the immobilization tag can be administered *in vitro* and *in vivo* as the affinity tag can be used to purify the mass tags from body fluids or ECM supernatant. The soluble system is not applicable in an *in vitro* setting because cleaved and non-cleaved mass reporters cannot be distinguished by affinity purification because non-cleaved mass reporters are not hold back. Therefore, a further purification process based on molecular weight would be necessary. The immobilization process by FXIIIa has the advantage to control more reliably the amount of applied mass reporters at the application site. After co-administration of mass reporters and transglutaminase, the immobilized and unspecific adsorbed peptide amount on ECM is constant with each application (assuming constant constitution of ECM). Potentially, there is an initial burst of unspecific adsorbed mass reporters, which might be decreased by more washing steps after immobilization in the *in vitro* setting. Another advantage is, that the enzymatic transglutaminase reaction catalyzes quickly, highly specific and reliably the formation of an isopeptide bond between lysine and glutamine residues and leave a stable and endogenous linkage behind. This makes the mass reporters highly biocompatible in case of *in vivo* application. The soluble mass reporter system was applied locally that hold the advantages of reduced off-site cleavage, higher local concentrations and no necessity of a targeting strategy. Its ability to be retained at the injection site *in vivo* might be dependent on the molecular weight of the attached polymer and the permeability of synovial basal membrane and the lymphatic drainage system. The higher the molecular weight, the greater the retention ability of the polymer. The polymer's molecular weight might also influence the MSS cleavage efficiency as a higher MW or branched polymers constitute a sterically barrier, thus leading to reduced or slower cleavage. By selecting the clicked polymer, the MSS cleavage might be controlled, but the postulated influence has to be confirmed by future cleavage experiments.

In our study from chapter 1 and 2, ECM served as scaffold for immobilizing mass reporters by FXIIIa. Extracellular matrix was recently moved into focus as scaffold in tissue engineering either natural-derived from tissues[43, 44] or cell-derived from fibroblasts,[45] chondrocytes,[46] or mesenchymal stem cells.[47] It also established its role in drug delivery techniques as drug depot or as novel biomaterial to control drug release.[48, 49] Its use is favored because of its biocompatibility, biodegradability, biomechanical and bioinductive properties, that impart a complex, three-dimensional, viscoelastic environment providing optimal conditions for host cell attachment and interaction, and promote tissue remodeling processes.[50, 51] ECM structure and constitution are versatile depending on the cells or tissues it is derived from.[52] The ECM was selected as immobilization site as MMPs play a pivotal role in its remodelling in health and disease. The matrix metalloproteinase family possess the combined ability to degrade all types of collagen and other matrix and non-matrix proteins.[53] The activity of the zinc-dependent proteases is tightly regulated on transcriptional and post-transcriptional level and via their activators (active MMPs or serine proteinases) and inhibitors (tissue inhibitor of metalloproteinase (TIMP), α2-macroglobulin).[54] In our *in vitro* experiment, ECM was used as depot for a diagnostic system helping to further characterize ECM in terms of MMP activity and turnover. ECM is constantly undergoing remodelling, especially during normal processes of development, differentiation and wound healing. When assembly and degradation fall out of balance by dysregulated activating and inhibiting processes of MMPs, this can contribute to disease development, e.g. tissue fibrosis,[55, 56] cancer,[57] chronic wounds,[58] chronic obstructive pulmonary disease (COPD),[59, 60] or arthritis.[61, 62] Therefore, it is crucial to study and understand enzyme activity in healthy and diseased ECM. The mass reporters present an appealing method for this task. In our experiments we applied two MSS with different MMP sensitivity. This initial study showed, that MMP activity can be monitored over a certain time. Due to its modular structure the diagnostic system is not restricted to these substrate sequences, but the MSS may be exchanged by more specific substrate sequences, substrate sequences for other proteases,[63, 64] or by linkers sensitive to temperature,[65] pH,[66] or reactive oxygen species (ROS).[67] For example, in cell culture models studying osteoarthritis (OA) our mass reporter system with a specific MMP-3 MSS might help further characterize these models in terms of MMP activity over time. One synovitis translational *ex vivo* OA model consisted of human primary fibroblast-like synoviocytes and synovial membrane explants and observed MMP-derived collagen degradation fragments of collagen type I and III and activated MMP-3 to identify these as osteoarthritis

biomarkers.[68] With our mass reporter system MMP-3 activity can be detected but not only at one time point but it can also be detected qualitatively over time. The knowledge of the spatio-temporal MMP activity details the enzyme activity and impart MMP-3 as biomarker for synovitis a stronger significance. Furthermore, cell culture models constitute an important function in studying disease pathology, interactions between cellular mediators and tissue and response to therapy. In recent years the importance of 3D cell culture models compared to 2D monolayer cell culture models gained attention because of their more precise mimicking of the *in vivo* microenvironment.[69] ECM or some of its components are often used as 3D-scaffold, as ECM affects cell proliferation, differentiation, migration, survival and adhesion it is not surprising that the ECM's composition and physical properties influence cell behavior.[70] The cell response to therapeutics in response to ECM remodeling was subject to previous studies and was not only observed for cancer,[71] but also for insulin resistance in obesity,[72, 73] or fibrotic tissue.[74, 75] As our mass reporter system is immobilized on ECM, it sure is a system that can provide information on ECM degradation. Either the information is on degradation mediated by MMPs since our mass reporters have two incorporated MSS and their activity can be relatively quantified by LC-MS/MS or on general degradation, when the MSS module is omitted during peptide synthesis and mass reporters are only released due to ECM turnover.

While the soluble mass reporters are designed to retain in the synovial gap by their high molecular weight, the immobilized mass reporters would be covalently attached to fibronectin by co-administration of FXIIIa in a potential *in vivo* application in the synovial gap. The calcium-dependent crosslinking reaction was previously used to PEGylate proteins,[76] load cytokines, growth factors or peptides into (fibrin) hydrogels,[77-79] tether biological active peptides to surfaces,[80] or for drug delivery purposes.[81, 82] Using the transglutaminase reaction to form a peptide depot on cell-derived extracellular matrix is a unique idea. Previous studies demonstrated the integration of functional groups in ECM, like azides for click chemistry to prepare ECM as drug depot.[83, 84] Fibrin and fibronectin are the major physiological substrates and provide both, the acetyl-donor glutamine, and the acetyl-acceptor amine residue. There is no obvious consensus sequence for the glutamine as acyl-donor but there are some structural requirements for its surroundings being relevant to function as FXIIIa substrate.[85] In our study, the mass reporters provide the acyl-acceptor group (lysine) and the glutamines in fibronectin are the acyl-donor residues. During the reaction a binary complex of glutamine and enzyme via a thioester

bond is formed, ammonia released, and the subsequent attack of the primary amine transfers the glutamine's acyl group to the primary ε-amine of the lysin side chain. The transamidation reaction compete with deamidation (by water, hydrolysis) and esterification, which lead to the transformation of glutamine to glutamic acid or a glutamic ester derivatives, respectively.[86] These side reactions reduce glutamine availability as acyl-donors. To ensure that the immobilized peptide amount only depend on the applied amount of mass reporters, we chose to provide the acyl-acceptor lysine with our mass reporters since it is not prone to hydrolysis or esterification thus always available for the transamidation reaction.[87] The transglutaminase reaction may be applied to design drug delivery systems for inflammatory disease that are immobilized at the sight of injection and release a therapeutic (growth factor, cytokine) in response to an inflammatory stimulus. A similar study was performed with the anti-inflammatory interleukin-4 (IL-4), that provided significant cartilage repair upon release in an *in vivo* osteoarthritic rabbit model after successful immobilization on ECM (data not published yet).[88] Instead of IL-4, the application of anti-TNF-α or IL-1 receptor antagonists[89] might help as well to reduce inflammation, enhance cartilage repair and have reduced systemic side effects. The risk linked to co-administration of FXIIIa *in vivo* was not evaluated. FXIIIa has pleiotropic functions, beside its involvement in blood coagulation by fibrin cross-linking, studies demonstrated its participation in wound healing, tissue remodeling or influence on cell adhesion and behavior. Previous studies showed that FXIIIa enhanced migration and proliferation of monocytes and fibroblasts and inhibited their apoptosis.[90, 91] Furthermore, a pro-angiogenic effect of FXIIIa associated with thrombospondin-1 expression was demonstrated *in vitro*[92] and *in vivo.*[93] In our study, FXIIIa was used in an *in vitro* setting so far. The possible structural changes of ECM due to cross-linking of ECM components like fibronectin and collagen by FXIIIa,[94] its effect on mass reporter's binding capacity or the effect of mass reporter binding on ECM need further investigation. FXIIIa's potential use in the synovial gap as highly competent enzyme lead to the question if there are any expected side effects. Previous studies indicated, that FXIIIa in an interplay with tissue transglutaminase (TG2) could play a major role in osteoblast differentiation and collagen type I matrix formation[95, 96] and induce TG2 externalization, which stimulate chondrocyte maturation to hypertrophy[97] and cartilage calcification.[98] These mechanisms might be linked to early stage OA, thus it is unclear, if transglutaminases aggravate or resolve damages in OA.[99] *In vivo* models with TG2- or FXIIIa-deficient mice showed that cartilage destruction is significantly reduced,[100, 101] arguing for an aggravating role of

transglutaminases in OA. But also studies exist, where FXIIIa contrasts effectively harmful action of collagenases in human fibroblast cultured cells.[102] Therefore, the effect on chondrocyte and osteoblast differentiation due to the administration of 20 U/mL FXIIIa must be subject of a following study.

The mass reporter system from chapter 1 and 2 was successfully used to demonstrate the measurement of MMP activity from cell-derived ECM in an in vitro setting. The proof of concept study established the basis for diagnostic systems using ECM as depot scaffold and performing multiplexed detection of mass-encoded peptides by LC-MS/MS. The mass reporters were covalently attached to fibronectin by FXIIIa and the mass-encoded peptides were released in response to MMPs. The simultaneous detection of four mass tags by LC-MS/MS and the relative quantification was shown. The soluble reporter system from chapter 3 was used in a mouse model for arthritis. Various studies indicate that MMP activity correlates with disease progression of RA[103-105] and some patient groups are non-responders to conventional therapy with biological therapeutics.[106] Thus, we hypothesized that each patient has a distinct MMP activity profile, which should have been demonstrated in the OA mouse model. According to their enzyme profile patients might be stratified and subjected to a special personalized treatment. In our study we were able to show biocompatibility of the soluble reporter system, but the *in vivo* experiment could not provide enzyme activity results. The evaluation of the hypothesis, therefore, is yet to be performed and might reveal personalized treatment in arthritic diseases.

References

1. Yoshihara, Y.; Nakamura, H.; Obata, K.; Yamada, H.; Hayakawa, T.; Fujikawa, K.; Okada, Y., Matrix metalloproteinases and tissue inhibitors of metalloproteinases in synovial fluids from patients with rheumatoid arthritis or osteoarthritis. *Ann Rheum Dis* **2000,** *59* (6), 455-461.
2. Meijer, M. J.; Mieremet-Ooms, M. A.; van der Zon, A. M.; van Duijn, W.; van Hogezand, R. A.; Sier, C. F.; Hommes, D. W.; Lamers, C. B.; Verspaget, H. W., Increased mucosal matrix metalloproteinase-1, -2, -3 and -9 activity in patients with inflammatory bowel disease and the relation with Crohn's disease phenotype. *Dig Liver Dis* **2007,** *39* (8), 733-9.
3. Dahlen, B.; Shute, J.; Howarth, P., Immunohistochemical localisation of the matrix metalloproteinases MMP-3 and MMP-9 within the airways in asthma. *Thorax* **1999,** *54* (7), 590-6.
4. Sukhova, G. K.; Schonbeck, U.; Rabkin, E.; Schoen, F. J.; Poole, A. R.; Billinghurst, R. C.; Libby, P., Evidence for increased collagenolysis by interstitial collagenases-1 and -3 in vulnerable human atheromatous plaques. *Circulation* **1999,** *99* (19), 2503-9.
5. Keyszer, G.; Lambiri, I.; Nagel, R.; Keysser, C.; Keysser, M.; Gromnica-Ihle, E.; Franz, J.; Burmester, G. R.; Jung, K., Circulating levels of matrix metalloproteinases MMP-3 and MMP-1, tissue inhibitor of metalloproteinases 1 (TIMP-1), and MMP-1/TIMP-1 complex in rheumatic disease. Correlation with clinical activity of rheumatoid arthritis versus other surrogate markers. *J Rheumatol* **1999,** *26* (2), 251-8.
6. Posthumus, M. D.; Limburg, P. C.; Westra, J.; van Leeuwen, M. A.; van Rijswijk, M. H., Serum matrix metalloproteinase 3 in early rheumatoid arthritis is correlated with disease activity and radiological progression. *Journal of Rheumatology* **2000,** *27* (12), 2761-2768.
7. Kanesaka, T.; Mori, M.; Hattori, T.; Oki, T.; Kuwabara, S., Serum matrix metalloproteinase-3 levels correlate with disease activity in relapsing-remitting multiple sclerosis. *J Neurol Neurosurg Psychiatry* **2006,** *77* (2), 185-8.
8. Sambursky, R., Presence or absence of ocular surface inflammation directs clinical and therapeutic management of dry eye. *Clin Ophthalmol* **2016,** *10*, 2337-2343.
9. Kaufman, H. E., The practical detection of mmp-9 diagnoses ocular surface disease and may help prevent its complications. *Cornea* **2013,** *32* (2), 211-6.
10. Alassiri, S.; Parnanen, P.; Rathnayake, N.; Johannsen, G.; Heikkinen, A. M.; Lazzara, R.; van der Schoor, P.; van der Schoor, J. G.; Tervahartiala, T.; Gieselmann, D.; Sorsa, T., The Ability of Quantitative, Specific, and Sensitive Point-of-Care/Chair-Side Oral Fluid Immunotests for aMMP-8 to Detect Periodontal and Peri-Implant Diseases. *Dis Markers* **2018,** *2018*, 1306396.
11. Hernández-Ríos, P.; Hernández, M.; Garrido, M.; Tervahartiala, T.; Leppilahti, J.; Kuula, H.; Heikkinen, A. M.; Mäntylä, P.; Rathnayake, N.; Nwhator, S., Oral fluid matrix metalloproteinase (MMP)-8 as a diagnostic tool in chronic periodontitis. *Metalloproteinases in Medicine* **2016,** *3*, 11-18.
12. Doyle, M. K.; Rahman, M. U.; Frederick, B.; Birbara, C. A.; de Vries, D.; Toedter, G.; Wu, X.; Chen, D.; Ranganath, V. K.; Westerman, M. E.; Furst, D. E., Effects of subcutaneous and intravenous golimumab on inflammatory biomarkers in patients with rheumatoid arthritis: results of a phase 1, randomized, open-label trial. *Rheumatology (Oxford)* **2013,** *52* (7), 1214-9.
13. Catrina, A. I.; Lampa, J.; Ernestam, S.; af Klint, E.; Bratt, J.; Klareskog, L.; Ulfgren, A. K., Anti-tumour necrosis factor (TNF)-alpha therapy (etanercept) down-regulates serum matrix metalloproteinase (MMP)-3 and MMP-1 in rheumatoid arthritis. *Rheumatology (Oxford)* **2002,** *41* (5), 484-9.
14. Rousseau, J. C.; Delmas, P. D., Biological markers in osteoarthritis. *Nature clinical practice. Rheumatology* **2007,** *3* (6), 346-56.
15. Gavrilă, B.; Ciofu, C.; Stoica, V., Biomarkers in rheumatoid arthritis, what is new? *Journal of medicine and life* **2016,** *9* (2), 144.

16. Hadler-Olsen, E.; Winberg, J. O.; Uhlin-Hansen, L., Matrix metalloproteinases in cancer: their value as diagnostic and prognostic markers and therapeutic targets. *Tumour Biol* **2013,** *34* (4), 2041-51.
17. Watt, F. E., Osteoarthritis biomarkers: year in review. *Osteoarthritis and cartilage* **2018,** *26* (3), 312-318.
18. Hanemaaijer, R.; Visser, H.; Konttinen, Y.; Koolwijk, P.; Verheijen, J. H., A novel and simple immunocapture assay for determination of gelatinase-b (MMP-9) activities in biological fluids: Saliva from patients with Sjögren's Syndrome contain increased latent and active gelatinase-b levels. *Matrix Biology* **1998,** *17* (8-9), 657-665.
19. Brownell, J.; Earley, W.; Kunec, E.; Morgan, B. A.; Olyslager, B.; Wahl, R. C.; Houck, D. R., Comparison of native matrix metalloproteinases and their recombinant catalytic domains using a novel radiometric assay. *Arch Biochem Biophys* **1994,** *314* (1), 120-5.
20. Stock, U. A.; Wiederschain, D.; Kilroy, S. M.; Shum-Tim, D.; Khalil, P. N.; Vacanti, J. P.; Mayer, J. E.; Moses, M. A., Dynamics of extracellular matrix production and turnover in tissue engineered cardiovascular structures. *Journal of Cellular Biochemistry* **2001,** *81* (2), 220-228.
21. Toth, M.; Sohail, A.; Fridman, R., Assessment of gelatinases (MMP-2 and MMP-9) by gelatin zymography. *Methods Mol Biol* **2012,** *878*, 121-35.
22. Hawkes, S. P.; Li, H.; Taniguchi, G. T., Zymography and reverse zymography for detecting MMPs and TIMPs. *Methods Mol Biol* **2010,** *622*, 257-69.
23. Chang, Y. H.; Lin, I. L.; Tsay, G. J.; Yang, S. C.; Yang, T. P.; Ho, K. T.; Hsu, T. C.; Shiau, M. Y., Elevated circulatory MMP-2 and MMP-9 levels and activities in patients with rheumatoid arthritis and systemic lupus erythematosus. *Clin Biochem* **2008,** *41* (12), 955-9.
24. Kim, G. B.; Kim, K. H.; Park, Y. H.; Ko, S.; Kim, Y. P., Colorimetric assay of matrix metalloproteinase activity based on metal-induced self-assembly of carboxy gold nanoparticles. *Biosens Bioelectron* **2013,** *41*, 833-9.
25. Chen, P.; Selegard, R.; Aili, D.; Liedberg, B., Peptide functionalized gold nanoparticles for colorimetric detection of matrilysin (MMP-7) activity. *Nanoscale* **2013,** *5* (19), 8973-6.
26. Oshita, Y.; Koga, T.; Kamimura, T.; Matsuo, K.; Rikimaru, T.; Aizawa, H., Increased circulating 92 kDa matrix metalloproteinase (MMP-9) activity in exacerbations of asthma. *Thorax* **2003,** *58* (9), 757-60.
27. Nagase, H.; Fields, C. G.; Fields, G. B., Design and characterization of a fluorogenic substrate selectively hydrolyzed by stromelysin 1 (matrix metalloproteinase-3). *J Biol Chem* **1994,** *269* (33), 20952-7.
28. Fields, G. B., Using fluorogenic peptide substrates to assay matrix metalloproteinases. *Methods Mol Biol* **2010,** *622*, 393-433.
29. Ryu, J. H.; Lee, A.; Huh, M. S.; Chu, J.; Kim, K.; Kim, B. S.; Choi, K.; Kwon, I. C.; Park, J. W.; Youn, I., Measurement of MMP Activity in Synovial Fluid in Cases of Osteoarthritis and Acute Inflammatory Conditions of the Knee Joints Using a Fluorogenic Peptide Probe-Immobilized Diagnostic Kit. *Theranostics* **2012,** *2* (2), 198-206.
30. Lombard, C.; Saulnier, J.; Wallach, J., Assays of matrix metalloproteinases (MMPs) activities: a review. *Biochimie* **2005,** *87* (3-4), 265-72.
31. Kleiner, D. E.; Stetler-Stevenson, W. G., Quantitative zymography: detection of picogram quantities of gelatinases. *Anal Biochem* **1994,** *218* (2), 325-9.
32. Goodlett, D. R.; Keller, A.; Watts, J. D.; Newitt, R.; Yi, E. C.; Purvine, S.; Eng, J. K.; von Haller, P.; Aebersold, R.; Kolker, E., Differential stable isotope labeling of peptides for quantitation and de novo sequence derivation. *Rapid Commun Mass Spectrom* **2001,** *15* (14), 1214-21.
33. Gygi, S. P.; Rist, B.; Gerber, S. A.; Turecek, F.; Gelb, M. H.; Aebersold, R., Quantitative analysis of complex protein mixtures using isotope-coded affinity tags. *Nature biotechnology* **1999,** *17* (10), 994-9.

34. Han, D. K.; Eng, J.; Zhou, H.; Aebersold, R., Quantitative profiling of differentiation-induced microsomal proteins using isotope-coded affinity tags and mass spectrometry. *Nature biotechnology* **2001,** *19* (10), 946-51.
35. Tam, E. M.; Morrison, C. J.; Wu, Y. I.; Stack, M. S.; Overall, C. M., Membrane protease proteomics: Isotope-coded affinity tag MS identification of undescribed MT1-matrix metalloproteinase substrates. *Proc Natl Acad Sci U S A* **2004,** *101* (18), 6917-22.
36. Kwong, G. A.; von Maltzahn, G.; Murugappan, G.; Abudayyeh, O.; Mo, S.; Papayannopoulos, I. A.; Sverdlov, D. Y.; Liu, S. B.; Warren, A. D.; Popov, Y.; Schuppan, D.; Bhatia, S. N., Mass-encoded synthetic biomarkers for multiplexed urinary monitoring of disease. *Nature biotechnology* **2013,** *31* (1), 63-70.
37. Ross, P. L.; Huang, Y. N.; Marchese, J. N.; Williamson, B.; Parker, K.; Hattan, S.; Khainovski, N.; Pillai, S.; Dey, S.; Daniels, S.; Purkayastha, S.; Juhasz, P.; Martin, S.; Bartlet-Jones, M.; He, F.; Jacobson, A.; Pappin, D. J., Multiplexed protein quantitation in Saccharomyces cerevisiae using amine-reactive isobaric tagging reagents. *Mol Cell Proteomics* **2004,** *3* (12), 1154-69.
38. Thompson, A.; Schafer, J.; Kuhn, K.; Kienle, S.; Schwarz, J.; Schmidt, G.; Neumann, T.; Johnstone, R.; Mohammed, A. K.; Hamon, C., Tandem mass tags: a novel quantification strategy for comparative analysis of complex protein mixtures by MS/MS. *Anal Chem* **2003,** *75* (8), 1895-904.
39. Dayon, L.; Hainard, A.; Licker, V.; Turck, N.; Kuhn, K.; Hochstrasser, D. F.; Burkhard, P. R.; Sanchez, J. C., Relative quantification of proteins in human cerebrospinal fluids by MS/MS using 6-plex isobaric tags. *Anal Chem* **2008,** *80* (8), 2921-31.
40. Hardt, M.; Witkowska, H. E.; Webb, S.; Thomas, L. R.; Dixon, S. E.; Hall, S. C.; Fisher, S. J., Assessing the effects of diurnal variation on the composition of human parotid saliva: quantitative analysis of native peptides using iTRAQ reagents. *Anal Chem* **2005,** *77* (15), 4947-54.
41. Kridel, S. J.; Chen, E.; Kotra, L. P.; Howard, E. W.; Mobashery, S.; Smith, J. W., Substrate hydrolysis by matrix metalloproteinase-9. *J Biol Chem* **2001,** *276* (23), 20572-8.
42. Deng, S. J.; Bickett, D. M.; Mitchell, J. L.; Lambert, M. H.; Blackburn, R. K.; Carter, H. L., 3rd; Neugebauer, J.; Pahel, G.; Weiner, M. P.; Moss, M. L., Substrate specificity of human collagenase 3 assessed using a phage-displayed peptide library. *J Biol Chem* **2000,** *275* (40), 31422-7.
43. Eitan, Y.; Sarig, U.; Dahan, N.; Machluf, M., Acellular cardiac extracellular matrix as a scaffold for tissue engineering: in vitro cell support, remodeling, and biocompatibility. *Tissue Eng Part C Methods* **2010,** *16* (4), 671-83.
44. Yang, Q.; Peng, J.; Guo, Q.; Huang, J.; Zhang, L.; Yao, J.; Yang, F.; Wang, S.; Xu, W.; Wang, A.; Lu, S., A cartilage ECM-derived 3-D porous acellular matrix scaffold for in vivo cartilage tissue engineering with PKH26-labeled chondrogenic bone marrow-derived mesenchymal stem cells. *Biomaterials* **2008,** *29* (15), 2378-87.
45. Xing, Q.; Yates, K.; Tahtinen, M.; Shearier, E.; Qian, Z.; Zhao, F., Decellularization of fibroblast cell sheets for natural extracellular matrix scaffold preparation. *Tissue Eng Part C Methods* **2015,** *21* (1), 77-87.
46. Jin, C. Z.; Park, S. R.; Choi, B. H.; Park, K.; Min, B. H., In vivo cartilage tissue engineering using a cell-derived extracellular matrix scaffold. *Artif Organs* **2007,** *31* (3), 183-92.
47. Lu, H.; Hoshiba, T.; Kawazoe, N.; Koda, I.; Song, M.; Chen, G., Cultured cell-derived extracellular matrix scaffolds for tissue engineering. *Biomaterials* **2011,** *32* (36), 9658-66.
48. Xu, H. L.; Mao, K. L.; Lu, C. T.; Fan, Z. L.; Yang, J. J.; Xu, J.; Chen, P. P.; ZhuGe, D. L.; Shen, B. X.; Jin, B. H.; Xiao, J.; Zhao, Y. Z., An injectable acellular matrix scaffold with absorbable permeable nanoparticles improves the therapeutic effects of docetaxel on glioblastoma. *Biomaterials* **2016,** *107*, 44-60.
49. Almeida, H. V.; Liu, Y.; Cunniffe, G. M.; Mulhall, K. J.; Matsiko, A.; Buckley, C. T.; O'Brien, F. J.; Kelly, D. J., Controlled release of transforming growth factor-beta3 from cartilage-extra-

cellular-matrix-derived scaffolds to promote chondrogenesis of human-joint-tissue-derived stem cells. *Acta Biomater* **2014,** *10* (10), 4400-9.
50. Badylak, S. F., The extracellular matrix as a biologic scaffold material. *Biomaterials* **2007,** *28* (25), 3587-93.
51. Badylak, S. F.; Freytes, D. O.; Gilbert, T. W., Extracellular matrix as a biological scaffold material: Structure and function. *Acta Biomater* **2009,** *5* (1), 1-13.
52. Fitzpatrick, L. E.; McDevitt, T. C., Cell-derived matrices for tissue engineering and regenerative medicine applications. *Biomater Sci* **2015,** *3* (1), 12-24.
53. Nagase, H.; Visse, R.; Murphy, G., Structure and function of matrix metalloproteinases and TIMPs. *Cardiovasc Res* **2006,** *69* (3), 562-73.
54. Sternlicht, M. D.; Werb, Z., How matrix metalloproteinases regulate cell behavior. *Annu Rev Cell Dev Biol* **2001,** *17*, 463-516.
55. Bedossa, P.; Paradis, V., Liver extracellular matrix in health and disease. *J Pathol* **2003,** *200* (4), 504-15.
56. Daley, W. P.; Peters, S. B.; Larsen, M., Extracellular matrix dynamics in development and regenerative medicine. *J Cell Sci* **2008,** *121* (Pt 3), 255-64.
57. Lu, P.; Takai, K.; Weaver, V. M.; Werb, Z., Extracellular matrix degradation and remodeling in development and disease. *Cold Spring Harb Perspect Biol* **2011,** *3* (12).
58. Hodde, J. P.; Johnson, C. E., Extracellular matrix as a strategy for treating chronic wounds. *Am J Clin Dermatol* **2007,** *8* (2), 61-6.
59. Bidan, C. M.; Veldsink, A. C.; Meurs, H.; Gosens, R., Airway and Extracellular Matrix Mechanics in COPD. *Front Physiol* **2015,** *6*, 346.
60. Annoni, R.; Lancas, T.; Yukimatsu Tanigawa, R.; de Medeiros Matsushita, M.; de Morais Fernezlian, S.; Bruno, A.; Fernando Ferraz da Silva, L.; Roughley, P. J.; Battaglia, S.; Dolhnikoff, M.; Hiemstra, P. S.; Sterk, P. J.; Rabe, K. F.; Mauad, T., Extracellular matrix composition in COPD. *Eur Respir J* **2012,** *40* (6), 1362-73.
61. Dean, D. D.; Martel-Pelletier, J.; Pelletier, J. P.; Howell, D. S.; Woessner, J. F., Jr., Evidence for metalloproteinase and metalloproteinase inhibitor imbalance in human osteoarthritic cartilage. *The Journal of clinical investigation* **1989,** *84* (2), 678-85.
62. Shiozawa, S.; Tsumiyama, K.; Yoshida, K.; Hashiramoto, A., Pathogenesis of joint destruction in rheumatoid arthritis. *Arch Immunol Ther Exp (Warsz)* **2011,** *59* (2), 89-95.
63. Basel, M. T.; Shrestha, T. B.; Troyer, D. L.; Bossmann, S. H., Protease-sensitive, polymer-caged liposomes: a method for making highly targeted liposomes using triggered release. *ACS Nano* **2011,** *5* (3), 2162-75.
64. Park, C.; Kim, H.; Kim, S.; Kim, C., Enzyme responsive nanocontainers with cyclodextrin gatekeepers and synergistic effects in release of guests. *J Am Chem Soc* **2009,** *131* (46), 16614-5.
65. Choi, S. W.; Zhang, Y.; Xia, Y., A temperature-sensitive drug release system based on phase-change materials. *Angew Chem Int Ed Engl* **2010,** *49* (43), 7904-8.
66. Lee, E. S.; Na, K.; Bae, Y. H., Super pH-sensitive multifunctional polymeric micelle. *Nano Lett* **2005,** *5* (2), 325-9.
67. de Gracia Lux, C.; Joshi-Barr, S.; Nguyen, T.; Mahmoud, E.; Schopf, E.; Fomina, N.; Almutairi, A., Biocompatible polymeric nanoparticles degrade and release cargo in response to biologically relevant levels of hydrogen peroxide. *J Am Chem Soc* **2012,** *134* (38), 15758-64.
68. Kjelgaard-Petersen, C.; Siebuhr, A. S.; Christiansen, T.; Ladel, C.; Karsdal, M.; Bay-Jensen, A. C., Synovitis biomarkers: ex vivo characterization of three biomarkers for identification of inflammatory osteoarthritis. *Biomarkers* **2015,** *20* (8), 547-56.
69. Ravi, M.; Paramesh, V.; Kaviya, S. R.; Anuradha, E.; Solomon, F. D., 3D cell culture systems: advantages and applications. *J Cell Physiol* **2015,** *230* (1), 16-26.
70. Langhans, S. A., Three-Dimensional in Vitro Cell Culture Models in Drug Discovery and Drug Repositioning. *Front Pharmacol* **2018,** *9*, 6.

71. Candido, S.; Abrams, S. L.; Steelman, L. S.; Lertpiriyapong, K.; Fitzgerald, T. L.; Martelli, A. M.; Cocco, L.; Montalto, G.; Cervello, M.; Polesel, J.; Libra, M.; McCubrey, J. A., Roles of NGAL and MMP-9 in the tumor microenvironment and sensitivity to targeted therapy. *Biochim Biophys Acta* **2016,** *1863* (3), 438-448.
72. Williams, A. S.; Kang, L.; Wasserman, D. H., The extracellular matrix and insulin resistance. *Trends Endocrinol Metab* **2015,** *26* (7), 357-66.
73. Lin; Chun, T. H.; Kang, L., Adipose extracellular matrix remodelling in obesity and insulin resistance. *Biochem Pharmacol* **2016,** *119*, 8-16.
74. Wynn, T. A.; Ramalingam, T. R., Mechanisms of fibrosis: therapeutic translation for fibrotic disease. *Nat Med* **2012,** *18* (7), 1028-40.
75. Bonnans, C.; Chou, J.; Werb, Z., Remodelling the extracellular matrix in development and disease. *Nat Rev Mol Cell Biol* **2014,** *15* (12), 786-801.
76. Braun, A. C.; Gutmann, M.; Mueller, T. D.; Luhmann, T.; Meinel, L., Bioresponsive release of insulin-like growth factor-I from its PEGylated conjugate. *J Control Release* **2018,** *279*, 17-28.
77. Ehrbar, M.; Rizzi, S. C.; Hlushchuk, R.; Djonov, V.; Zisch, A. H.; Hubbell, J. A.; Weber, F. E.; Lutolf, M. P., Enzymatic formation of modular cell-instructive fibrin analogs for tissue engineering. *Biomaterials* **2007,** *28* (26), 3856-66.
78. Ehrbar, M.; Rizzi, S. C.; Schoenmakers, R. G.; Miguel, B. S.; Hubbell, J. A.; Weber, F. E.; Lutolf, M. P., Biomolecular hydrogels formed and degraded via site-specific enzymatic reactions. *Biomacromolecules* **2007,** *8* (10), 3000-7.
79. Schense, J. C.; Hubbell, J. A., Cross-linking exogenous bifunctional peptides into fibrin gels with factor XIIIa. *Bioconjug Chem* **1999,** *10* (1), 75-81.
80. Sala, A.; Ehrbar, M.; Trentin, D.; Schoenmakers, R. G.; Voros, J.; Weber, F. E., Enzyme mediated site-specific surface modification. *Langmuir* **2010,** *26* (13), 11127-34.
81. Song, W.; Tang, Z.; Zhang, D.; Li, M.; Gu, J.; Chen, X., A cooperative polymeric platform for tumor-targeted drug delivery. *Chem Sci* **2016,** *7* (1), 728-736.
82. McCarthy, J. R.; Sazonova, I. Y.; Erdem, S. S.; Hara, T.; Thompson, B. D.; Patel, P.; Botnaru, I.; Lin, C. P.; Reed, G. L.; Weissleder, R.; Jaffer, F. A., Multifunctional nanoagent for thrombus-targeted fibrinolytic therapy. *Nanomedicine (Lond)* **2012,** *7* (7), 1017-28.
83. Fruh, S. M.; Spycher, P. R.; Mitsi, M.; Burkhardt, M. A.; Vogel, V.; Schoen, I., Functional modification of fibronectin by N-terminal FXIIIa-mediated transamidation. *Chembiochem* **2014,** *15* (10), 1481-6.
84. Gutmann, M.; Bechold, J.; Seibel, J.; Meinel, L.; Lühmann, T., Metabolic Glycoengineering of Cell-Derived Matrices and Cell Surfaces: A Combination of Key Principles and Step-by-Step Procedures. *ACS Biomaterials Science & Engineering* **2018**.
85. Penzes, K.; Kover, K. E.; Fazakas, F.; Haramura, G.; Muszbek, L., Molecular mechanism of the interaction between activated factor XIII and its glutamine donor peptide substrate. *J Thromb Haemost* **2009,** *7* (4), 627-33.
86. Lorand, L.; Graham, R. M., Transglutaminases: crosslinking enzymes with pleiotropic functions. *Nat Rev Mol Cell Biol* **2003,** *4* (2), 140-56.
87. Hu, B. H.; Messersmith, P. B., Rational design of transglutaminase substrate peptides for rapid enzymatic formation of hydrogels. *J Am Chem Soc* **2003,** *125* (47), 14298-9.
88. Spieler, V., Bio-inspired delivery of interleukin-4. *Univeristy of Wuerzburg* **2019**.
89. Calich, A. L.; Domiciano, D. S.; Fuller, R., Osteoarthritis: can anti-cytokine therapy play a role in treatment? *Clin Rheumatol* **2010,** *29* (5), 451-5.
90. Dardik, R.; Krapp, T.; Rosenthal, E.; Loscalzo, J.; Inbal, A., Effect of FXIII on monocyte and fibroblast function. *Cell Physiol Biochem* **2007,** *19* (1-4), 113-20.
91. Brown, L. F.; Lanir, N.; McDonagh, J.; Tognazzi, K.; Dvorak, A. M.; Dvorak, H. F., Fibroblast migration in fibrin gel matrices. *Am J Pathol* **1993,** *142* (1), 273-83.

92. Dardik, R.; Solomon, A.; Loscalzo, J.; Eskaraev, R.; Bialik, A.; Goldberg, I.; Schiby, G.; Inbal, A., Novel proangiogenic effect of factor XIII associated with suppression of thrombospondin 1 expression. *Arterioscler Thromb Vasc Biol* **2003,** *23* (8), 1472-7.
93. Inbal, A.; Leor, J.; Skutelsky, E.; Castel, D.; Holbova, R.; Schibi, G.; Goldberg, I.; Eskaraev, R.; Dardik, R., Evaluation of pro-angiogenic activity of factor XIII (FXIII) in ischemic tissue, heart transplantation and FXIII-deficient mice. *Blood* **2004,** *104* (11), 816a-816a.
94. Greenberg, C. S.; Birckbichler, P. J.; Rice, R. H., Transglutaminases: multifunctional cross-linking enzymes that stabilize tissues. *FASEB J* **1991,** *5* (15), 3071-7.
95. Al-Jallad, H. F.; Nakano, Y.; Chen, J. L.; McMillan, E.; Lefebvre, C.; Kaartinen, M. T., Transglutaminase activity regulates osteoblast differentiation and matrix mineralization in MC3T3-E1 osteoblast cultures. *Matrix Biol* **2006,** *25* (3), 135-48.
96. Al-Jallad, H. F.; Myneni, V. D.; Piercy-Kotb, S. A.; Chabot, N.; Mulani, A.; Keillor, J. W.; Kaartinen, M. T., Plasma membrane factor XIIIA transglutaminase activity regulates osteoblast matrix secretion and deposition by affecting microtubule dynamics. *PLoS One* **2011,** *6* (1), e15893.
97. Johnson, K. A.; Rose, D. M.; Terkeltaub, R. A., Factor XIIIA mobilizes transglutaminase 2 to induce chondrocyte hypertrophic differentiation. *J Cell Sci* **2008,** *121* (Pt 13), 2256-64.
98. Aeschlimann, D.; Mosher, D.; Paulsson, M., Tissue transglutaminase and factor XIII in cartilage and bone remodeling. *Semin Thromb Hemost* **1996,** *22* (5), 437-43.
99. Adamczyk, M., Transglutaminase 2 in cartilage homoeostasis: novel links with inflammatory osteoarthritis. *Amino Acids* **2017,** *49* (3), 625-633.
100. Raghu, H.; Cruz, C.; Rewerts, C. L.; Frederick, M. D.; Thornton, S.; Mullins, E. S.; Schoenecker, J. G.; Degen, J. L.; Flick, M. J., Transglutaminase factor XIII promotes arthritis through mechanisms linked to inflammation and bone erosion. *Blood* **2015,** *125* (3), 427-37.
101. Orlandi, A.; Oliva, F.; Taurisano, G.; Candi, E.; Di Lascio, A.; Melino, G.; Spagnoli, L. G.; Tarantino, U., Transglutaminase-2 differently regulates cartilage destruction and osteophyte formation in a surgical model of osteoarthritis. *Amino Acids* **2009,** *36* (4), 755-63.
102. Zamboni, P.; De Mattei, M.; Ongaro, A.; Fogato, L.; Carandina, S.; De Palma, M.; Tognazzo, S.; Scapoli, G. L.; Serino, M. L.; Caruso, A.; Liboni, A.; Gemmati, D., Factor XIII contrasts the effects of metalloproteinases in human dermal fibroblast cultured cells. *Vasc Endovascular Surg* **2004,** *38* (5), 431-8.
103. Yamanaka, H.; Matsuda, Y.; Tanaka, M.; Sendo, W.; Nakajima, H.; Taniguchi, A.; Kamatani, N., Serum matrix metalloproteinase 3 as a predictor of the degree of joint destruction during the six months after measurement, in patients with early rheumatoid arthritis. *Arthritis & Rheumatism* **2000,** *43* (4).
104. Brennan, F. M.; Browne, K. A.; Green, P. A.; Jaspar, J. M.; Maini, R. N.; Feldmann, M., Reduction of serum matrix metalloproteinase 1 and matrix metalloproteinase 3 in rheumatoid arthritis patients following anti-tumour necrosis factor-alpha (cA2) therapy. *Br J Rheumatol* **1997,** *36* (6), 643-50.
105. Green, M. J.; Gough, A. K.; Devlin, J.; Smith, J.; Astin, P.; Taylor, D.; Emery, P., Serum MMP-3 and MMP-1 and progression of joint damage in early rheumatoid arthritis. *Rheumatology (Oxford)* **2003,** *42* (1), 83-8.
106. van der Laken, C. J.; Voskuyl, A. E.; Roos, J. C.; Stigter van Walsum, M.; de Groot, E. R.; Wolbink, G.; Dijkmans, B. A.; Aarden, L. A., Imaging and serum analysis of immune complex formation of radiolabelled infliximab and anti-infliximab in responders and non-responders to therapy for rheumatoid arthritis. *Ann Rheum Dis* **2007,** *66* (2), 253-6.

ABBREVIATIONS

AA	Amino acid
ACN	Acetonitrile
AF488	Alexa fluor 488
AGC	Automated gain control
ANP	Fmoc-(*S*)-3-amino-3-(2-nitrophenyl)propionic acid
APTES	(3-Aminopropyl)triethoxysilane
au	Arbitrary units
BCA	Bicinchoninic acid
BCS	Bovine calf serum
Bio-Ahx	Biotin-aminohexanoic acid
BSA	Bovine serum albumin
CID or HCD	collision induced dissociation or high-energy collision dissociation
CLSM	Confocal laser scanning microscopy
COPD	Chronic obstructive pulmonary disease
CuAAC	Copper (I)-catalyzed azide-alkyne cycloaddition
DBCO	Dibenzo cyclooctyne
DCM	Dichloromethane
DIC	N,N′-Diisopropylcarbodiimide
DIPEA	Diisopropylethylamine
DMEM	Dulbecco's Modified Eagle Medium
DMM	Destabilization of medial meniscus
DMF	Dimethylformamide
DMSO	Dimethyl sulfoxide
DTT	Dithiothreitol
ECM	Extracellular matrix
EDTA	Ethylenediaminetetraacetate
ELISA	Enzyme linked immunosorbent assay
ESI-MS	Electrospray ionization mass spectrometry
FPLC	Fast protein liquid chromatography
FXIIIa	activated factor XIII
HE	Haematoxylin and eosin
HPLC	High-performance liquid chromatography

HRP	Horseradish peroxidase
IA	Iodoacetamide
IGF-I	Insulin-like growth factor I
LAF	Laminar Air Flow
LC-MS/MS	Tandem mass spectrometry
MALDI-MS	Matrix-assisted laser desorption ionization mass spectrometry
Mt	Mass tag
MMP	Matrix metalloproteinase
MS	Mass spectrometry
MS/MS or MS^2	Tandem mass spectrometry
MQW	Milli-Q® purified water
MWCO	Molecular weight cut-off
NHS	N-hydroxy succinimide
m/z	mass to charge ratio
OA	Osteoarthritis
PBS	Phosphate buffered saline
PEG	Polyethylene glycol
Pen/Strep or P/S	Penicillin and Streptomycin
PSS	Protease-sensitive sequence
PTFE	Polytetrafluoroethylene
RA	Rheumatoid arthritis
RT	Room temperature
RPM	Rounds per minute
SPAAC	Strain-promoted alkyne-azide cycloadditions
SPPS	Solid phase peptide synthesis
ST	Streptag II
TEV	Tobacco Etch Virus
TFA	Trifluoracetic acid
TIS	Triisopropylsilane
TMB	3,3′,5,5′-Tetramethylbenzidine
UV	Ultraviolet

ACKNOWLEDGMENTS

I would like to sincerely thank my supervisor Prof. Dr. Dr. Lorenz Meinel for giving me the opportunity to perform my PhD at his Chair, to receive an insight in a variety of scientific methods and to be able to work in excellent equipped laboratories. His scientific knowledge, constructive feedback and enthusiastic character are greatly appreciated as they helped me to stay motivated and succeed in writing my thesis.

Furthermore, I am very grateful for the scientific guidance and support PD Dr. Tessa Lühmann gave me and for always having an open door.

I would also like to express my gratitude to Stephanie Lamer and Dr. Andreas Schlosser of the Rudolf Virchow Center for Experimental Biomedicine. I appreciate your time and support with the tandem mass spectrometry measurements and analysis and your constant and competent support in designing the mass-encoded peptides.

I would like to thank the "Deutsche Forschungsgemeinschaft" (DFG) and the Sino German Center for my financial support and the opportunity to spend four weeks at Zhejiang University in the lab of our cooperation partner Prof. Ouyang and for being able to witness an expert environment for animal studies. Special thanks go to Yejun Hu, who was an enormous help in organizing, performing and analyzing the animal experiment and who made my stay in Hangzhou an unforgettable experience.

Thanks to Juliane Adelmann from the organic chemistry department of the University of Würzburg for MALDI and ESI-MS measurements.

Many thanks to my great PhD colleagues that became friends. Thank you, Eleonora Cataldi, Simon Hanio and Marco Saedtler for interesting conversations and moral support. Thanks to Martina Raschig for a great holiday, for proofreading and for your input. Thanks to my office mate Matthias Ruopp for educational discussions and your help with mathematics. Björn ter Mors, thank you for your motivation and your supply of chewing gums and tea. Valerie Spieler, thanks for your humor, your scientific input and the cleanliness in our labs. Thank you, Tobias Miesler, for your scientific expertise and fun facts that lifted the mood. Thanks to Marcus Gutmann, Matthias Beudert and Niklas Hauptstein for spending many hours with me at the confocal laser scanning microscopy and for the fruitful discussions. Thanks, Magdalena Nowak, for peptide synthesis with the LibertyBlue and a huge thanks

to Christine Schneider for all your organizational talent and keeping things running. Thank you all for making my time in Würzburg memorable inside and outside the lab.

A special thanks to Judith for supporting me in difficult times, laughing in good times and being the perfect yoga buddy.

I would also like to thank my friends, Martina and Viki, outside of Würzburg for all the great experiences we share and the constant support and motivation I received.

Finally, I would like to express my greatest gratitude to my parents and to my brother for their immeasurable support, unlimited advice, constant encouragement and relaxing holidays.

DOCUMENTATION OF AUTHORSHIP

This section contains a list of the individual contribution for each author to the publication reprinted in this thesis. Unpublished manuscripts are handled, accordingly.

1	**K. Dodt, M. Drießen, S. Lamer, A. Schlosser, T. Lühmann, L. Meinel** A complete and versatile protocol: Decoration of cell-derived matrices with mass-encoded peptides for multiplexed protease activity detection. ACS Biomater. Sci. Eng. 2020 [Epub ahead of print]						
Author		**1**	**2**	**3**	**4**	**5**	**6**
Design of mass reporters		x			x		
Tandem mass spectrometry measurements of mass tags				x			
Analysis of tandem mass spectrometry measurements		x		x			
Synthesis of mass reporters by SPPS		x					
Characterization of mass reporters by MMP and TEV protease incubation, UV irradiation, and affinity purification		x					
Cell culture and ECM production		x					
Immobilization of mass reporters on ECM		x					
Visualization of mass reporters on ECM		x					
Incubation of immobilized reporters on ECM		x					
Statistical analysis		x					
Development of concept		x				x	x
Preparation of manuscript		x	x	x	x	x	x
Design of figures		x	x				x
Revision of manuscript		x	x			x	x
Supervision of K. Dodt							x

2	**K. Dodt, S. Lamer, M. Drießen, S. Bölch, A. Schlosser, T. Lühmann, L. Meinel** Mass-encoded reporters reporting proteolytic activity from within the extracellular matrix. ACS Biomater. Sci. Eng. 2020, 6, 9, 5240-5253							
Author		**1**	**2**	**3**	**4**	**5**	**6**	**7**
Design of mass reporters		x				x		
Tandem mass spectrometry measurements of mass reporters			x					
Analysis of tandem mass spectrometry measurements		x	x					
Synthesis of mass reporters by SPPS		x						
Characterization of mass reporters by MMP and TEV incubation, UV irradiation and affinity purification		x						
Cell culture and ECM production		x						
Immobilization of mass reporters on ECM		x						
Visualization of mass reporters on ECM		x						

Incubation of immobilized reporters on ECM	x						
Statistical analysis	x						
Development of concept	x					x	x
Preparation of manuscript	x	x	x	x	x	x	x
Design of figures	x		x				x
Revision of manuscript	x		x			x	x
Supervision of K. Dodt							x

3	**K. Dodt, Y. Hu, S. Lamer, A. Schlosser, T. Lühmann, H. Ouyang, L. Meinel** Soluble mass reporters for detection of enzyme activity and multiplexed analysis. (2020) [unpublished]

Author	**1**	2	**3**	**4**	**5**	**6**	**7**
Design of mass tags	**x**			x			
Tandem mass spectrometry measurements of mass tags			x				
Analysis of tandem mass spectrometry	**x**		x				
Synthesis of mass reporters	**x**						
Characterization of mass reporters by MMP incubation, UV irradiation, affinity purification and TEV protease incubation	**x**						
Mouse model of partial meniscectomy		x					
Macroscopic and histological assessment		x					
Immunohistochemistry		x					
Statistical analysis		x					
Development of concept	**x**			x	x	x	x
Preparation of manuscript	**x**						
Design of figures	**x**	x					
Correction of manuscript	**x**				x		x
Supervision of K. Dodt							x

Erklärung zu den Eigenanteilen des Doktoranden sowie der weiteren Doktoranden als Koautoren an Publikationen und Zweitpublikationsrechten bei einer kumulativen Dissertation.

Für alle in dieser kumulativen Dissertation verwendeten Manuskripte liegen die notwendigen Genehmigungen der Verlage (‚reprint permission') für die Zweitpublikation vor, außer das betreffende Kapitel ist noch gar nicht publiziert. Dieser Umstand wird einerseits durch die genaue Angabe der Literaturstelle der Erstpublikation auf der ersten Seite des betreffenden Kapitels deutlich gemacht oder die bisherige Nichtveröffentlichung durch den Vermerk „unpublished" oder „nicht veröffentlicht" gekennzeichnet.

Die Mitautoren der in dieser kumulativen Dissertation verwendeten Manuskripte sind sowohl über die Nutzung als auch über die oben angegebenen Eigenanteile informiert.

Die Anteile der Mitautoren an den Publikationen sind in den vorausgehenden Tabellen aufgeführt.

Prof. Dr. Dr. Lorenz Meinel	Unterschrift
Katharina Dodt	Unterschrift